NASA
CR
3558-
pt.2
c.1

TECH LIBRARY KAFB, NM

0062176

LOAN COPY
AFWL TECHNI

NASA Contractor Report 3558
Part 2

# LSST (Hoop/Column) Maypole Antenna Development Program

Marvin R. Sullivan

CONTRACT NAS1-15763
JUNE 1982

24 JUN 1982
Technical Library
AF Weapons
Laboratory

NASA

TECH LIBRARY KAFB, NM
0062176

# LSST (Hoop/Column) Maypole Antenna Development Program

NASA Contractor Report 3558
Part 2

# LSST (Hoop/Column) Maypole Antenna Development Program

Marvin R. Sullivan
*Harris Corporation*
*Melbourne, Florida*

Prepared for
Langley Research Center
under Contract NAS1-15763

National Aeronautics
and Space Administration

**Scientific and Technical
Information Office**

1982

Use of trade names or names of manufacturers in this report does not constitute an official endorsement of such products or manufacturers, either expressed or implied, by the National Aeronautics and Space Administration.

CONTENTS

Part 1*



*Chapters 1 to 5 are published under separate cover.

## 6.0 MATERIAL DEVELOPMENT - CABLE TECHNOLOGY

This section documents the activities and results of the LSST Task II Material development.

### 6.1 Objectives and Requirements

#### 6.1.1 Study Objectives

The objective of the Task II Material Development is to provide the necessary materials and material properties to support the Hoop/Column antenna design task. An early survey of the antenna design and required materials indicated that cable technology was the most needed area of study. Cables are very important structural elements of the Maypole Hoop/Column antenna design. They structurally connect and stabilize the hoop and column assemblies and contour the flexible RF reflective mesh surface. The cables are major contributors in attaining high structural natural frequency and good thermal elastic performance in space. Their prominence and importance in the Hoop/Column design resulted in directing the activities of this task to cable development.

Objectives of the task are shown in Figure 6.1.1-1. They consist of defining cable requirements, researching existing data, evaluating candidate materials and configurations, fabricating samples, testing, and determining material properties of selected candidates.

#### 6.1.2 Cable Requirements

The cables control the reflector configuration, and to a large degree determine antenna performance. To accomplish this, the cables must possess high static and thermal stability and high EA (modulus of elasticity times the area). The cables must also be capable of sustained exposure to the harsh environment of space without appreciable degradation, and be flexible so they can be stowed for launch. A more detailed summary of these requirements is shown in Figure 6.1.2-1. They have been categorized under the three general areas of survival, structural, and cost.

## OBJECTIVES

- DEFINE CABLE REQUIREMENTS, STRUCTURAL, THERMAL, ENVIRONMENTAL
- PERFORM DATA RESEARCH
- EVALUATE CANDIDATE MATERIALS AND CONFIGURATIONS
- FABRICATE SAMPLES OF SELECTED CABLE MATERIAL/ CONFIGURATION COMBINATIONS
- DETERMINE MATERIAL PROPERTIES OF SELECT CONFIGURATIONS VIA APPROPRIATE TESTS
- PROVIDE DESIGN DATA AS INPUT TO OTHER TASKS

Figure 6.1.1-1. Objectives

## CORD REQUIREMENTS

- SURVIVAL REQUIREMENTS
  - SPACE ENVIRONMENTAL
    - THERMAL
    - RADIATION
    - VACUUM
  - HANDLING*
    - SPOOLING
    - PACKAGING
  - STRENGTH
    - DESIGN LOADS*
    - FAILSAFE MODE LOADS
- STRUCTURAL REQUIREMENTS
  - STABILITY
    - THERMAL*
    - CREEP/RESIDUAL STRAIN*
  - STIFFNESS*
  - WEIGHT*
- COST
  - MATERIAL (AVAILABILITY)*
  - MANUFACTURING*

*ADDITIONAL DEFINITION SUPPLIED IN VIEWGRAPHS WHICH FOLLOW

Figure 6.1.2-1. Cord Requirements

The survival requirements override all other requirements. The cords must be able to survive the expected space environment and ground handling for them to be viable candidates. They must also have sufficient strength to survive all expected load conditions.

The key structural requirements may be listed in descending order of importance as: stability, stiffness, and weight. Experience has shown that thermal and creep stability properties are the most difficult cord properties to obtain and have the greatest influence on antenna performance. Cord strains of $50 \times 10^{-6}$ have a significant effect on the antenna performance as shown in Figure 6.1.2-2. Cord stiffness, or EA, is an important parameter of the deployed reflector natural frequency. Figure 6.1.2-3 shows the relationship of cord EA and antenna natural frequency. The natural frequency is shown as a percent of nominal which is assumed to be for an antenna using graphite cords with an EA of 4500. If quartz cords with an EA of 1600 is used, the natural frequency is 57 percent of the nominal. It is important to note, however, that the frequency modes in which the cables effect, are not the lowest modes as described in Section 5.0 of this report. Cord EA also influences the thermal elastic performance of the antenna. In general, the higher the stiffness the better the antenna performance.

Cost is another requirement that must be considered when evaluating candidate cable materials. No specific cost requirement has been established; however, cost related parameters such as material availability and manufactureability of the candidates are important considerations in establishing feasibility.

The 100-meter antenna design was inspected to determine the cord load and quantity requirements. The results are shown in Figure 6.1.2-4. The total cord length per antenna is approximately 22.5 km (14 miles) and the loads vary from 0.27 newtons (0.06 pounds) to 180 newtons (40 pounds).

## 6.2 Study Approach

The study approach is best described in the task flow illustrated in Figure 6.2-1. The task is initiated by identifying the requirements as summarized in the preceding section. After the requirements are established, candidate cable designs are identified by surveying existing literature,

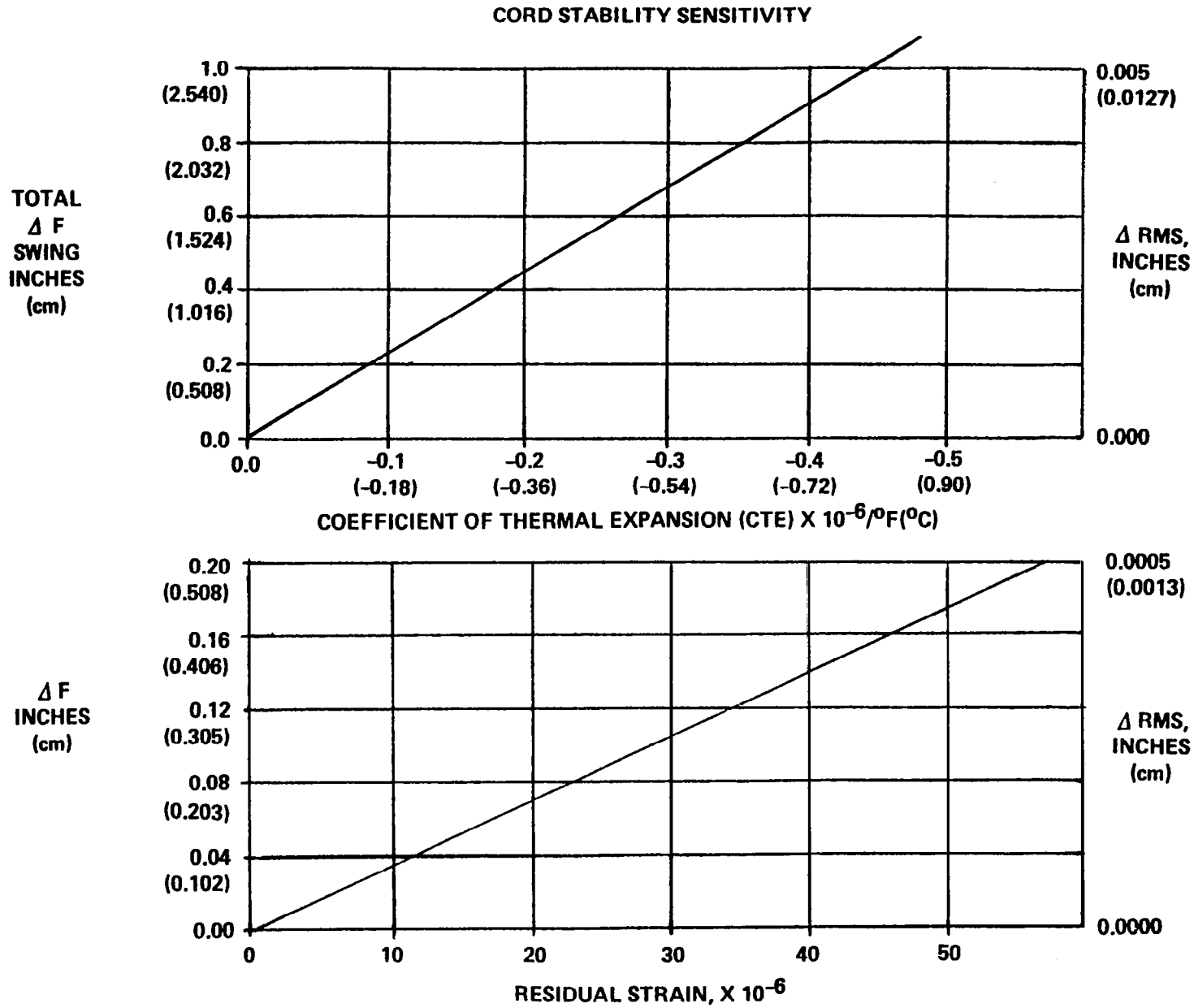


Figure 6.1.2-2. Cord Stability Sensitivity

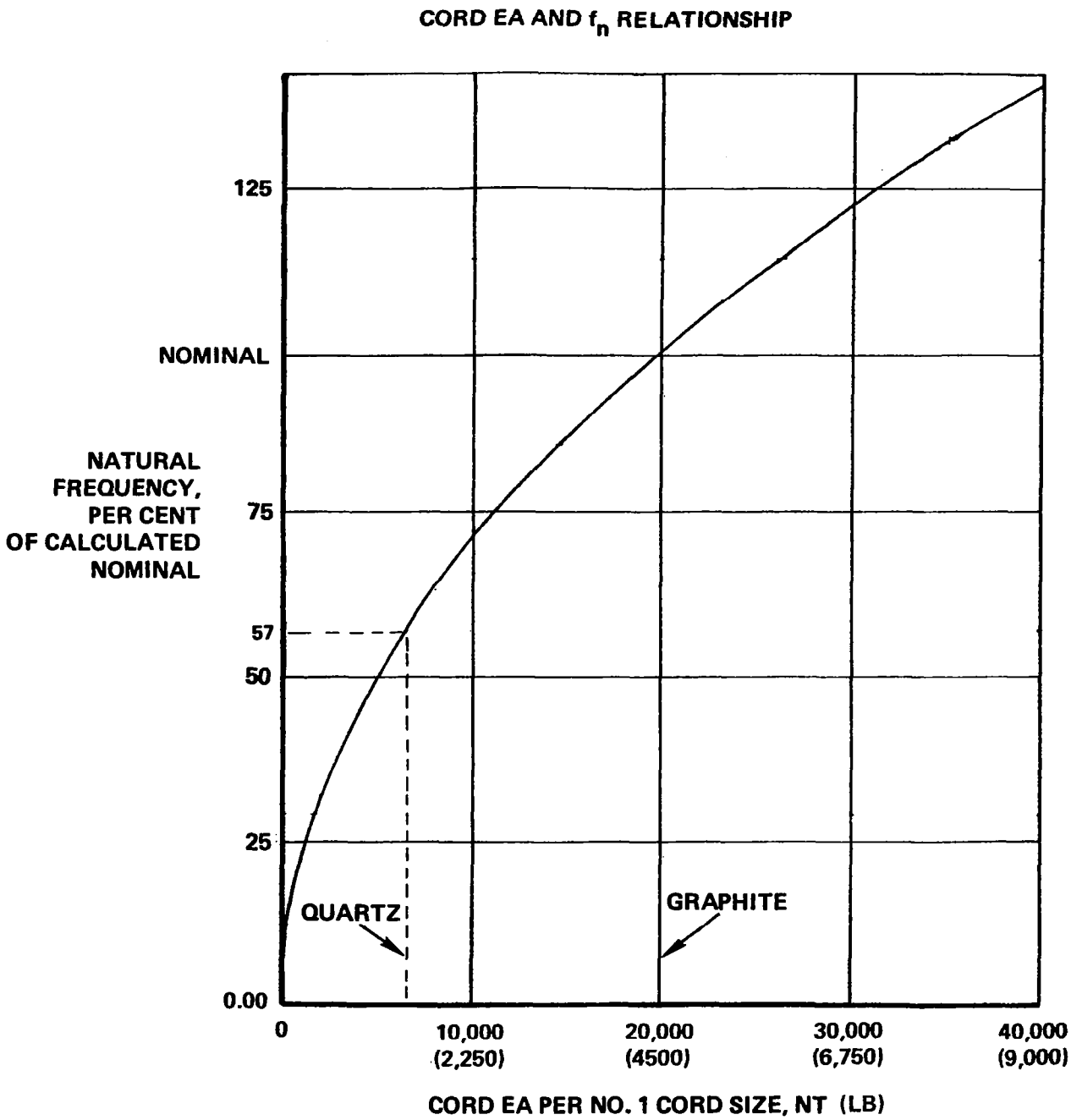


Figure 6.1.2-3. Cord EA and $f_n$ Relationship

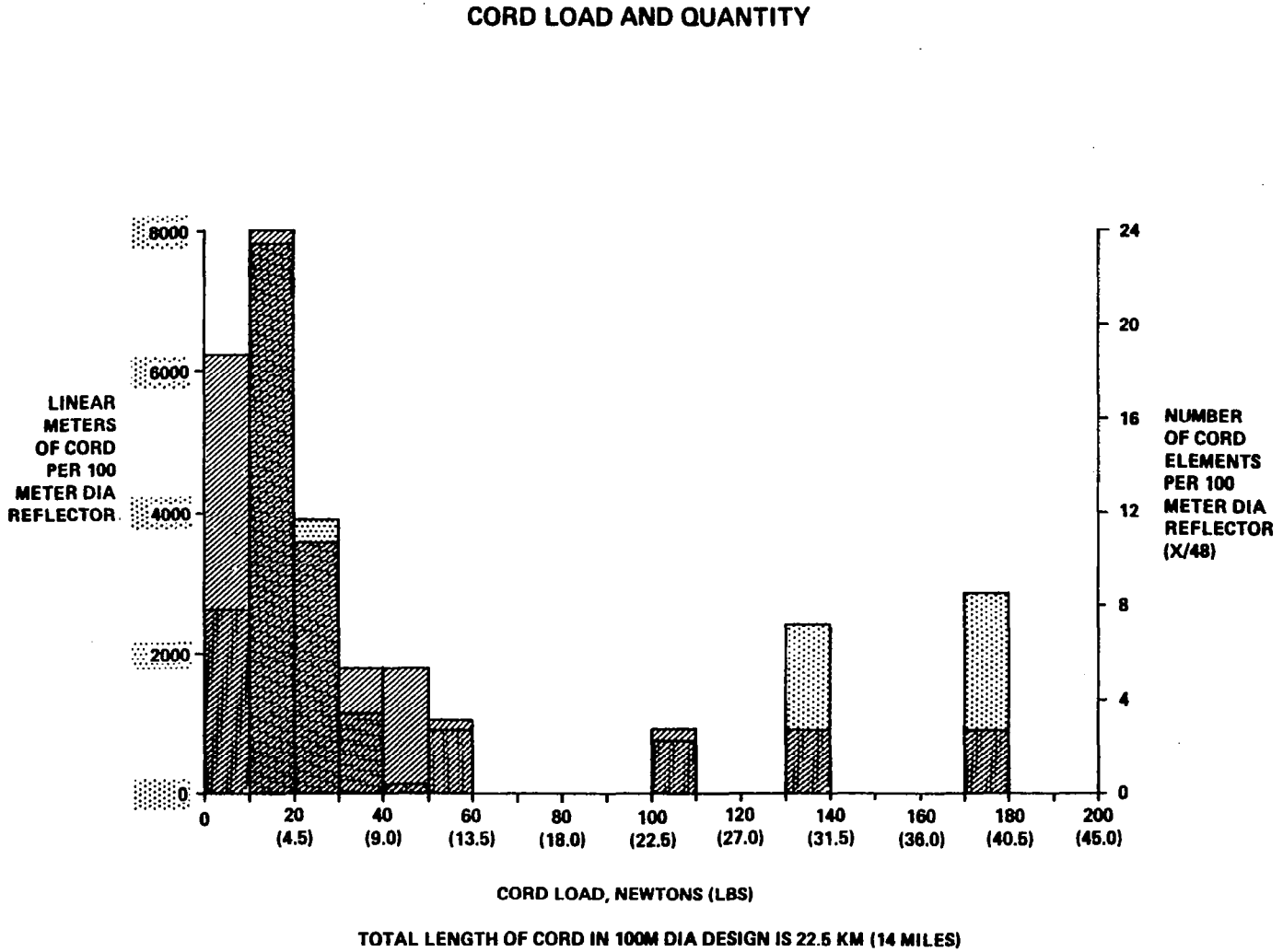


Figure 6.1.2-4. Cord Load and Quantity

## TASK 2 FLOW

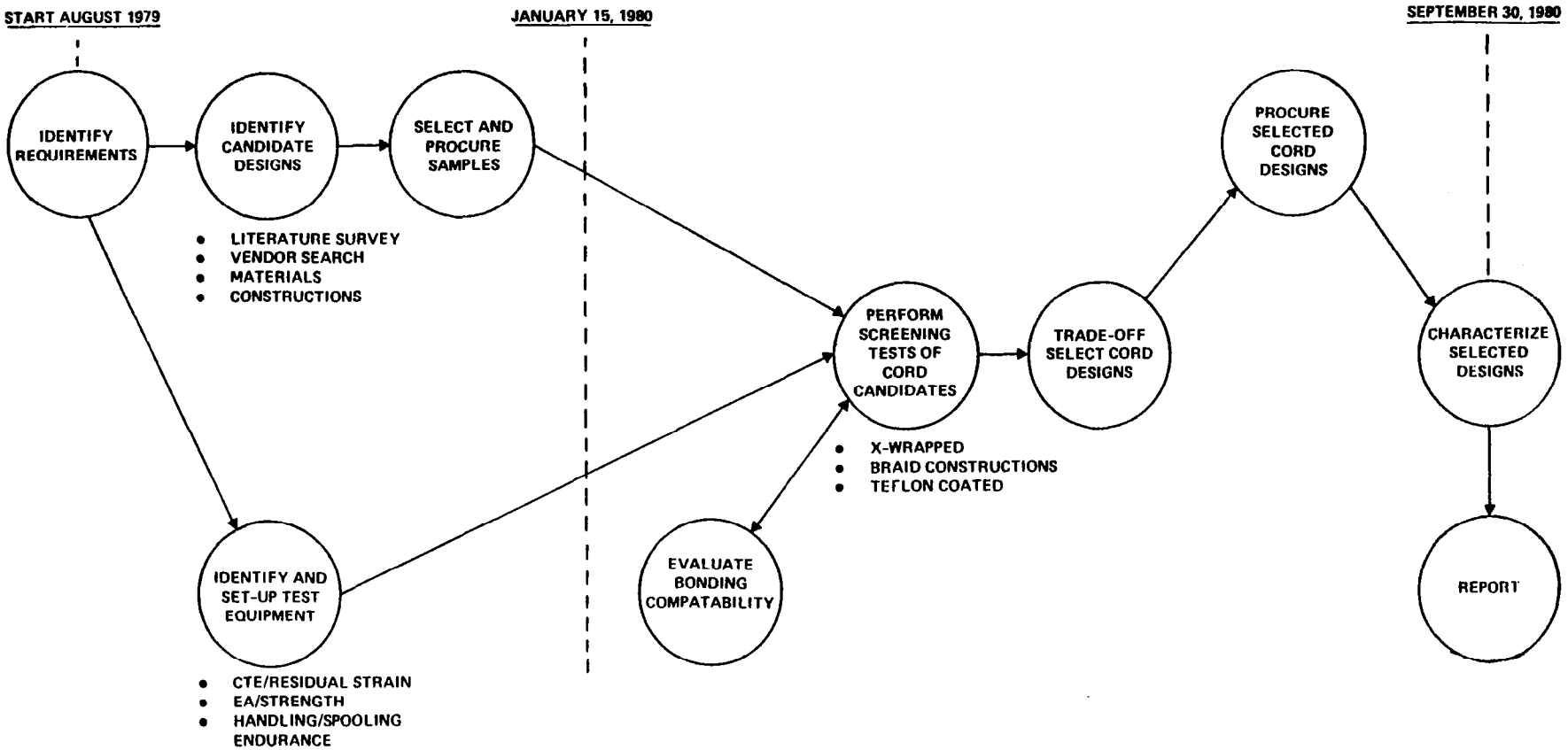


Figure 6.2-1. Task 2 Flow

contacting cable vendors and material suppliers, and identifying potential construction methods. From these activities, candidate cable designs are selected and samples are procured for evaluation. Concurrent with these activities, the necessary testing and test equipment are identified to evaluate the samples relative to the defined requirements. The evaluation tests chosen are: coefficient of thermal expansion, initial cord stretch or residual strain, EA (modulus of elasticity times area), tensile strength, and handling and spooling endurance. These tests are described in more detail in Paragraph 6.3 which follows. After the cable samples are received they are tested and the most favorable candidates are identified in a trade-off study. Following the trade-off study additional samples of the winning candidates are procured and characterized by materials property testing.

## 6.3 Test Methods

The required tests which have been identified in the preceding paragraph may be accomplished on three separate test equipment. The coefficient of thermal expansion (CTE) and residual strain of the cables are measured on the test equipment illustrated in Figure 6.3-1. The equipment consists of a 120 inches tall test fixture which will accept cable specimen of 100 inches in length. The fixture is constructed of upper and lower plates separated by three 100-inch long quartz rods, 1/4-inch in diameter. The high thermal stability of the quartz rods negate thermal expansion of the test fixture. The cable test samples are attached to the upper plate. A weighted plumb bob is attached to the other end of the samples. The weighted plumb bob is constructed so that visual contact with a micrometer can be accurately determined as shown in Figure 6.3-2. The sample is suspended in a 2-inch diameter copper tube, 100 inches long to provide a shroud for heating and cooling. The specimen may be cycled from -156$^{o}$C (-250$^{o}$F) to +93$^{o}$C (+200$^{o}$F). The fixture is instrumented with thermalcouples to allow recording of the average specimen temperature at any point in time. Load may be added or subtracted from the plumb bob to allow mechanical load cycling on the specimen. Both thermal and mechanical load cycling are done to determine the residual strain of a cable sample. The coefficient of thermal expansion of the samples are determined from the thermal strain data received from the test.

An Instron Tensile Test machine is used to measure the EA and tensile strength of the cable specimen (see Figure 6.3-3).

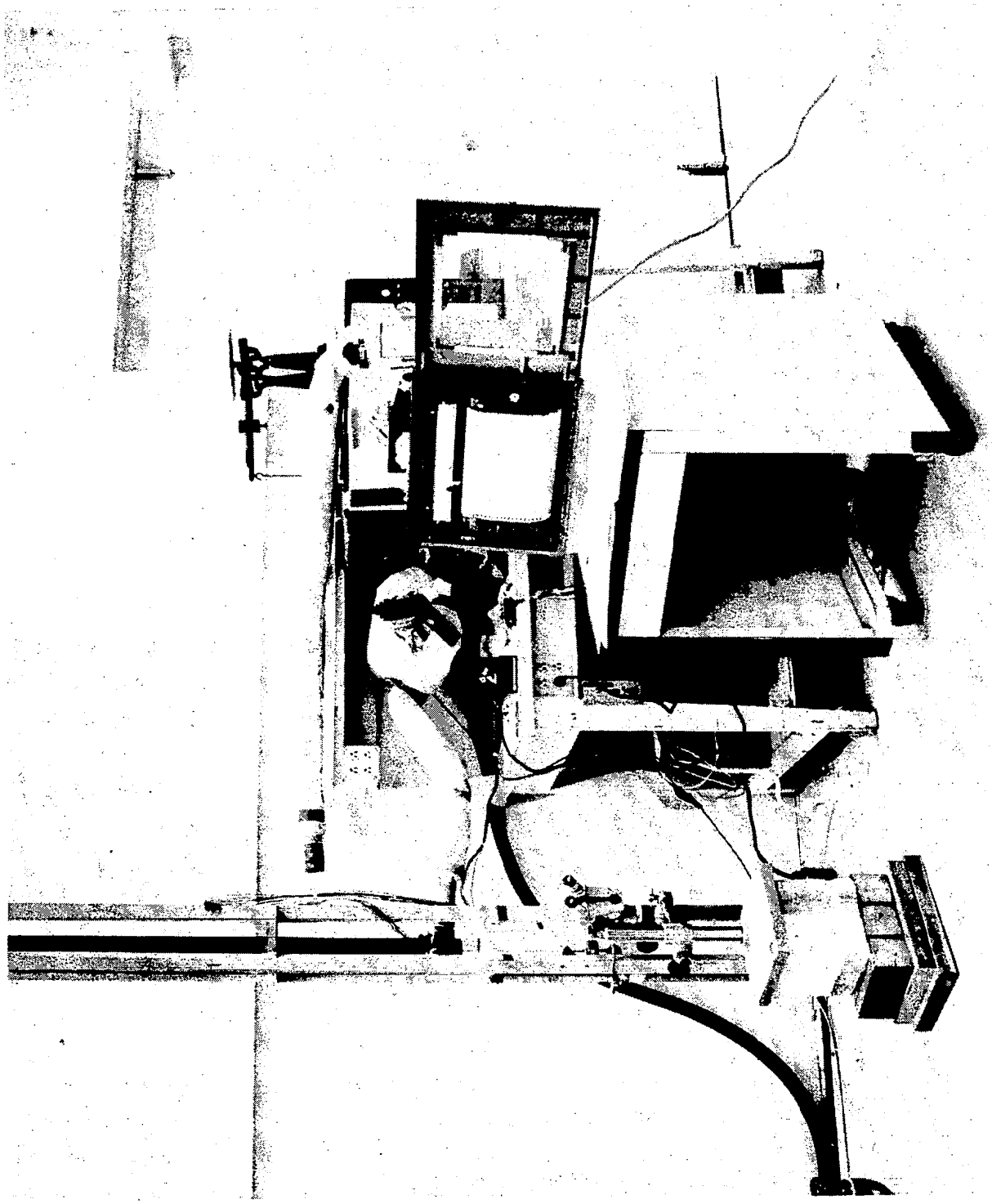

CTE/RESIDUAL STRAIN TEST FIXTURE

FIGURE 6.3-1

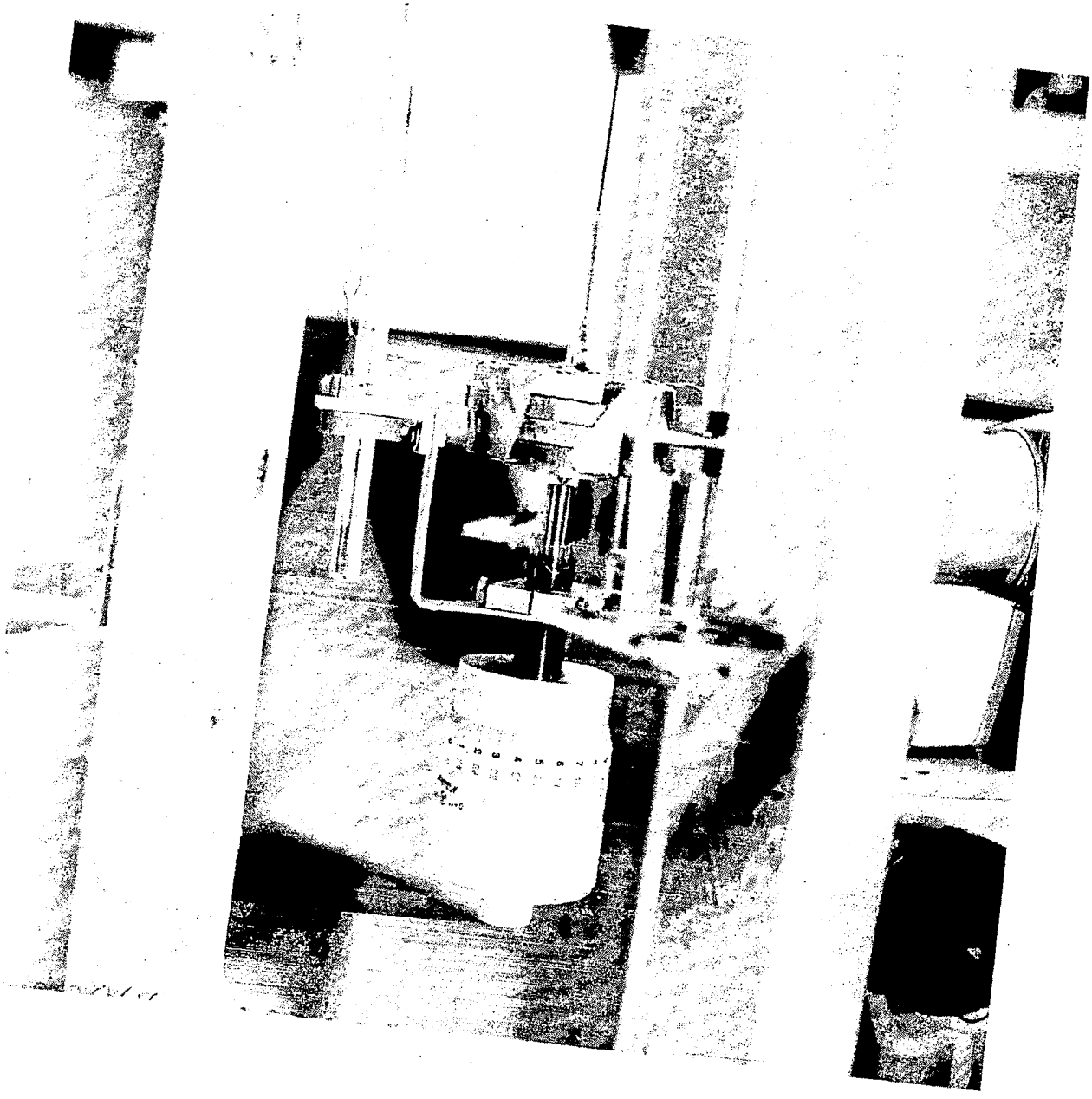

MICROMETER LENGTH MEASUREMENT

FIGURE 6.3-2

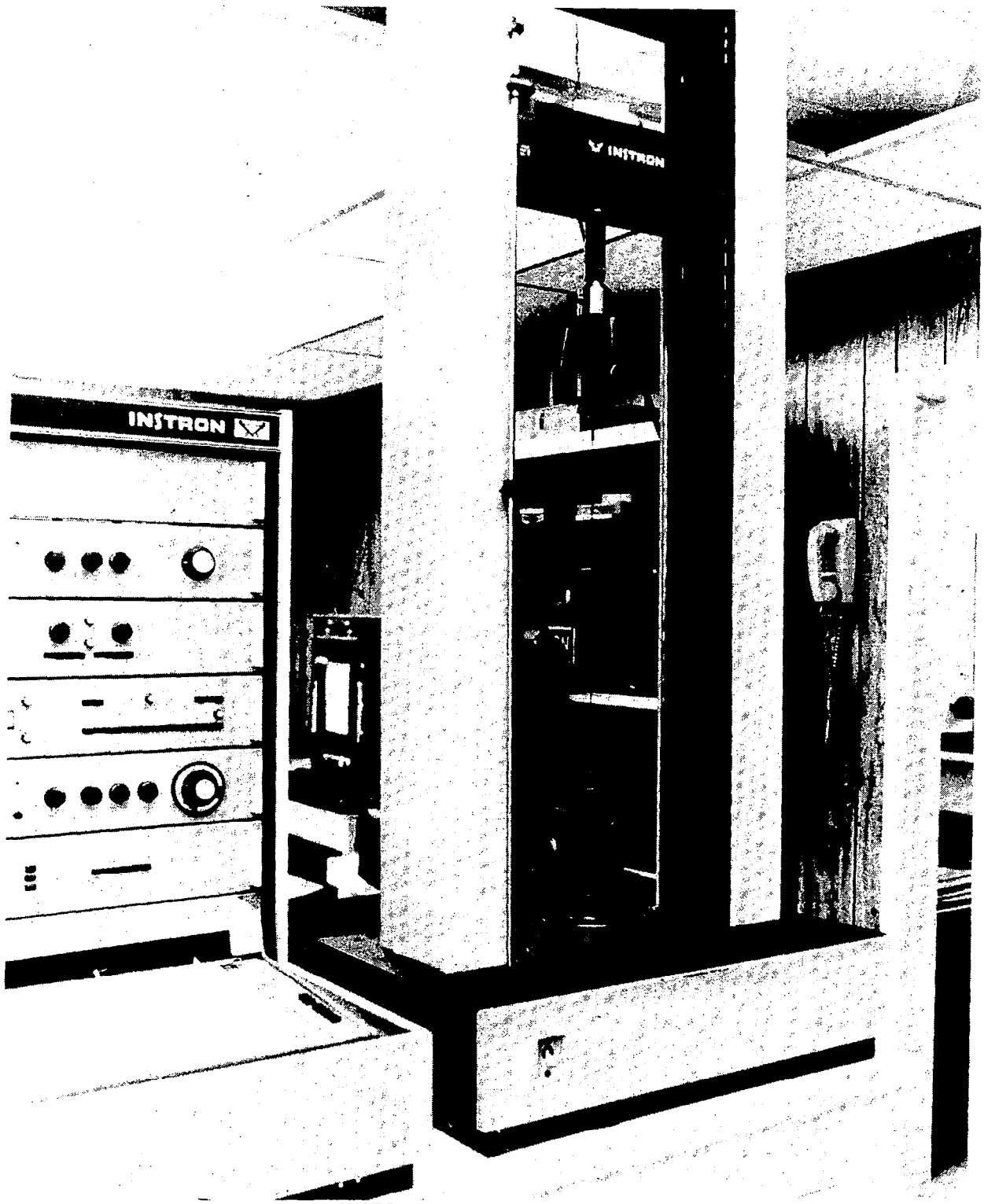


INSTRON TENSION TESTER

FIGURE 6.3-3

A third test apparatus was fabricated to evaluate the spooling and handling endurance of the cables. This equipment is shown in Figures 6.3-4 and 6.3-5. The fixture provides a method of oscillating cable specimens back and forth over pulleys. Pulleys of different diameters may be used and the tension in the specimen may be varied by interchanging weights attached to the fixture. The specimen are flexed thousands of times over the pulleys to obtain relative endurance data. Another test which may be performed on the fixture is illustrated in Figure 6.3-6. This test configuration provides stow and deploy endurance data for mesh and cord assemblies. A mesh and cord assembly in a cylindrical shape is attached to a top and bottom plate which can be extended in a taut condition, simulating deployed position, or collapsed to simulate a stowed condition. It is almost impossible to simulate the actual cable flex history which occurs in an antenna assembly, but the fixture does provide a relative rating of the candidates for both spool flexing and mesh/cord deploy and stow cycling. The assumed pass/fail criteria of the test is that the sample degradation is equal to or better than the cables presently used in existing Harris deployable antenna designs. These existing cables consist of continuous quartz filament yarn cross-wrapped with Teflon.

## 6.4 Results

### 6.4.1 Cable Candidates

Two areas of cable development are materials and construction techniques. The candidates evaluated in these two areas are discussed in the following paragraphs.

#### 6.4.1.1 Materials

There are many different types of fiberous materials which may be used to manufacture cables. However, viable material candidates were narrowed down to just a few when considering the combined requirements of thermal stability, mechanical stability (no creep), and space survivability. Some potential material candidates are shown in Figure 6.4.1.1-1. The figure shows the relative position of the materials when plotted on a graph depicting the

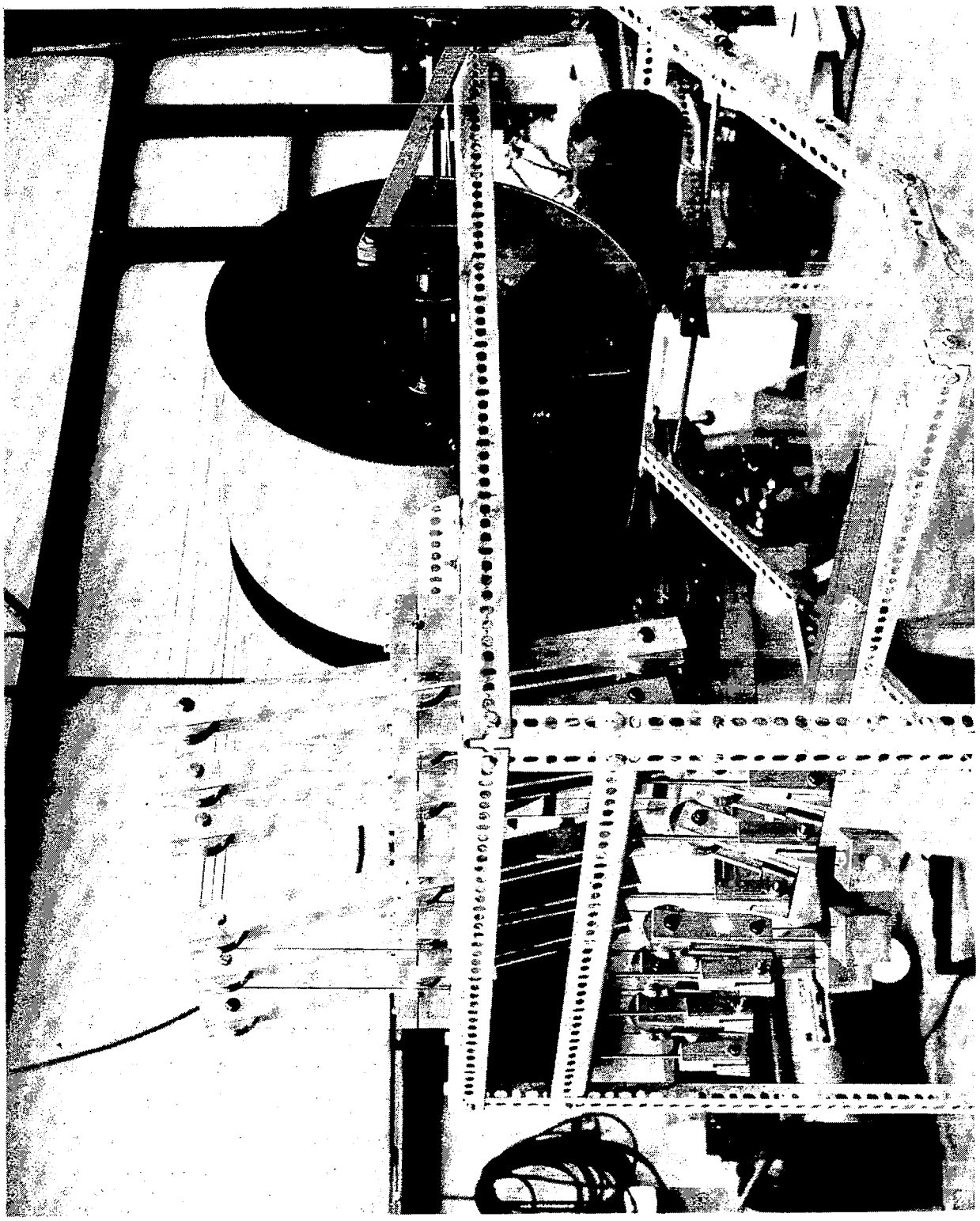

CYCLIC ENDURANCE TEST FIXTURE

FIGURE 6.3-4

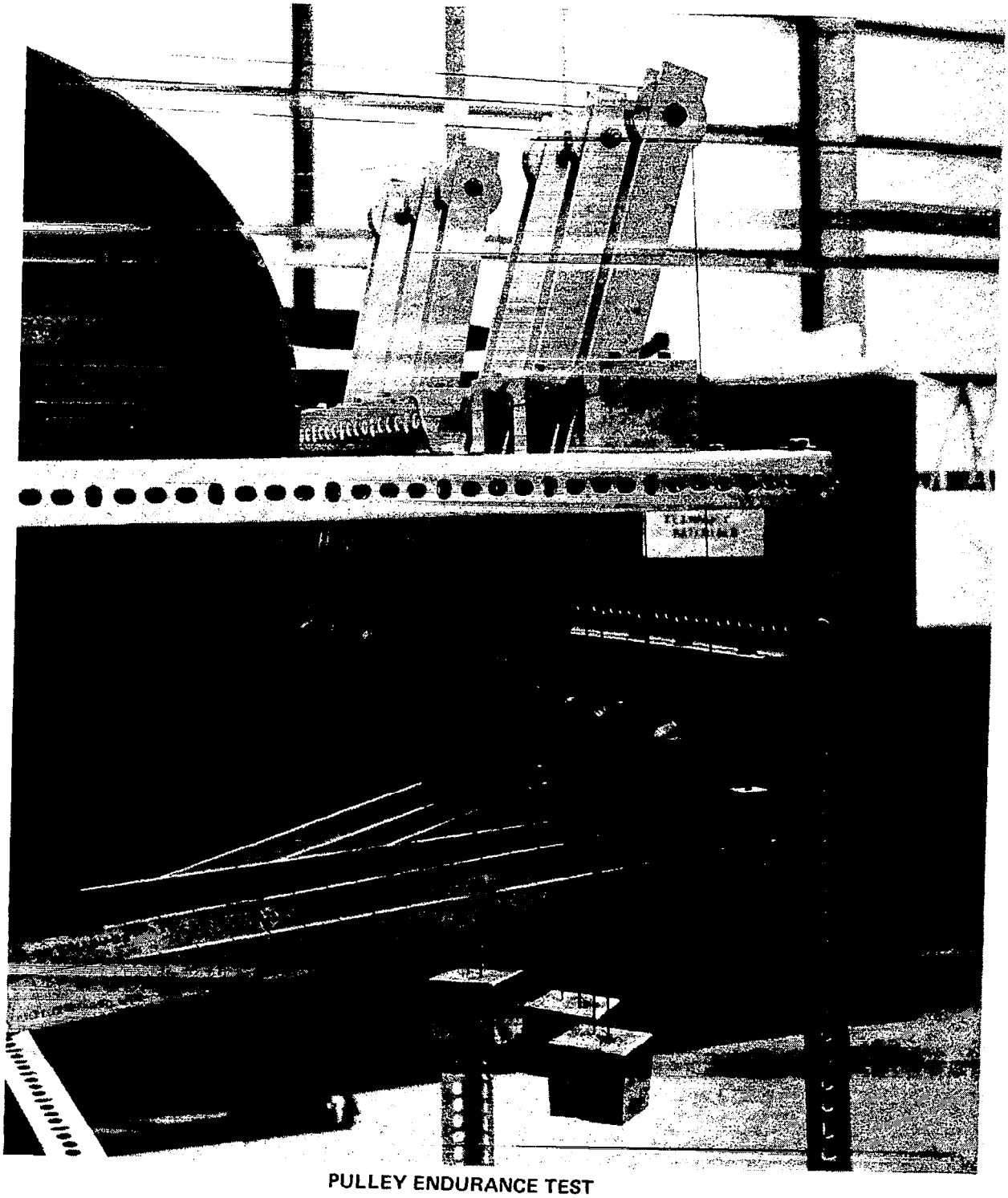

PULLEY ENDURANCE TEST

FIGURE 6.3-5

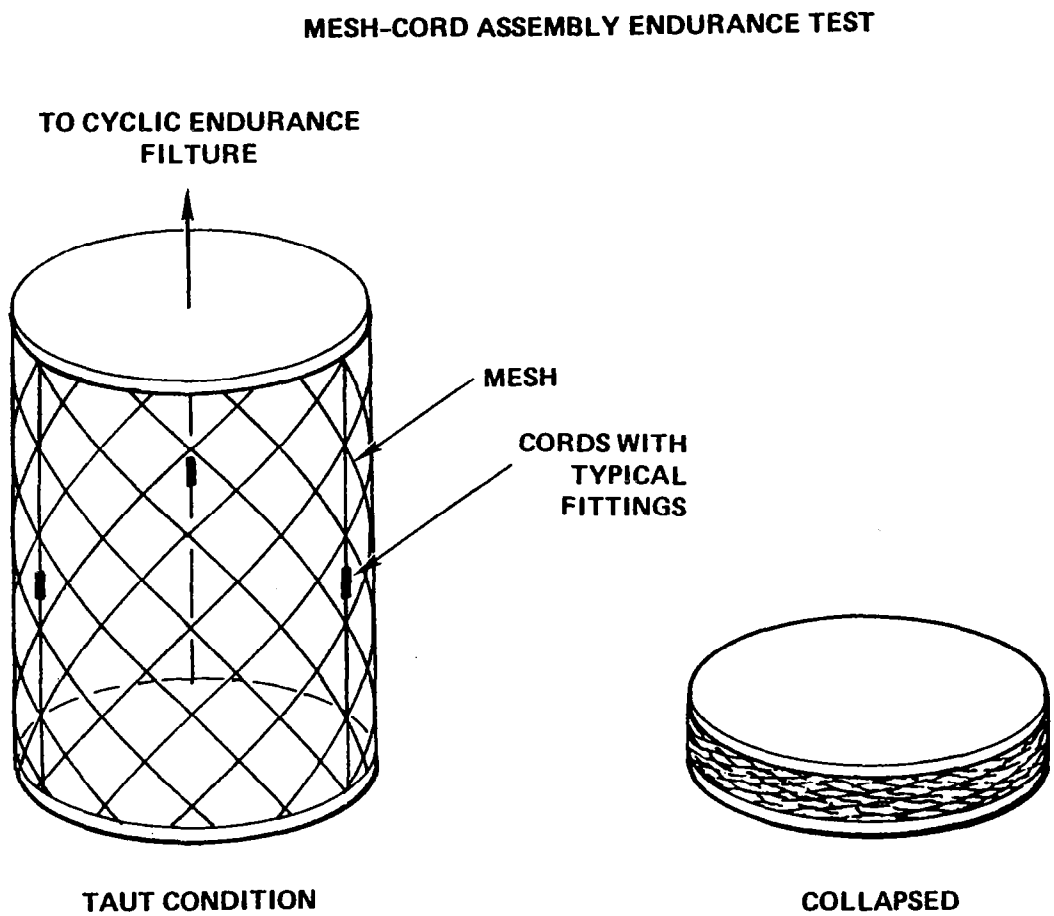


Figure 6.3-6. Mesh-Cord Assembly Endurance Test

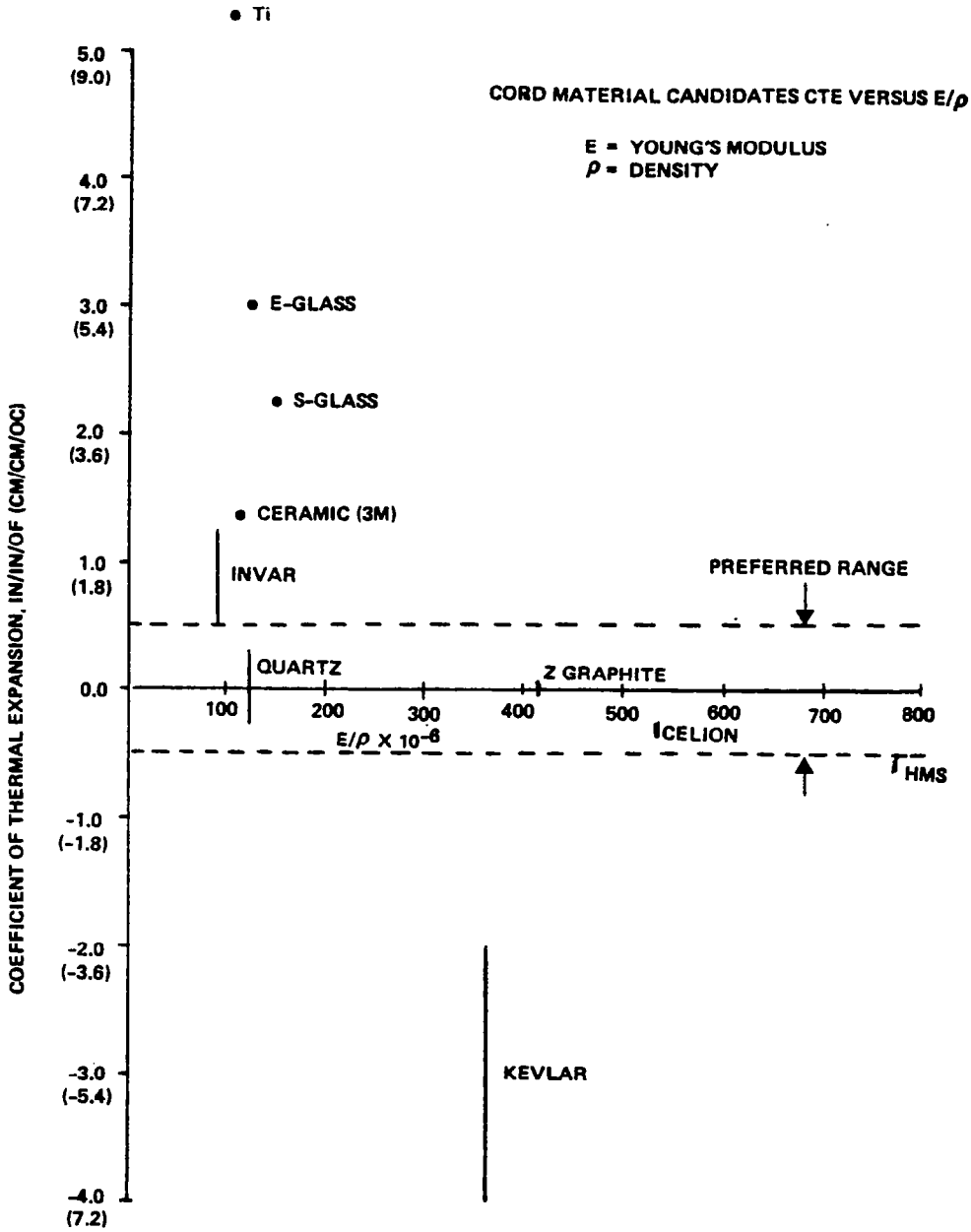


Figure 6.4.1.1-1. Cord Material Candidates CTE Versus E/ρ

specific modulus and the coefficient of thermal expansion (CTE). Quartz and graphite are the only materials in the preferred CTE range of plus and minus $0.9 \times 10^{-6}$ cm/cm/$^{o}$C ($0.5 \times 10^{-6}$ in/in/$^{o}$F). Graphite is available with a number of different E (modulus of elasticity) values. In general, the higher the E value the more negative the CTE. Graphite fibers with an E equal to $25 \times 10^{6}$ psi has a CTE of approximately zero. Whereas, graphite fibers with an E equal to $50 \times 10^{6}$ psi and above, have CTE's of $0.5 \times 10^{-6}$ cm/cm/$^{o}$C ($-0.3 \times 10^{-6}$ in/in/$^{o}$F) or less. Graphite is the highest performance material for this application, and quartz is a very close alternate with an E of approximately 1/3 of graphite. Kevlar may be considered a low performance alternate, with a much larger negative CTE and instability problems due to moisture absorption.

Quartz and graphite are selected for use as the principle load carrying materials in the cables developed in this task. As previously stated, quartz has been used for a number of years as a cable material in antennas built by Harris. They have performed very well in the systems they have been used in; however, they are not of sufficient size to meet the load requirements of the Hoop/Column antenna design. The existing quartz cable materials will be used as a standard in which to compare the cables developed in this task.

### 6.4.1.2 Construction Techniques

Cord construction methods, which were discovered through literature and vendor surveys and evaluated in this task, are shown in Figure 6.4.1.2-1. Each of the construction methods listed in the figure will be briefly described and their relative merits discussed. The construction technique successfully used in existing Harris deployable antenna designs consist of wrapping a tow of longitudinal fibers with a fine yarn in double cross wrap. The wrapping is done in a rather loose configuration so that it does not influence the thermal and mechanical stability of the cable material. Typical wrap materials include polyester, Teflon, and glass. Teflon had been favored for most of the existing cable designs because of its low abrasion and excellent UV radiation resistance. Wrapping is an acceptable cable construction method for the

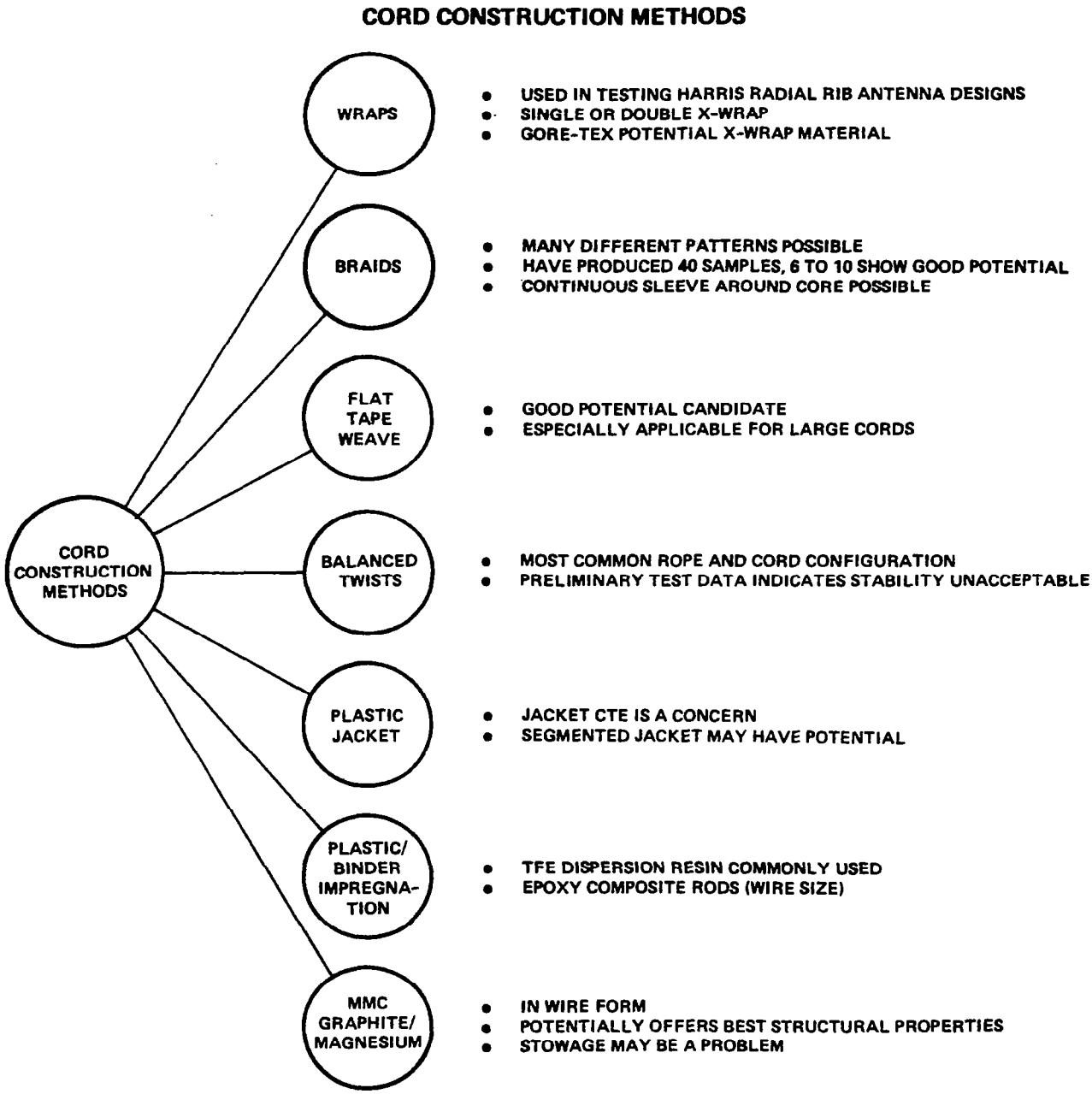


Figure 6.4.1.2-1. Cord Construction Methods

smaller cable sizes. One of the disadvantages of wrapping is that the wrap material is easily slid down the length of the cable, causing bunching of the wrapping to occur. This is not a significant problem for cable sizes in the 0.025 to 0.05 inches in diameter, but for larger cables a more stable construction method is desireable. An excellent alternate construction method is braiding. There are many different types of braid patterns that can be used. Many of these appear very similar to wrapping with exception that the braiding yarns are interlaced so that sliding and bunching does not occur as it does in wrapped cords.

The geometry of a typical braiding machine is depicted in Figure 6.4.1.2-2 and a photograph of a braiding machine is shown in Figure 6.4.1.2-3. There are three different parts to a braided cables as shown in the figure; namely, warps, core and carrier yarns. The warps and core contain the unidirectional load carrying fiber materials and the carrier wraps around these bundles in circular patterns. There are many possible pattern combinations from this basic geometry. A few are shown in Figure 6.4.1.2-4. Photographs of a couple of typical braided cord samples are shown in Figures 6.4.1.2-5 and 6.4.1.2-6. Also shown in the photographs are samples of some woven flat tapes. Weaving is an excellent construction method for large cables as it produces a flat configuration which accommodates spooling of large cords much easier than round configurations. The challenge of producing tapes with high mechanical stability (low-stretch) is to weave in very fine and low- tensioned crossed weaving yarns (or picks) which do not deflect or crimp the unidirectional load carrying cord materials. This has been most successfully accomplished using very fine polyester cross weaved yard. Figure 6.4.1.2-7 is a photograph of woven graphite tape being produced on a loom.

A fourth and most common method of cable construction is balanced twist. It is an effective and simple method of binding cable fibers together. However, twisting introduces additional mechanical instability (residual strain) into the cord and is, therefore, not considered a promising candidate for this task.

# BRAIDER GEOMETRY

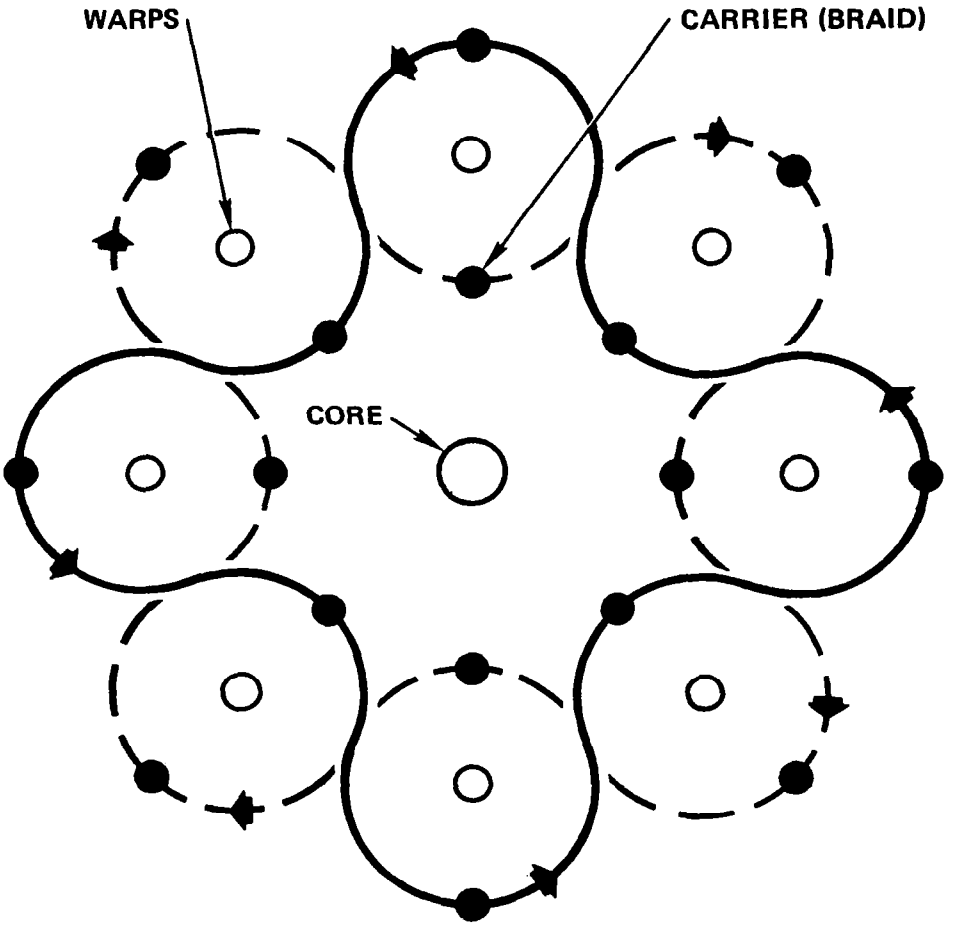


**WORKED WITH TWO DIFFERENT BRAIDERS:**

A. **8 WARP (SHOWN ABOVE)**
B. **16 WARP**

Figure 6.4.1.2-2. Braider Geometry

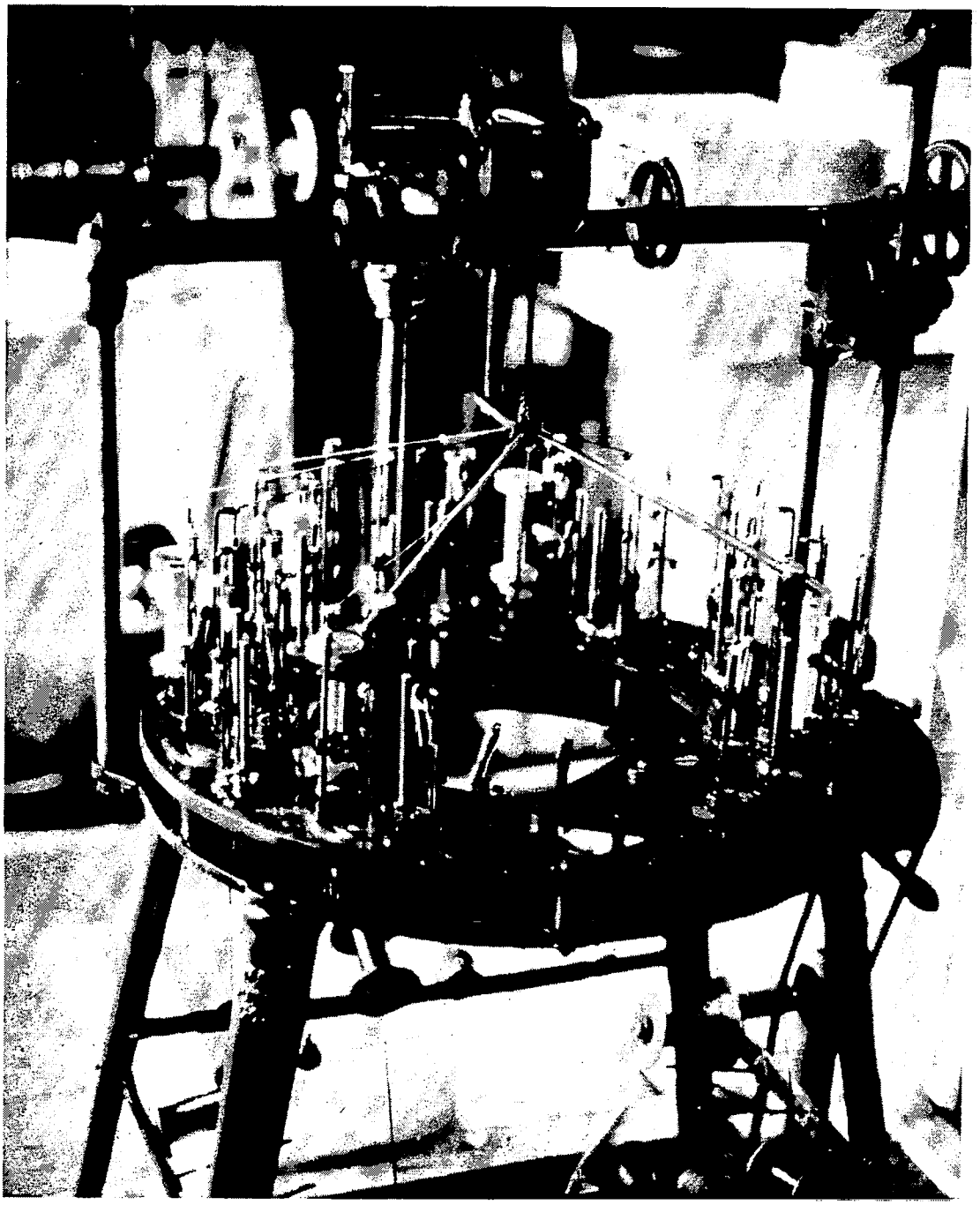

CABLE BRAIDING MACHINE

FIGURE 6.4.1.2-3

# BRAID PATTERNS

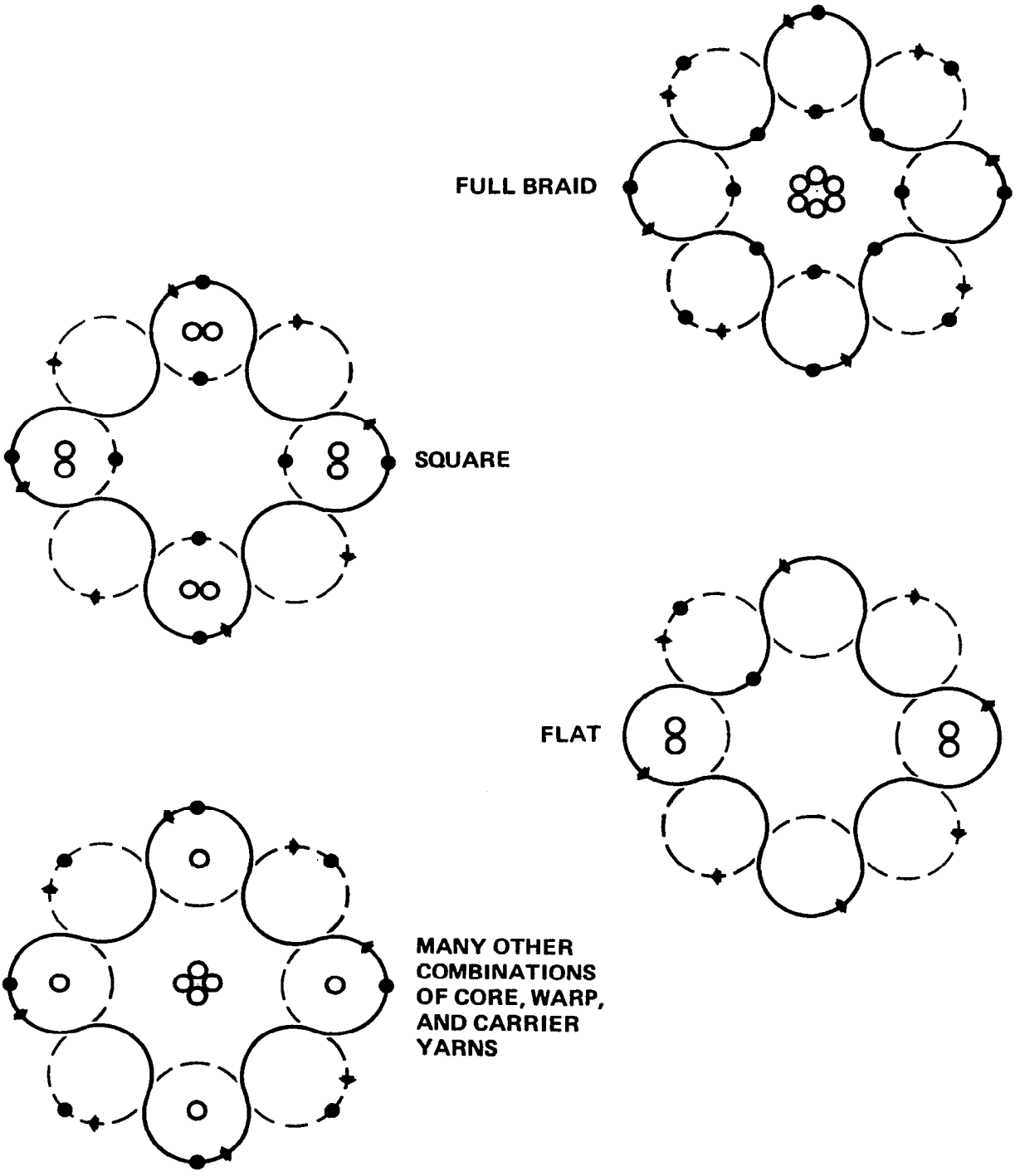


Figure 6.4.1.2-4. Braid Patterns

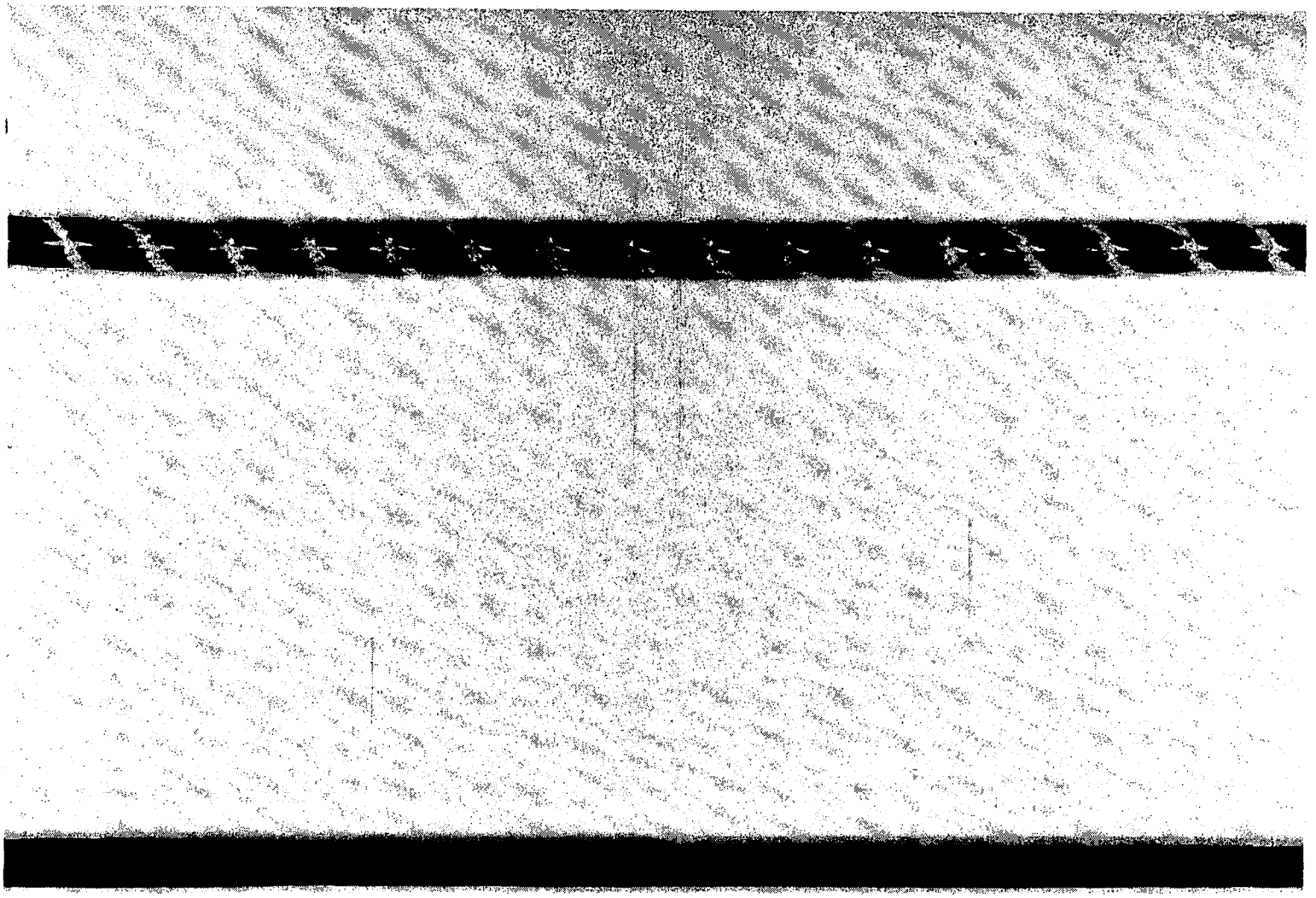

Figure 6.4.1.2-5. Typical Cord Samples

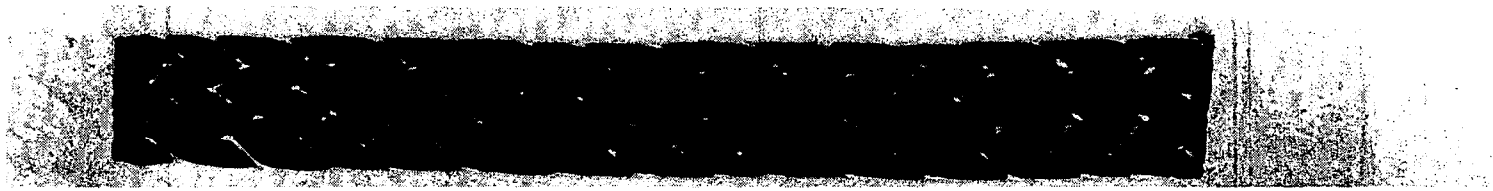

BRAIDED NO. 20 CORD
5 CELION 12000
200 DENIER KEVLAR

WOVEN NO. 20 CORD
5 CELION 12000
70 DENIER POLYESTER PICKS

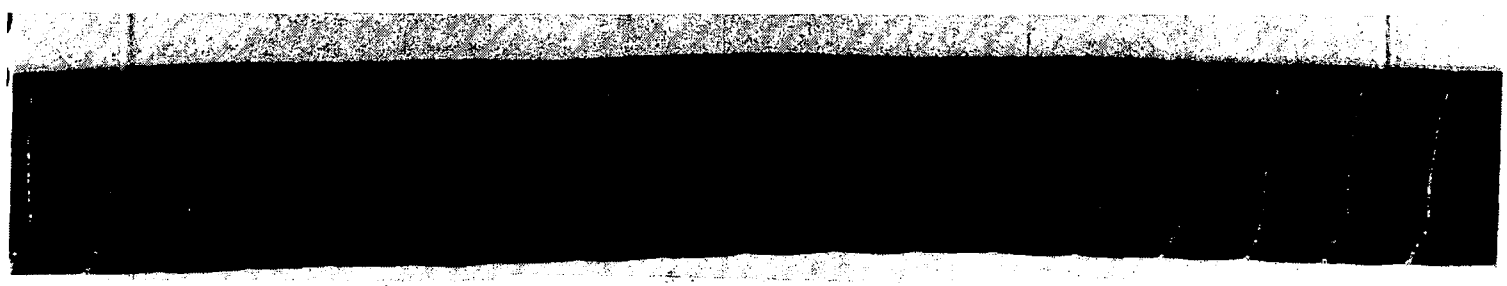

WOVEN NO. 40 CORD
10 CELION 12000
70 DENIER POLYESTER PICKS

Figure 6.4.1.2-6. Typical Cord Samples

GRAPHITE TAPE BEING PRODUCED ON A WEAVING LOOM

FIGURE 6.4.1.2-7

There are many different types of plastic jacketing materials used in the electrical cabling industry that could be considered for this application. Many of the jacketing materials have poor space survivability characteristics. Teflon is a viable plastic jacket material that has good space survivability and was investigated in this study. Compared to other cord construction methods, Teflon jacketing results in high weight and problems with the high CTE of the jacket influencing the cable thermal expansion characteristics.

A more favorable plastic covering method is impregnation of a cord with appropriate plastic. Most plastic polymers when combined with graphite or quartz fibers produce a very stiff composite material, and are not appropriate for the flexible cable materials being developed in this task. Examples of these are epoxy, polyester, phenolic, and nylon. Weight is another important consideration when choosing a plastic impregnation material. Most of the available materials increase weight by 40 to 60 percent.

The polymer which has been found to be most satisfactory for cable impregnation is Teflon dispersion resin (TFE). It has been used for years to impregnate glass yarns used in the construction of astronauts suits, thermal control coatings, and other space applications. In these applications Teflon is added to the yarn to provide toughness and flexibility, and allows the glass yarns to be handled through commercial sewing machines. For the Hoop/Column antenna design, toughness is a very desirable characteristic. But in addition to providing toughness, Teflon also provides a construction technique which binds the load carrying fibers together in a consolidated bundle and yet maintains flexibility. The TFE resin is an aqueous solution which may be deluted to any concentration to provide the desired amount by weight of dried and sintered Teflon added to the cable. Experience has shown that for graphite and quartz cables, Teflon amounts of 7 to 10 percent by weight are adequate to provide a good flexible cable bundle. The manufacturing process for Teflon coated graphite cables is shown in Figure 6.4.1.2-8.

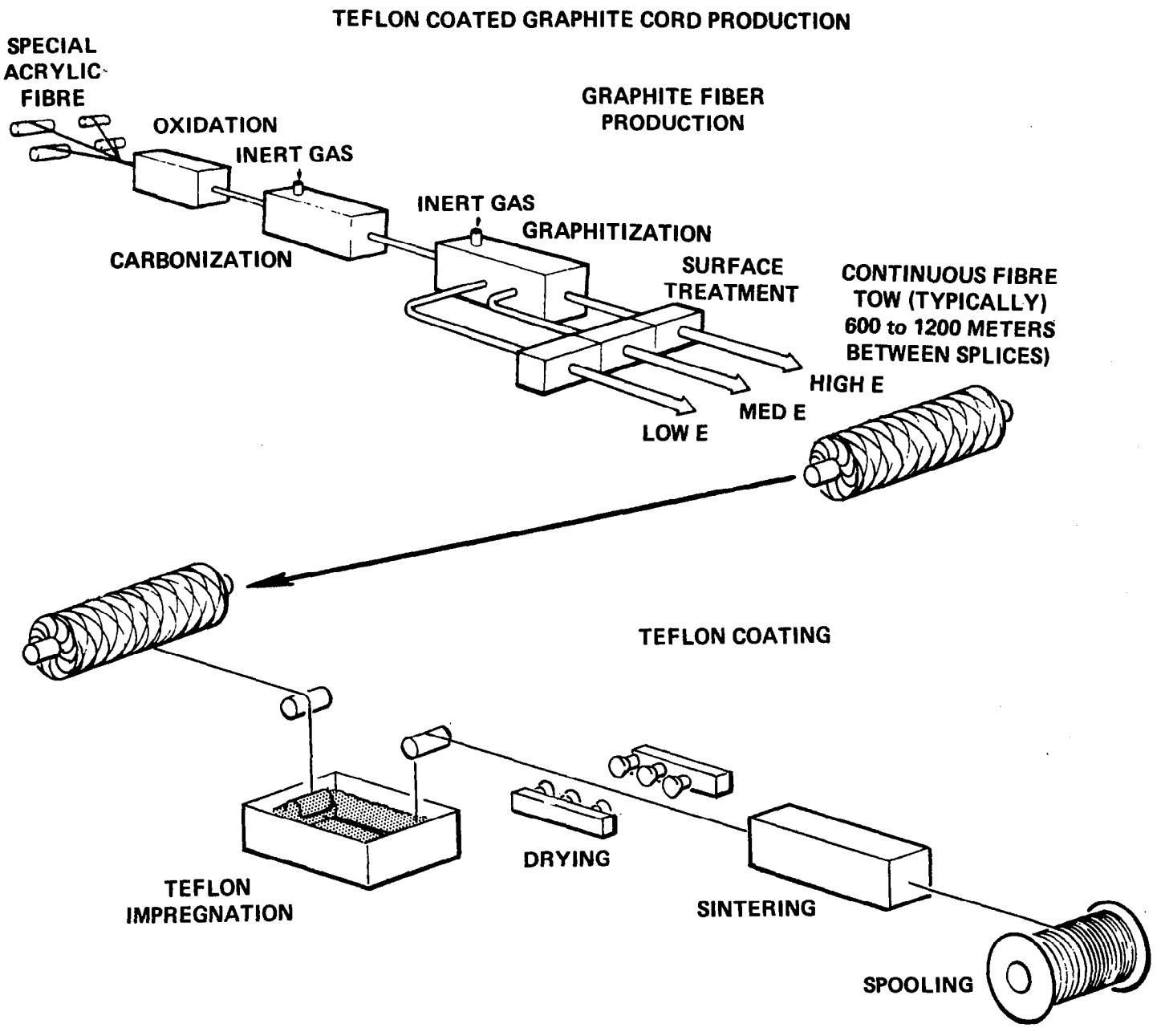


Figure 6.4.1.2-8. Teflon Coated Graphite Cord Production

Graphite is made from an acrylic fiber which is oxidized, carbonized and graphitized in an inert atmosphere at high temperature. The fibers are stretched during graphitization to produce the high strength and modulus crystalline structure. Different values of modulus of elasticity (E) of graphite can be produced by increasing or decreasing the temperature and elongation during graphitization. The finished graphite yarn is spooled and sent to the Teflon coating vendor where it is run through an aqueous Teflon resin solution, dried, and sintered at approximately 800$^{o}$F. The entire process is done with the graphite yarn under tension. The resulting product is a uniformly coated yarn with fibers lightly bonded together in a straight compact configuration.

A final material and construction method which was investigated for applicability was Metal Metric Composites (MMC). Samples of graphite/aluminum wire were obtained from Material Concepts, Inc. in Cleveland, Ohio, and tests were conducted to determine their flexibility. It was determined that a 10-inch diameter pulley was the minimum size that the wire could be wrapped around without breakage. MMC is a very strong, stiff and brittle material and perhaps could be used for special applications as tension members; however, for the application it would place undue restraint on the stowed antenna design.

In summary, all the construction methods discussed above were investigated by acquiring samples and performing preliminary tests. The winning candidates from these preliminary tests were: wraps, braids, flat-tape weaves and Teflon impregnation. These four construction methods were carried forward for additional testing and the results are discussed in Paragraph 6.4.2.

### 6.4.1.3 Vendors

There were a number of material suppliers and cable manufacturing companies which participated in preparation of samples for this task. These vendors are depicted in Figure 6.4.1.3-1. Initially, the staple yarns are procured from the appropriate suppliers and sent to cable manufacturing companies for construction of samples. Graphite yarns are available from many

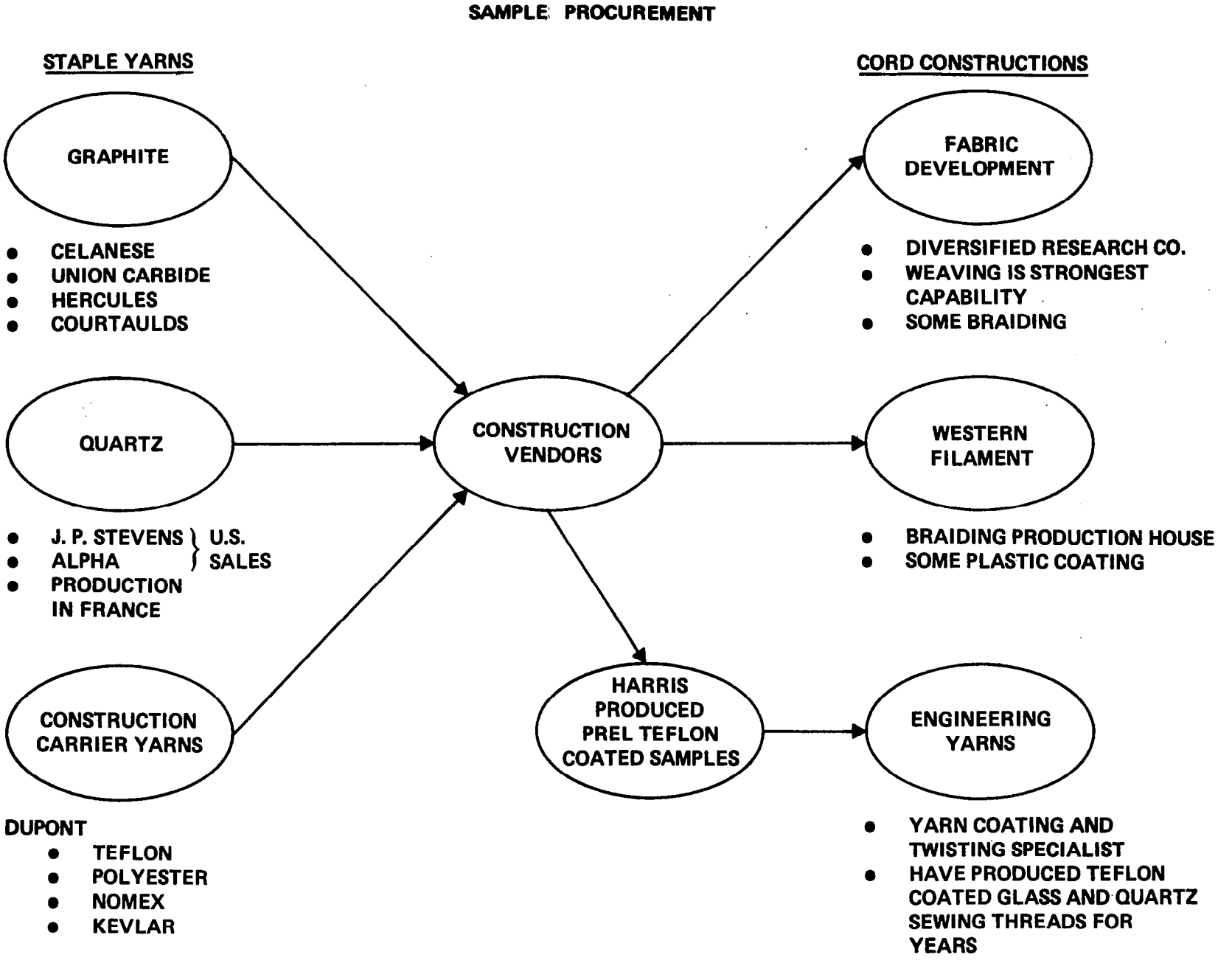


Figure 6.4.1.3-1. Sample Procurement

different suppliers, with a wide selection of fiber properties. In this task, graphite materials were purchased from Celanese Corporation, Union Carbide, Hercules, and Courtaulds. They all supply essentially equivalent graphite fiber materials. To select a graphite vendor is somewhat arbitrary; however, it was found that the CELION fiber from Celanese Corporation produced the minimum amount of fuzzing in braiding and weaving operations and for this reason it was the most used material in this task. Hercules Corporation supplied a fiber material which exhibited zero CTE which shows good promise.

All of the industrial quartz cord materials available today are produced in France. The U.S. distributors for these materials are J. P. Stevens, and Alpha Associates. There were other yarn materials purchased from Du Pont which were used for cross wrapping, weaving and braiding operations. These materials include Teflon, polyester, Nomex[6], and Kevlar.

There are many companies in the textile industry which have braiding and weaving equipment to produce cables. The two selected to make samples in this task are Fabric Development, and Western Filament. Fabric Development is a diversified textile research company. They have good weaving capability and can do some braiding. Western Filament specialized in braiding. They are primarily a braiding production house; however, they were willing to participate in the research and development work needed in this task. A third company which participated in the manufacturing of cable samples for this task was Engineering Yarns. Their speciality is twisting and coating of yarns for use in commercial applications like vinyl coated awnings. They have also produced beta glass yarns coated with Teflon for use in the aerospace industry. Their Teflon coating experience is valuable for this task.

[6] Nomex: Trademark of E.I. DuPont de Nemour & Company, Inc.

### 6.4.2 Screening Test Results

There were many screening tests performed early in the task which will not be described in detail in this report. Included in these early tests were approximately 40 different types of braid, 10 different weaving constructions and preliminary Teflon coated samples that were coated at Harris. Both graphite and quartz were used in these early cable samples. The results from some of these preliminary screening tests are shown in Figure 6.4.2-1. Significant conclusions made from these preliminary tests results are:

- The Teflon wrapped quartz cord material, used as a standard in the test, yielded the expected results in terms of EA and CTE. This validated the test setup.
- Cross wrapped graphite is a good candidate for small cables.
- The test results from most of the remaining braided samples indicated efficiencies in the constructions. The fine strands of Dacron or Kevlar used in the braided constructions influenced both EA and coefficient of thermal expansion of the cable.

The EA's and tensile strengths (not shown in Figure 6.4.2-1) of the braided samples are not consistent with expected values, indicating that there is poor fiber load sharing in the samples. The assumed mechanism which causes this poor load sharing is unequal fiber lengths caused by crimping and twisting of the graphite or quartz fibers. Teflon coating has also been found to enhance the tensile properties of quartz and graphite yarns. This is depicted in Figure 6.4.2-2 where two different sizes of graphite cables are compared. The number 2* size Teflon coated cables produced high and consistent tensile strengths. The number 20 graphite cords which are ten times larger than the number 2 cords and had no Teflon coating, produced tensile strenths of about half the expected value. The poor performance

*A number 2 graphite cable is defined as having 6000 fibers; see Figure 6.4.4-1.

PRELIMINARY TEST RESULTS

| SAMPLE | EA (LB)* | EA SIZE CORRECTED FOR COMPARISON WITH STANDARD | CTE ($10^{-6}/^{o}F$) | COMMENTS |
|---|---|---|---|---|
| QUARTZ (Q) STANDARD (X-WRAPPED) | 1500 | 1500 | -0.3 TO +0.3 | ——— |
| GRAPHITE (G) STANDARD (X-WRAPPED) | 4500 | 4500 | -0.35 | ——— |
| *Q5 (BRAID) | 1850 (HIGH) | 1500 | -1.0 | HIGH WRAP INTERACTION, TIGHT 8 STRAND DACRON |
| Q11 (BRAID) | 1850 (HIGH) | 1500 | -0.4 TO +0.3 | TWO STRANDS OF KEVLAR WRAP HAS NEGLIGIBLE EFFECT |
| *G15 (BRAID) | 5630 | 6000 | -2.7 | HIGH WRAP INTERACTION, FULL BRAID |
| G17 (BRAID) | 7150 (LOW) | 9000 | -1.4 | HIGH WRAP INTERACTION, FULL BRAID |
| G22 (BRAID) | 3350 (LOW) | 4500 | 0.44 | ONE LONGITUDINAL KEVLAR STRAND |
| G23 (BRAID) | 7925 | 9000 | 0.42 | |
| G24 (BRAID) | 2775 | 3000 | 0.44 | FLAT CONSTRUCTION WITH MANDRELS |
| G25 (BRAID) | 4600 (LOW) | 6000 | 0.39 | |
| G30 (BRAID) | 4900 | 4500 | 0.35 | IDENTICAL TO STANDARD |
| G81A (BRAID) | 3900 | 4500 | 3.5 | HIGH WRAP INTERACTION, FULL BRAID |
| *K1 | 6100 | - | -5.5 | CTE AGREES WITH LITERATURE |
| E GLASS/ TEFLON COATING | 3355 | - | 3.0 | PURE E-GLASS HAS A CTE OF 3.0 |
| QUARTZ/ TEFLON COATING | - | - | -0.3 TO +0.3 | TEFLON CAUSED NO CTE EFFECT |

*ACCURACY ±15% DUE TO POOR CHOICE OF INSTRON CHART SPEED

*Q - QUARTZ
G - GRAPHITE
K - KEVLAR

Figure 6.4.2-1. Preliminary Test Results

**ULTIMATE STRENGTH**
**KG (LB)**

| SAMPLE | NO. 2 CORD (TEFLON COATED) | NO. 20 CORD (NO TEFLON) |
|---|---|---|
| 1 | 40 (88) | 184 (406) |
| 2 | 39 (85) | 174 (384) |
| 3 | 44 (96) | |
| 4 | 38 (83) | |
| 5 | 35 (77) | |
| AVERAGE | 39 (86) | 179 (395) |
| | | ↓ |
| | | WOULD EXPECT 390 (860) |

Figure 6.4.2-2. Ultimate Strength
KG (Lb)

of the number 20 cord is attributed to poor fiber load sharing caused by the larger size and no coating to hold the fibers in a linear configuration. Conversely, the Teflon coated cords have fibers which are very compactly consolidated without any crimping or twisting of the fibers, thus fiber load sharing is more readily achieved. Following the favorable tensile tests results of the Teflon coated yarns, preliminary tests were performed to determine residual strain and CTE of Teflon coated quartz and graphite yarn samples. Before these results are presented, background residual strain data is discussed in the following paragraph.

The residual strain characteristics of Teflon cross wrapped quartz cords was established by Harris on the Tracking and Data Relay Satellite System (TDRSS) Program previous to this task. This data, shown in Figure 6.4.2-3, is used as a baseline for comparison of results obtained in this task. The figure shows the strain of ten samples which were subjected to a combination of thermal and mechanical cycles. Strain in the cords occurred during the first 30 or 40 cycles, after which they stabilized to a constant length. The average total strain of the ten samples is approximately 60 micro-strains. This phenomena of cord elongation due to mechanical and thermal cycling has been repeated many times with similar results. A detailed evaluation of residual strain was performed and recorded in a Master degree thesis by F. C. Koblank, Harris Corporation. In his thesis, Koblank attributes residual strain to the nonlinearity of the fibers caused by twisting. A typical quartz cord section is illustrated in Figure 6.4.2-4. The quartz cables consists of five individual strands which are held together with Teflon cross wrap. The individual quartz strands are supplied from the vendor with 0.2 to 0.5 twists per inch. Koblank derived a formula for calculating the amount of residual strain resulting from twist (see Figure 6.4.2-5). The calculated residual strain using this formula is compared to measured data in Figure 6.4.2-6, which indicates Koblank's hypothesis is a close approximation.

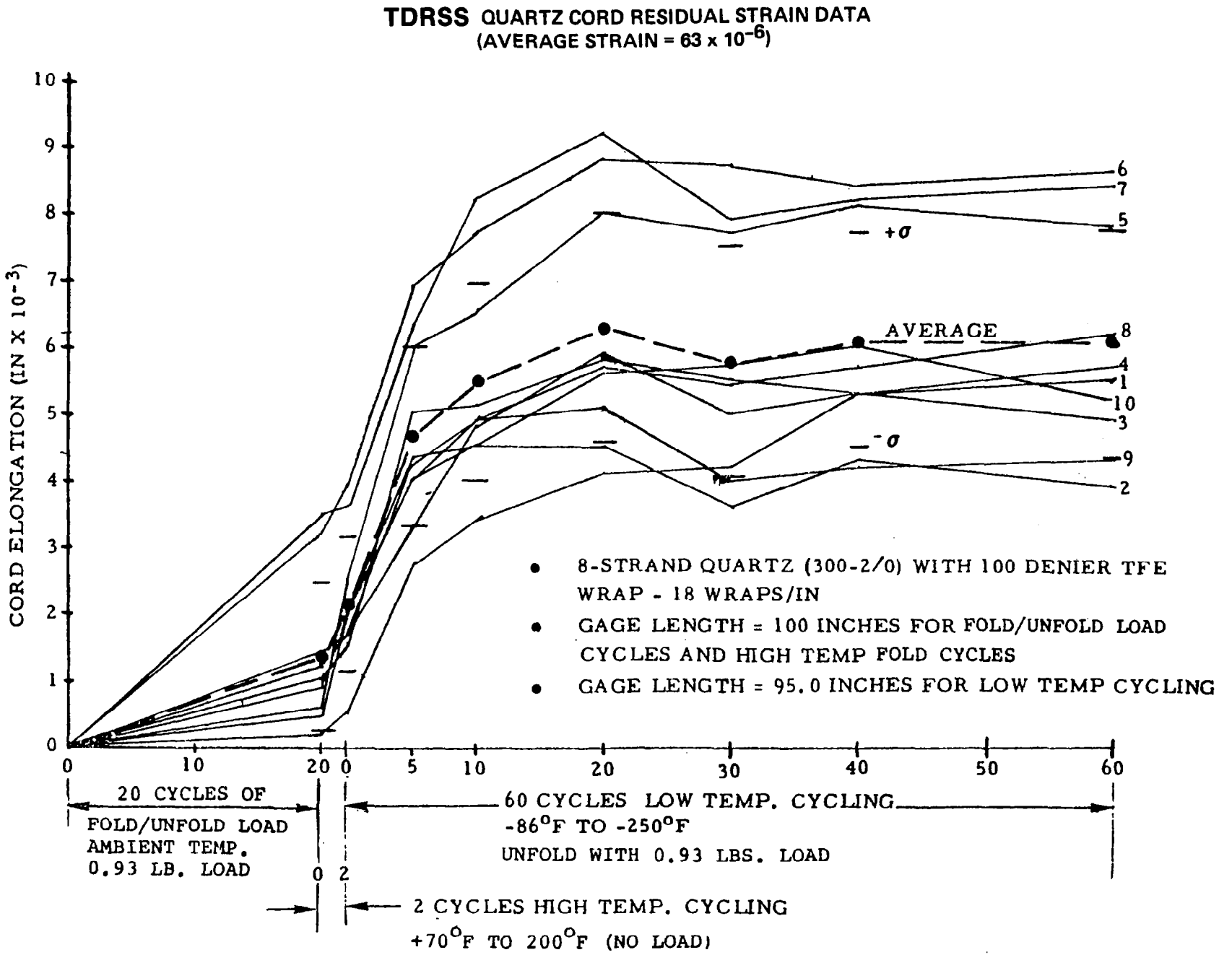


Figure 6.4.2-3. TDRSS Quartz Cord Residual Strain Data

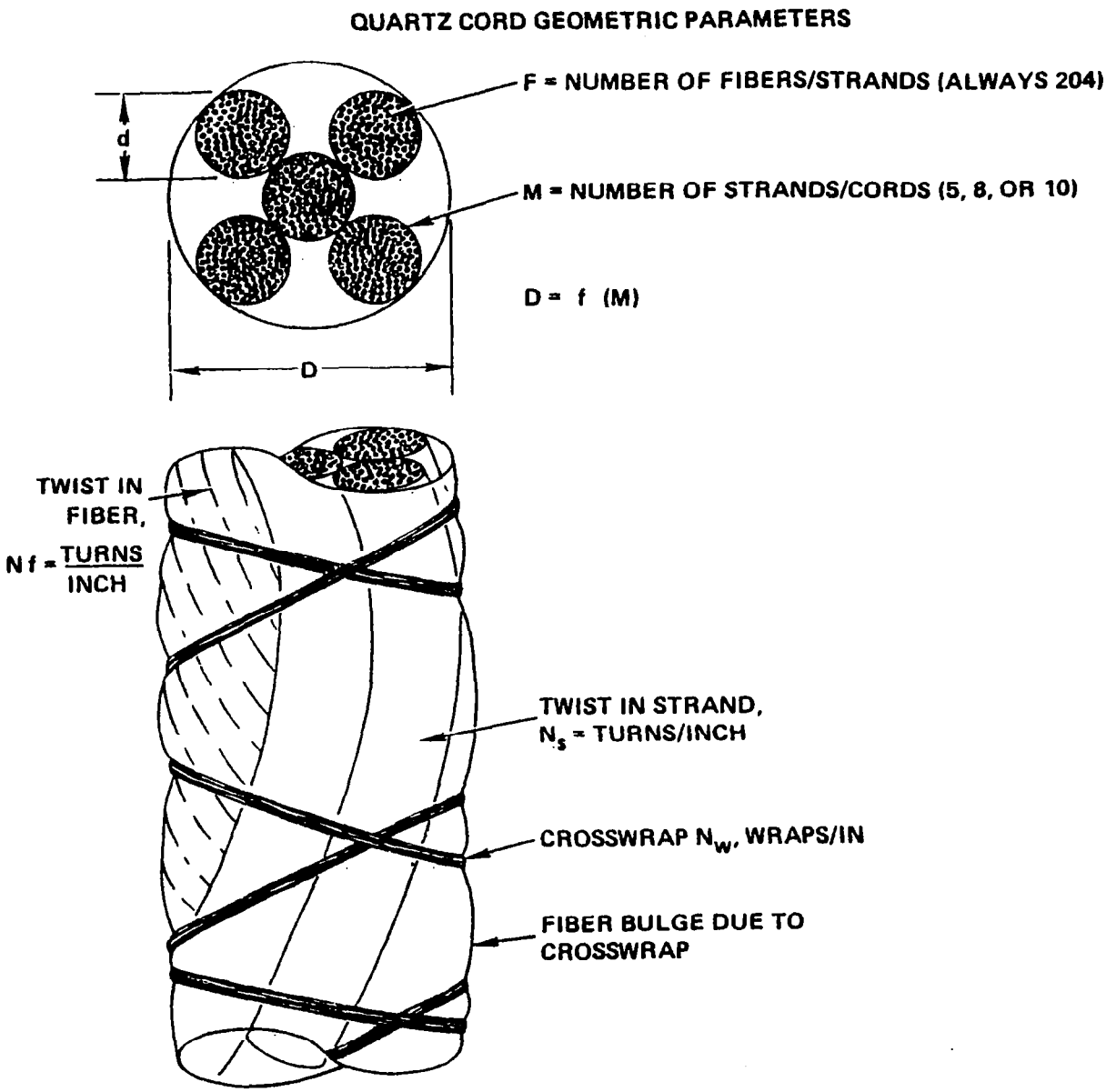


Figure 6.4.2-4. Quartz Cord Geometric Parameters

RESIDUAL STRAIN ANALYTICAL PREDICTIONS
(F. C. KOBLANK MASTERS DEGREE THESIS)

CORD RESIDUAL STRAIN

$$\frac{\Delta L}{L} = \frac{N_c \pi D}{\cos\left[\tan^{-1}\left(\frac{1}{\pi D N_c}\right)\right]} + \frac{N_s \pi d}{\cos\left[\tan^{-1}\left(\frac{1}{\pi d N_s}\right)\right]} - 2$$

WHERE:
- $\Delta L$ = CHANGE IN CORD LENGTH
- $L$ = CORD LENGTH
- $N_e$ = CORD TWIST PER UNIT LENGTH (MEASURED 0.2 FOR QUARTZ CORD)
- $N_s$ = STRAND TWIST PER UNIT LENGTH (ASSUMED 0.2 FOR BALANCED QUARTZ CORD)
- $D$ = CORD DIAMETER
- $d$ = STRAND DIAMETER (142 MICRONS FOR QUARTZ STRAND)

Figure 6.4.2-5. Residual Strain Analytical Predictions (F. C. Koblank Masters Degree Thesis)

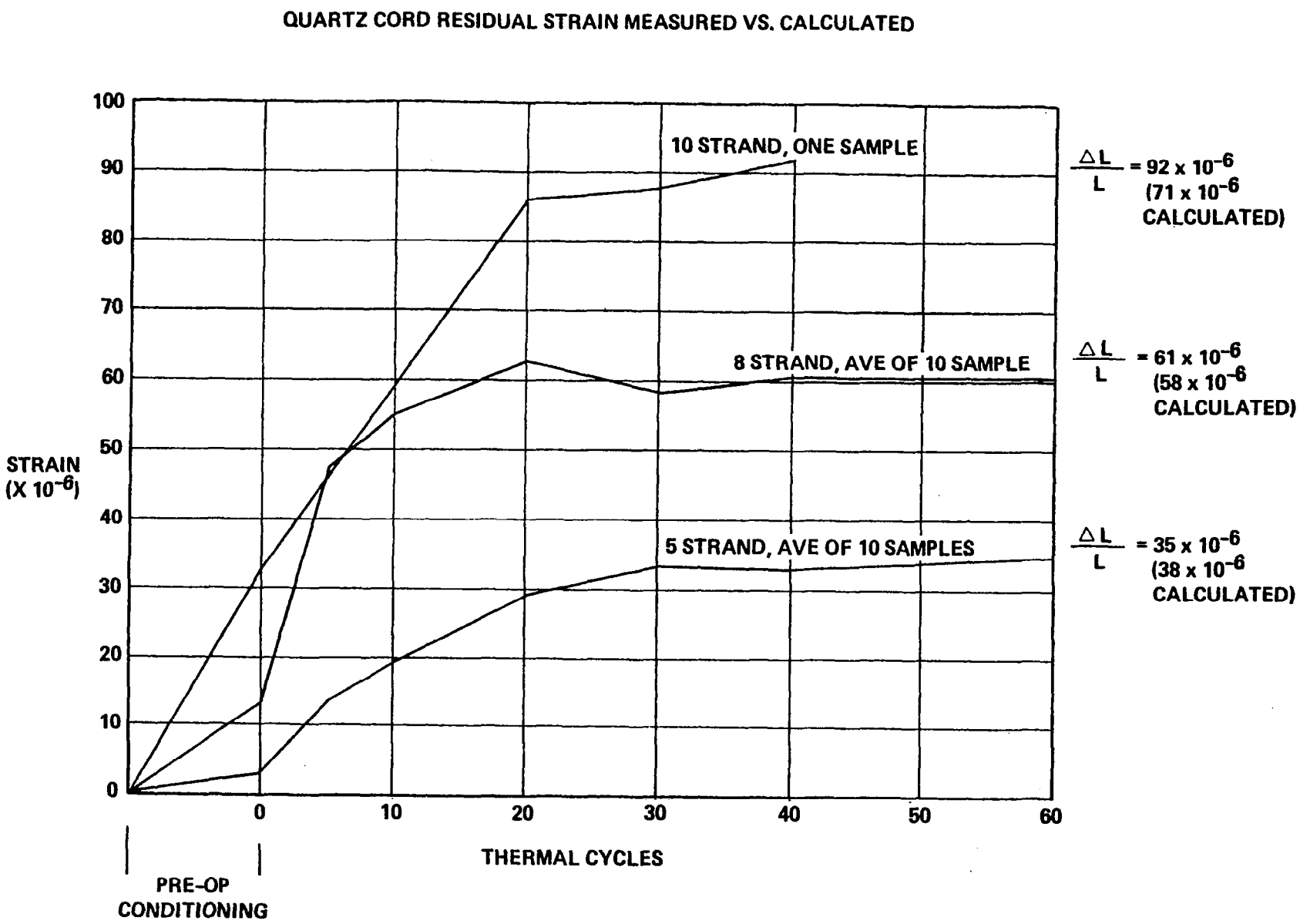


Figure 6.4.2-6. Quartz Cord Residual Strain Measured Versus Calculated

The residual strain test setup used in this task was validated by initially testing Teflon cross wrapped quartz control samples. The results from two control samples is given in Figures 6.4.2-7 and 6.4.2-8. Many thermal and load cycles of varying types were imposed on these control samples, and the residual strain was measured to be 60 and 75 micro-strains which is in good agreement with the previous TDRSS data. Following the control sample validation tests, preliminary tests were performed on Teflon coated quartz and graphite cables. The samples used in these preliminary tests were coated by Harris. Quartz cable samples were produced and tested with varying amounts of Teflon. The results (see Figure 6.4.2-9) indicate that the average residual strain is about half of the uncoated quartz control samples. These same samples were tested for coefficient of thermal expansion (CTE) and the data is presented in Figure 6.4.2-10. This data indicates that samples with the higher concentration of Teflon coating have a more positive coefficient of thermal expansion than the lightly coated or uncoated quartz samples. Uncoated quartz cords have a CTE which varies from $-0.5 \times 10^{-6}$ to $+0.5 \times 10^{-6}/^{o}C$ ($-0.3 \times 10^{-6}$ to $+0.3 \times 10^{-6}/^{o}F$). The heavier Teflon coated samples resulted in a constant positive $0.7 \times 10^{-6}/^{o}C$ CTE. Similar tests were performed for Teflon coated graphite cables. The residual strain data, presented in Figure 6.4.2-11, indicates approximately zero residual strain, which is very encouraging data. Three more graphite samples were prepared and the test repeated with the results shown in Figure 6.4.2-12. Unfortunately, the data did not repeat, but indicated an average residual strain of approximately 50 micro-strains. In an effort to explain these results, the samples were closely inspected and it was found that the Teflon coating was not uniformly sintered in the cord nor was the coating penetration consistent through the cables. The conclusion was that future tests should be performed on samples from qualified Teflon coating vendors.

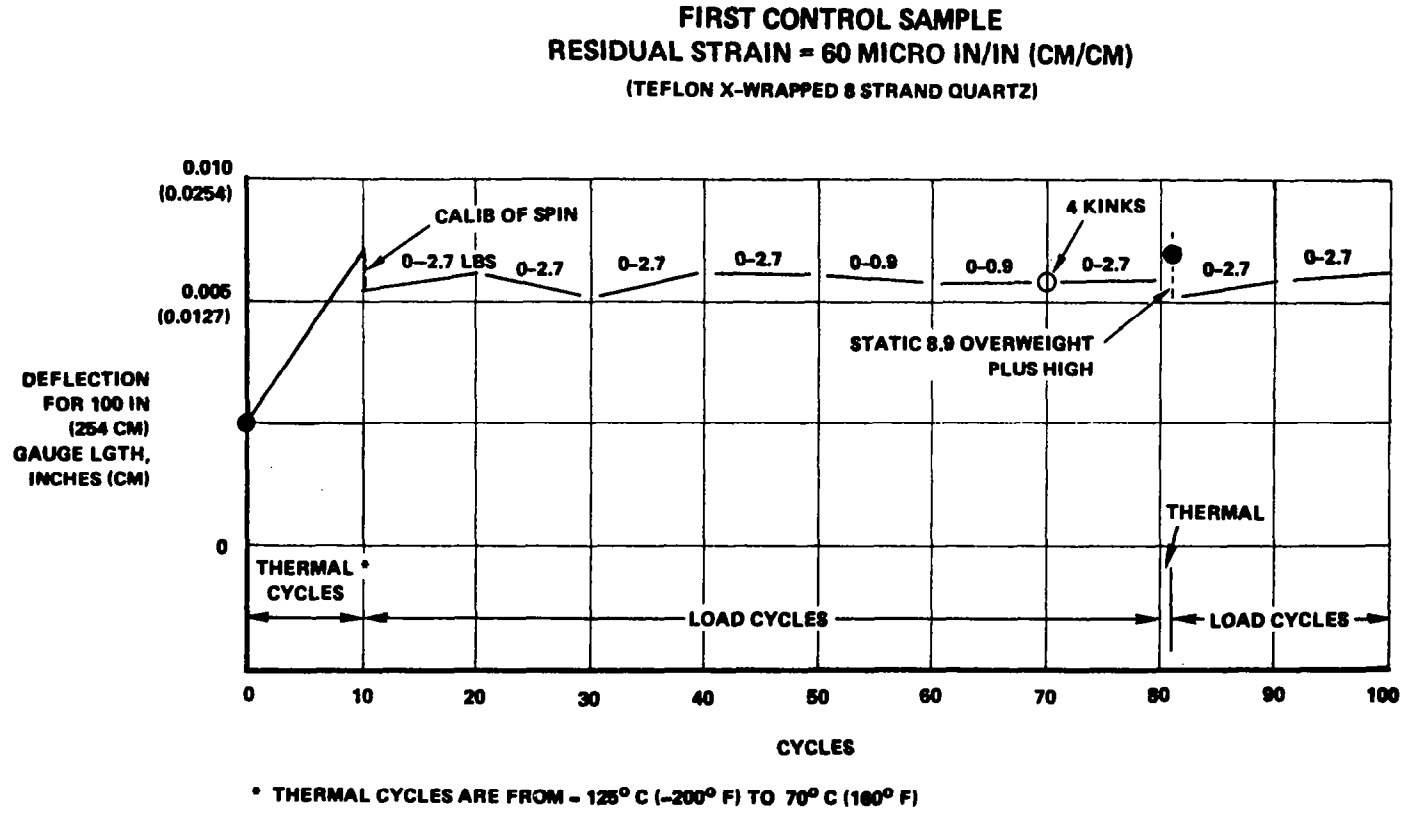


Figure 6.4.2-7. First Control Sample
Residual Strain = 60 Micro in/in (cm/cm)

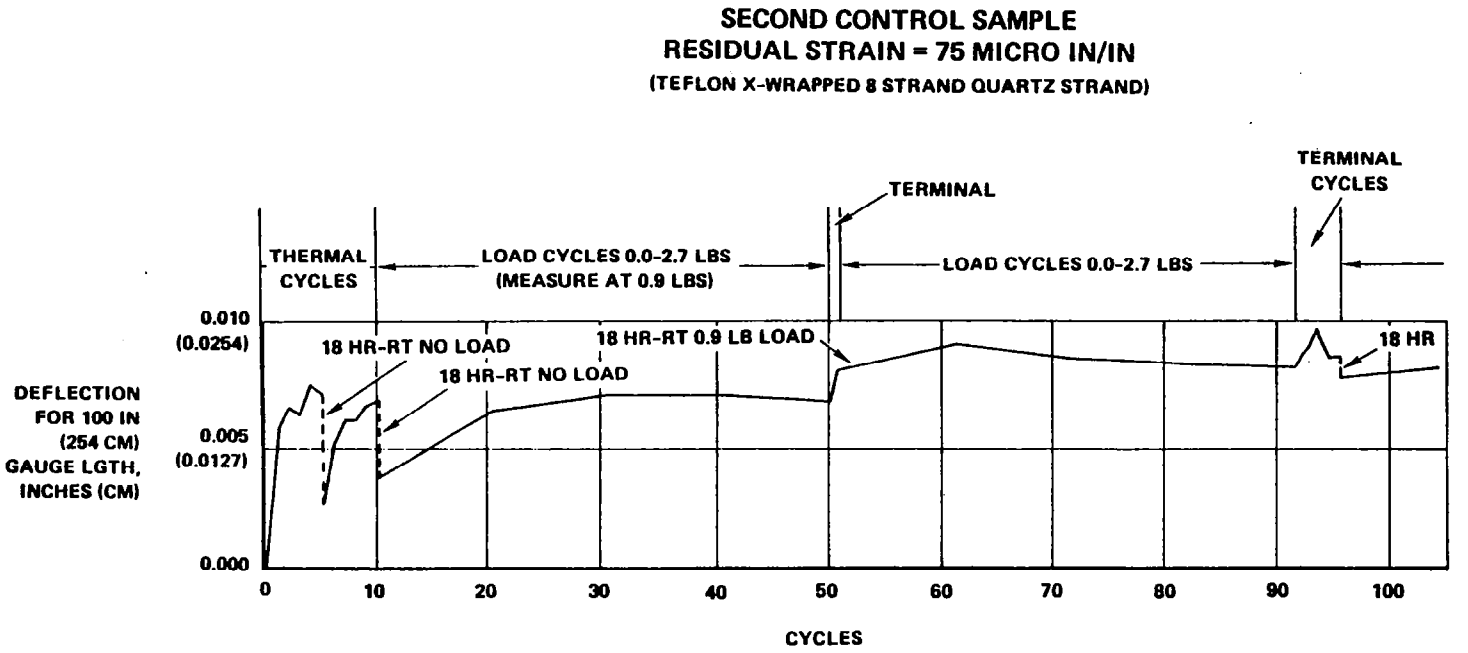


Figure 6.4.2-8. Second Control Sample
Residual Strain = 75 Micro in/in (cm/cm)

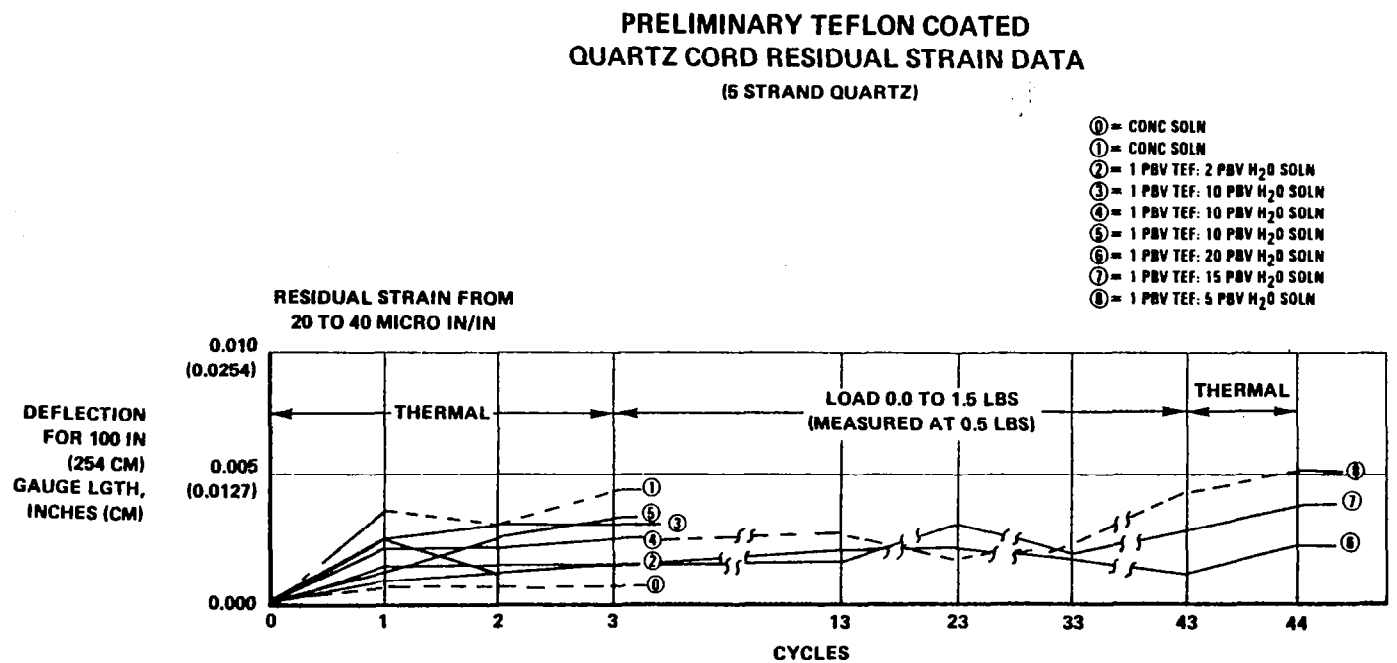


Figure 6.4.2-9. Preliminary Teflon Coated
Quartz Cord Residual Strain Data

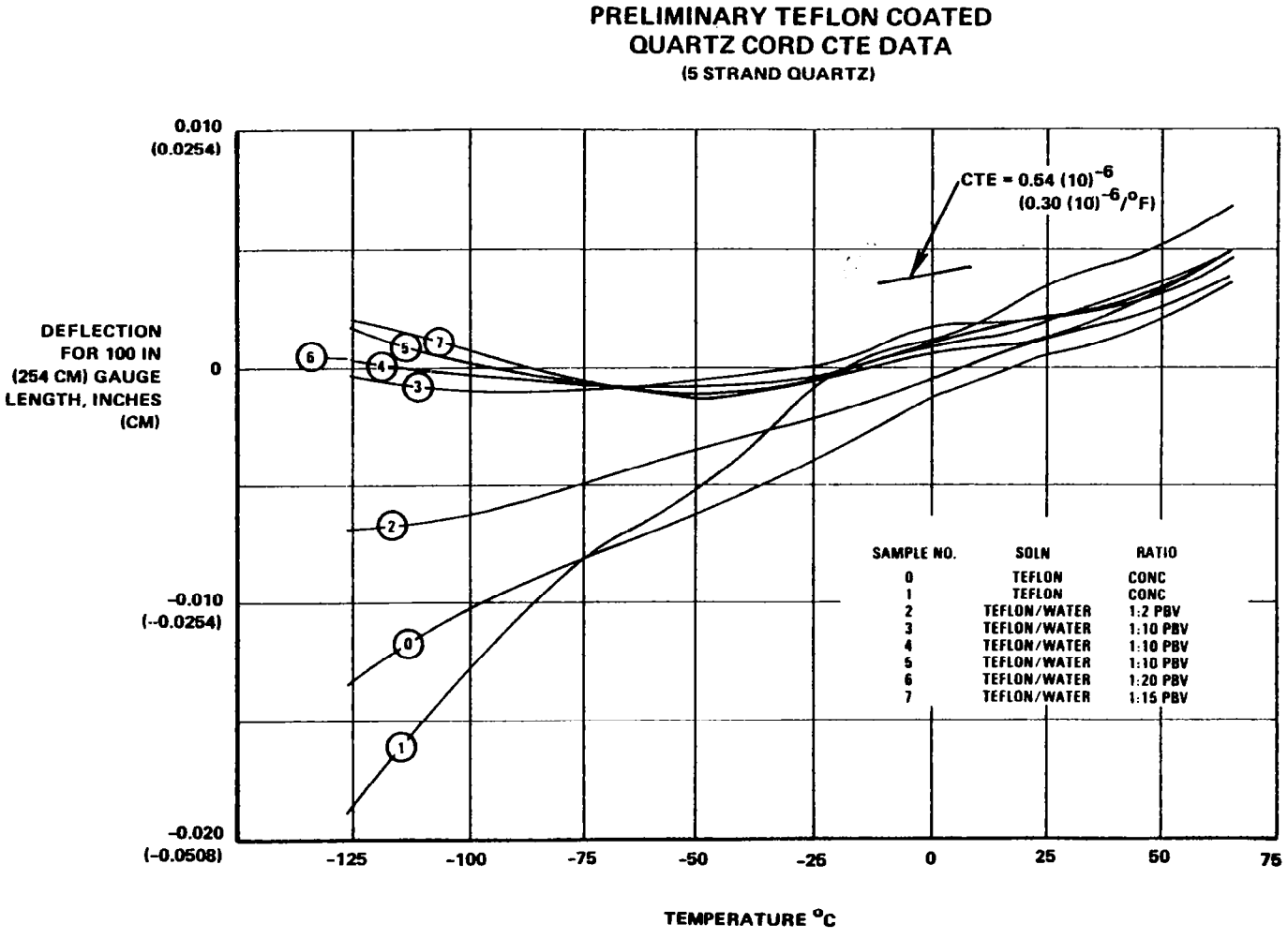


Figure 6.4.2-10. Preliminary Teflon Coated Quartz Cord CTE Data

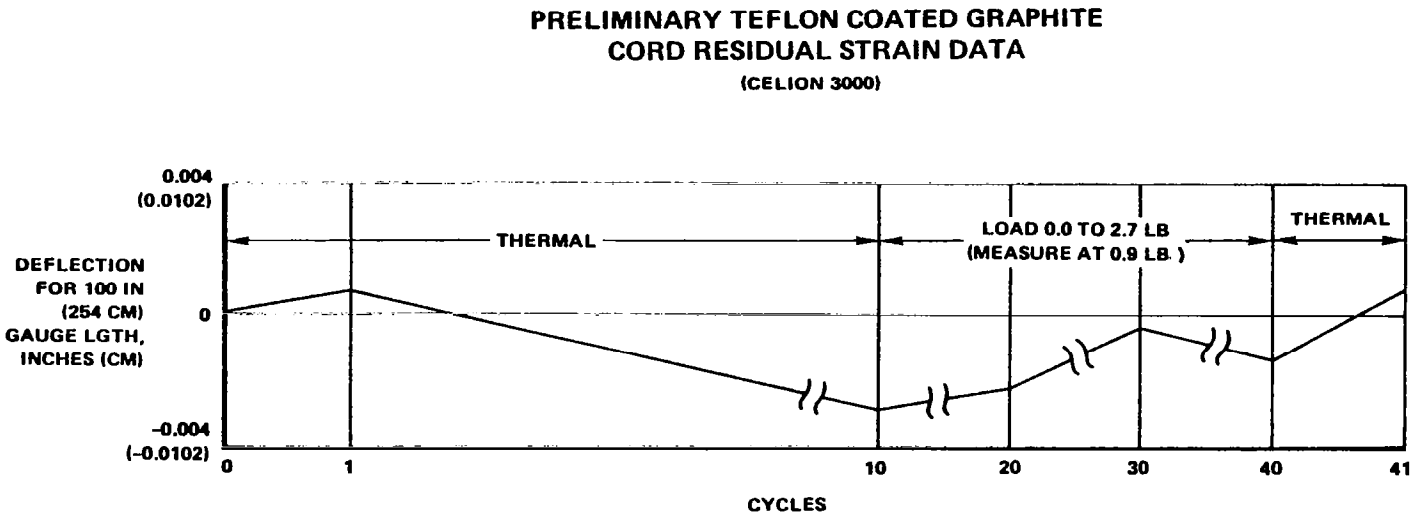


Figure 6.4.2-11. Preliminary Teflon Coated Graphite Cord Residual Strain Data

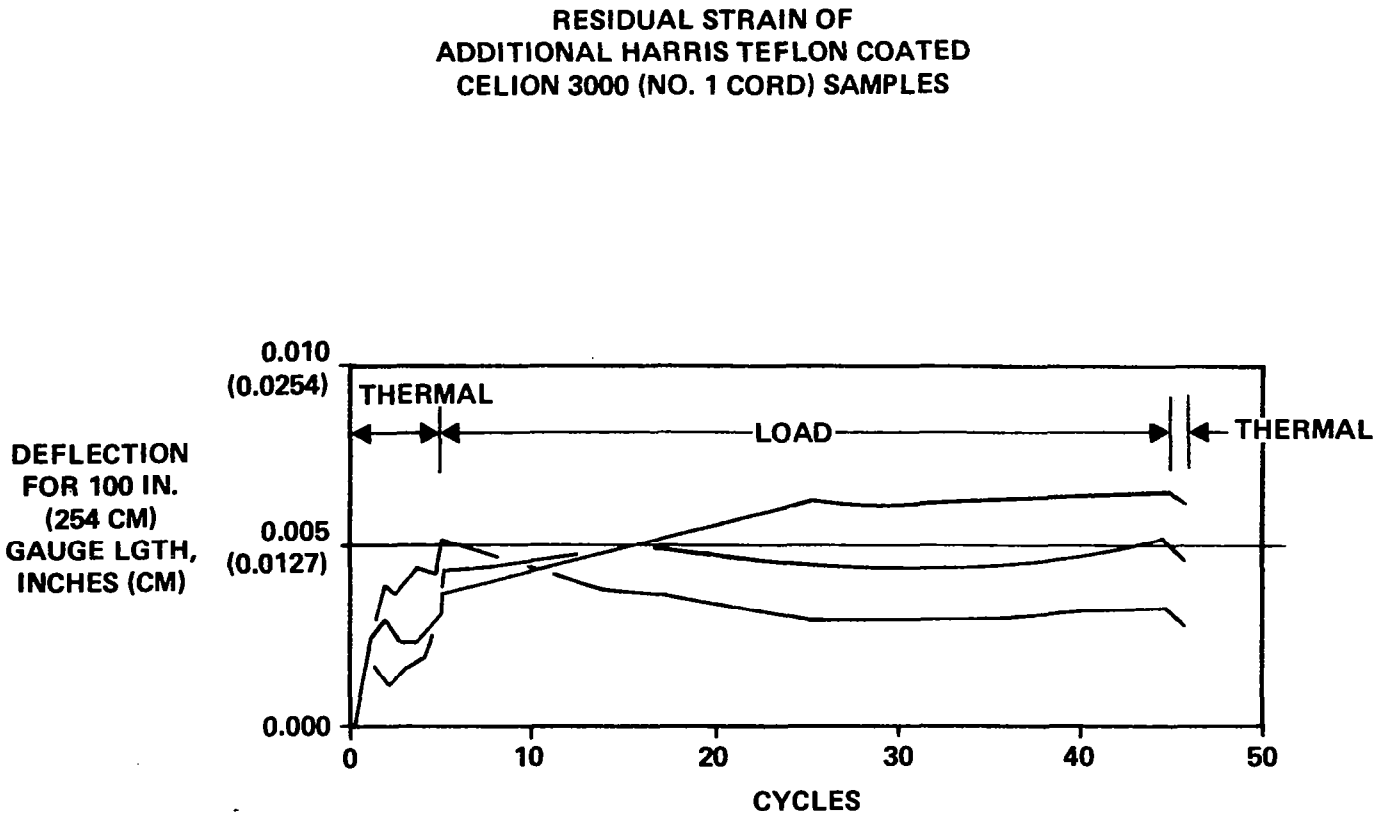


Figure 6.4.2-12. Residual Strain of Additional Harris Teflon Coated CELION 3000 (No. 1 Cord) Samples

The CTE data from these preliminary Teflon coated graphite cable samples is presented in Figure 6.4.2-13. The data indicates that Teflon has a negligible effect on the graphite cord, which has an approximate CTE of 0.5 x $10^{-6}/^{o}C$.

The conclusions from the screening test results are:

- Teflon coated graphite cables show the best performance potential considering residual strain, CTE, EA, strength, and handling toughness.
- Testing of higher quality samples is needed to substantiate an initial selection of Teflon coated graphite cables for this design application. Samples should be procured from a vendor which has the experience and equipment to provide uniform and consistent coating on the graphite cables.
- Future cable test specimen should have end fittings which are consistent with the Hoop/Column antenna design to ensure that the cable test data is valid for the antenna cable assemblies. This requires that joint designs and fabrication processes be developed for the Hoop/Column antenna.
- Teflon coated quartz cable is a good alternate cable design with lower EA and strength compared to graphite cables.

As a result of the screening test described above, two activities were initiated. These activities were the procurement of higher quality Teflon coated graphite cable materials from qualified vendors, and secondly, cable joint design and process development. The following section will describe the cable joint development activities and results.

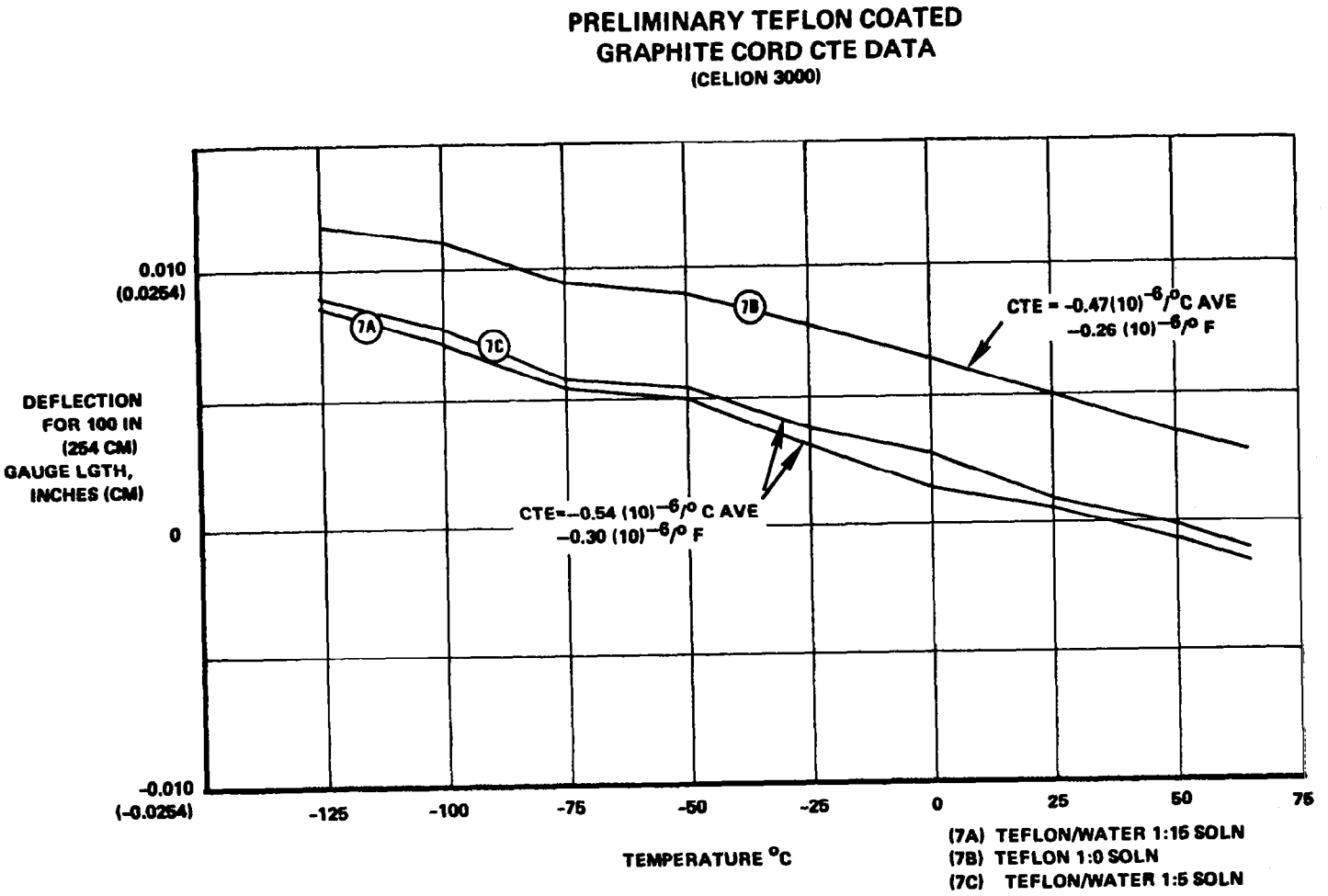


Figure 6.4.2-13. Preliminary Teflon Coated Graphite Cord CTE Data

## 6.4.3 Joint Development

The cable configurations and manufacturing criteria of the Hoop/Column antenna design are important considerations for cable joint development. The antenna cord assemblies are shown in Figures 6.4.3-1 and 6.4.3-2. The cable assemblies are fabricated to design length and load in the configurations shown. This is accomplished with tooling pegs laid out on a flat pattern and cables tensioned around these pegs to form the cord paths necessary in the design. The configuration contains a large number of cord joints with converging or diverging cord junctions in a "Y" configuration. In addition to these "Y" junction joints there are cable end fitting joints which attach to the hoop and hub portions of the Hoop/Column antenna design. The joint design must secure the "Y" junctions and end fittings with the cables in a tensioned condition. Many cord joint approaches were considered, including: clamping, swagging, tieing, and soldering (see Figure 6.4.3-3), but the only reliable cord joining technique is bonding. The most common use of graphite and quartz fibers in industry is as reinforcements in composites of epoxy, polyester and other resins. The yarns are sized with the appropriate materials to ensure good wetting of the resin materials. The yarns used in this task are sized with an epoxy compatible system at the fiber manufacturers. The introduction of Teflon in the cords complicates the cord bonding process. Teflon coated cords cannot be bonded unless the Teflon is chemically treated with an etching agent or the Teflon is removed. It was found that strong bonds could be produced by chemically etching the Teflon coated cables, however, the chemicals used are strong acid materials which are dangerous and difficult to use. It would be very difficult to use a chemical etching agent on the cable joints in the stretch configurations required by the antenna design. A much better technique is to remove the Teflon from the graphite with heat. Teflon will oxidize at approximately 550° C in air which is well below to graphitizing temperature of 1000 to 3000° C of the fibers. Graphite fibers are stable and retain most of their strength up to the graphitizing temperature. A number of heat sources were investigated which would provide the Teflon oxidation temperature and not exceed the graphitizing temperature of the fibers. Heat sources which were investigated are depicted

## CORD JOINT DESIGN MANUFACTURING CRITERIA

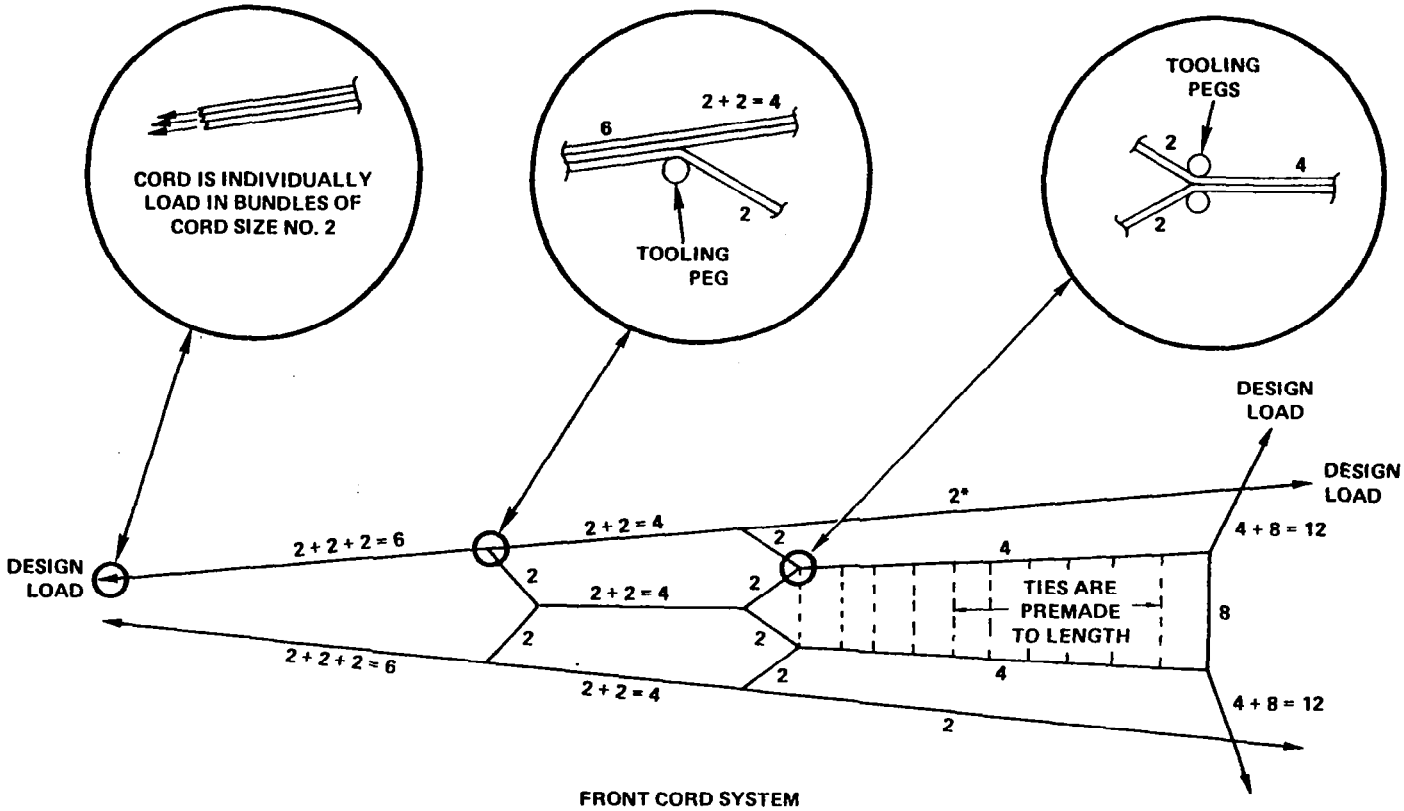


FRONT CORD SYSTEM

*NUMBERS INDICATE CORD SIZE

Figure 6.4.3-1. Cord Joint Design Manufacturing Criteria

## CORD JOINT DESIGN
## MANUFACTURING CRITERIA (CONTINUED)

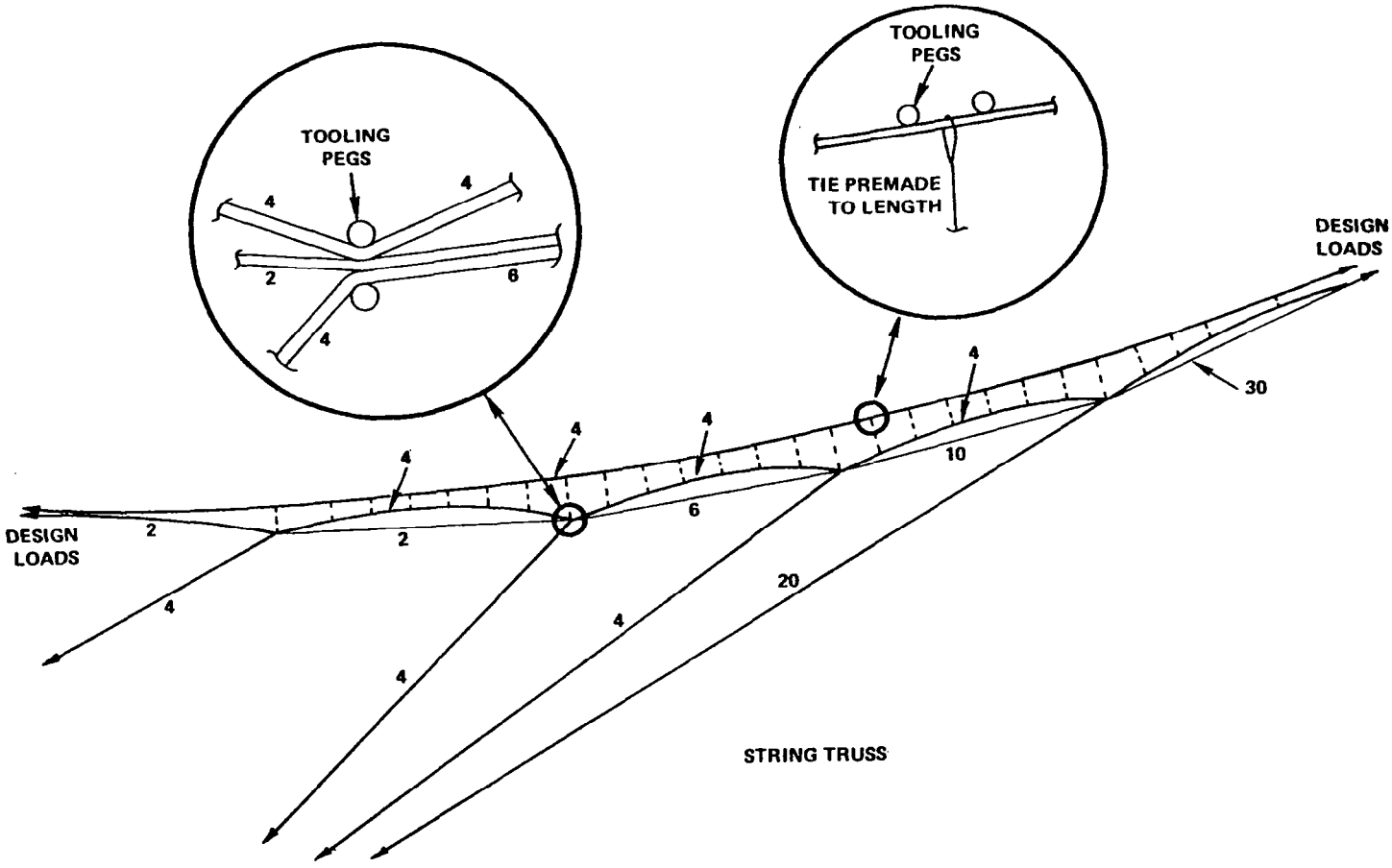


Figure 6.4.3-2. Cord Joint Design Manufacturing Criteria

## CORD JOINT APPROACH

**BONDING IS THE ONLY RELIABLE CORD JOINING TECHNIQUE**

- **CLAMPING**
  - **SLIPPAGE**
  - **BREAKAGE**
- **SWAGING**
  - **LOW STRENGTH**
  - **SLIPPAGE**
- **TIEING**
  - **MODERATE STRENGTH**
  - **POOR LOAD SHEARING CONTROL**
  - **POOR LENGTH ACCURACY**
- **SOLDERING**
  - **NO WETTING (QUARTZ)**

Figure 6.4.3-3. Cord Joint Approach

in Figure 6.4.3-4. The only sources found which provided local heat a high enough temperature were infrared heaters and miniature butane torches. The infrared heaters used were small reflector types which are capable of producing temperatures of over 2000°C. To achieve these temperatures the cable must be held at the focal point of the miniature reflectors, making it difficult to control the temperature. The heaters are not very versatile tools to work in close areas as required by the antenna design. It was found that miniature butane torches are much better heat sources. Torches are available with butane only, or with butane and oxygen mixed. Butane by itself in air has a flame temperature of approximately 1400°C. When oxygen is mixed in the flame the temperature goes up to 2800°C. These temperatures may be varied by the shape and size of the flame. A very small needle-point type flame is possible with these miniature torches, providing good control of stripping area. The torches are hand-held and easy to use in most any position. Many cable lap joint test specimen were fabricated by stripping the Teflon and bonding with epoxy and no failures in the bond areas have occurred.

There were initial concerns about the health hazards of Teflon fumes generated in the removal process. The concerns were answered in a Du Pont Bulletin T-13, "Properties, Processing and Applications of Teflon Fibers," which says in part,

> "Although there is no record of workers being seriously injured by fumes from heated Teflon or its thermal decomposition products, fumes are increasingly toxic in heavy concentrations, just as are the fumes or decomposition products of many common resins, paints, elastomers, and solvents, as well as naturally occurring polymeric materials like wood, silk, wool, and rubber. Therefore, the ventilation precautions to be observed when heating Teflon are the same as those which should be observed in heating many types of conventional materials."

## TEFLON STRIPPING DEVELOPMENT

- TEFLON WILL OXIDIZE AT 550°C IN AIR
- THE GRAPHITIZING TEMPERATURE OF GRAPHITE FIBERS IS FROM 1000°C TO 3000°C
- FOLLOWING HEAT SOURCES WERE INVESTIGATED:

### ELECTRIC

- SMALL NOZZLE, FORCED AIR TYPE
- TEMPERATURE UP TO 538°C (1000°F)
- COULD NOT REMOVE TEFLON

### INFRARED

- SMALL REFLECTOR TYPE
- TEMPERATURES OF 2000°C PLUS
- POOR TEMPERATURE CONTROL
- DIFFICULT CONFIGURATION TO USE
- TEFLON WAS SUCCESSFULLY REMOVED FOR TEST SAMPLES

### MINIATURE BUTANE TORCH

- BUTANE FLAME TEMP. IS 1400°C
- BUTANE/OXYGEN FLAME TEMP. UP TO 2800°C
- PROVIDE NEEDLE FLAME
- GOOD TEMPERATURE CONTROL
- EASY TO USE
- SELECTED TEFLON STRIPPING METHOD

Figure 6.4.3-4. Teflon Stripping Development

The bulletin continues to say that if adequate ventilation is not provided and workers inhale the fumes of heated Teflon resins in sufficient quantities, influenza-like symptoms may follow. Observations indicate that there are no lasting or cumulative effects. They define adequate ventilation to be an air flow of 180 $ft^3$/min/lb of Teflon resin. There is approximately 7 x $10^{-6}$ lbs of Teflon resin removed from the average antenna cord joint during the stripping process. This requires an air flow of 0.0013 $ft^3$/min (1.57 $in^3$/min) which is well within the range of most industrial air conditioning systems.

It was found that the Teflon coating on the cords provide a very effective epoxy wicking control. In uncoated cords the epoxy wicks down the length of the cord some distance away from the joint area before curing. These wicking areas must be protected to avoid flexing of the cables, or breakage will occur at the hard cured epoxy interface. In other Harris antenna programs where uncoated quartz cords have been used, Teflon sleeves are used at the cord joints to protect these wicking interface areas. A typical joint using Teflon sleeves are shown in Figure 6.4.3-5. In Teflon coated cables, the Teflon can be removed in the desired area and epoxy adhesive will not wick beyond that area. The Teflon provides a wicking stop which deletes the requirement for Teflon strain relief sleeves; thus allowing a simpler cord joint design to be developed. A simpler joint design is also shown in Figure 6.4.3-5. The joint consists of an epoxy graphite laminate machined to the "Y" configuration to allow the cables to be bonded to a Teflon stripped portion of the cable. In the final configuration, the joint consists of a flat sandwich graphite epoxy laminate. The manufacturing process developed for this joint is illustrated in Figure 6.4.3-6. The first step in producing a joint is to tension the cables around the tooling pegs provided by the flat pattern tooling. Teflon is then removed from the cables in the appropriate locations using miniature butane torches. The cables are then impregnated with an epoxy resin in the stripped areas. Epoxy adhesive is then applied to a graphite epoxy laminate fitting and placed over the tooling pegs and against the stripped and epoxy impregnated cable areas. After adhesive cure, the joint is removed from the tooling pegs and a second laminate cap is bonded over the joint to complete the flat graphite epoxy laminate joint. A very similar process was developed for end fittings and is depicted in Figure 6.4.3-7.

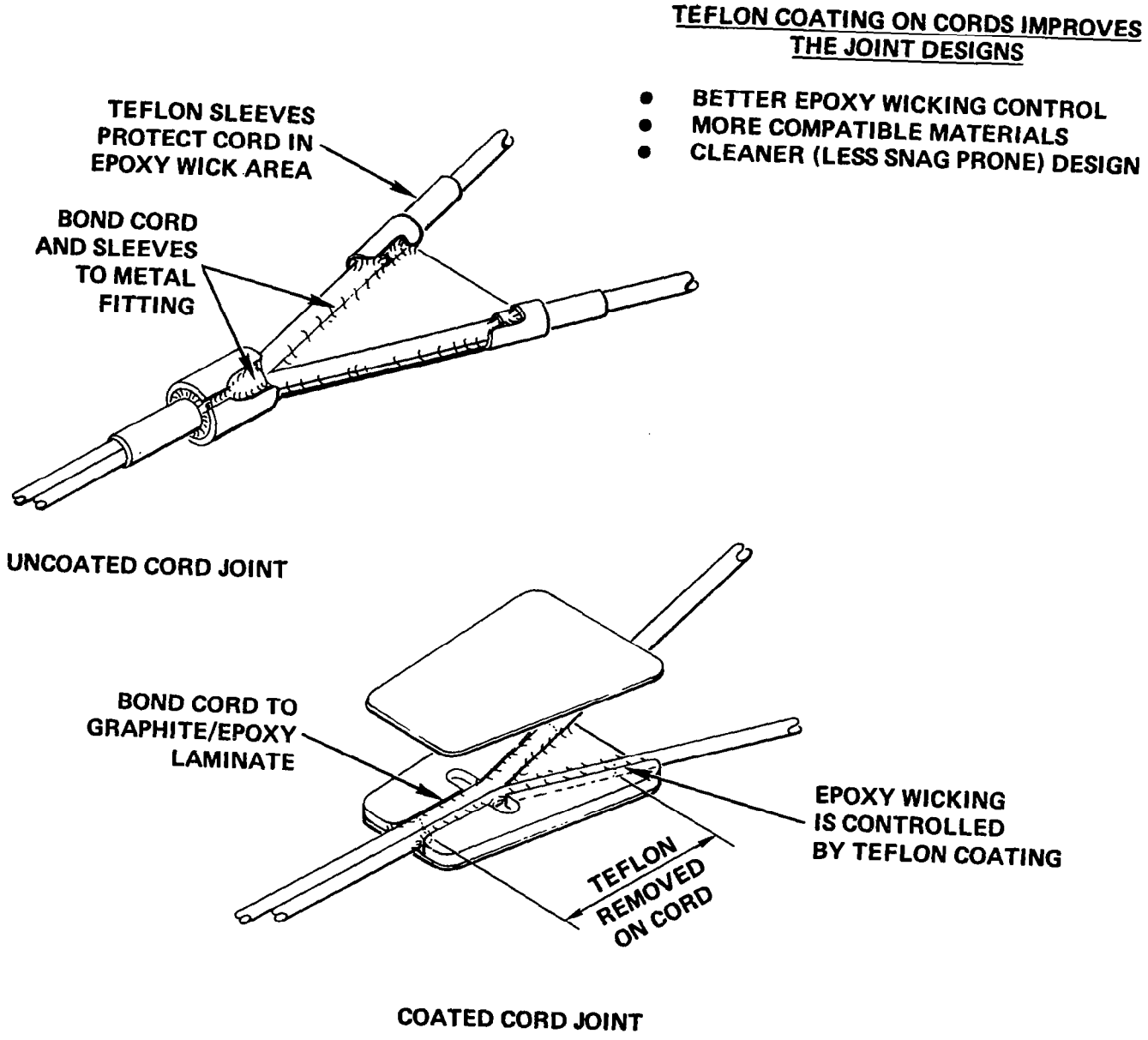


Figure 6.4.3-5. Coated Cord Joint

## CORD JOINT MANUFACTURING PROCESS

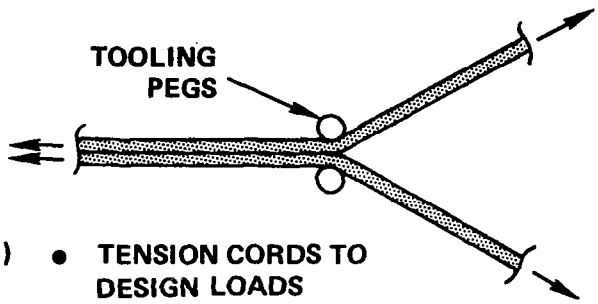


1) • TENSION CORDS TO DESIGN LOADS

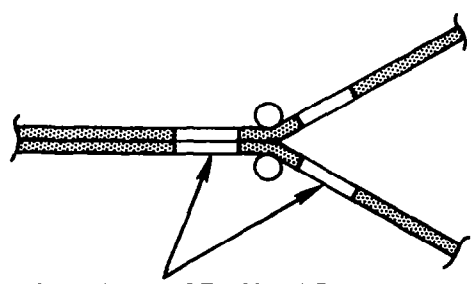

2) • REMOVE TEFLON WITH MINIATURE BUTANE TORCH

• APPLY EPOXY ADHESIVE TO CORD AREAS

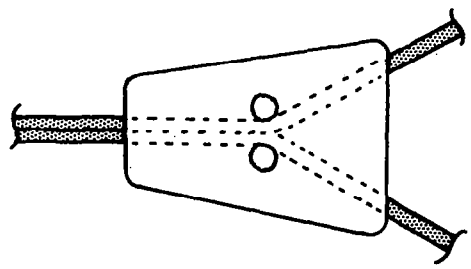

3) • TO APPLY EPOXY ADHESIVE TO GRAPHITE/EPOXY FITTING

• PLACE FITTING OVER TOOLING PEGS WITH ADHESIVE IN CONTACT WITH CORDS

• ALLOW 24 HOURS FOR ADHESIVE CURE

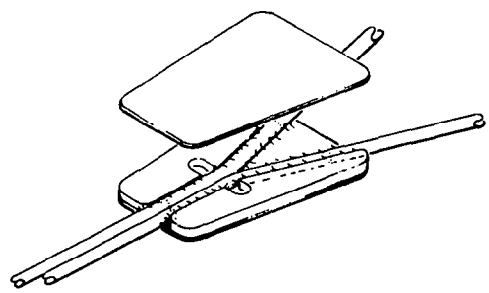

4) • REMOVE FITTING AND CORDS FROM TOOLING PEGS AND BOND LAMINATE CAP TO EXPOSED CORD SIZE OF FITTING

Figure 6.4.3-6. Cord Joint Manufacturing Process

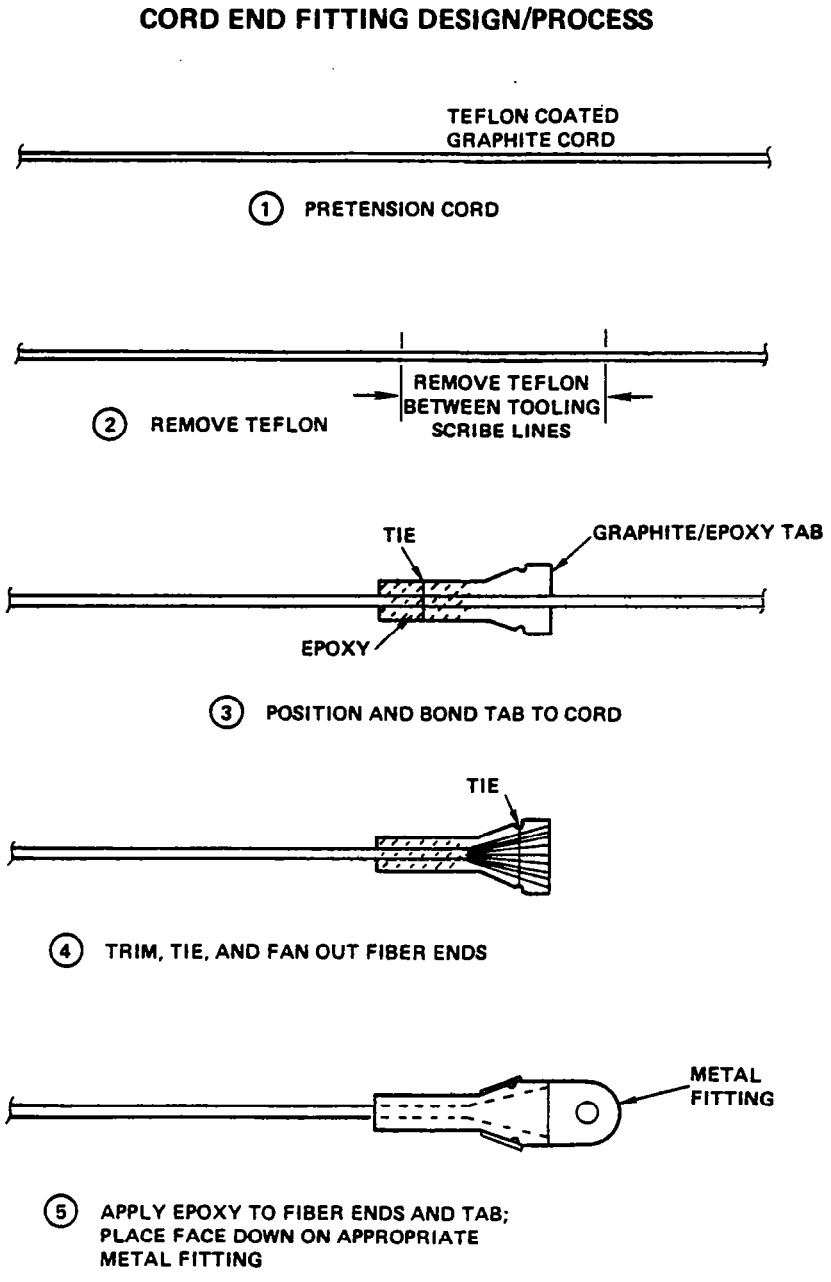


Figure 6.4.3-7. Cord End Fitting Design/Process

Again, the cable is first tensioned, then the Teflon is removed from the bond area, and a graphite epoxy tab is bonded to the cable. After adhesive cure, excess cable is cut from the joint and a second bonding operation bonds the tab to the appropriate metal fitting for end connection. Figures 6.4.3-8 through 6.4.3-15 illustrate how the cable joint design described above has been applied in the Hoop/Column antenna design.

### 6.4.4 Final Test Results

The final testing performed in this phase of the program was done with number 2 Teflon coated graphite cables purchased from Engineering Yarns. The cord number sizes was assigned in this task for convenience. A description/definition of number 1 cord size graphite and quartz is presented in Figure 6.4.4-1. For graphite it is defined as 3000 fibers of seven microns in diameter to produce a total cable diameter of 450 microns (0.018 inch). A number 1 quartz cable is of equivalent diameter but consists of 1920 fibers of 9 microns in diameter. Additional material properties data is given in the figure for comparison. The number 2 graphite cables procured from Engineering Yarns consisted of 6000 fibers uniformly compacted and coated with Teflon. Test specimens were fabricated with end fittings like those described in the preceding section. A fixture was fabricated to bond the end fittings to the specimens and ensure good alignment is achieved (see Figure 6.4.4-2). A typical specimen end fittting attached to the Instron Tensile Testing machine is shown in the photograph of Figure 6.4.4-3.

Cable specimen were tested to determine EA and strength properties. The average load/strain curve of three specimens are plotted in the chart of Figure 6.4.4-4. There is a small and repeatable historesis in the loading and unloading curves of these specimens. The design load range for this cord size has been chosen between 500 and 1000 grams. The average EA in this range is approximately 17.6 grams (8000 pounds). The same samples were tested to a higher load range cycle and the data is shown in Figure 6.4.4-5. The load/deflection curve is a little nonlinear giving an EA of approximately 22.2 grams (10,000 pounds) at loads over 10 kilograms. These

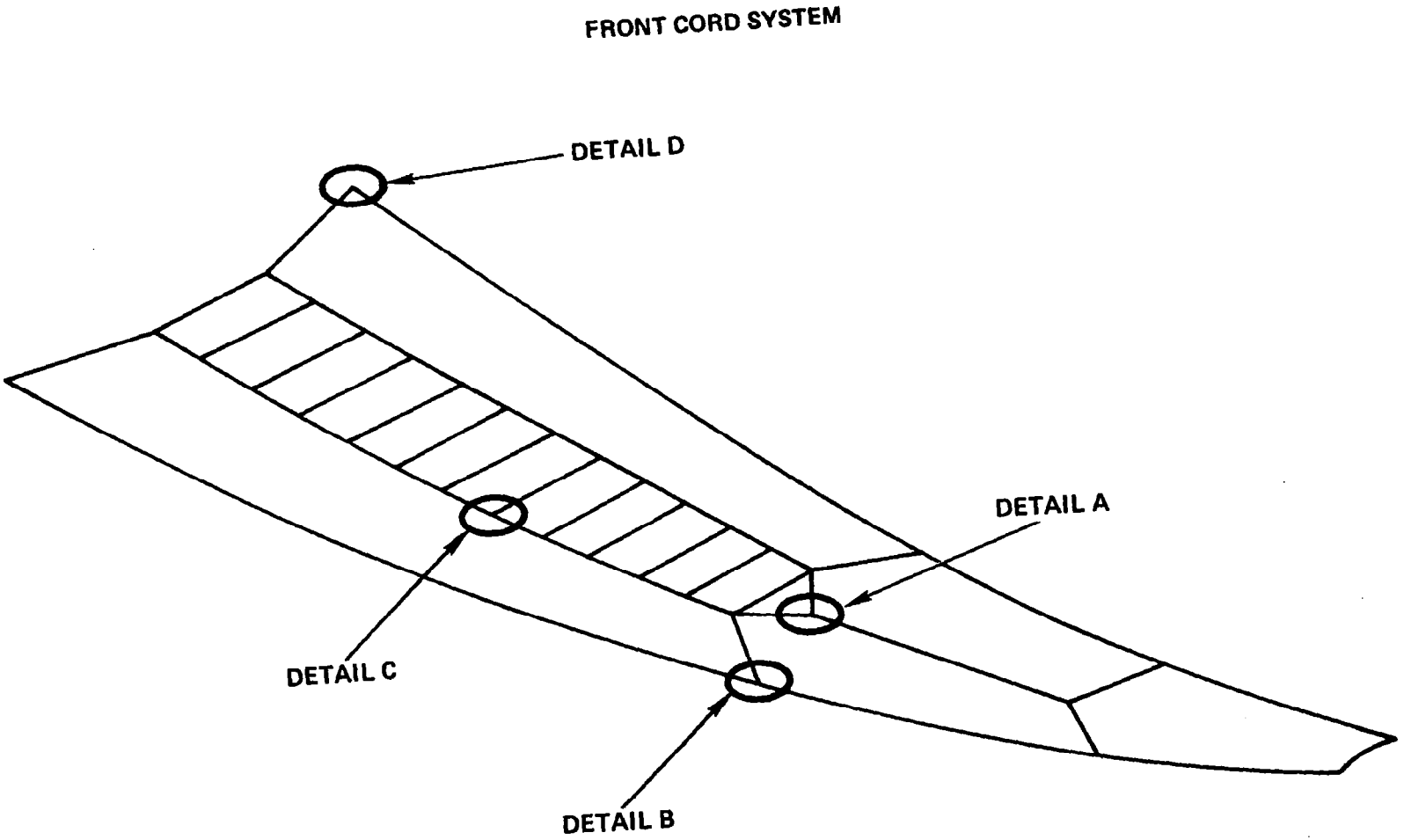


Figure 6.4.3-8. Front Cord System

**DETAIL A**

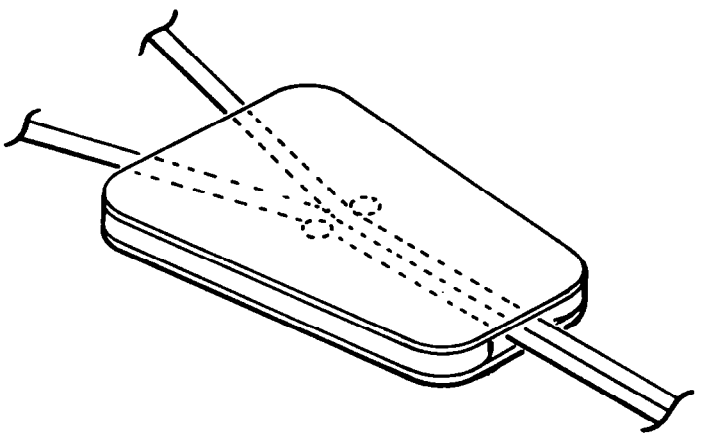

Figure 6.4.3-9. Detail A

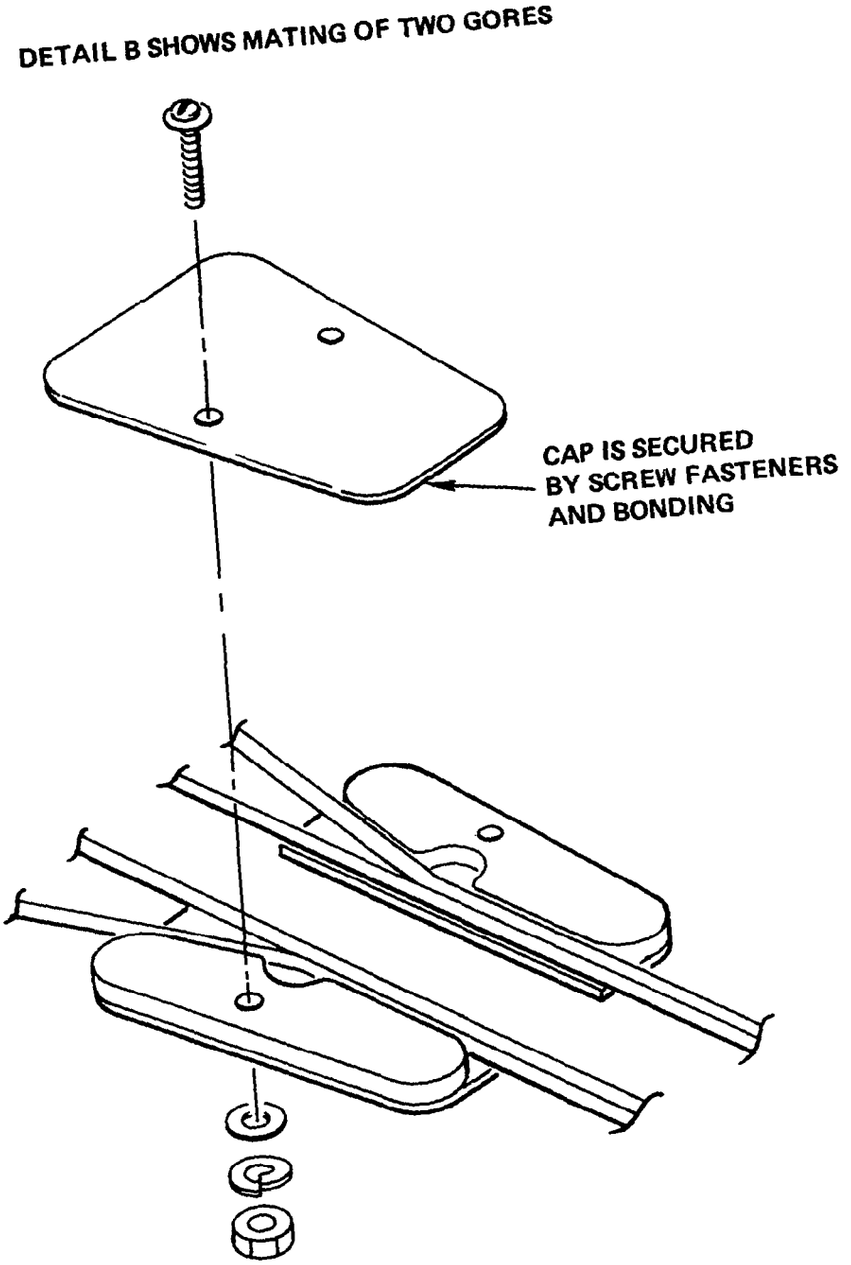


Figure 6.4.3-10. Detail B Shows Mating of Two Gores

DETAIL C

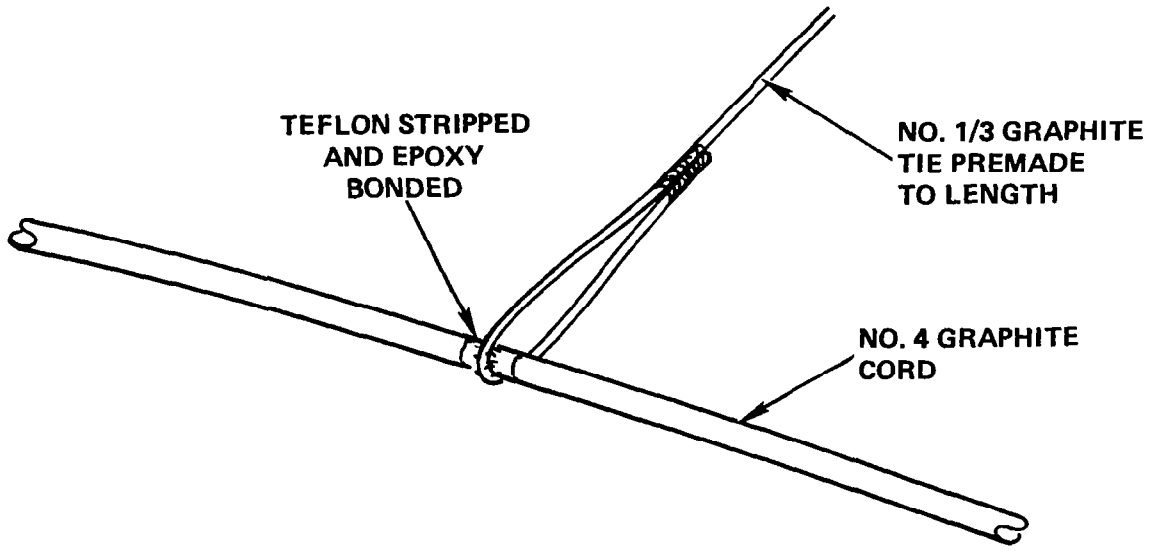


Figure 6.4.3-11. Detail C

**DETAIL D**

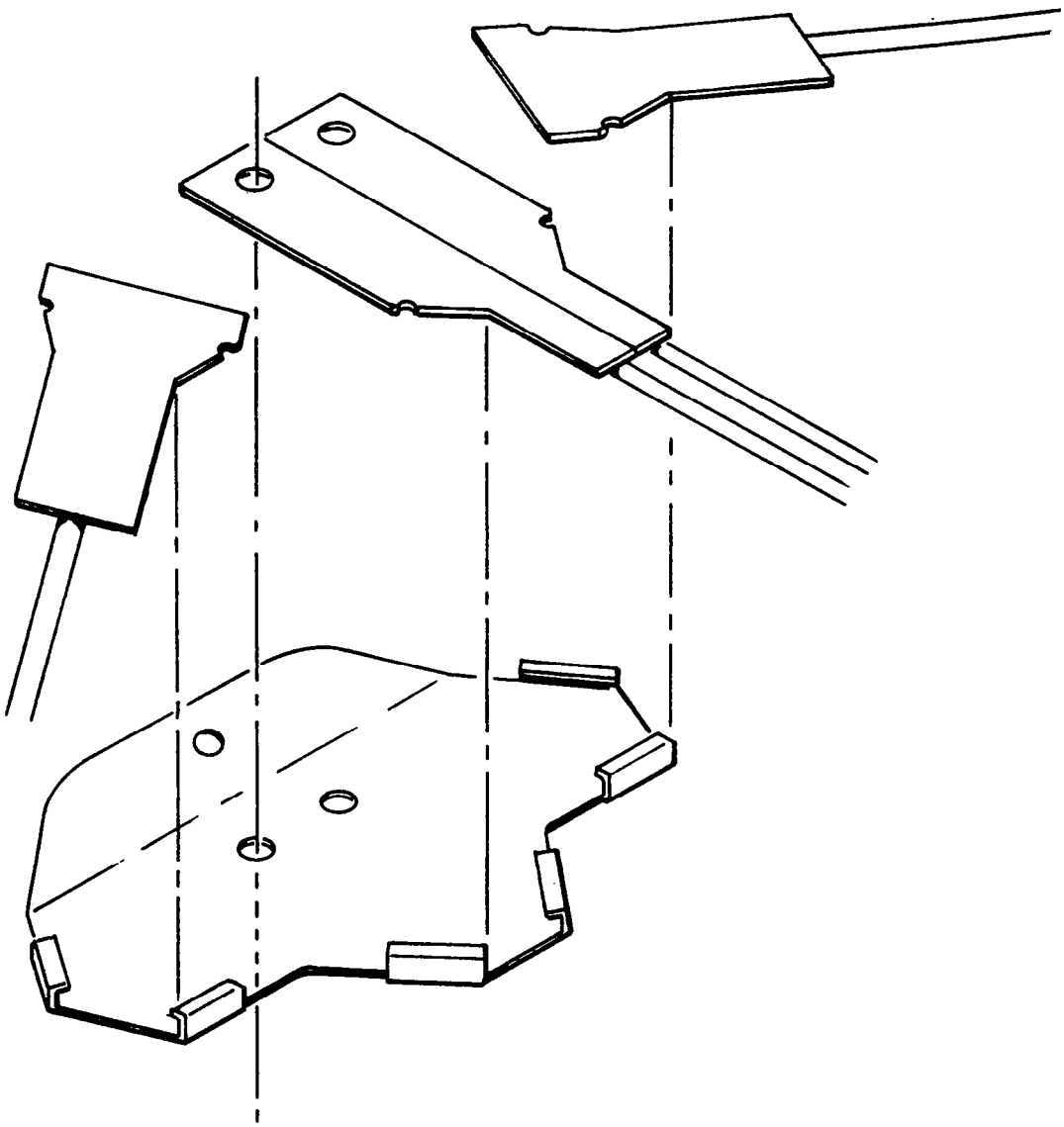

Figure 6.4.3-12. Detail D

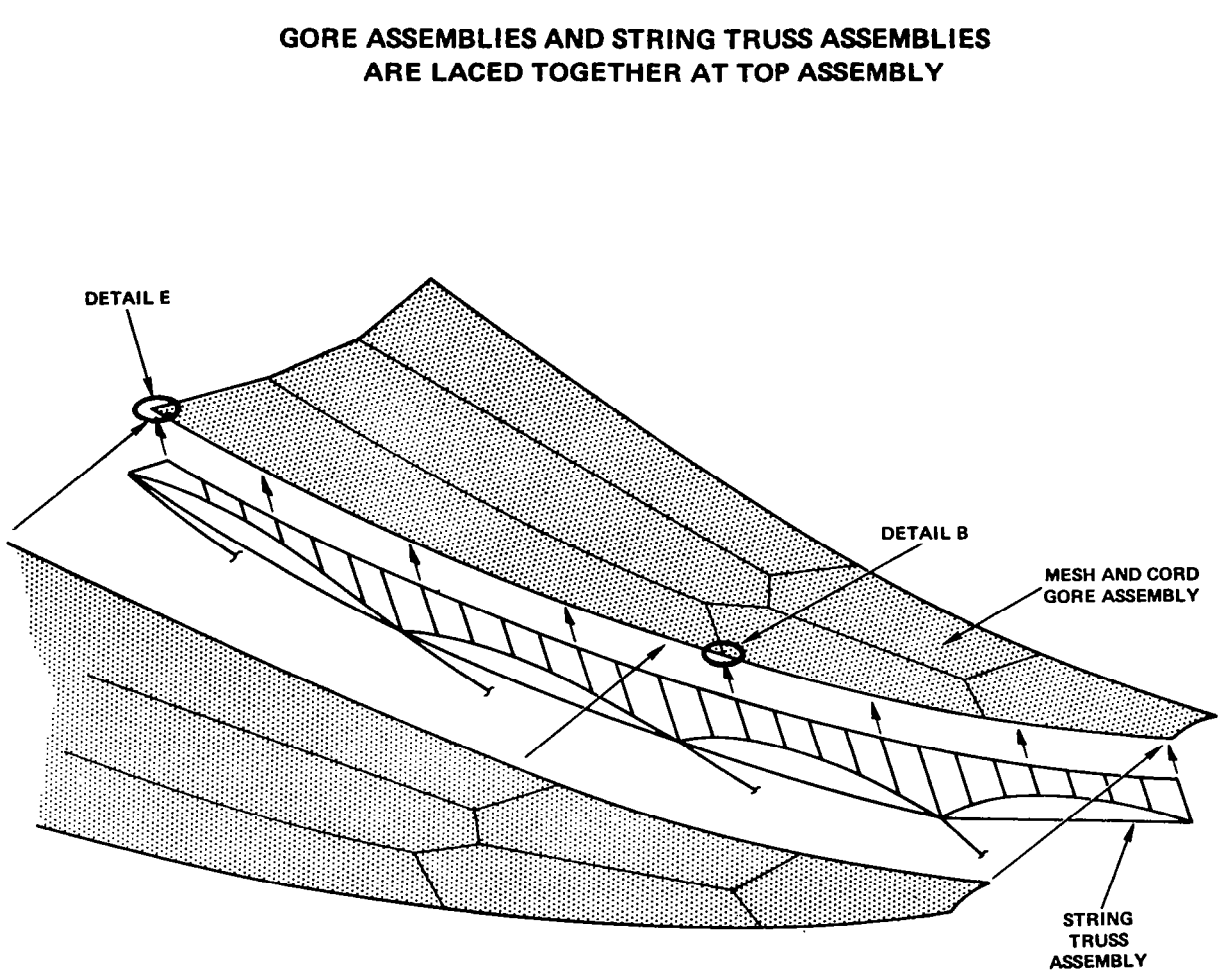


Figure 6.4.3-13. Gore Assemblies and String Truss Assemblies are Laced Together at Top Assembly

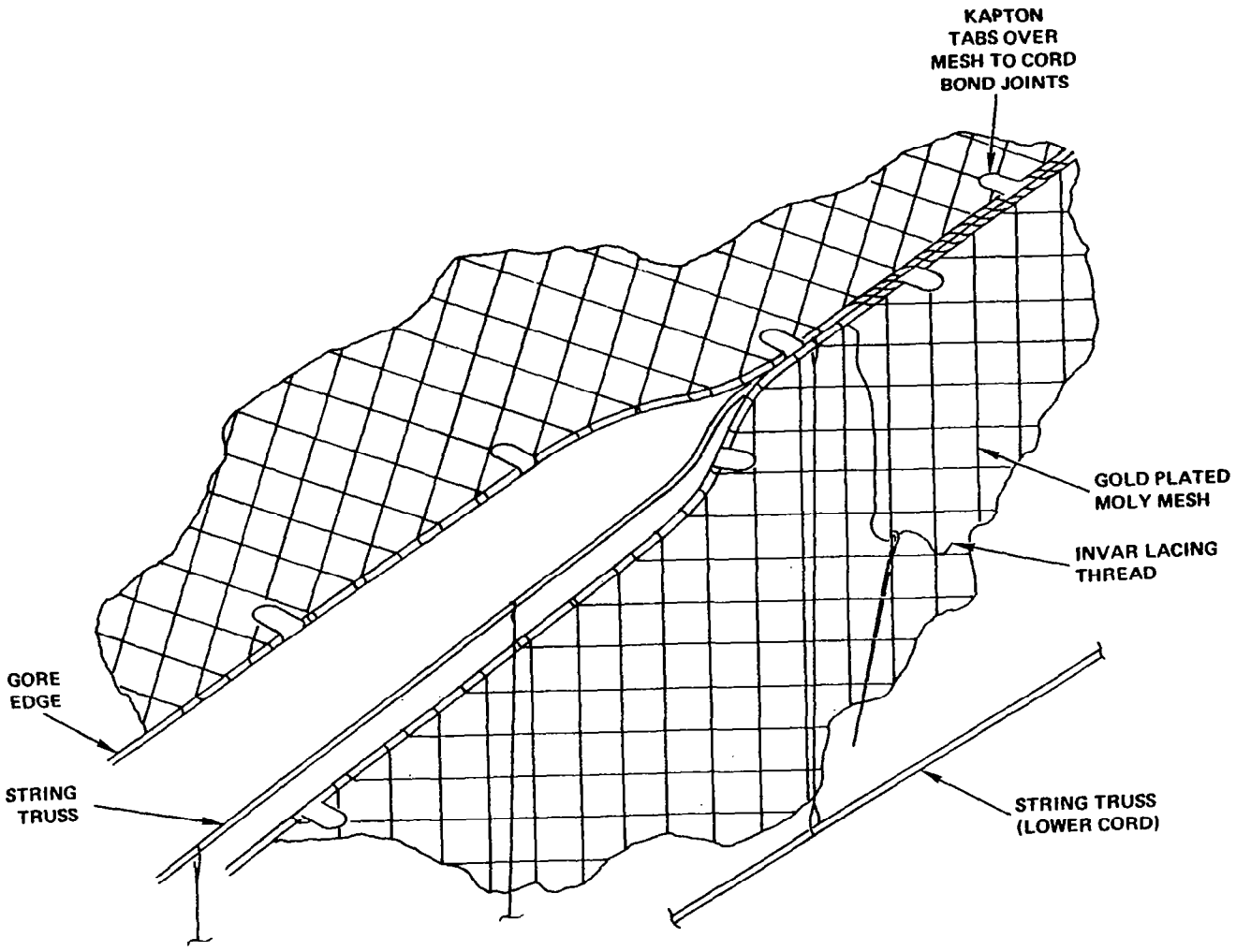


Figure 6.4.3-14. Adjacent Gores and String Truss are Laced Together

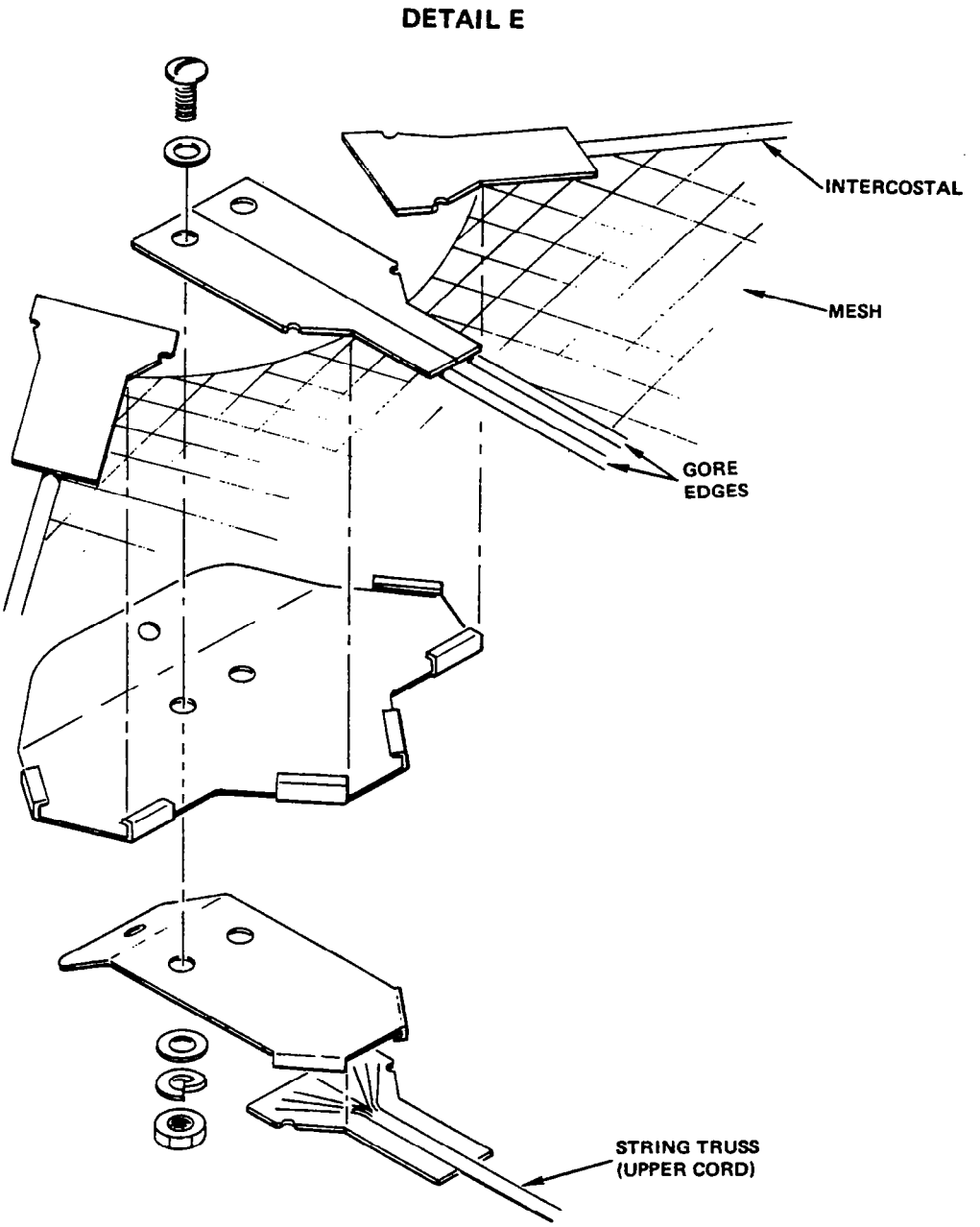


Figure 6.4.3-15. Detail E

## TASK 2 HAS DEFINED THE FOLLOWING FIBER BUNDLES AS NO. 1 CORD SIZES

| | QUARTZ | GRAPHITE |
|---|---|---|
| PLIES/CORD | 8 | 1 |
| FIBERS/PLY | 240 | 3000 |
| FIBERS/CORD | 1920 | 3000 |
| FIBER DIAMETER | 9 $\mu$m (0.0004 IN.) | 7 $\mu$m (0.00028 IN.) |
| CORD DIAMETER | 450 $\mu$m (0.018 IN.) | 450 $\mu$m (0.018 IN.) |
| *DESIGN LOAD RANGE (APPROXIMATE) | 2.5 – 5.0 NT (0.5 – 1.0 LB) | 2.5 – 5.0 NT (0.5 – 1.0 LB) |
| E (MODULUS) | 73 GPa (10.4 X $10^6$ psi) | 227 GPa (33 X $10^6$ psi) |
| EA | 6500 – 7000 NT (1500 – 1600 LB) | 18,000 – 20,000 NT (4000 – 4500 LB) |
| TENSILE STRENGTH | 70 NT (15 LB) | 180 NT (40 LB)** |
| WEIGHT | 0.265 g/m (1.482 X $10^{-5}$ LB/IN.) ADD 16% FOR TEFLON X-WRAP | 0.201 g/m (1.125 X $10^{-5}$ LB/IN.) ADD 10% FOR TEFLON COATED |

*THE DESIGN LOAD RANGE IS SOMEWHAT ARBITARILY SELECTED, BUT IS BASED ON THE MINIMUM LOAD REQUIRED TO OPERATE IN THE LINEAR RANGE OF THE LOAD/DEFLECTION CURVE OF THE CORD. THIS MAXIMIZES CORD EA (MODULUS X AREA) FOR A PARTICULAR LOAD.

**NUMBERS SHOWN ARE FOR CORDS WITH TEFLON COATING. CORDS WITHOUT TEFLON COATING HAVE ABOUT HALF THE STRENGTH

Figure 6.4.4-1. Task 2 Has Defined the Following Fiber Bundles as No. 1 Cord Sizes

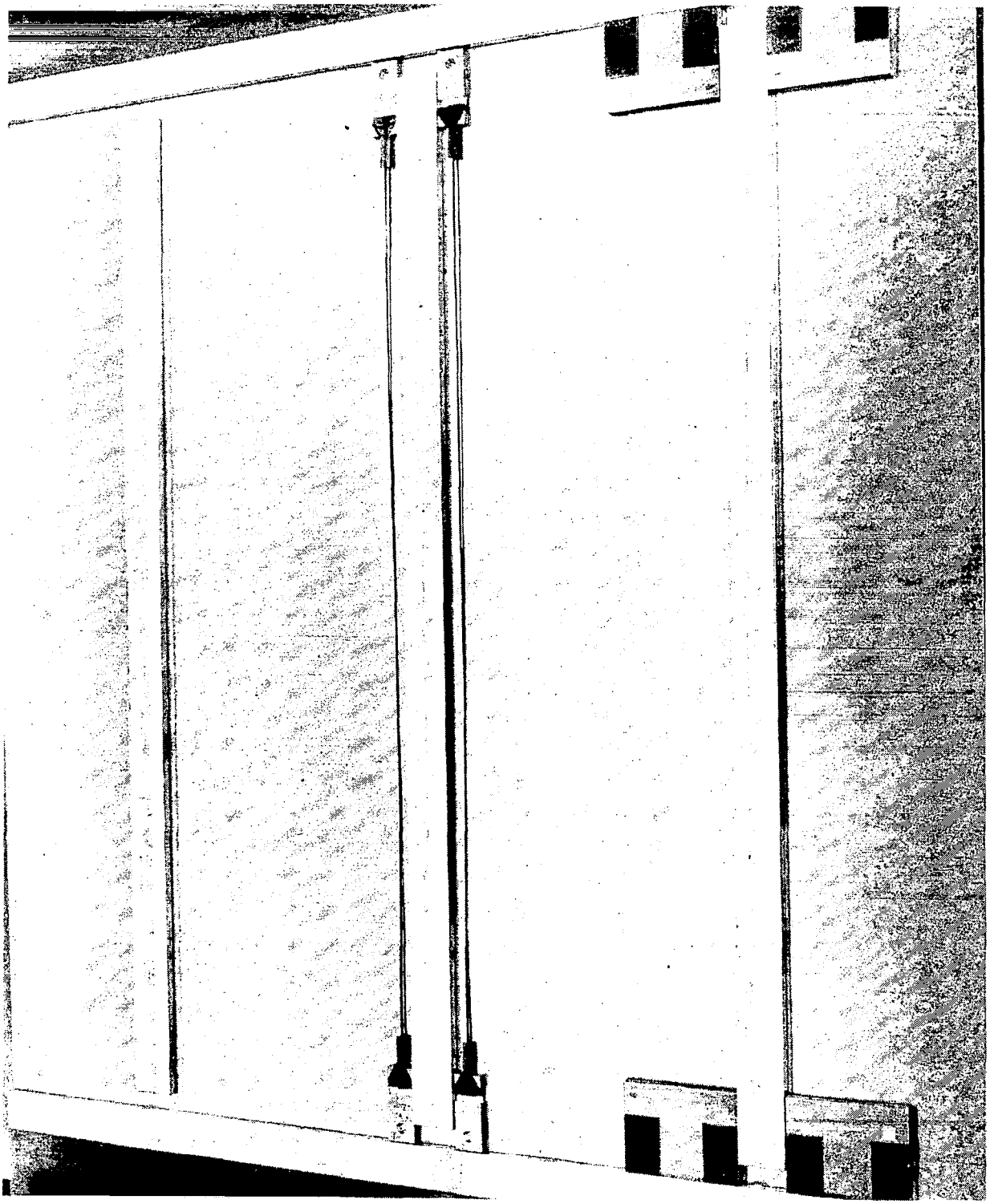

SPECIMEN FABRICATION FIXTURE

FIGURE 6.4.4-2

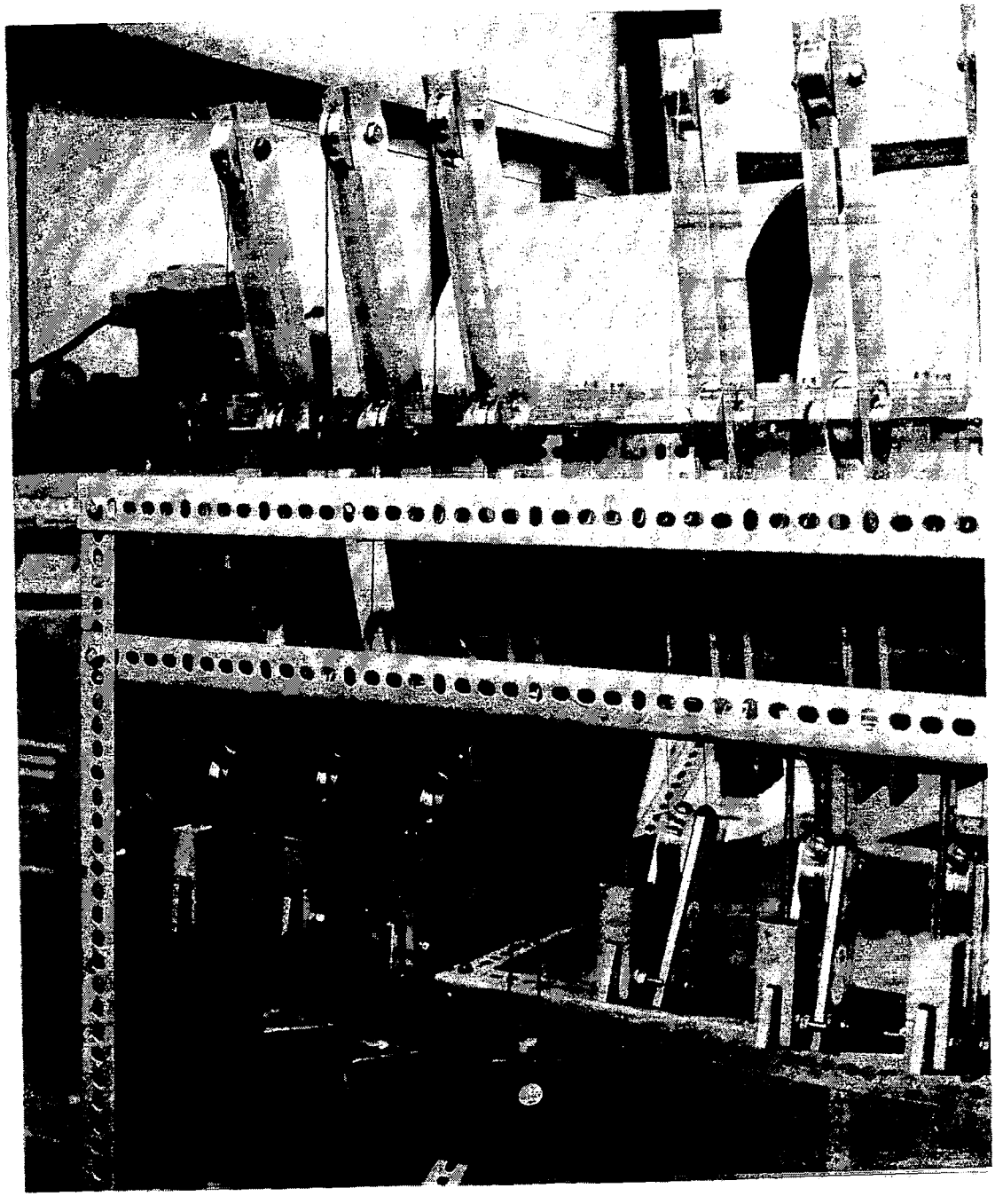

INSTRON SPECIMEN END FITTING

FIGURE 6.4.4-3

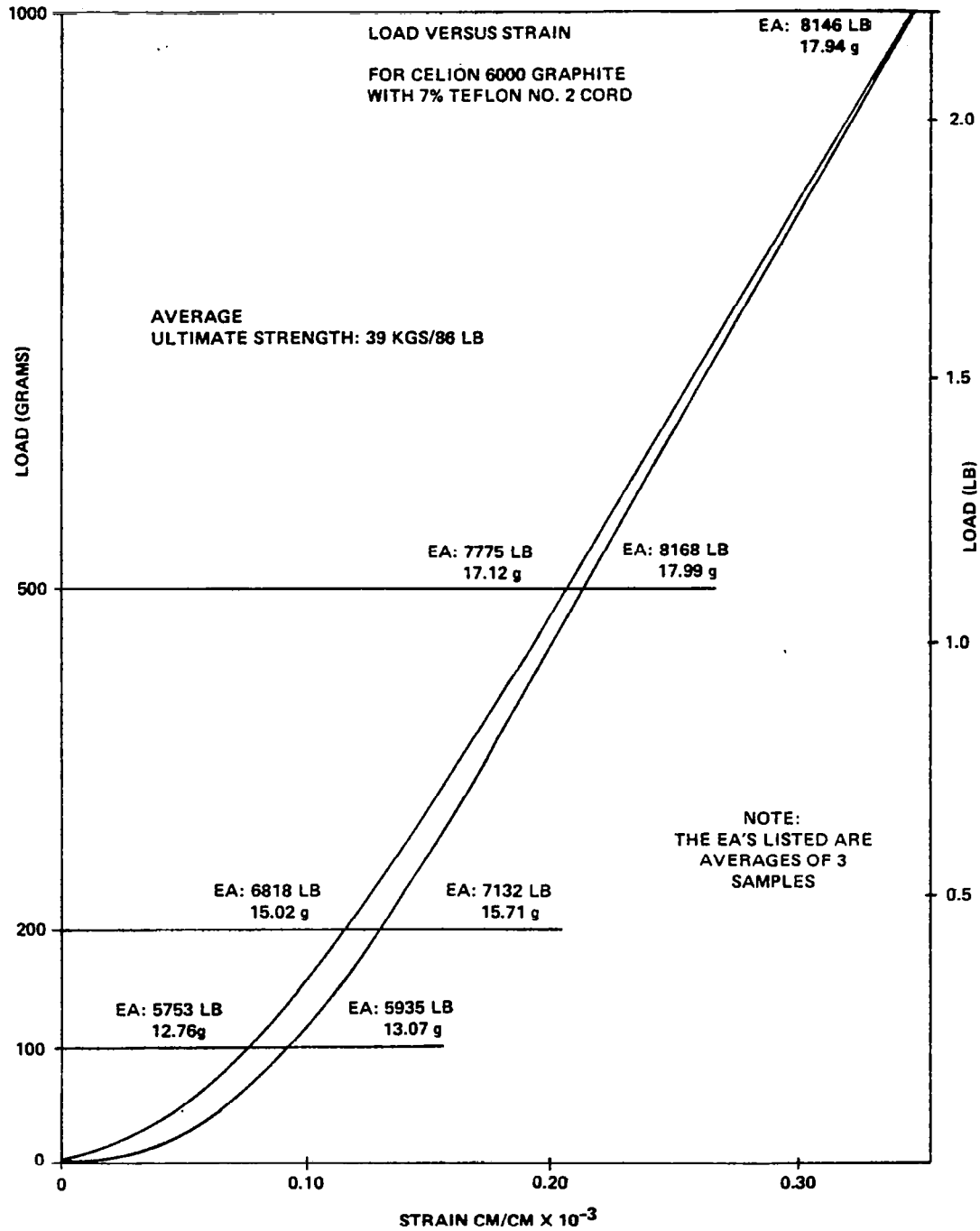


Figure 6.4.4-4. Load Versus Strain for CELION 6000 Graphite With 7% Teflon No. 2 Cord

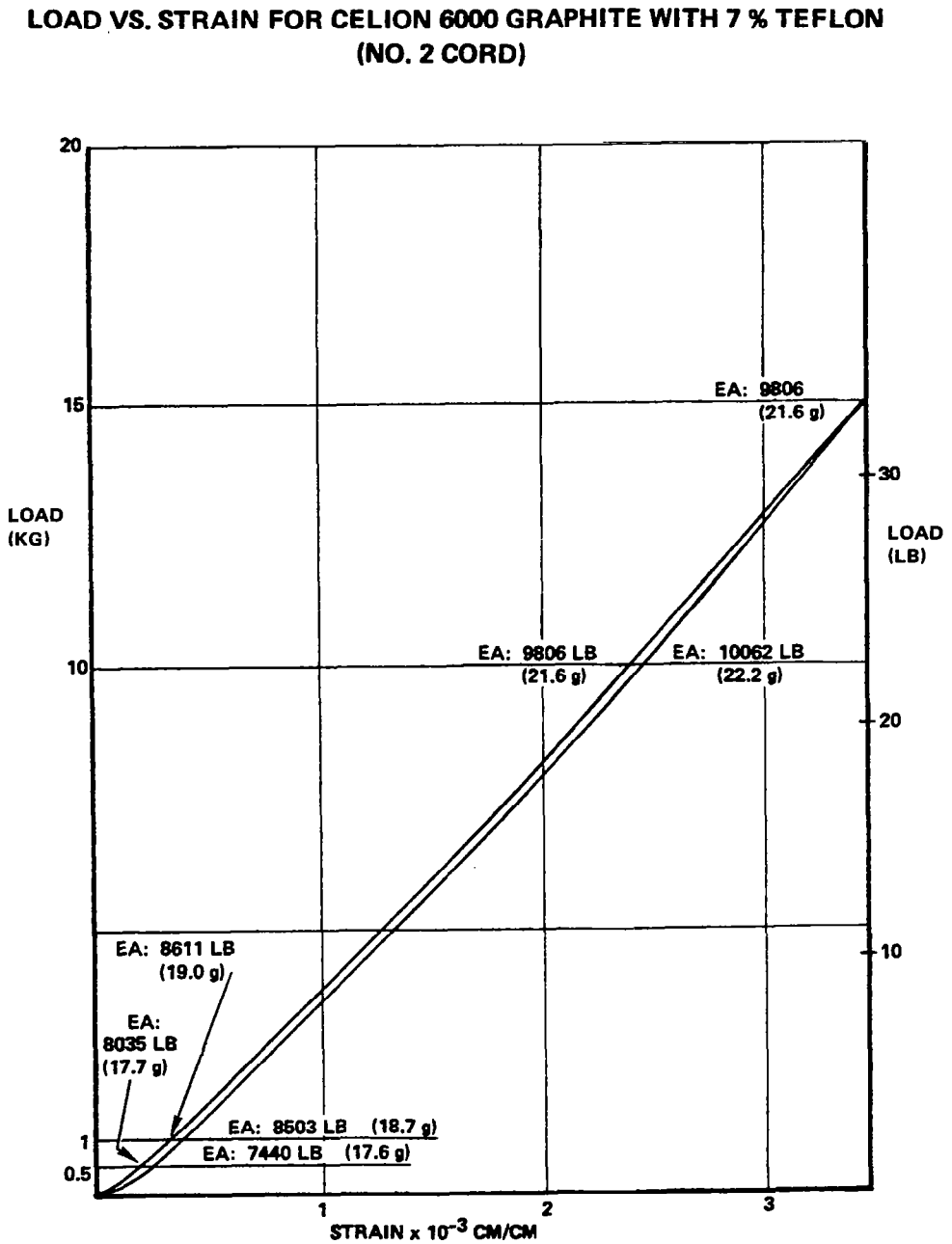


Figure 6.4.4-5. Load Versus Strain for CELION 6000 Graphite With 7% Teflon (No. 2 Cord)

specimens were loaded to failure, yielding an average tensile strength of 39 kilograms (86 pounds). The specimens failed by a catastropic breakage of all fibers at the same moment which could be seen as well as heard. In preliminary testing of cords without Teflon coating, failure did not occur in such a pronounced way but rather with a gradual breaking of fibers due to unequal load sharing, resulting in a total break strength of approximately half of those tested with Teflon coating.

One hundred inch long test specimens were fabricated from the number 2 Teflon coated graphite material for testing of residual strain and coefficient of thermal expansion. The residual strain test data results of three samples are shown in Figure 6.4.4-6. The average residual strain is approximately zero, a very significant result. The deflection versus temperature of three samples is shown in Figures 6.4.4-7 through 6.4.4-9. It can be seen by the curves that good repeatability of strain versus temperature occurs and the resulting coefficient of thermal expansion is very low (approximately $-0.42 \times 10^{-6}/^{o}C$).

## 6.5 Conclusions and Recommendations

The Phase I Material Development Task has identified Teflon coated graphite as a superior cable material for the Hoop/Column antenna design application. The benefits of the material is best described by comparing it witn quartz cables presently being used on existing space deployable antenna structures. This comparison is made in Figure 6.5-1. Graphite offers significant advantages in stiffness (EA) and residual strain. The coefficient of thermal expansion (CTE) of the graphite tested is similar to quartz, nowever, the CTE of graphite may be altered to produce zero $\pm 0.05/^{o}C$. In addition, it is concluded that the Teflon coating used on the graphite has facilitated the development of improved joint designs by being an effective stop of epoxy adhesive wicking.

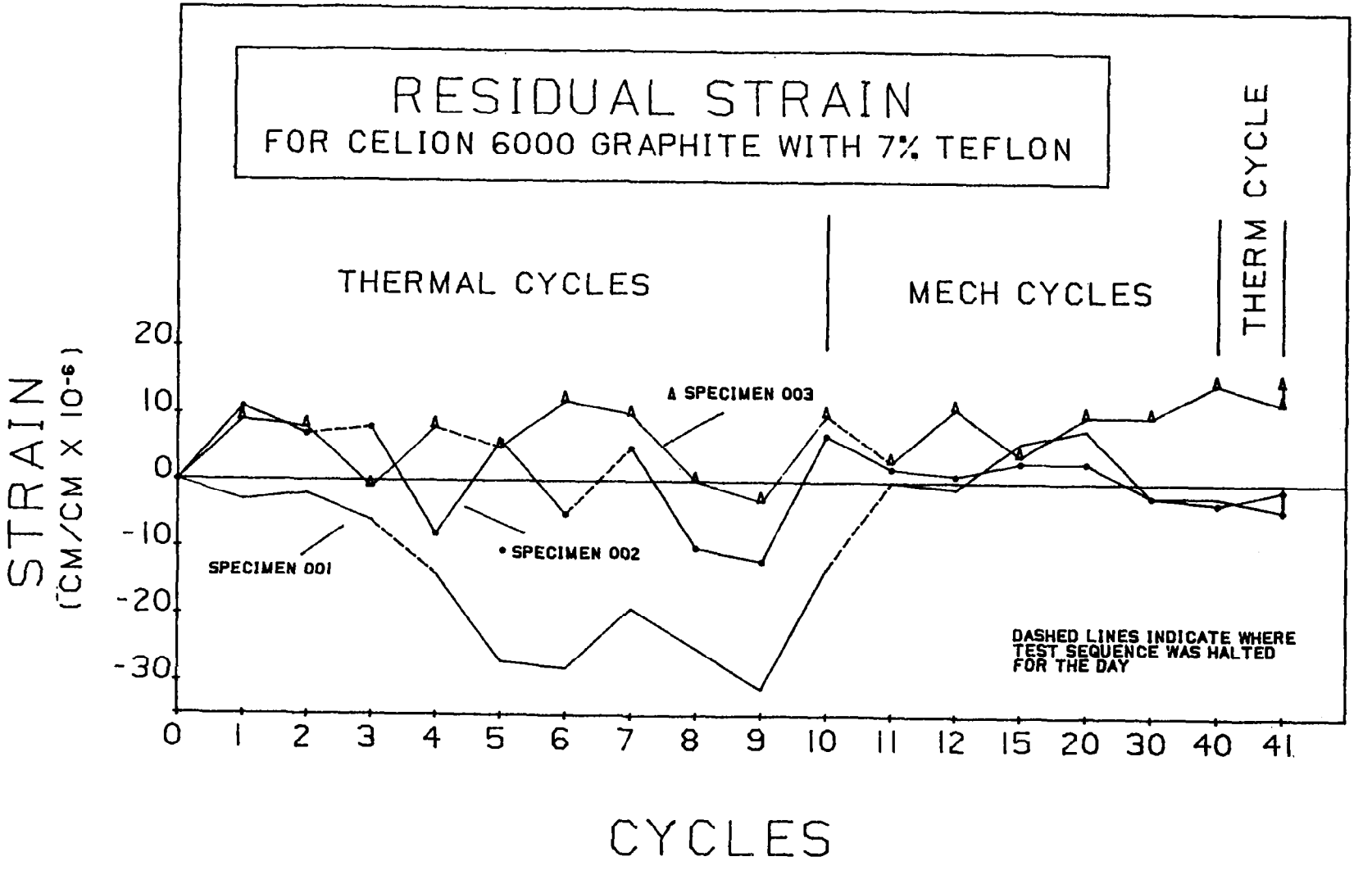


Figure 6.4.4-6. *Residual Strain for CELION 6000 Graphite With 7% Teflon*

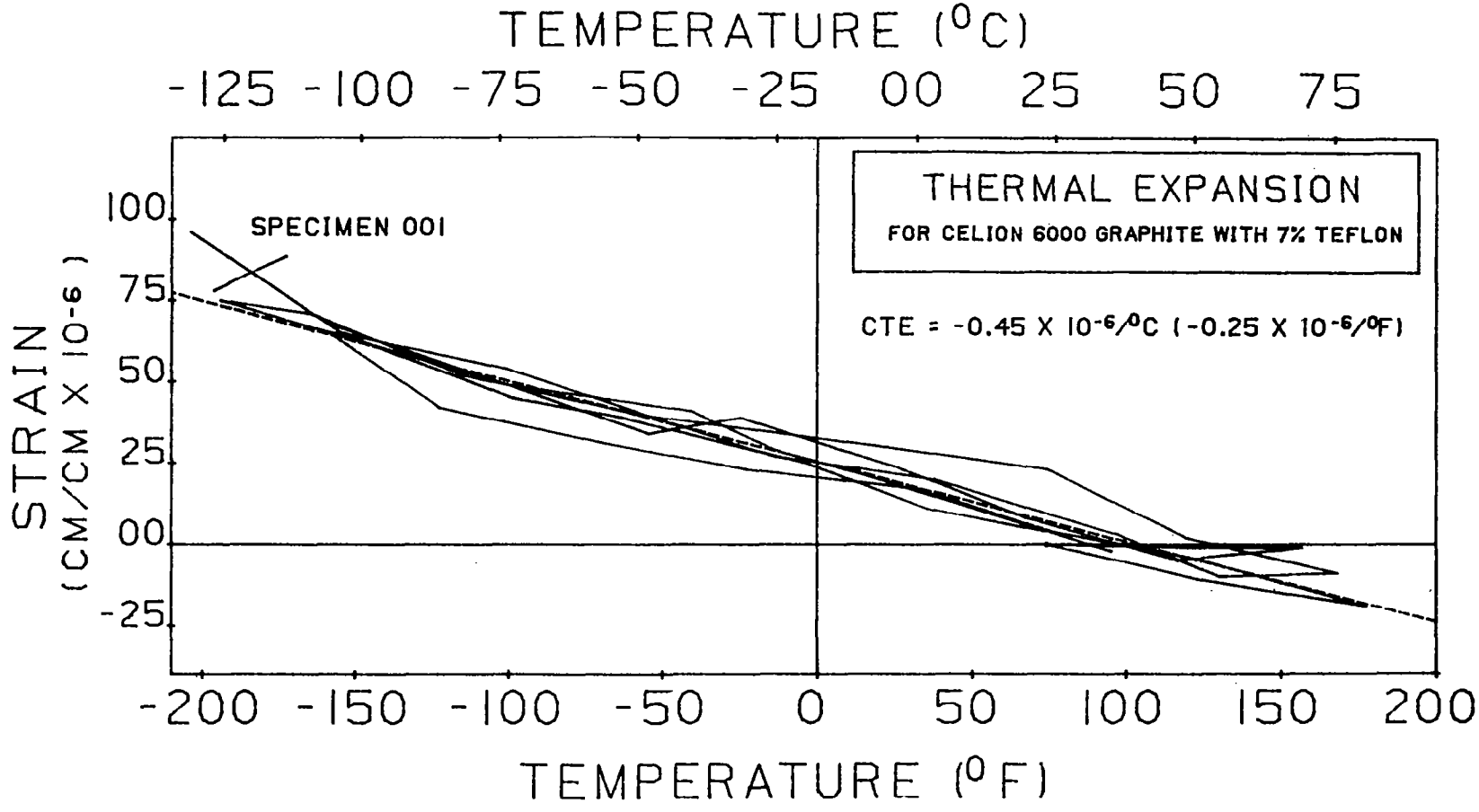


Figure 6.4.4-7. Thermal Expansion for CELION 6000 Graphite With 7% Teflon

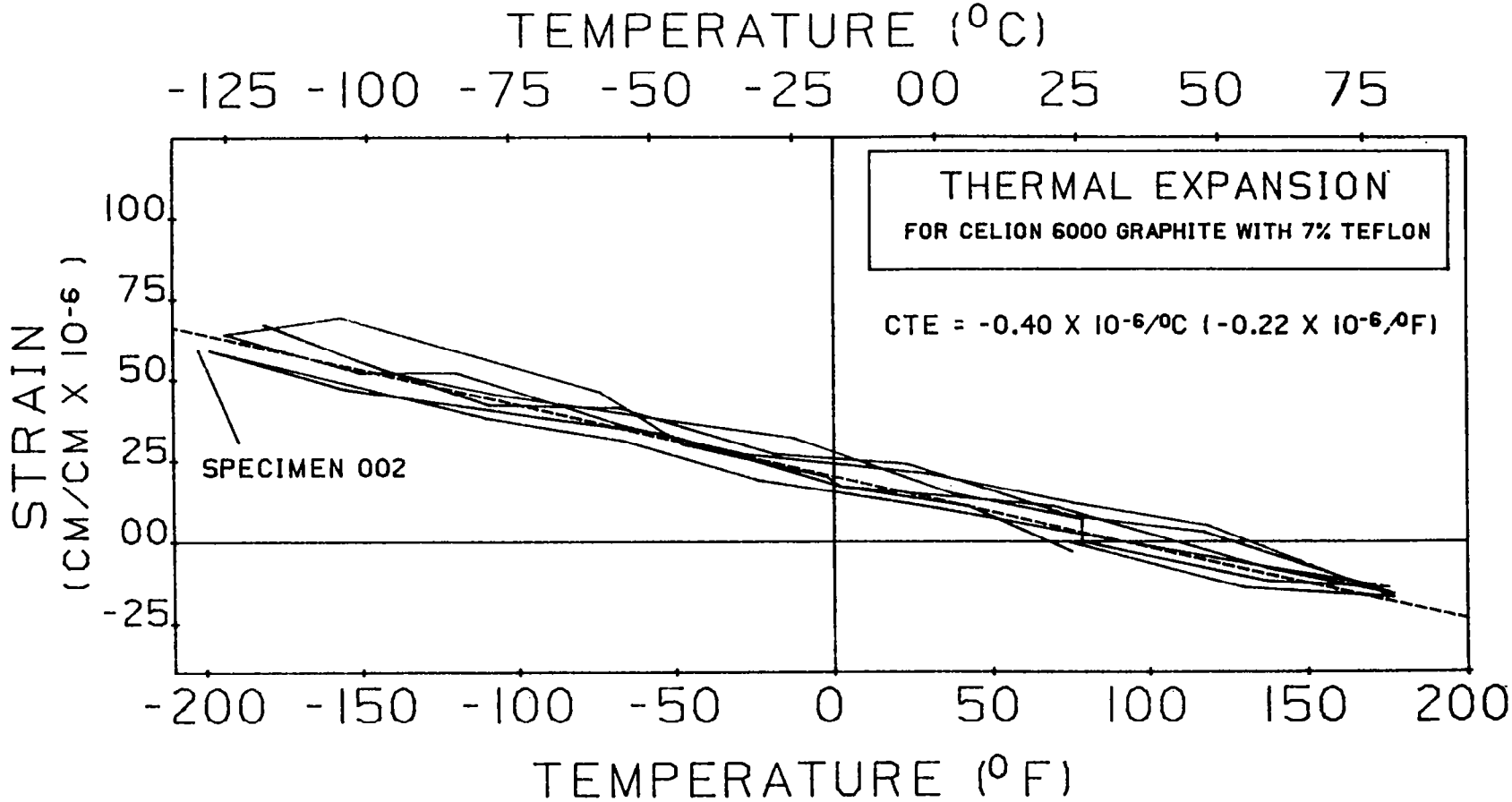


Figure 6.4.4-8. Thermal Expansion for CELION 6000 Graphite With 7% Teflon

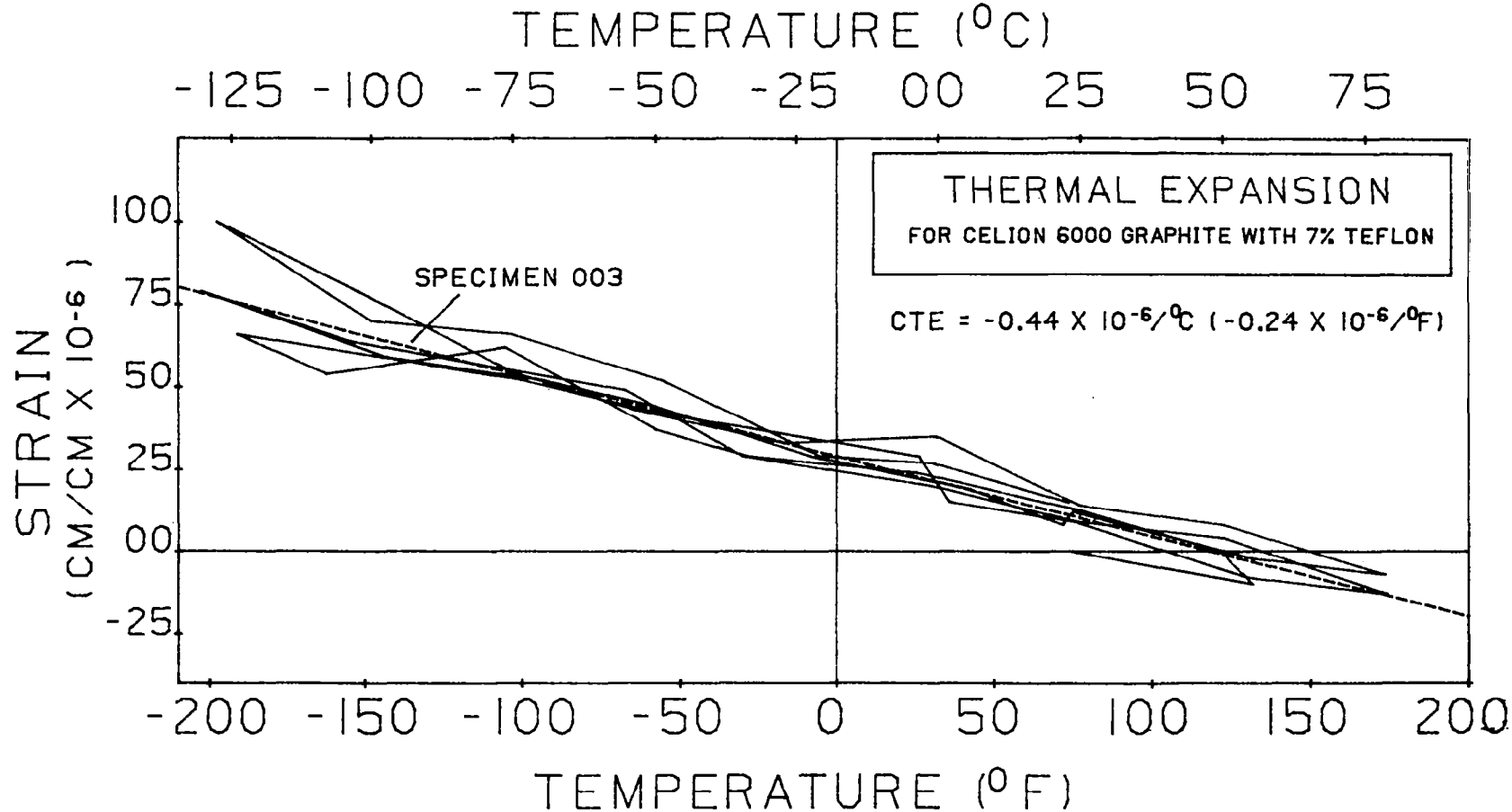


Figure 6.4.4-9. Thermal Expansion for CELION 6000 Graphite With 7% Teflon

## RESULTS SUMMARY (TASK 2)

- THE SELECTED TEFLON COATED GRAPHITE CABLE MATERIAL OFFERS THE FOLLOWING ADVANTAGES COMPARED TO EXISTING QUARTZ CABLE MATERIAL:
  - THREE TIMES HIGHER MODULUS (E)
  - TWICE THE STRENGTH
  - EXHIBITS NO RESIDUAL STRAIN (COMPARED TO 60 MICRO STRAINS FOR QUARTZ)
  - MEASURED CTE OF -0.41/$^{o}$C (-0.23/$^{o}$F) AND OTHER FIBERS FROM MANUFACTURERS WITH PREDICTED ZERO CTE
  - 30% LOWER WEIGHT
  - GOOD HANDLING TOUGHNESS
- TEFLON COATING ON CABLES FACILITATED THE DEVELOPMENT OF IMPROVED JOINT DESIGNS
- DEVELOPED LSST CABLE MANUFACTURING PHILOSOPHY
- DEVELOPED TEST PROCEDURES AND EQUIPMENT

Figure 6.5-1. Results Summary (Task 2)

The number 2 size cables developed in this task are used as singles or multiples for most cable requirements in the Hoop/Column antenna design. Requirements also exist for number 20 and 40 cables for lower and upper hoop control members. Woven and braided samples of these sizes, and without Teflon coating, were fabricated and tested. The results showed unsatisfactory residual strain, EA and strength properties due to poor fiber load sharing. It is recommended that continued development of these larger cables be performed and that the introduction of Teflon coatings be investigated to improve their performance. It is also recommended that more extensive testing be done to develop statistical basis allowables for cable properties.

## 7.0 MANUFACTURING FLOW AND PHILOSOPHY

Harris has developed an integrated approach to the design, production, and testing of space deployable antennas. The production organization consists of a team, ranging from senior engineering personnel to experienced, certified technicians. Production engineering specialist and quality control personnel ensure the antenna is built to specifications and under the proper environmental conditions. Harris production is capable of not only fabricating the antenna but also interfacing with cognizant design and test groups to build a reliable and space qualified antenna.

The LSST 100-Meter Antenna is built from subassemblies. The elements for each subassembly is organized into separate kits for easy construction. Functional testing is performed on the kit elements and completed subassemblies as required. The surface is built to dimension and load in subassemblies. The largest subassembly is planned to be a $60^{o}$ sector of the reflector surface.

In addition to the functional testing, steps are taken to ensure the accuracy and reliability of the antenna. All flight hardware fabrication occurs in clean rooms, and environmental conditions are monitored by quality control personnel. Construction is performed by technicians experienced in the handling of Hi-Rel hardware and lightweight materials such as graphite, aluminum, and titanium. The antenna is built in accordance to specific procedures written by production engineering specialist.

The following is a step-by-step description of the Hoop/Column reflector assembly. The reader should refer to the chart in Figure 7.0-1 to relate the paragraph bubbles to their corresponding illustration on the chart. Figures 7.0-1(a) through 7.0-1(p) further illustrate the assembly flow.

Upper and Lower Cable Storage Segments

The upper and lower cable storage segments consist of four parts: control cables, negator spring spools, and preload and surface control segments.

C1a The cables are arranged into hoop support cables and surface control cable kits. These are laid out under operating tensions and cut to length on tooling tables.

C1b The negator spring spools are assembled simultaneously with the cables.

C1c The preload and surface control cone segments are constructed on tooling tables.

C2a C2b The cables are wound on to the negator spring spools.

C3a C3b The hoop suport and surface control spools are attached to their respective mast segments.

4 The upper and lower cone segments are fastened and aligned to the upper and lower mast assembly, respectively.

Mast

M1 The various components of the mast are sorted into kits and labeled.

M2a The circumferentials and end fittings are assembled on a special tooling plate.

M2b The base plate, consisting of the drive motor, deployment spool and limit switch assemblies is fabricated at this point.

M3 The circumferentials are connected by tubes to make a section of the mast. The diagonals are installed at this point and their proper preload is accomplished by means of their turnbuckles.

(M4) The roller brackets and pulleys are fastened to the structure and adjusted to allow uniform travel of one section within another. The hub half section is then fastened to the base plate assembly.

(M5) Each segment is then assembled to its respective adjacent outer segment. Alignment of the segments, roller, and pulleys are verified at this time and the cable is installed.

(M6) Each segment is deployed with respect to its adjacent segment and latch alignment is checked.

(M7) The mast subassembly is stowed and stop alignment is attained. One-half of the structural mast is now complete; the other half is done in the same manner.

(M8) The two mast halves are mated at the midring and the stowed assembly of the structural mast is complete.

Hoop

The hoop is made up of four basic assemblies: pivot arm, hinge platform, graphite tubes, and synchronizing strips.

(H1) The elements for each assembly are labeled and sorted into their appropriate kits.

(H2) Each kit is then assembled on a tooling table.

(H3) The pivot arms are bonded to their respective GFRP tube to form a hoop segment. A tooling table is used to ensure the correct hoop segment length is maintained.

(H4) Two hoop segments are joined by a common hinge frame assembly and pushrod. One hinge frame is jointed to the adjacent hinge frames by synchronizing strips. Eight 6-segment sections are built up in this manner.

(H5) Linear activators located $90^{0}$ apart in the final assembly are fastened to four of the 48 hinge platforms.

Surface

The surface is fabricated from three types of assemblies: surface cord assemblies, radial truss assemblies, and mesh assembly.

(S1) Cords for the various assemblies are sorted and labeled along with their end fittings.

(S2) The diagonal cords are laid out on a tooling table, loaded to their operating tension and cut to proper length.

(S3) The surface cords are built up in panels. The outer panel is laid out on a tooling surface, loaded, and bonded. The diagonals are also bonded to the surface cords at this level. After the outer panel is bonded, the middle panel is laid out and bonded in the same manner. This is repeated for the inner panel.

(S3a) On a separate tooling surface, the radial trusses are laid out, loaded to their operating tensions, and bonded.

(S4) The mesh is placed over the surface cords, stretched to its operating tension field, and fastened to the surface cords.

(S5) The surface is now attached to the hoop and mast and built up to complete a 6-gore segment of the antenna. Two gores and a radial truss are joined at the same time. The radial truss cords are sandwiched between the gore-to-gore interface fittings. The panel assemblies are then tied to the antenna hub and their respective hoop segments.

Surface control and hoop support cables are deployed from the preload and surface control segments and fastened to the surface cords and hoop.

(S6) The 6-gore antenna segment is partially stowed by running the hoop segment in along a radial track.

The hoop skewers are aligned with the five parallel tooling cords which gather the mesh as the hoop is stowed.

(S7) The above procedure is repeated eight times to produce eight 6-gore sections of the antenna. Each new 6-gore section is partially stowed and fastened to the previous section until the antenna is complete.

(S8) The hoop and surface is then completely stowed.

(S9) The restraint cones, upper and lower, are attached to their respective interfaces and the reflector assembly is complete.

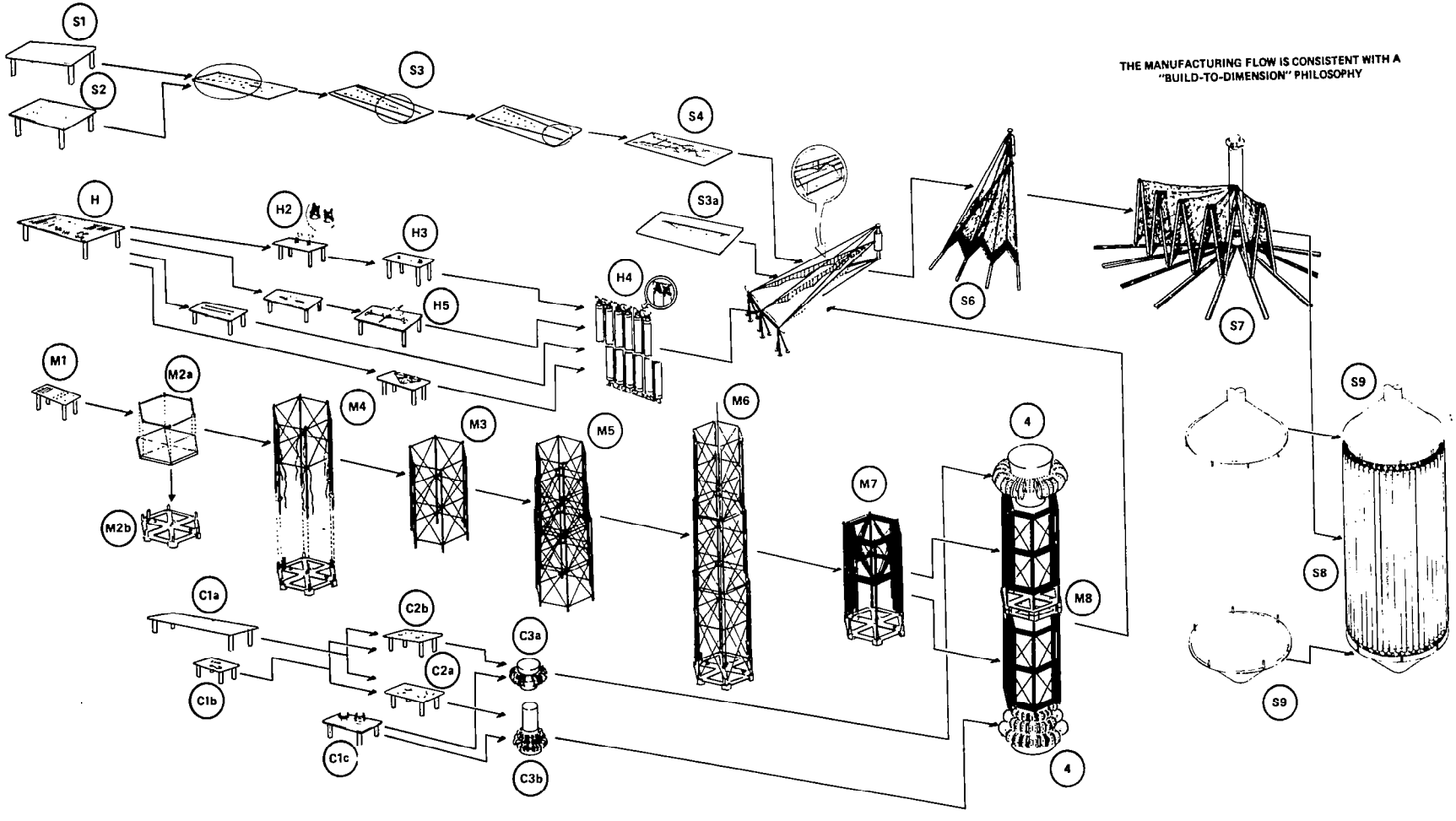


Figure 7.0-1. The Manufacturing Flow is Consistent With a "Build-to-Dimension" Philosophy

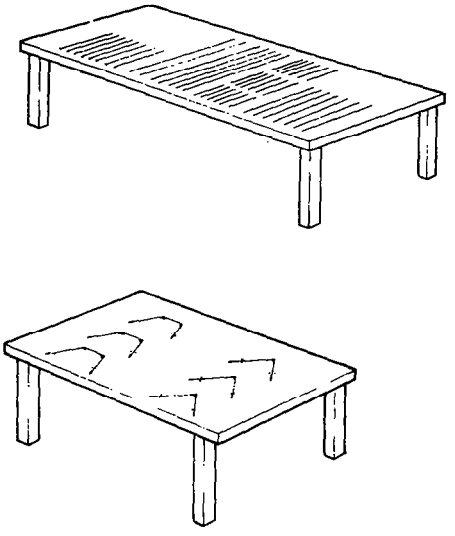

Figure 7.0-1(a). Surface Kits

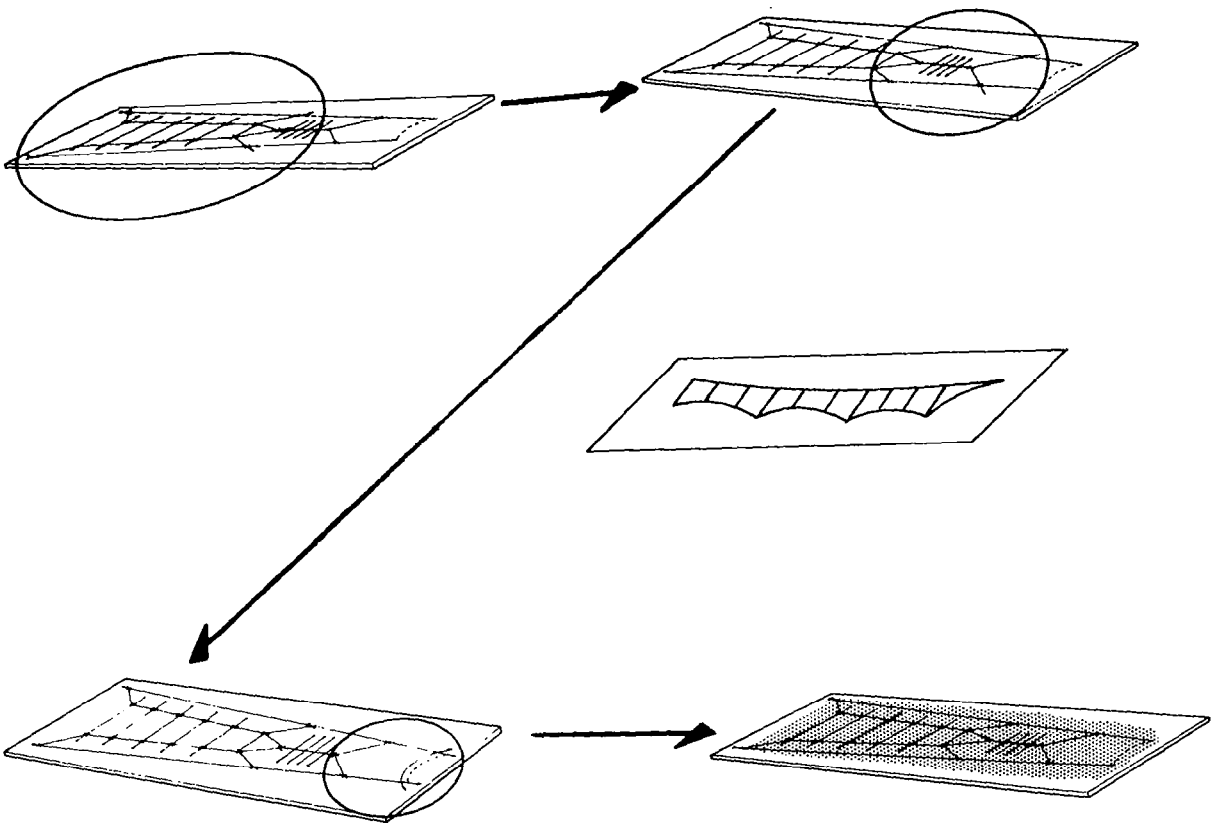

Figure 7.0-1(b). Surface Subassemblies

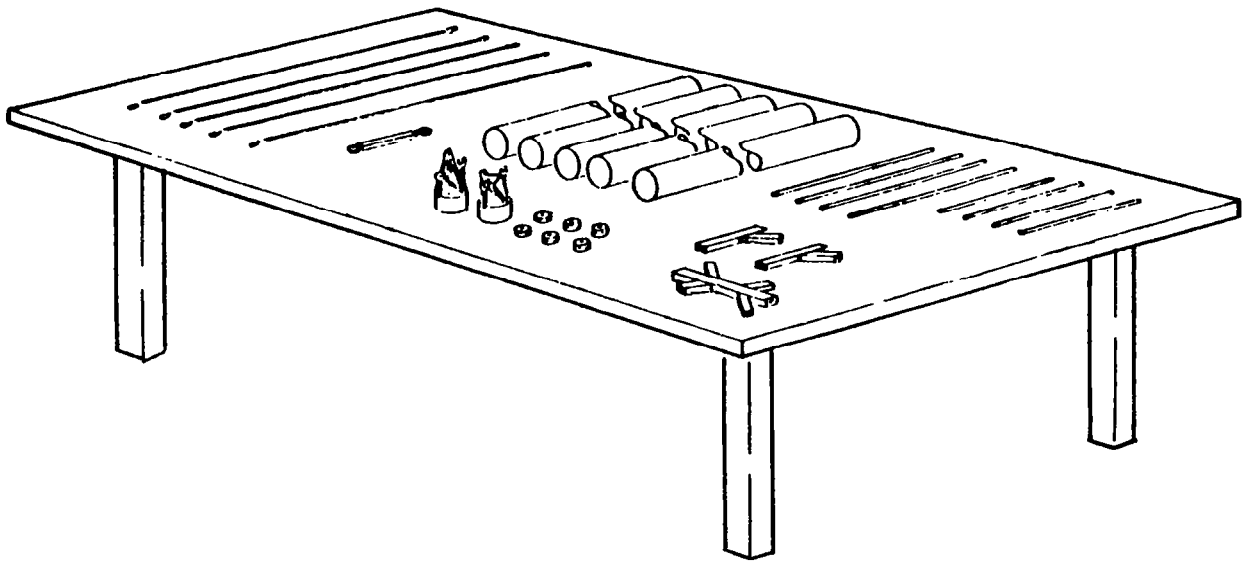

Figure 7.0-1(c). Hoop Kits

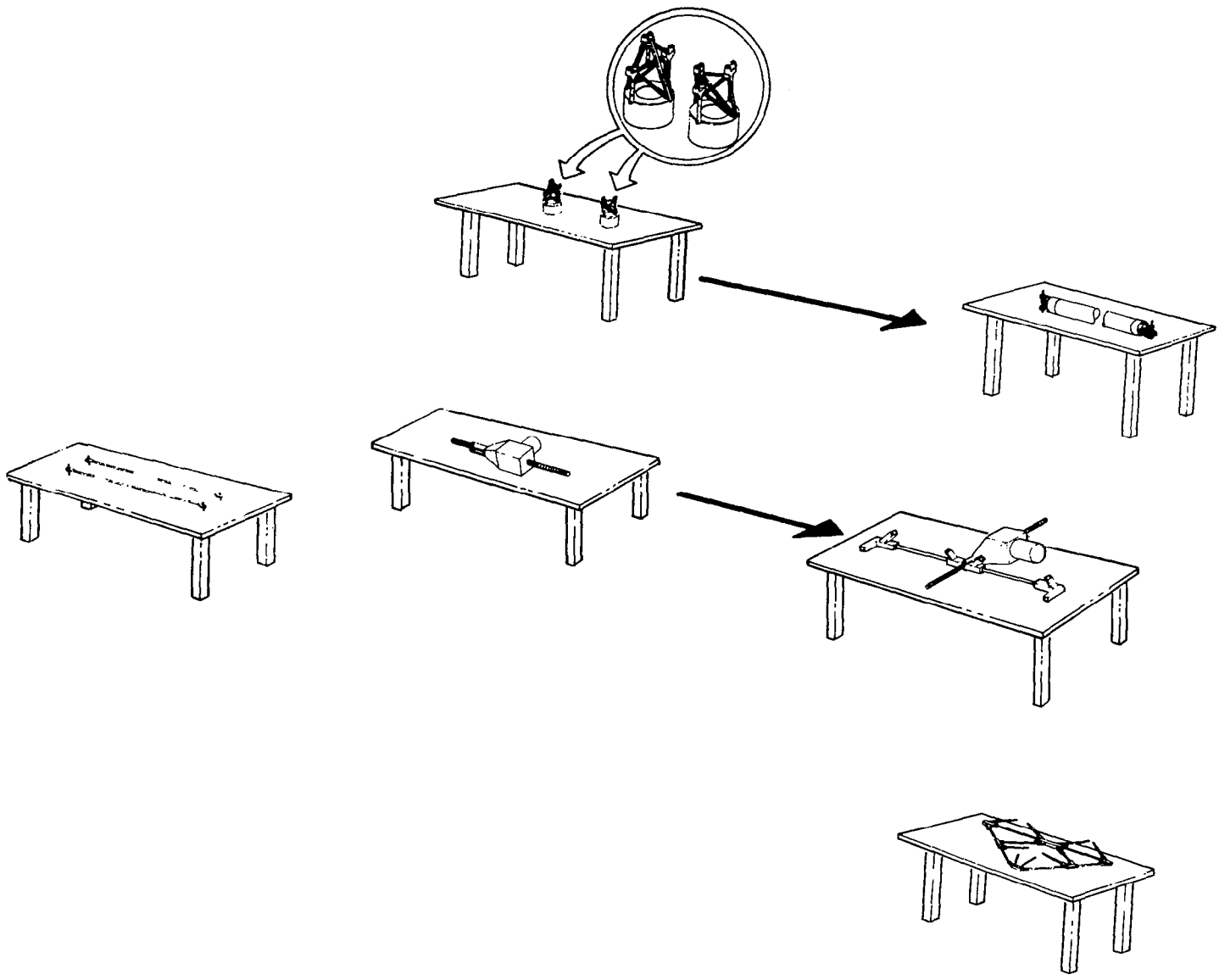

Figure 7.0-1(d). Hoop Fitting/Segment Subassemblies

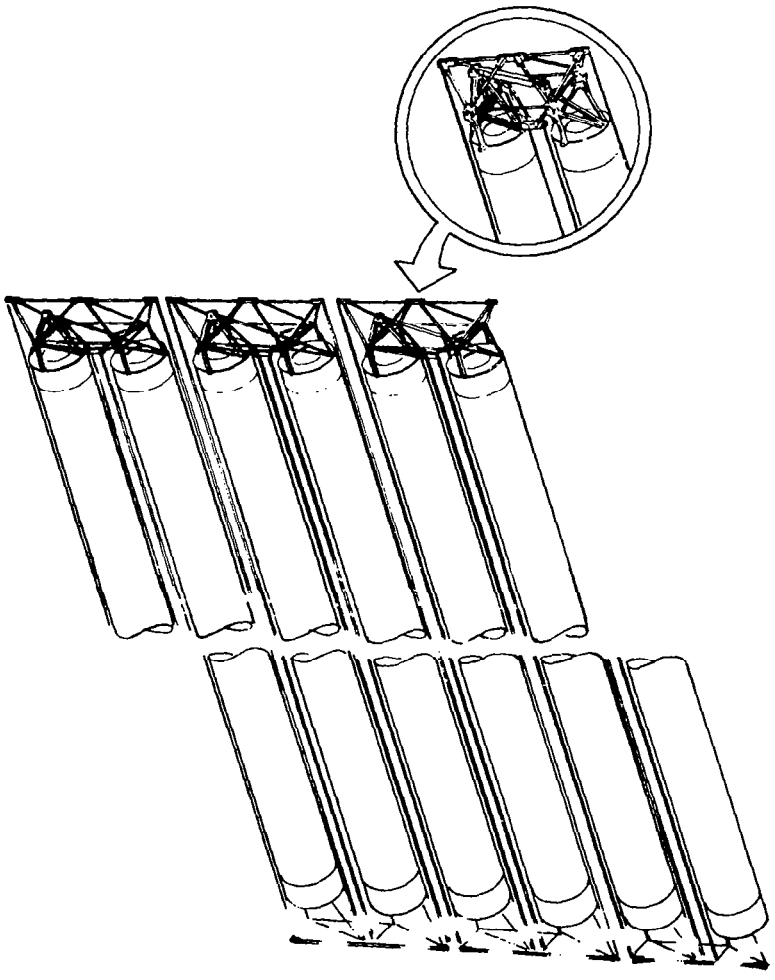

Figure 7.0-1(e). Hoop Subassembly

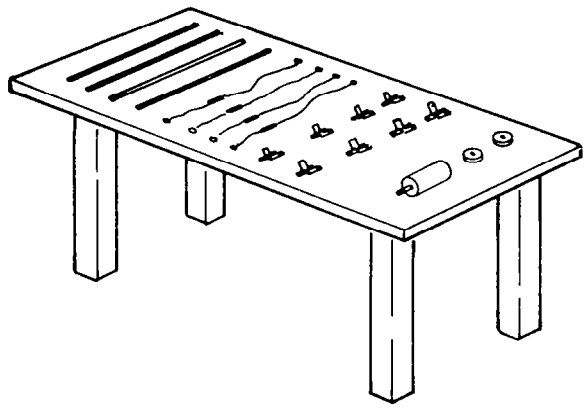

Figure 7.0-1(f). Mast Kits

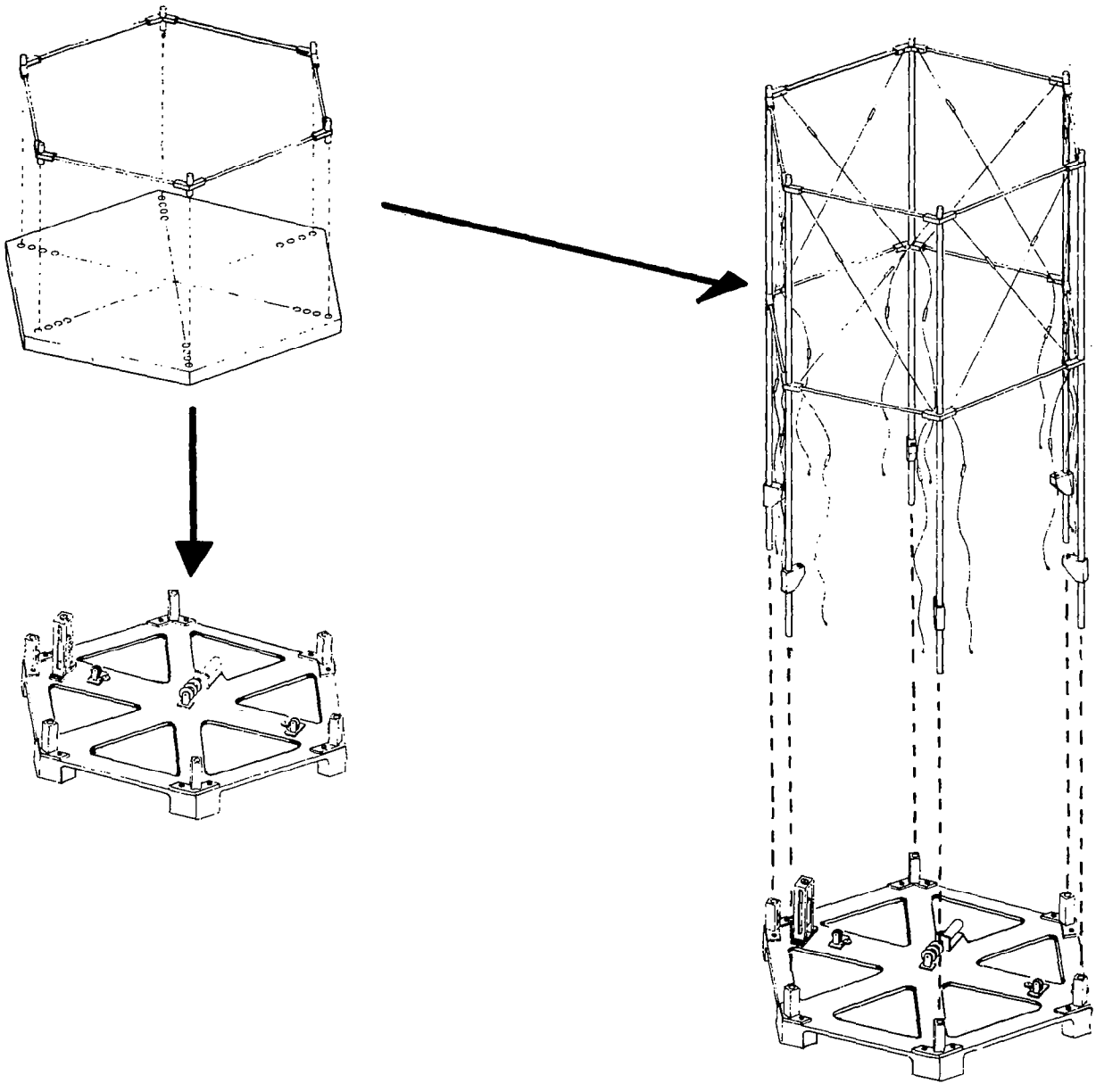

Figure 7.0-1(g). Hub Assembly

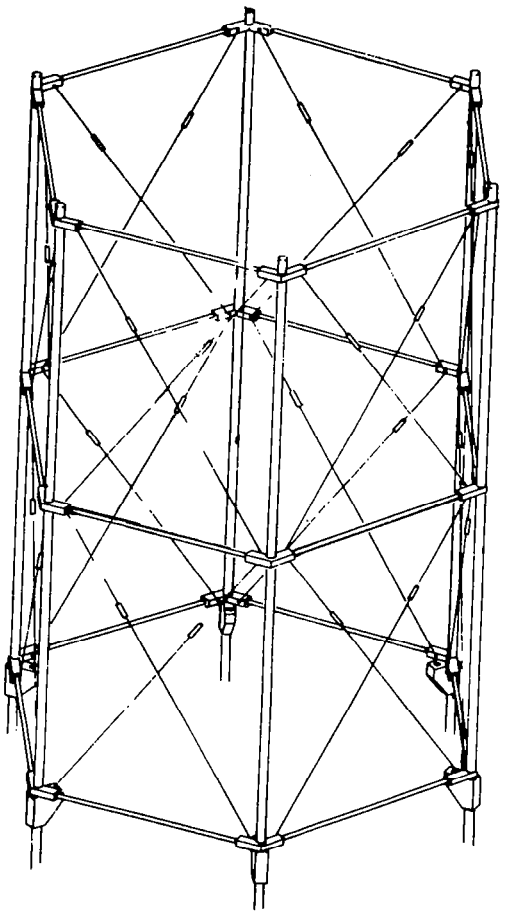

Figure 7.0-1(h). Typical Segment Assembly

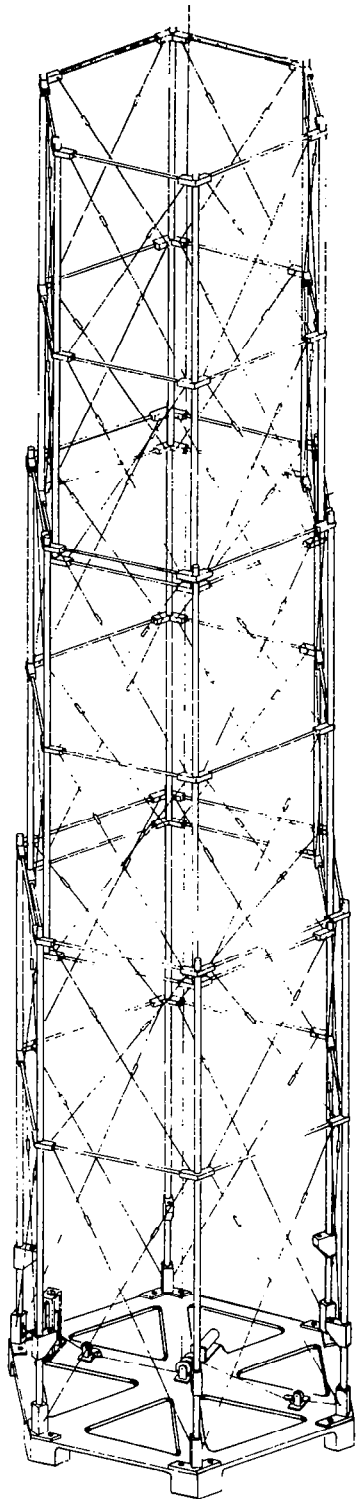

Figure 7.0-1(i). Mast Subassembly and Alignment

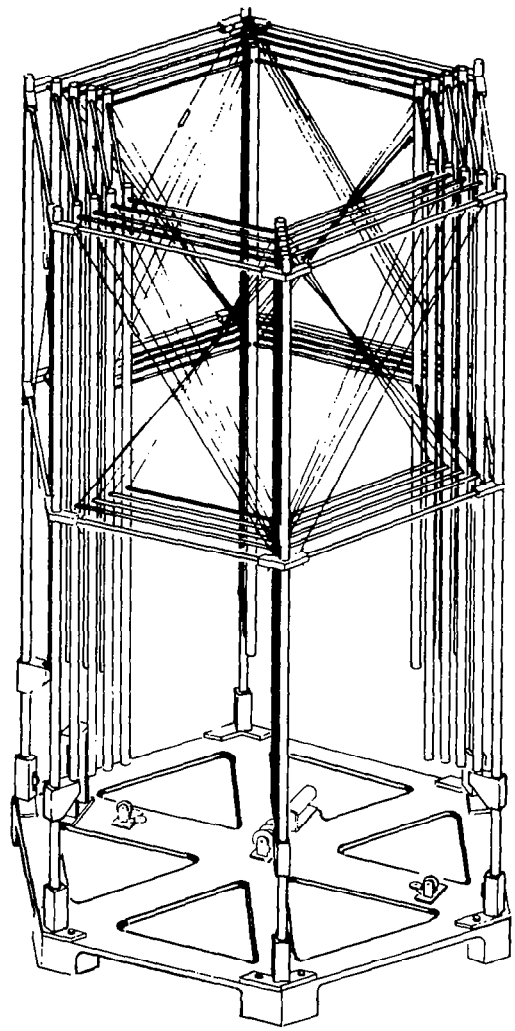

Figure 7.0-1(j). Mast Stowed Assembly and Alignment

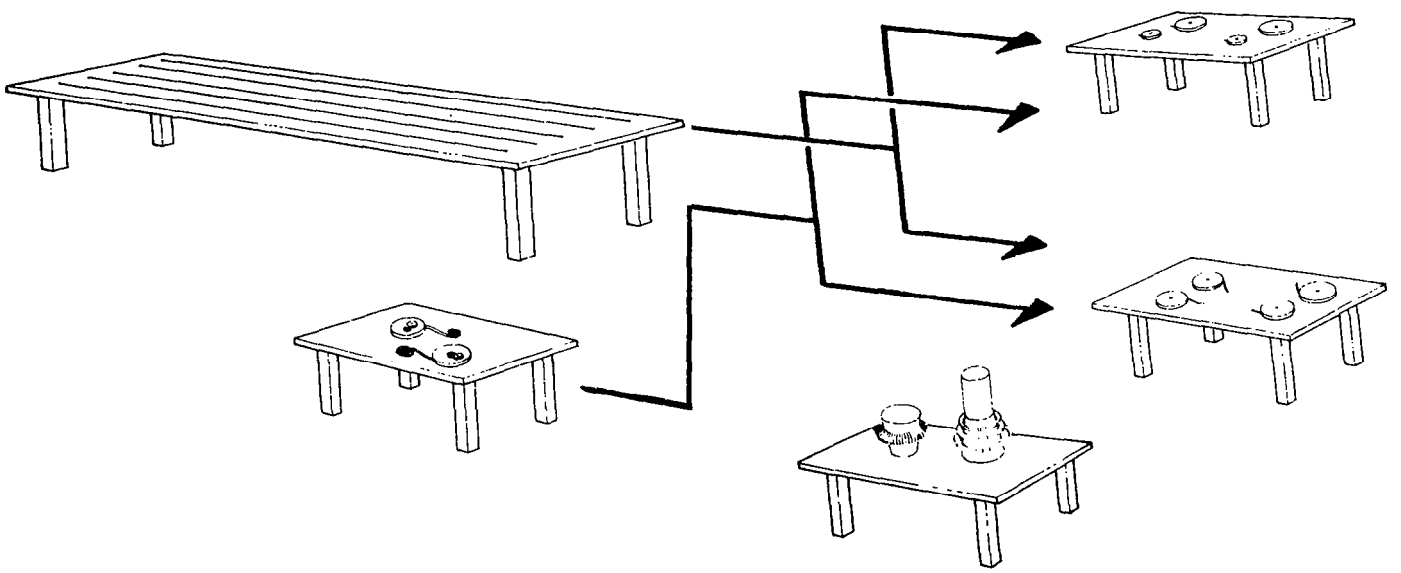

Figure 7.0-1(k). Control Cable Kits

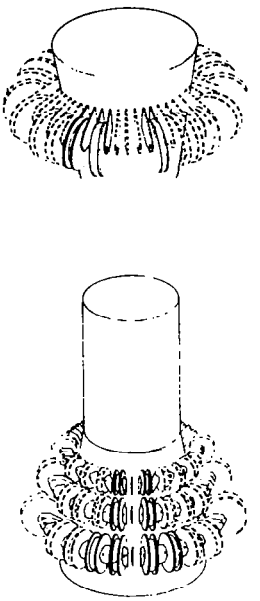

Figure 7.0-1(1). Cable Storage Segments Final Assembly

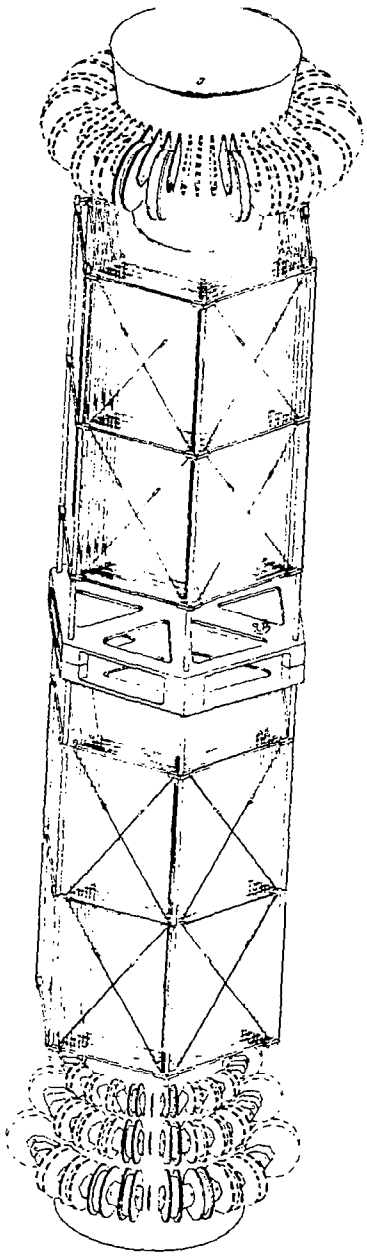

Figure 7.0-1(m). Hub/Mast Final Assembly

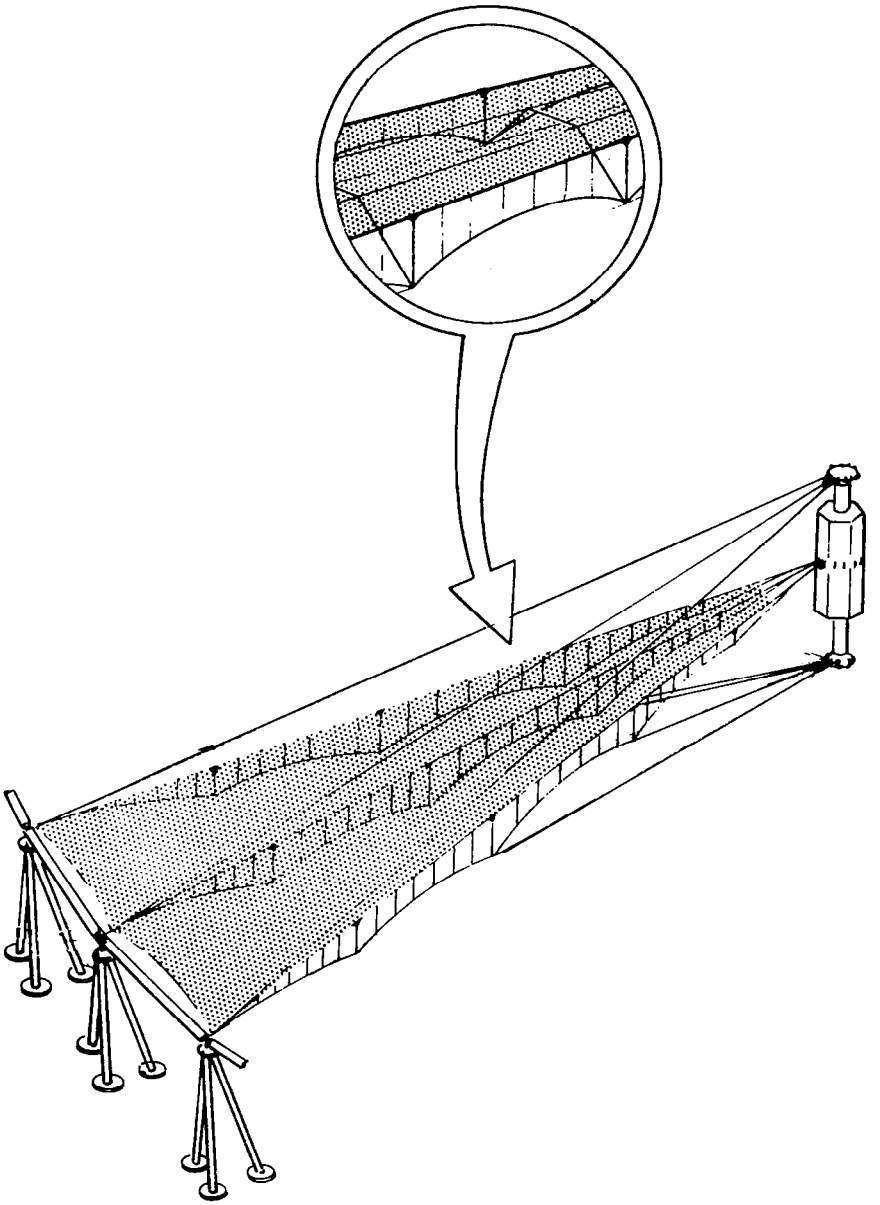

Figure 7.0-1(n). Surface to Structure Integration

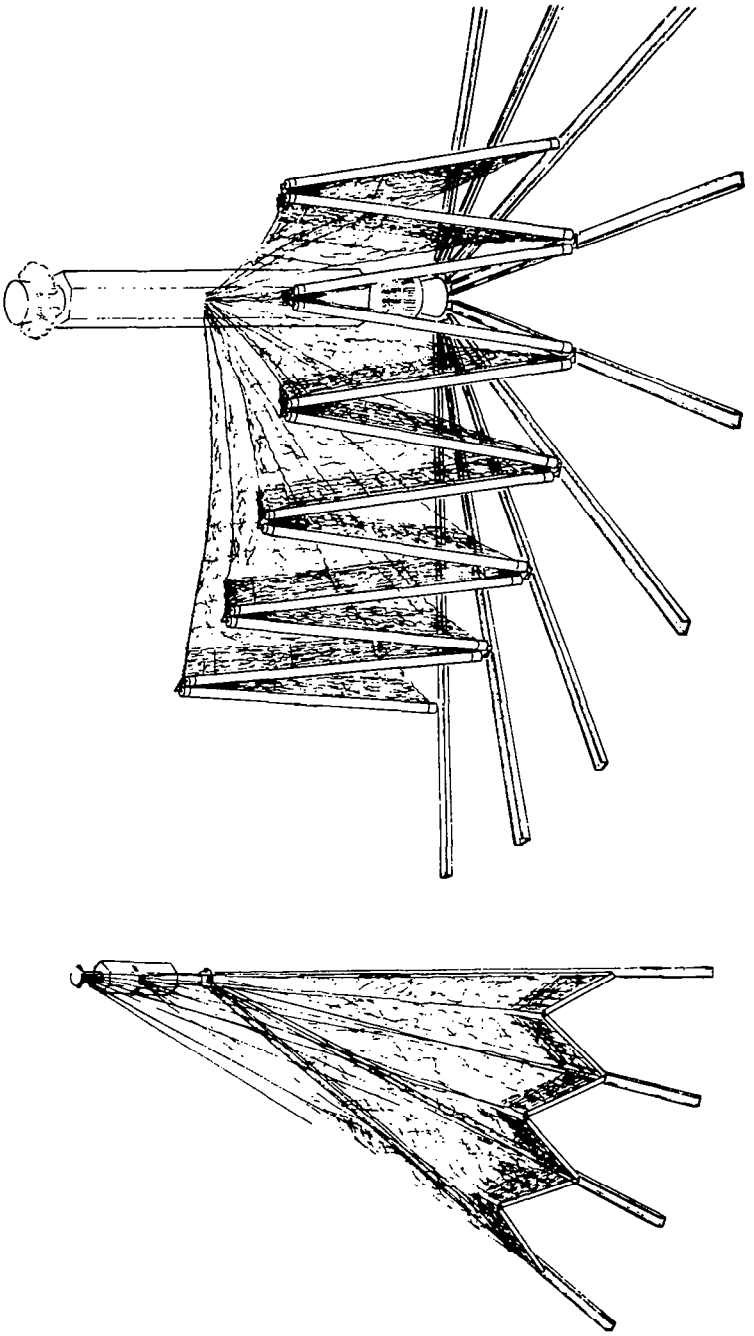

Figure 7.0-1(o). Gore-to-Gore Assembly

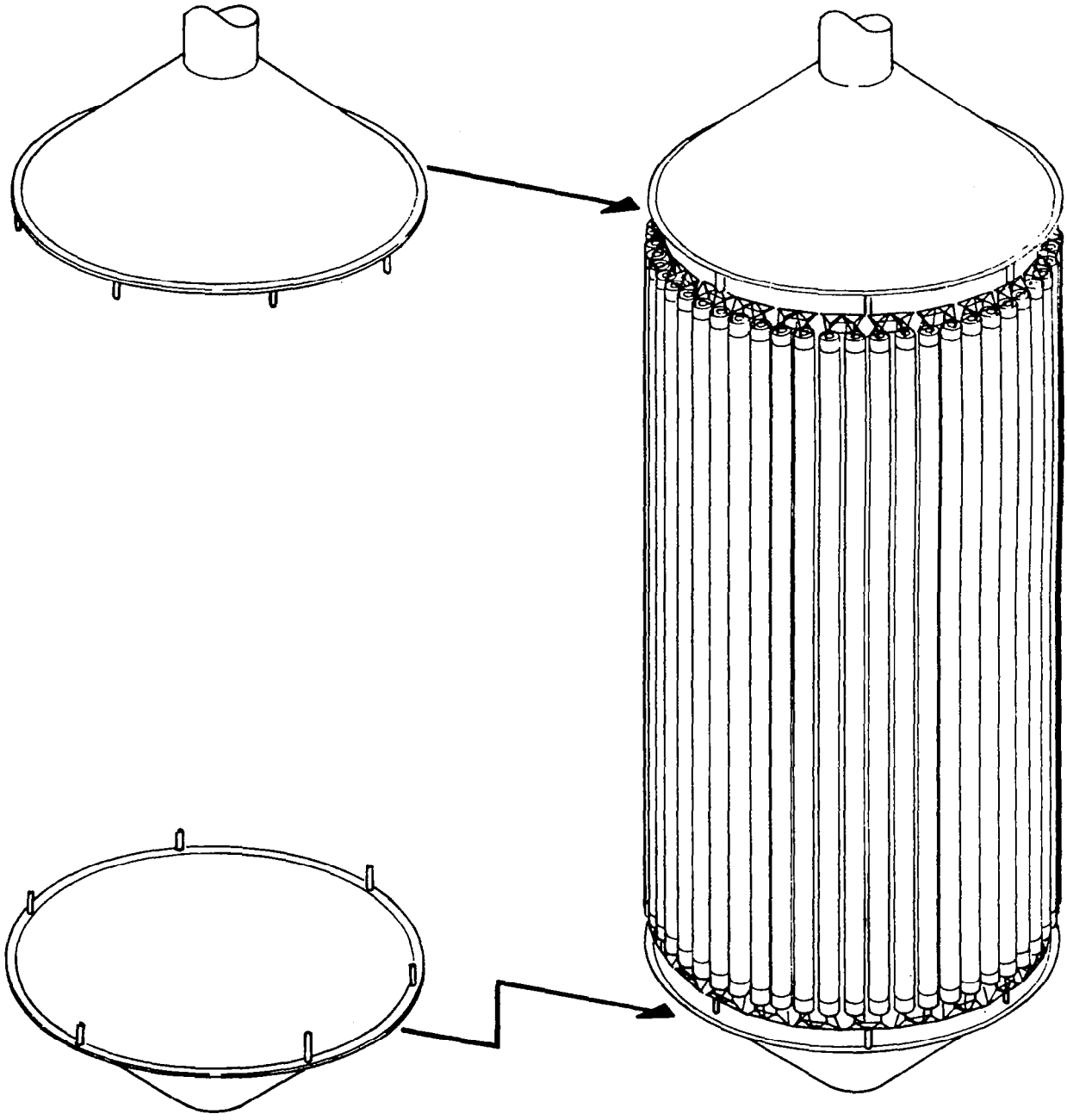

Figure 7.0-1(p). Stowed Reflector Final Assembly

# 8.0 TEST PLAN

## 8.1 Introduction

This test plan presents the verification test program for the LSST Hoop/Column Antenna design. The plan includes the test philosophy, the test flow for the Antenna System, a description of the test facilities required, and summary descriptions of the test performed.

The purpose of this plan is to define a coordinated verification test program during the early phase of the LSST Hoop/Column Antenna Program. The test plans and flows are improved, modified and corrected as the design matures. A summary of the test plan objectives are presented in Figure 8.1-1.

## 8.2 Test Philosophy and Approach

The LSST Hoop/Column Antenna test program provides a cost-effective approach to assuring a qualified flight design. Therefore, the philosophy used in developing the test program emphasizes the following points:

- Maximize ground testing for verification of the antenna design.
- Maximize testing to verify the analysis tools and methods to be used for orbital performance predictions.
- Identify those areas of performance that can only be verified by full scale flight tests and show how ground testing minimizes the risk in these area.
- Define the test program to be fluid in order to accommodate changes in the design as the design evolves.

The nature and size of the LSST Hoop/Column Antenna requires the development of a test program which emphasizes component and subassembly tests versus full assembly tests. Subassembly full scale and scale model tests are included in the program to verify the design performance and to verify the analysis which will be used for full scale performance predictions. The combination of an extensive subassembly test program with the analysis (verified by test) provides a logical and complete approach to qualifying the Hoop/Column Antenna for flight.

- **OBJECTIVE**
  - DEFINE A COORDINATED VERIFICATION TEST PROGRAM FOR DEVELOPMENT OF THE LSST HOOP/COLUMN ANTENNA
  - DEFINE THE ACCEPTANCE TEST PROGRAM FOR THE FULL SIZE LSST HOOP/COLUMN ANTENNA
  - PRESENT THE TEST PHILOSOPHY APPLIED TO THE LSST HOOP/COLUMN ANTENNA PROGRAM

Figure 8.1-1. Summary of Test Plan Objectives

To accomplish these test objectives, the following summarizes the major elements of the test program:

- Development of component/element material properties data base. The existing antenna component data base is expanded as required to cover new design elements. Test results from Task II of this study program provide significant inputs to this data base.
- Element and subsystem development tests for the purpose of validating the design concept and providing analysis correlation data for use in the design and performance analyses.
- Two major models to verify the design concept and provide analysis correlation data. These models have been defined as: 1) 50-Meter Surface Model, and 2) 15-Meter Model.
- Qualification and acceptance tests of the components and subassemblies during manufacturing and assembly.
- Acceptance testing of the stowed full assembly prior to delivery.
- Flight testing of a model or full assembly to verify the performance and analysis prediction.

## 8.3 Test Description

This section presents an overview of component, subassembly and full assembly testing of the LSST Hoop/Column Antenna (see Figure 8.3-1).

The top-level assembly test flow is shown in Figure 8.3-2. The flow is consistent with the manufacturing flow described in Section 7.0. It consists of the four major test areas of Mast, Hoop, Surface and Models which converge to final testing of the full antenna assembly. Addition breakdown of required component level tests is given in Figure 8.3-3. With the exception of spools, pulleys, and rollers, all of the identified component level tests have been performed by Harris or Harris vendors on previous programs.

# LSST POINT DESIGN – DEPLOYED

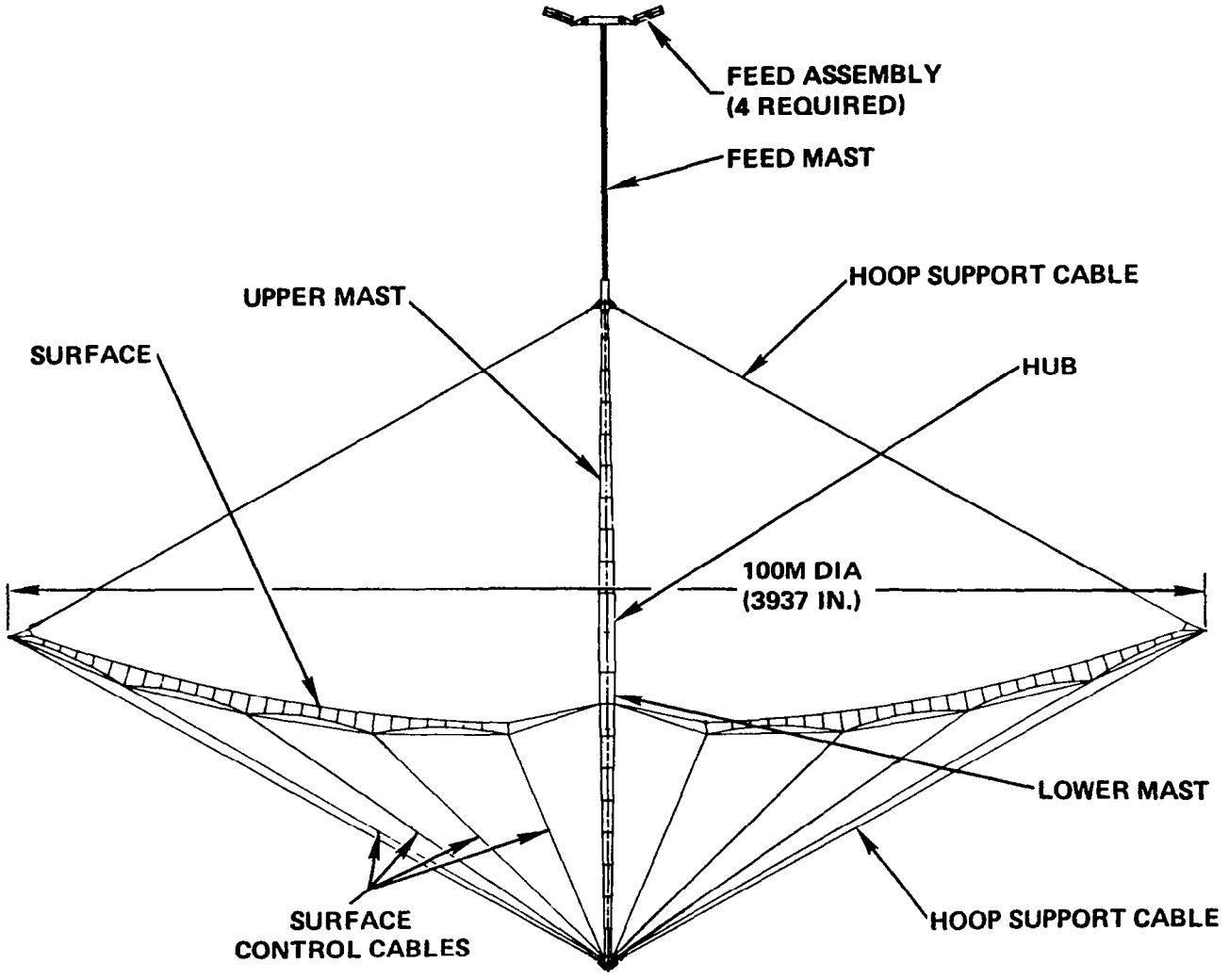


Figure 8.3-1. LSST Point Design - Deployed

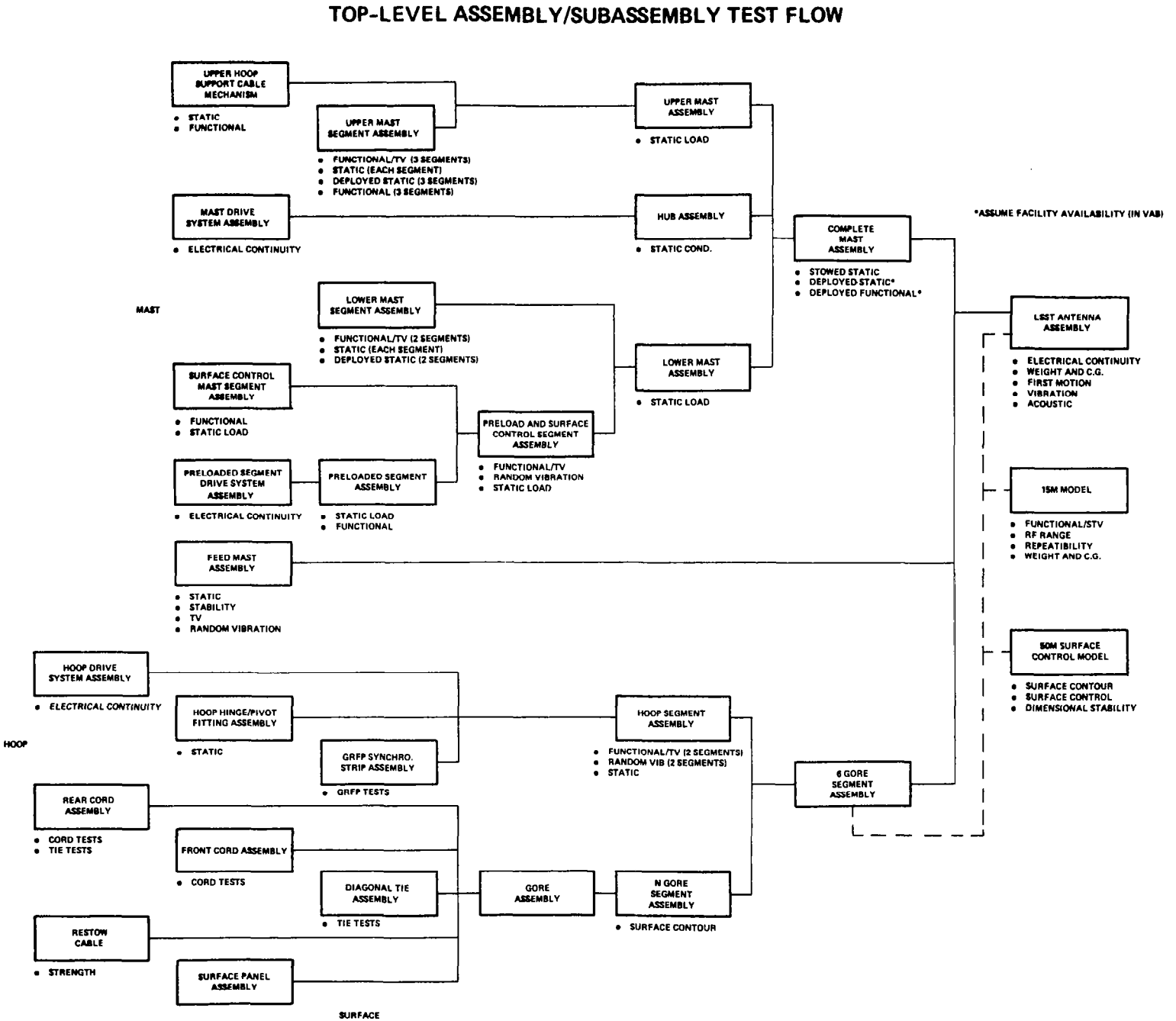


Figure 8.3-2. Top-Level Assembly/Subassembly Test Flow

Graphite

- Graphite components used for:
  - Tubes
  - Synchro strip
  - Shell
- Tests include:
  - Structural properties
  - Thermophysical properties

Drive Motors

- Drive motor components used for:
  - Hoop drive motors
  - Mast drive motors
  - Preloaded segment drive motors
  - Surface control servo drive motors
- Tests include:
  - Functional/TV
  - Random vibration
  - Backdriving torque

Mesh Wire

- Mesh wire component used for:
  - Mesh surface
- Tests include:
  - Tensile
  - Plating

Mesh

- Mesh component used for:
  - Surface
- Tests include:
  - Stiffness
  - RF reflectivity
  - Weight
  - Transmissivity
  - Microscopic examination

Figure 8.3-3. Component Level Tests (Sheet 1 of 3)

Spools, Pulleys, and Rollers

- Spools, pulleys, and rollers used for:
  - Mast deployment
  - Hoop support
  - Surface control
  - Mesh restraint system
- Tests include:
  - Functional/thermal-vacuum
  - Structural properties
  - Thermophysical

Ballscrews/Worm Gears/Push Rods

- Ballscrews, worm gears, and push rods used for:
  - Hoop drive system
  - Preloaded drive system
- Tests include:
  - Static loads

Cords/Cables

- Cords and cables used for:
  - Surface control
  - Hoop support
  - Retension system
  - Mast deployment
  - Tie assemblies
- Tests include:
  - Structural properties
  - Thermophysical properties
  - Residual strain
  - Joint strength

Figure 8.3-3. Component Level Tests (Sheet 2 of 3)

Latching Mechanisms

- Latching mechanisms used for:
  - Deployed mast
  - Deployed upper hoop support cable segment
- Tests include:
  - Dynamic loads
  - Static loads
  - Functional

Limit Switches

- Limit switches used for:
  - Mast drive system
  - Preloaded segment drive system
- Tests include:
  - Functional

Turnbuckles

- Turnbuckles used for:
  - Diagonal mast assembly
- Tests include:
  - Structural properties

Figure 8.3-3. Component Level Tests (Sheet 3 of 3)

Key subassembly level tests identified are:

- 50-Meter Surface Model tests
- 15-Meter Model tests
- N Gore surface contour test
- 3-Mast segment development tests
- 2-Mast segment development tests
- 2-Hoop segment development tests

These test activities are summarized in the following paragraphs.

The 50-Meter Surface Model tests verify feasibility of manufacturing large areas of mesh with ties and cords. This is performed by surface contour measurements and measuring tensions in surface control cords. The surface control cords are adjusted and surface contour measurements made to obtain surface enhancement capability data.

The 15-Meter Model is tested to verify antenna performance since a test of the completely assembled 100-meter antenna would be impractical to perform on the ground. Identified 15-Meter Model tests are functional/STV test, a RF range test, and a repeatability test. A weight and CG test are defined to help scale the 15-Meter Model with the full assembly.

The N gore surface tests provide contour tests for every section of surface at every level of testing up to and including acceptance tests. These tests qualify the surface before being installed on the complete 100-meter assembly.

The three-mast segment test includes static loads and functional development tests which verify the mast operation and structural margin. These tests allow the middle mast section to behave in a realistic fashion due to imposed boundary conditions.

Two segments of the mast and hoop are tested in thermal/vacuum conditions. A functional development test is performed under these conditions to verify the hoop and mast operation.

Additional details of the above defined tests are given in the appendices.

### 8.3.1 Acceptance Tests

The acceptance tests are better defined as the program evolves, but an initial test flow is shown in Figure 8.3.1-1. It is anticipated that the acceptance test program will consist of:

- LSST Antenna Assembly
  - Electrical continuity
  - Weight and CG
  - First motion
  - Vibration
  - Acoustic
  - Inspection
- Mast
  - Static loading of complete stowed mast, upper and lower mast assemblies, hub, preload segment, upper hoop support cable mechanism, and each mast segment including the surface control mast segment
  - Functional tests of complete mast, preload and surface control segment
- Hoop
  - Static loading of hoop segment assembly
- Surface
  - Surface contour measurement of N gore segments
- Components
  - Structural tests of graphite assemblies, mesh, spools, pulleys, rollers, ballscrews, worm gears, push rods, skewers, cable assemblies, latching mechanisms, turnbuckles
  - Thermal vacuum testing of drive motors, spools, pulleys, rollers, cable assemblies, limit switches
  - Functional testing of drive motors and limit switches
  - RF reflectivity testing of mesh
  - Weight of mesh
  - Transmissivity of mesh
  - Microscopic examination of mesh

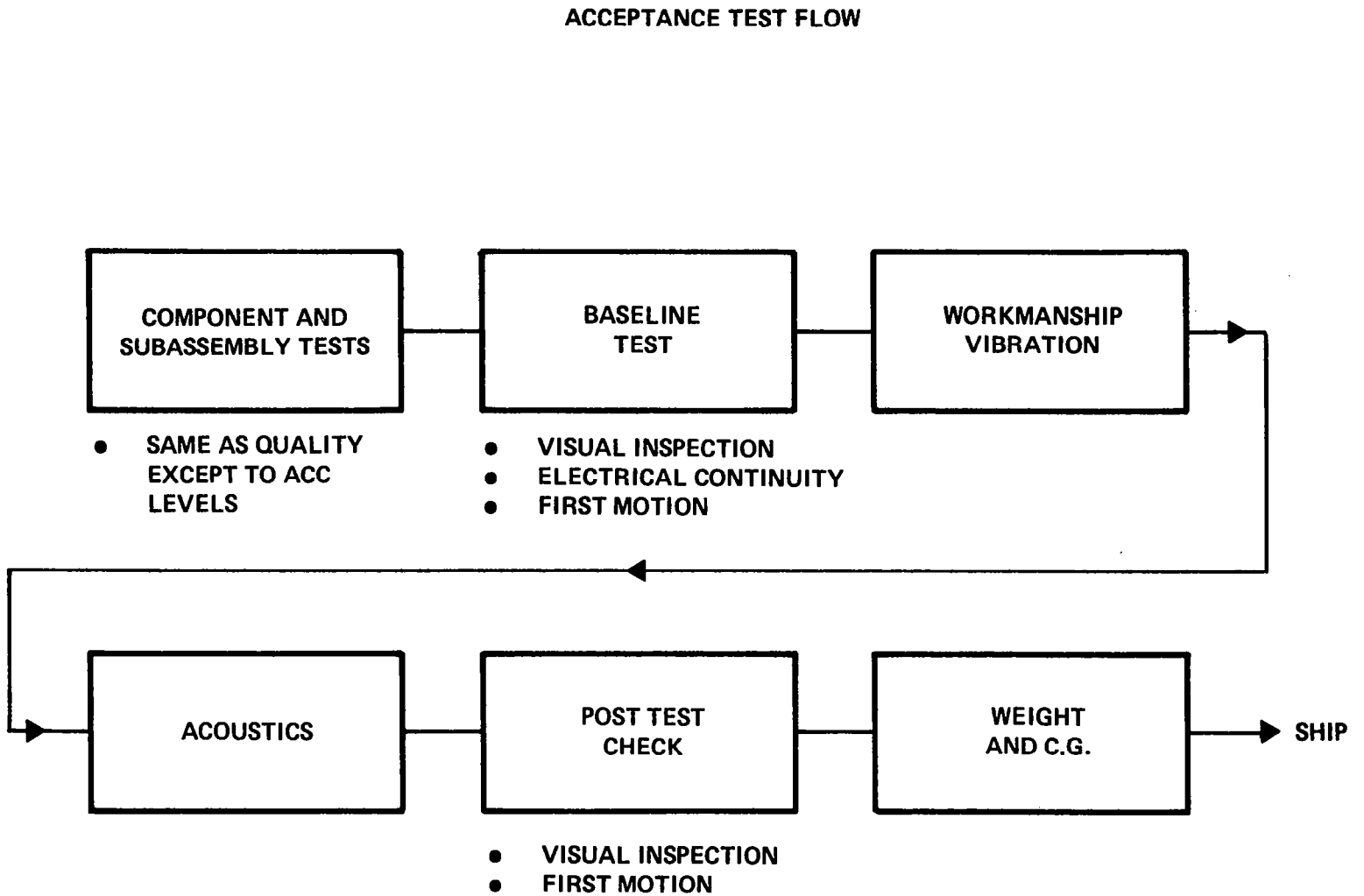


Figure 8.3.1-1. Acceptance Test Flow

### 8.3.2 Qualification Tests

Preliminary antenna qualification tests are defined in the flow shown in Figure 8.3.2-1.

### 8.3.3 Flight Tests

Flight tests onboard the shuttle orbiter are defined to gather further data on antenna performance before the system is put into a high energy orbit. In the top level subassembly/assembly test flow, many LSST Antenna assembly tests are impractical and will be covered by flight tests. Like acceptance tests the specific tests will be defined as the program evolves and are not addressed in detail here; however, it is anticipated that the flight test program will consist of:

- System thermal performance verification
- Functional - a complete deploy and stow operation
- RF - measurement to ensure RF performance including gain, beam-to-beam isolation, and aperture efficiency

## 8.4 Facilities Required

Harris GESD has dedicated significant resources for the development of specialized test facilities for the deployable antenna technology. This is especially evident in the mesh and cord test equipment which is currently being used for development testing to support LSST and other programs. Harris also has extensive environmental laboratory equipment, including vibration tables and space simulation chambers with $LN_2$ shrouds. Wherever possible, subassembly testing will be accomplished at the Melbourne plant location. Large system tests, however, may require use of other vendor facilities and possibly NASA facilities. For example, the Vehicle Assembly Building (VAB) at nearby Kennedy Space Center, could possibly meet the size and environment requirements for tests such as the first motion test of the full assembly, functional testing of the assembled mast, and the static testing of the deployed mast.

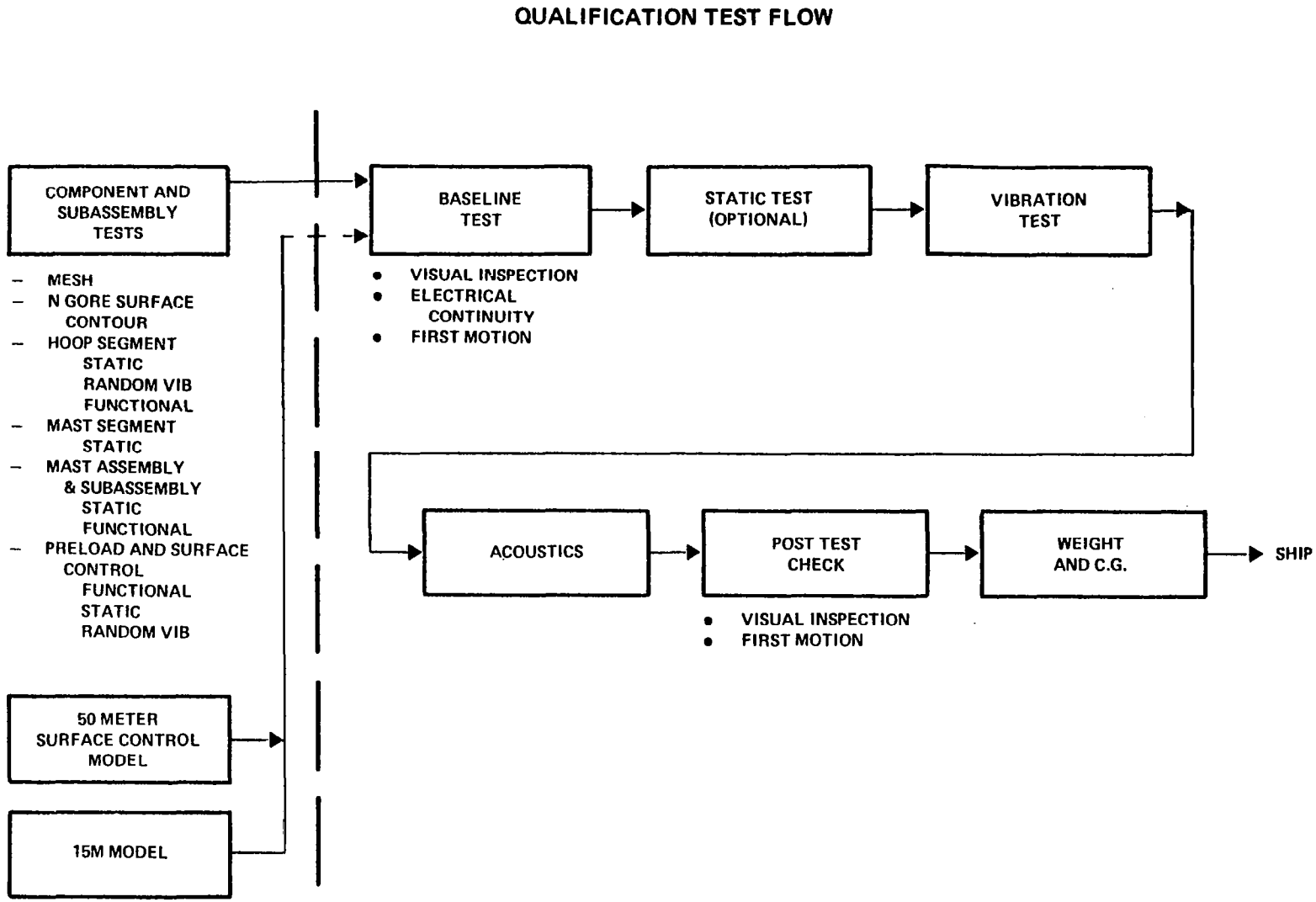


Figure 8.3.2-1. Qualification Test Flow

Solar thermal vacuum tests of the 15-Meter Model, thermal vacuum tests of large subassemblies, and RF range tests will be performed at qualified vendors or NASA facilities if HGESD facilities are not adequate or available. These tests will be performed once during development and will not be repeated for qualification or acceptance of the 100-meter design.

Components, such as drive motors, switches, and graphite structures, will most likely be tested at the vendors, under supervision of Harris.

New test facilities at HGESD will not be required to support the LSST 100-meter antenna program.

## 8.5 Failure Actions

In the event of a major failure or malfunction during qualification and acceptance testing of deliverable hardware, the customer will be notified immediately and a mutually accepted course of action will be selected prior to repair of the damage and test continuance or restarting. Failure reporting and corrective action will be accomplished in accordance with Paragraph 3.5 of PAR 700-1119.

## 8.6 Safety Philosophy

Safety considerations are factored into each test to protect personnel and the test article.

Safety program employed as follows:

- Each test procedure will contain a general paragraph on safety requirements.
- Potential failure modes and hazards will be identified for each test.
- Each test procedure will incorporate solutions to potential failure modes.
- Data sheets will be used to verify all critical procedure steps.
- Test procedures will have verification columns for critical events.

- All critical events will be identified and proper safety procedures employed.
- Safety Engineer must review and sign off all test procedures.
- All critical events will be monitored by Safety Officer.
- All test personnel will be instructed, briefed, and/or a dry run instituted when possible.
- Employ housekeeping practices per Harris Corporation procedures.
- Safety considerations will be reviewed at the readiness to test meeting.

## 8.7 Quality Control Requirements

### 8.7.1 Preacceptance Test Inspection

A final inspection will be accomplished prior to initiating acceptance testing. This inspection will consist of:

a. Visual inspection of the system for compliance with drawing requirements.
b. Verifying that all assemblies are properly installed.
c. Verifying that documentation exists to assure the previous acceptance of all assemblies. This documentation shall include: completed flow tags, configuration records, assembly acceptance test data, nonconformances properly dispositioned and accepted.

### 8.7.2 Acceptance Testing

A customer's Product Assurance Representative shall have the option of witnessing all acceptance testing and will be notified 48 hours prior to starting the tests.

8.7.3 Preparation

Before acceptance testing is initiated, Quality Control will verify that the system has been inspected and that no discrepancies remain to be cleared; test equipment and special fixtures are checked to assure current calibration; Acceptance Test Procedures (ATP's) and data sheets must conform to the requirements of the QA Program Plan.

The Quality Engineer reviews and approves the ATP before it is released and is conversant with the overall test plan. He will assure that the inspectors assigned to witness acceptance testing have sufficient training and experience to understand the testing procedures, the test equipment, and the test objective. Special instructions will be provided for inspectors, as required.

8.7.4 Test Data

All copies of the Acceptance Test Procedure and test data will be filed and maintained by Quality Control.

8.7.5 Test Failures

All failures occurring during acceptance testing will be documented on Failure Reports and processed per the Reliability Plan. The customer's Product Assurance Representative shall be immediately notified of any acceptance test failures as well as the test status, e.g., "Test Resumed" or "Test Discontinued Pending Customer Direction."

8.7.6 Qualification Tests

The first system completed will be subject to Qualification Testing. The Inspection, Functional and Environmental Tests will be as defined by an approved Qualification Test Plan to assure conformance. Quality Control will perform the required inspections and witness of the Qualification Testing to contractual requirements. Inspection and/or review of the design during the Qualification Test will be performed by Quality Assurance personnel to verify performance parameters, including, but not limited to, the following:

a. Service and access
b. Electrical interference
c. Configuration
d. Dimensions
e. Weight
f. Workmanship
g. Identification and marking
h. Safety
i. Selection of specifications and standards
j. Material, parts, and processs

## 9.0 50-METER SURFACE MODEL

The 50-Meter Surface Model is shown in Figure 9.0-1. The model is a face-down, four-gore segment of a half scale point design. The surface developed is representative of the point design with regard to geometry and all major elements. A fixed boundary is used to accurately simulate the proper boundary conditions.

The objectives of the 50-Meter Surface Model are:

- Verify analytical models
- Evaluate fabrication and assembly techniques
- Demonstrate surface adjustment capability
- Provide test bed for operational demonstration of Surface Accuracy Measurement System (SAMS)
- Provide data for input into scaling laws

### 9.1 Design Description

A design description summary of the 50-Meter Surface Model is provided in Figure 9.1-1. More detailed description of the model is given in the following paragraphs.

#### 9.1.1 Cord Elements

There are two types of cord assemblies in the model surface design: front surface cord assemblies and rear cord truss assemblies. These assemblies are shown in Figures 9.1.1-1 and 9.1.1-2, respectively. The cord material is Teflon impregnated graphite fibers described in Section 6.0.

Several trade-offs were performed in selecting the design concept for the front and rear cord systems. An incrementally constructed, one-piece cord system was selected because of several inherent advantages. Foremost is the fact that lower tolerances buildups are achievable. The number of fittings and hardware required are minimized, and the weight is reduced. These effects enable assembly of a more accurate surface with less manufacturing errors.

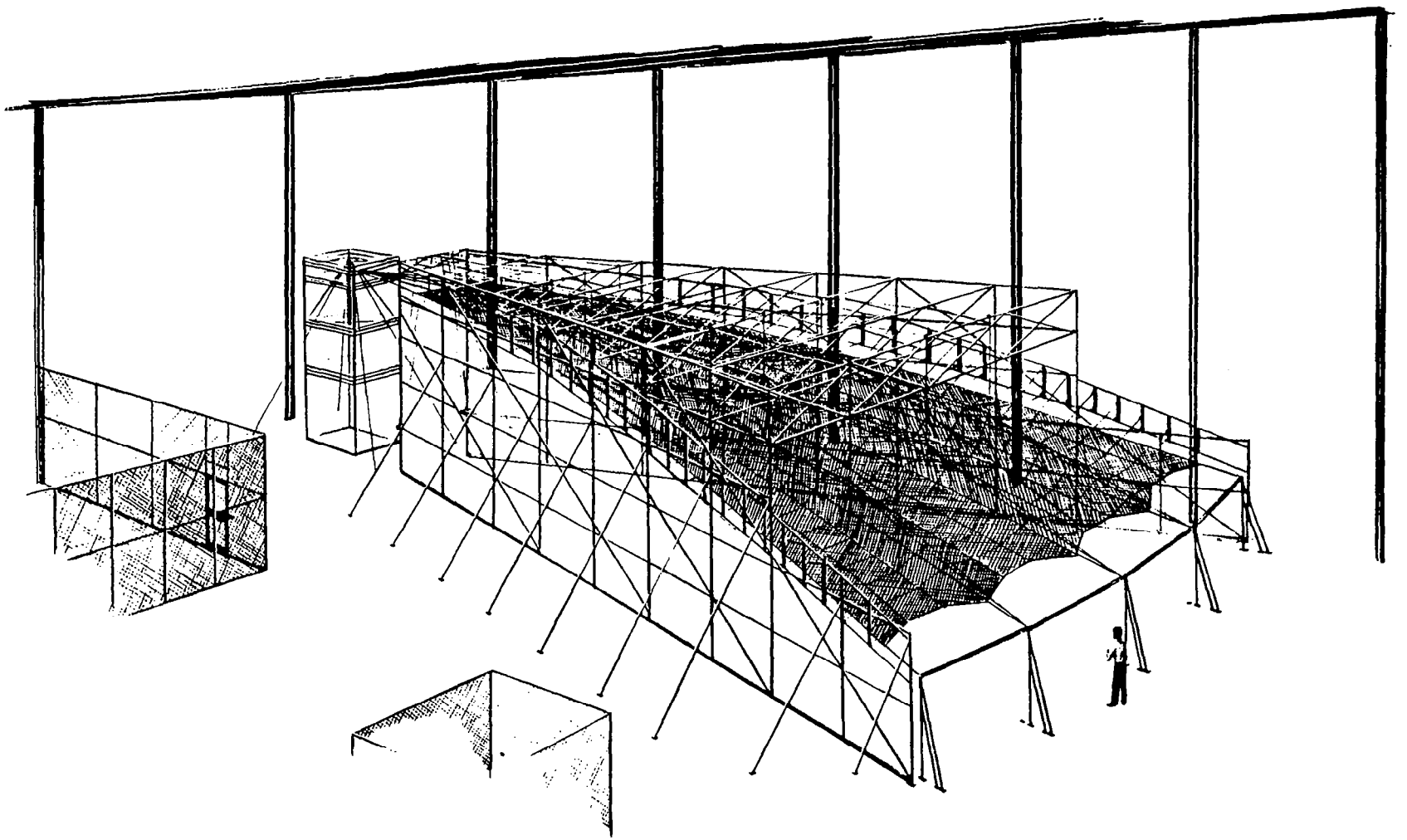

Figure 9.0-1. 50-Meter Surface Model

## 50M BASELINE DESIGN DESCRIPTION SUMMARY

- THE SURFACE ADJUSTMENT MODEL IS A NON-STOWABLE, FACE-DOWN, FOUR GORE SEGMENT OF A HALF SCALE POINT DESIGN SURFACE
- THE DEVELOPED SURFACE SIMULATES THE 0-G CONTOUR
- THE SURFACE IS REPRESENTATIVE OF THE POINT DESIGN WITH REGARD TO GEOMETRY AND ALL MAJOR ELEMENTS
- FIXED BOUNDARY STRUCTURES PROVIDE PROPER BOUNDARY CONDITIONS
- THE MAST AND HOOP ARE SIMULATED BY TOOLING STRUCTURES
- NO STOWAGE ELEMENTS OR MOTORS ARE REQUIRED

Figure 9.1-1. 50-Meter Baseline Design Description Summary

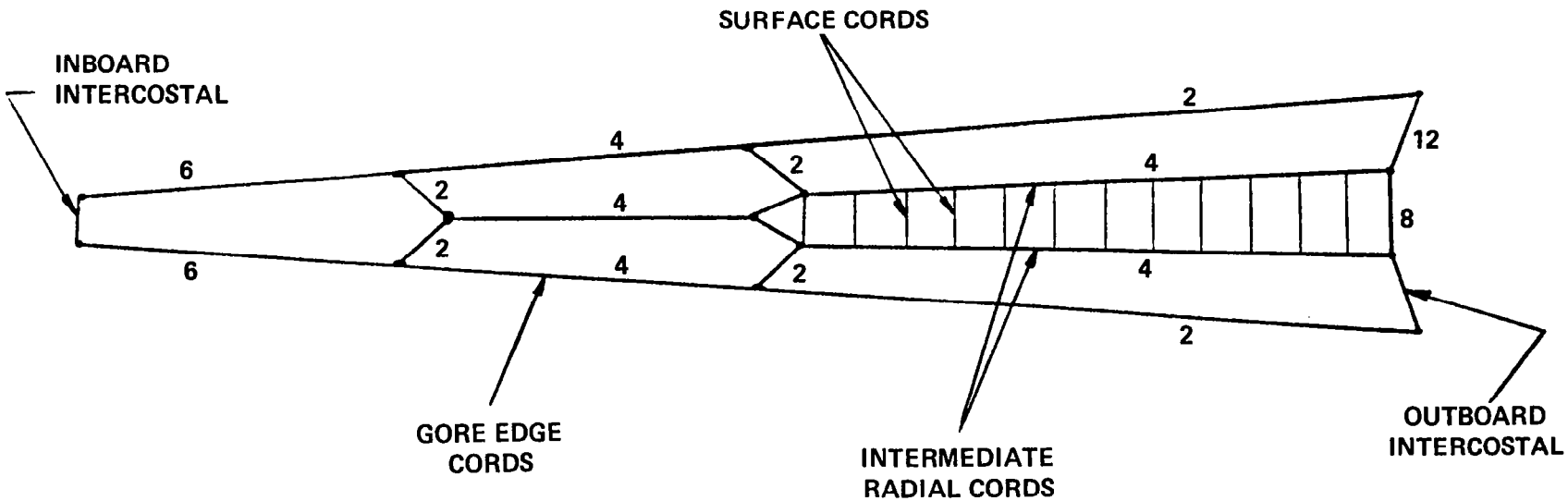


FRONT CORD SYSTEM

- THIS IS AN INTEGRATED CORD SYSTEM TO WHICH REFLECTIVE MESH IS ATTACHED TO FORM A PANEL. THE FRONT CORD SYSTEM SHAPES THE MESH CONTOUR AND IS CONTROLLED BY THE REAR CORD SYSTEM BY MEANS OF TIES.
- THE "ONE PIECE" APPROACH TAKEN IN THIS DESIGN MINIMIZES TOLERANCE BUILDUPS WHICH ADVERSELY AFFECT THE LOAD DISTRIBUTION.

Figure 9.1.1-1. Front Cord System

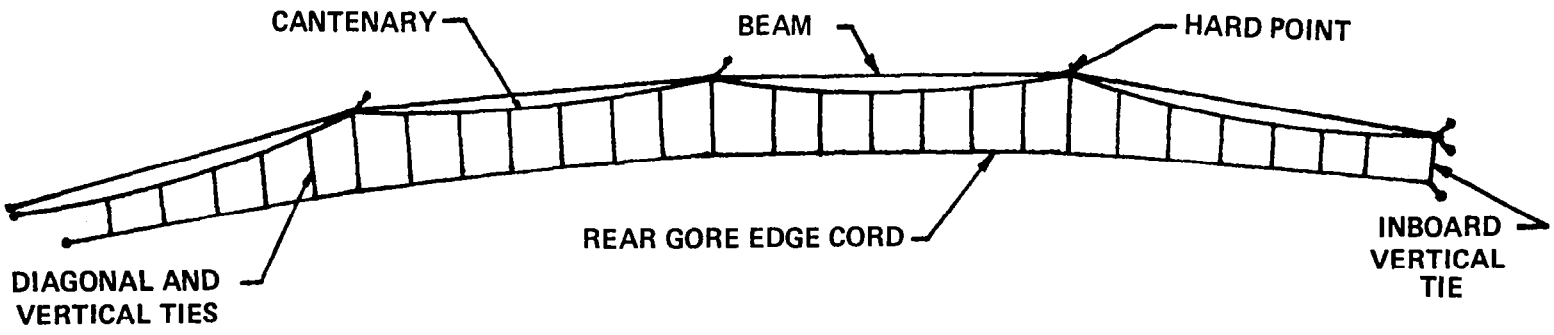


REAR CORD STRING TRUSS SYSTEM

- THIS IS A SET OF CORDS WHICH SUPPORT THE SURFACE BY MEANS OF TIES ATTACHED TO THE GORE EDGE CORDS AND INTERMEDIATE CORDS
- CORD SIZES:

  VERTICAL TIES: 1/3
  DIAGONAL TIES: 1/3
  CATENARIES: 4
  INBD TIE: 1

  BEAMS: 30, 10, 6, OR 2
  REAR GORE EDGE CORD: 4

- TIES ARE PRE-FABRICATED
- GEOMETRY AND CORD TENSIONS ESTABLISHED BY TOOLING AND CAPTURED BY BONDED JOINTS



Figure 9.1.1-2. Rear Cord String Truss System

The front cord system provides the periphery definition for the RF reflective mesh panels, plus when attached to the rear cords provide an effective method of contouring the surface. The periphery is created by the gore edge cords and inboard and outboard intercostals. Additional internal cords are added for surface contouring. The intersection of these cords at any of the 14 front cord junctions is maintained by G-10 plates bonded with the cords preloaded. These junctions are discussed in more detail in Paragraph 9.1.2.

Mesh is secured to the tensioned flat pattern front cord system while on the panel fabrication template using invar lacing wire. This lacing wire is spirally wrapped around the peripheral cords and through the large mesh openings (0.27 x 0.27 inch). Every 4 to 6 inches the lacing wire is tied off in a knot to prevent slippage of the mesh relative to the cord. The mesh is secured to the various junction covers or plates by pressure-sensitive tapes.

The mesh is a 0.27-inch opening tricot knit fabricated from 0.0012-inch diameter gold plated molybdenum wire. Attached to the mesh panels are 108 targets located at the node locations of the half-gore analytical model. These particular locations are chosen to minimize the errors in correlation of predicted versus measured surface contour. Each target is approximately 16 mm in diameter and is characterized by a central black dot on a white field enclosed by a concentric black ring.

The rear cord string truss system is a network of graphite cords lying in a radial and vertical plane passing through the central axis of the mast. One cord of this rear cord system (rear gore edge cord) is shaped into a parabolic curve corresponding to an F/D of 1.53 by means of ties and applied boundary loads. Each front surface cord is connected to a rear cord string truss system by vertical or diagonal ties.

The rear cord string truss system is fabricated on a template. Each hard point junction is constructed by a junction positioning device within the template frame. Theodolites are used to establish the correct geometry of all junction positioners, boundary attachments, and vertical

ties. The cords are tensioned to design load during truss fabrication. Once the system is bonded and cured, it is removed from the template and placed in storage until it is assembled to the front gore edge cords of the panel assemblies.

The 50-Meter Model is face-down, and as such, the rear cord string truss system is above the surface. Control cords passing through pulleys of the overhead boundary assembly trusses support the rear cords, which, in turn, support the mesh panels as shown in Figure 9.1.1-3.

The front and rear cord assemblies are assembled as shown in Figures 9.1.1-4 and 9.1.1-5. Two panel assemblies and one rear cord string truss system are simultaneously joined along the gore edge cords. Fittings at the outboard and inboard ends assure that the ends are terminated in a geometrically correct manner. Edge junctions of adjacent panels are joined by fiberglass plates to assure their proper alignment. The balance of the joining task involves lacing and tieing the gore edge cords together between the joint locations.

### 9.1.2 Cord Junctions

The cord junction of both the front and rear cord systems are discussed in this section. The front cord system has five types of cord junctions (refer to Figure 9.1.2-1):

a. Inboard Junction - Joining inboard intercostal to gore edge cords.
b. Edge Junction - Joining gore edge cord to intermediate cords.
c. Intermediate Junction - Providing separation of intermediate cords.
4. Intercostal Junction - Providing separation of intercostal cords into intercostal cords and intermediate cords.
5. Outboard Junction - Joining outboard intercostal to gore edge cords. The rear cord string truss system has two types of cord junctions (refer to Figure 9.1.1-2):

REAR CORD SYSTEM FAB

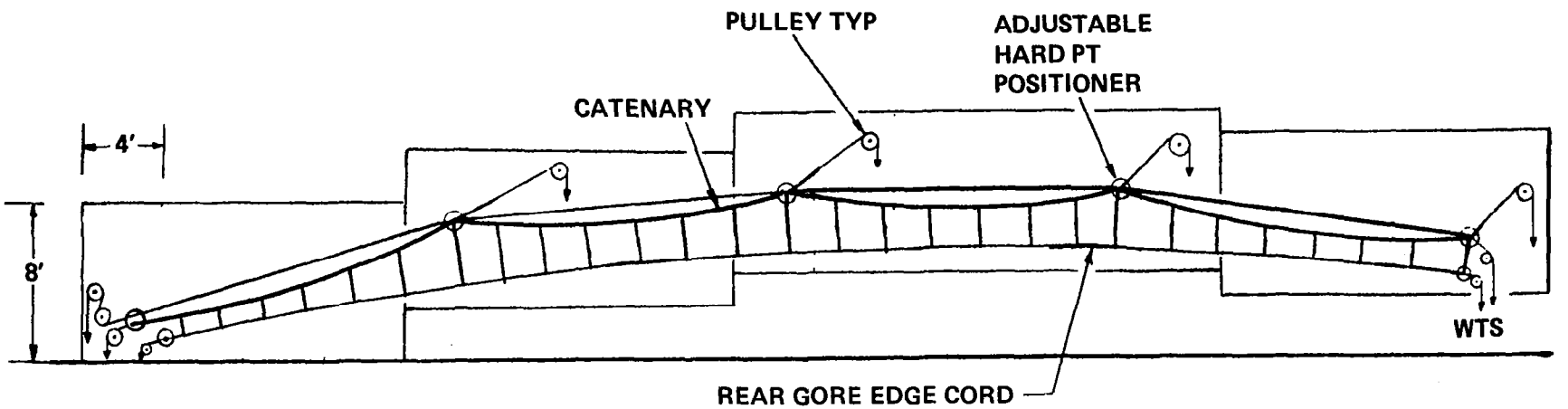


Figure 9.1.1-3. Rear Cord System Fab

**GORE ASSEMBLIES AND STRING TRUSS ASSEMBLIES ARE LACED TOGETHER AT TOP ASSEMBLY**

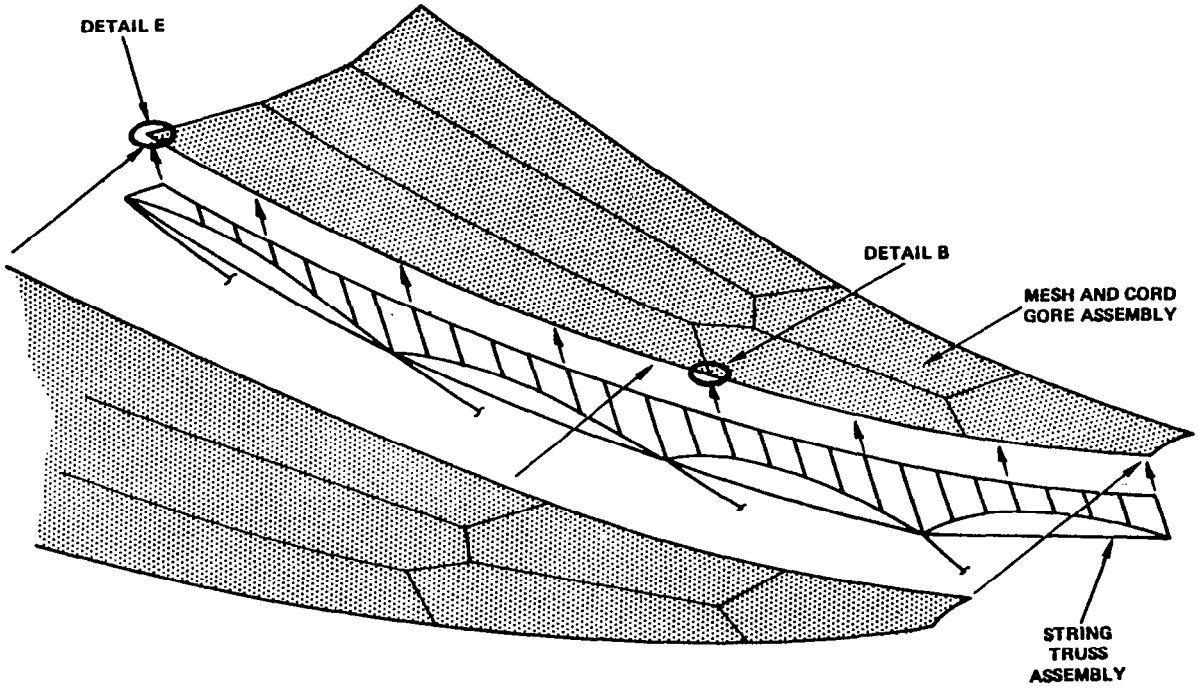


Figure 9.1.1-4. Gore Assemblies and String Truss Assemblies are Laced Together at Top Assembly

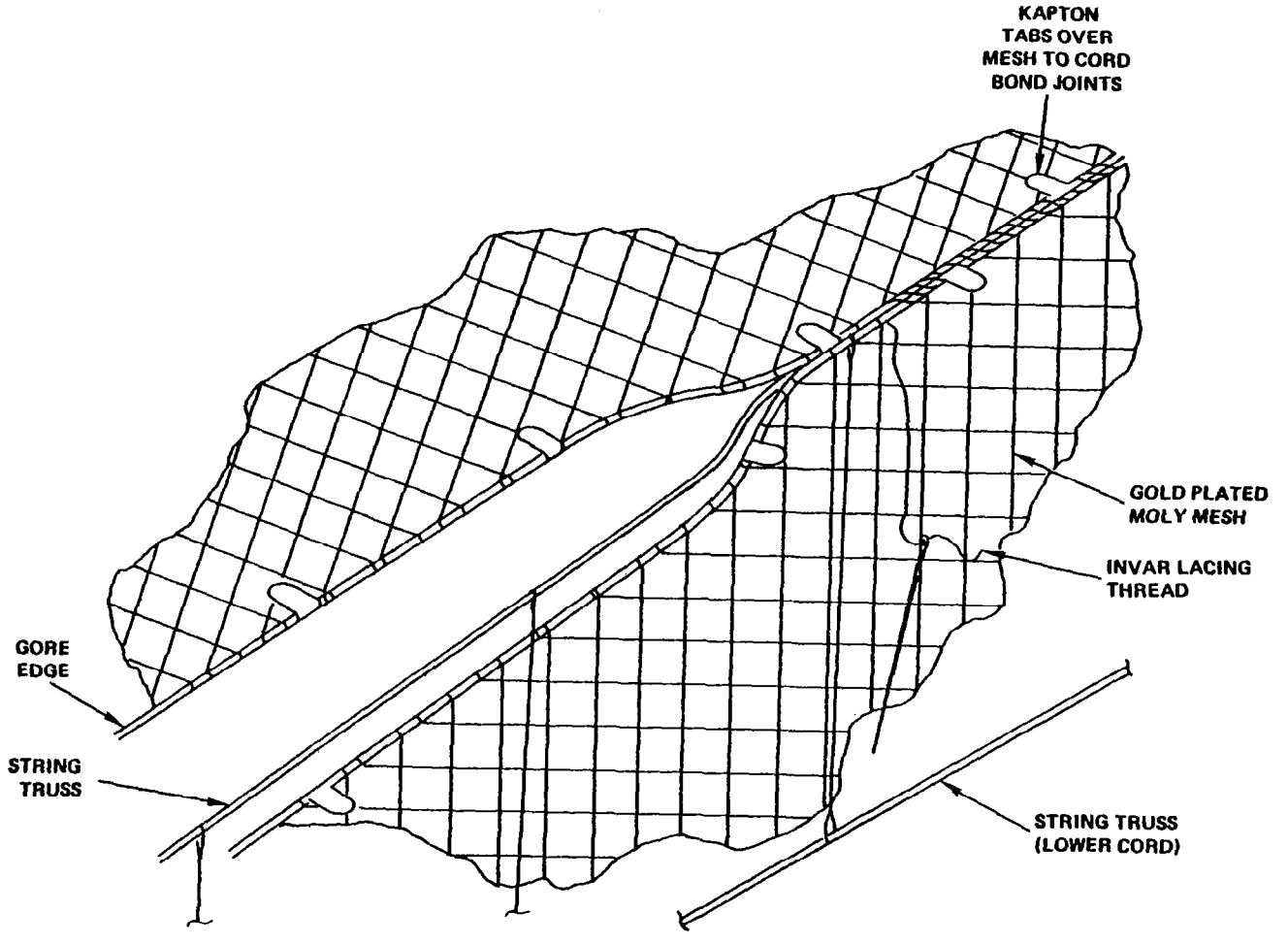


Figure 9.1.1-5. Adjacent Gores and String Truss are Laced Together

PANEL JUNCTIONS

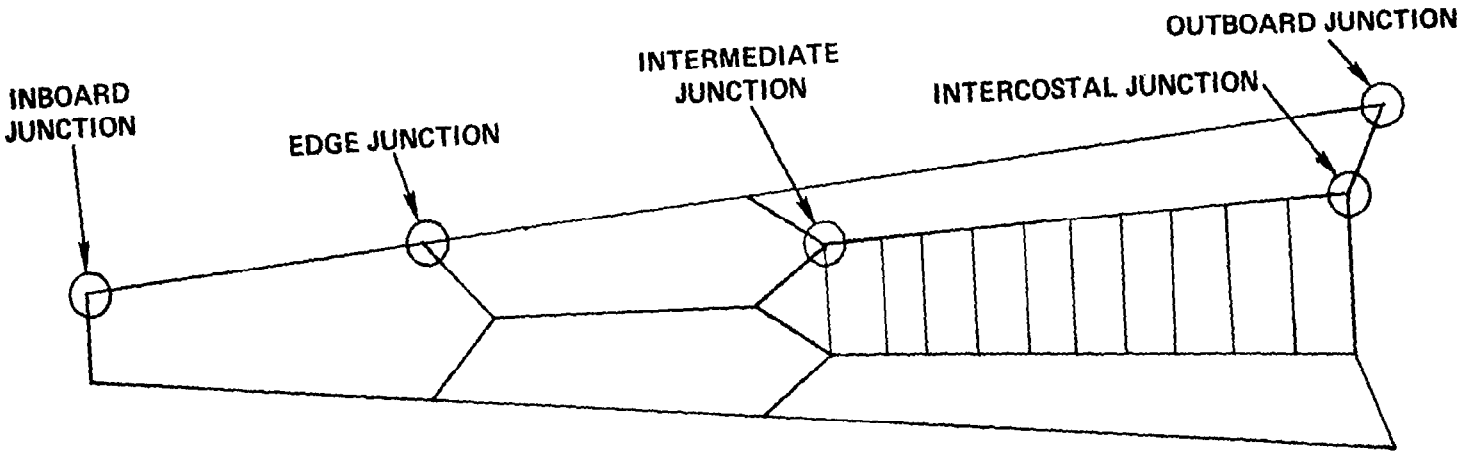


Figure 9.1.2-1. Panel Junctions

1. Hard Point Junctions - Convergence of vertical end diagonal ties, control cords, catenaries, and beams
2. Tie to Cord Junctions

The tooling and measurement system used to establish cord junction positions is significant in determining the achievable correlation between measured and predicted data. If incorrect geometry of cord junctions is established, tensions will exist in the cords which are not in agreement with the analytical model. Further, the error in tensions will be directly proportional to the error in length. Targets, load cells, stain gages, and bead tensioners are included in the model design specifically for the purpose of verifying the geometry and cord tensions, and updating the analytical model with "as-built" data. Cord tooling will be discussed further in Paragraph 9.4.

The cord junction design is the end result of several iterations of panel/system design. Earlier designs featured machined metal clevises to which the various ties and cords were attached. For each of the 17 major node junctions, a set of up to eight cords radiate from a single point. The disadvantages of the clevis joints are: the numerous angles that must be accurately integrated into a single part; cost and complexity; the system tolerances are additive; the CTE match to the cord material is poor; and high weight.

The chosen cord junction design is a three-layer fiberglass laminate which captures the pre-established cord geometry. Part costs are reduced by batch machining the flat laminate parts. System tolerances are not additive, resulting in improved as-built accuracy. The joint laminate parts of the 100-Meter Point Design are made of graphite/epoxy which gives excellent CTE match with the cords. Fiberglass/epoxy is used on the 50-Meter Model because it is lower cost and there is no requirement for thermal cycling on the model.

A description of joint manufacturing processes and each type of cord junction is provided in Figures 9.1.2-2 through 9.1.2-8.

CORD JOINT MANUFACTURING PROCESS

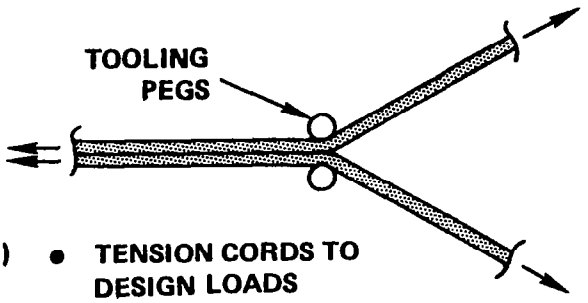


1) • TENSION CORDS TO DESIGN LOADS

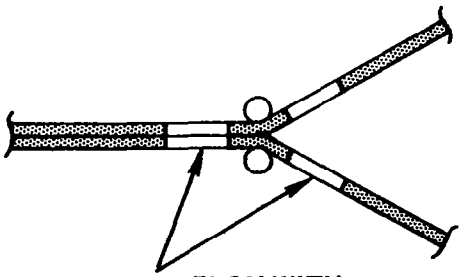

2) • REMOVE TEFLON WITH MINIATURE BUTANE TORCH

• APPLY EPOXY ADHESIVE TO CORD AREAS

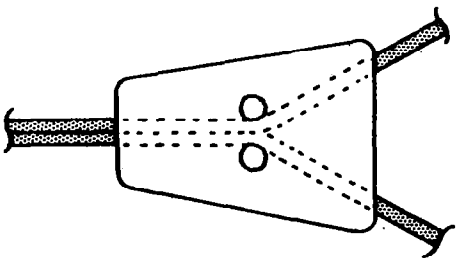

3) • TO APPLY EPOXY ADHESIVE TO GRAPHITE/EPOXY FITTING

• PLACE FITTING OVER TOOLING PEGS WITH ADHESIVE IN CONTACT WITH CORDS

• ALLOW 24 HOURS FOR ADHESIVE CURE

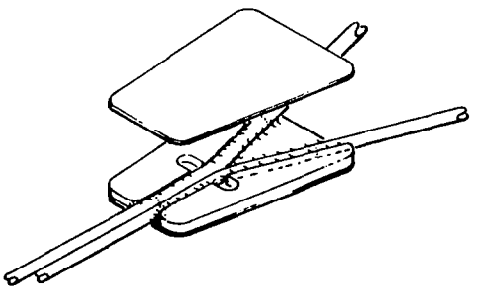

4) • REMOVE FITTING AND CORDS FROM TOOLING PEGS AND BOND LAMINATE CAP TO EXPOSED CORD SIZE OF FITTING

Figure 9.1.2-2. Cord Joint Manufacturing Process

## CORD END FITTING DESIGN/PROCESS

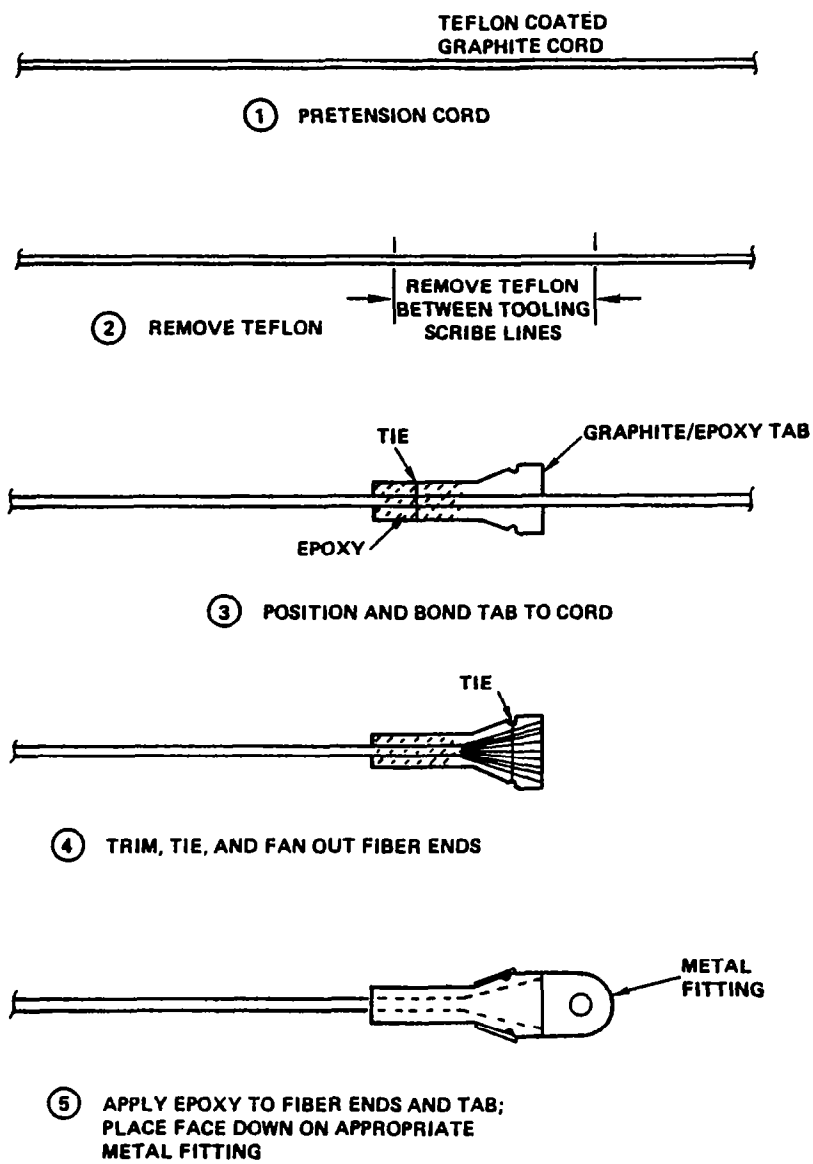


Figure 9.1.2-3. Cord End Fitting Design/Process

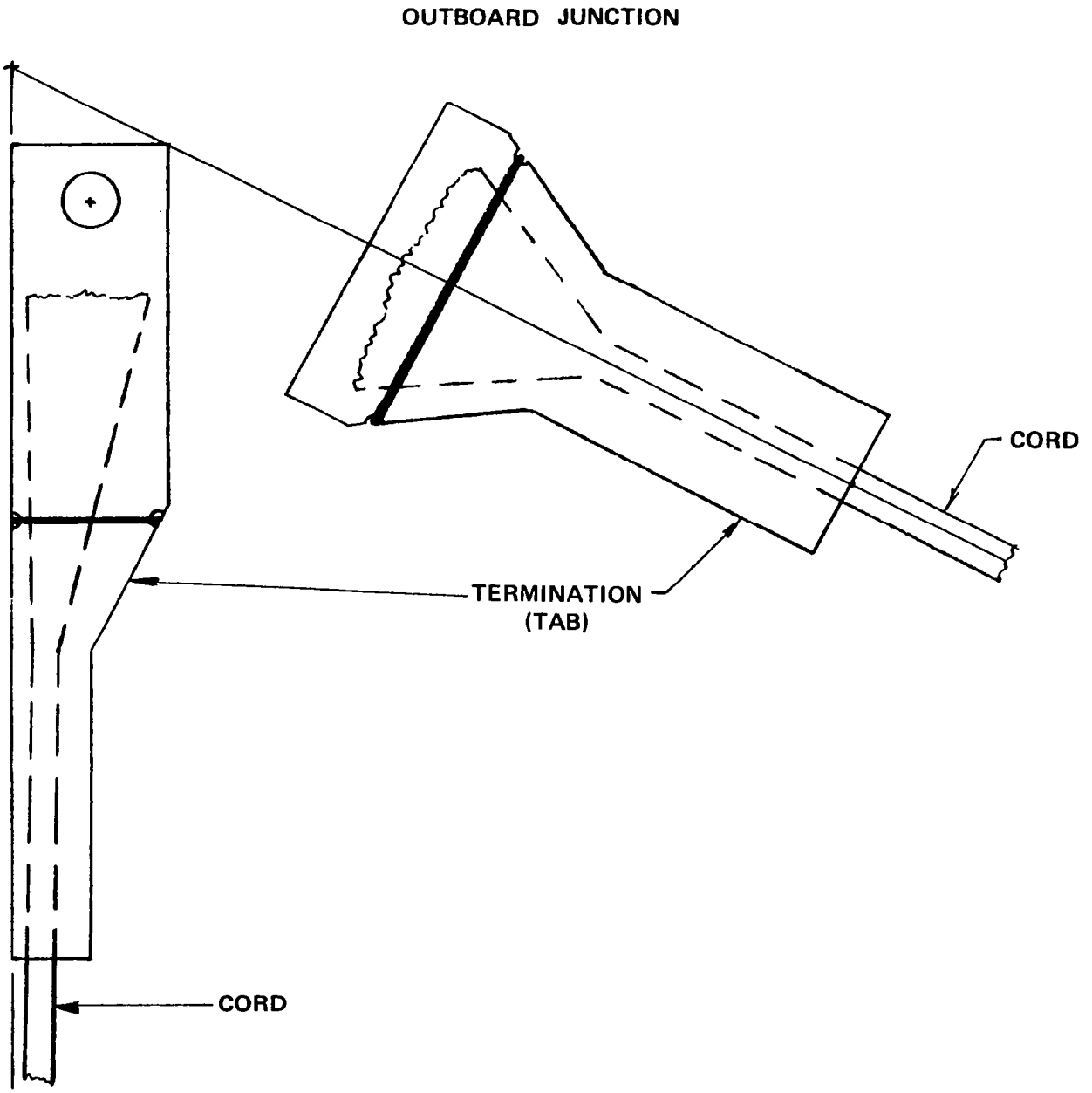


Figure 9.1.2-4. Outboard Junction

INTERCOSTAL JUNCTION

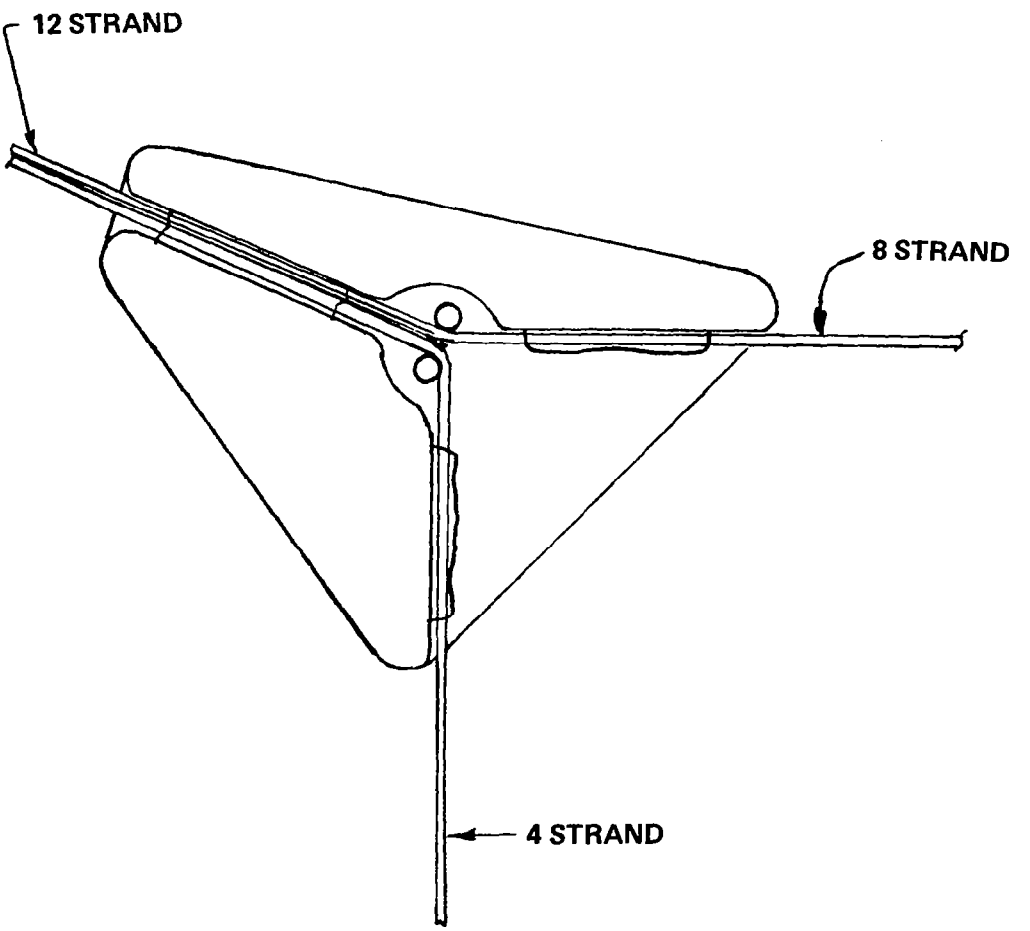


Figure 9.1.2-5. Intercostal Junction

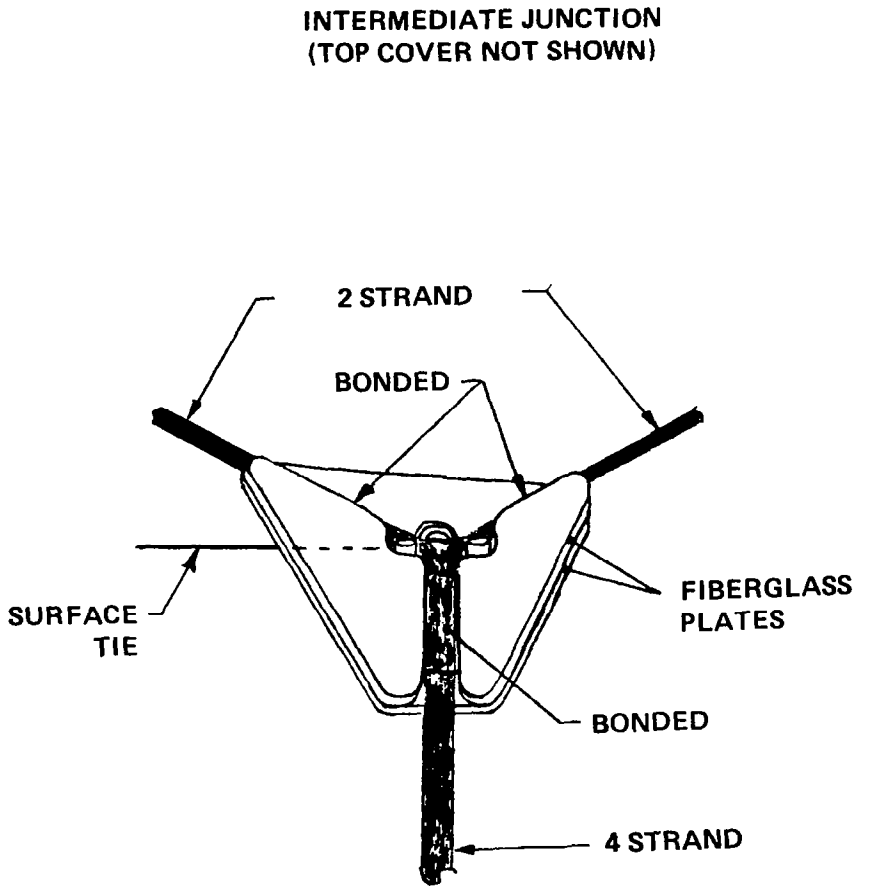


Figure 9.1.2-6. Intercostal Junction (Top Cover not shown)

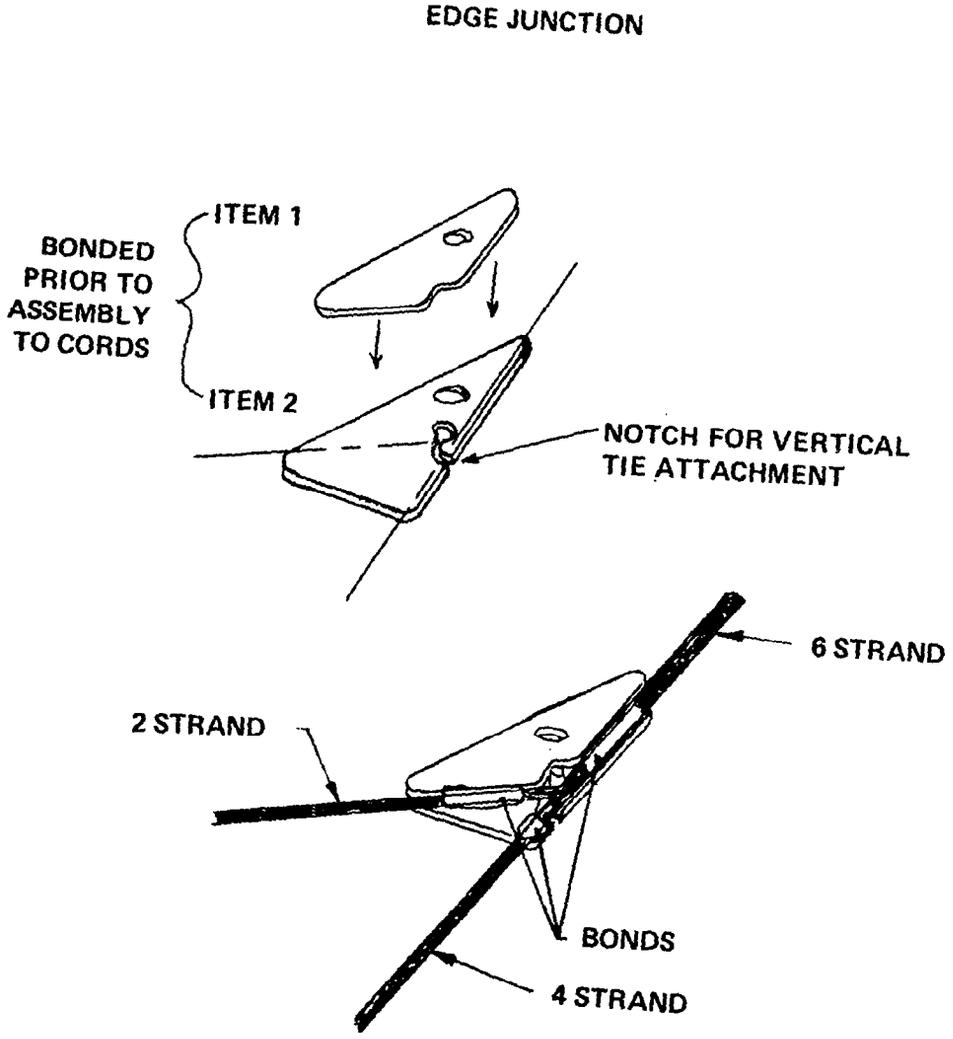


Figure 9.1.2-7. Edge Junction

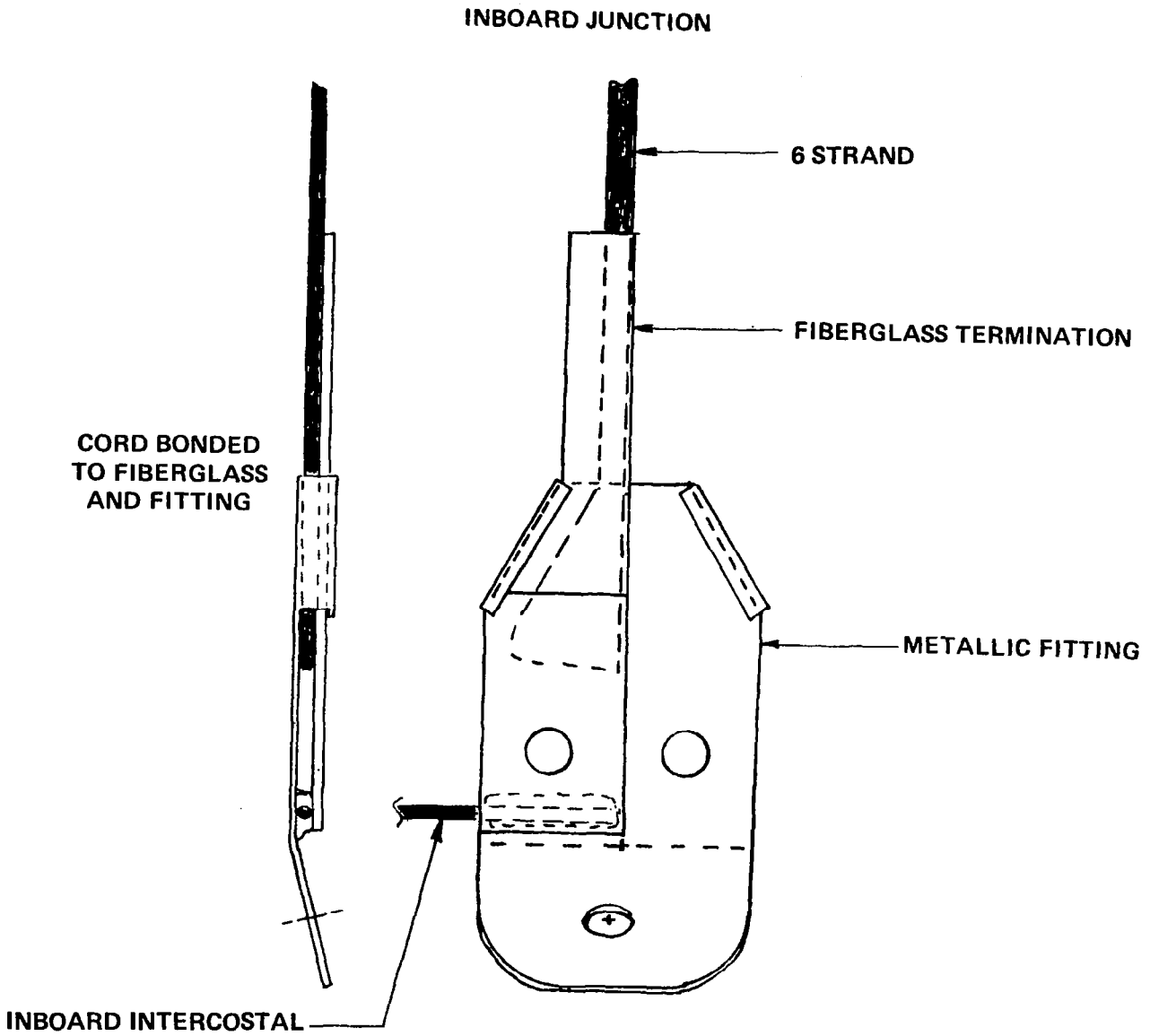


Figure 9.1.2-8. Inboard Junction

### 9.1.3 Model Interfaces to Boundary

The model surface is terminated at rigid radial plane boundaries, five hoop attachment points, and three mast attachment points. The test surface area is the two inner panels (gores) of the four-gore segments of the surface. Surface control adjustment is provided along the three radial seams bounding the two innermost gores.

The rationale for a rigid radial plane boundary is that the two outermost gores isolate the two innermost gores (adjustable test area) from the rigid boundaries. The boundary conditions of the model therefore are well-defined (relative to a floating boundary) and do not introduce spurious behavior into the performance of the test area. Tensions and positions of the boundary are capable of being verified and adjusted to provide consistency with the analytic model boundary constraints. The resultant two-gore test area is of sufficient size and possesses sufficient interaction to verify analytical models. The cost effectiveness of the rigid radial plane boundary is an important consideration, because a disproportionate amount of time and money can be consumed implementing a set of complicated boundary conditions.

The model surface interfaces with the simulated mast, simulated hoop, and boundary assembly which are discussed in more detail in Paragraph 9.3. The entire radial length of the outer gores is attached to steel strip assemblies which are clamped to the boundary assembly at 54 points. The hard points of the rear cord system are supported by counterbalances and control cables passing through pulleys on the overhead trusses of the boundary assembly. These pulleys are required for the boundary assembly because of the size constraints of the facility housing the surface adjustment breadboard model. All pulleys are located along radials in the trusses at a height of approximately 7 meters above the floor. The diagonal ties on the outer half of the outer gores have chain termination ends to provide adjustable attach points to the boundary assembly (see Figure 9.1.3-1).

## SURFACE ATTACHMENT

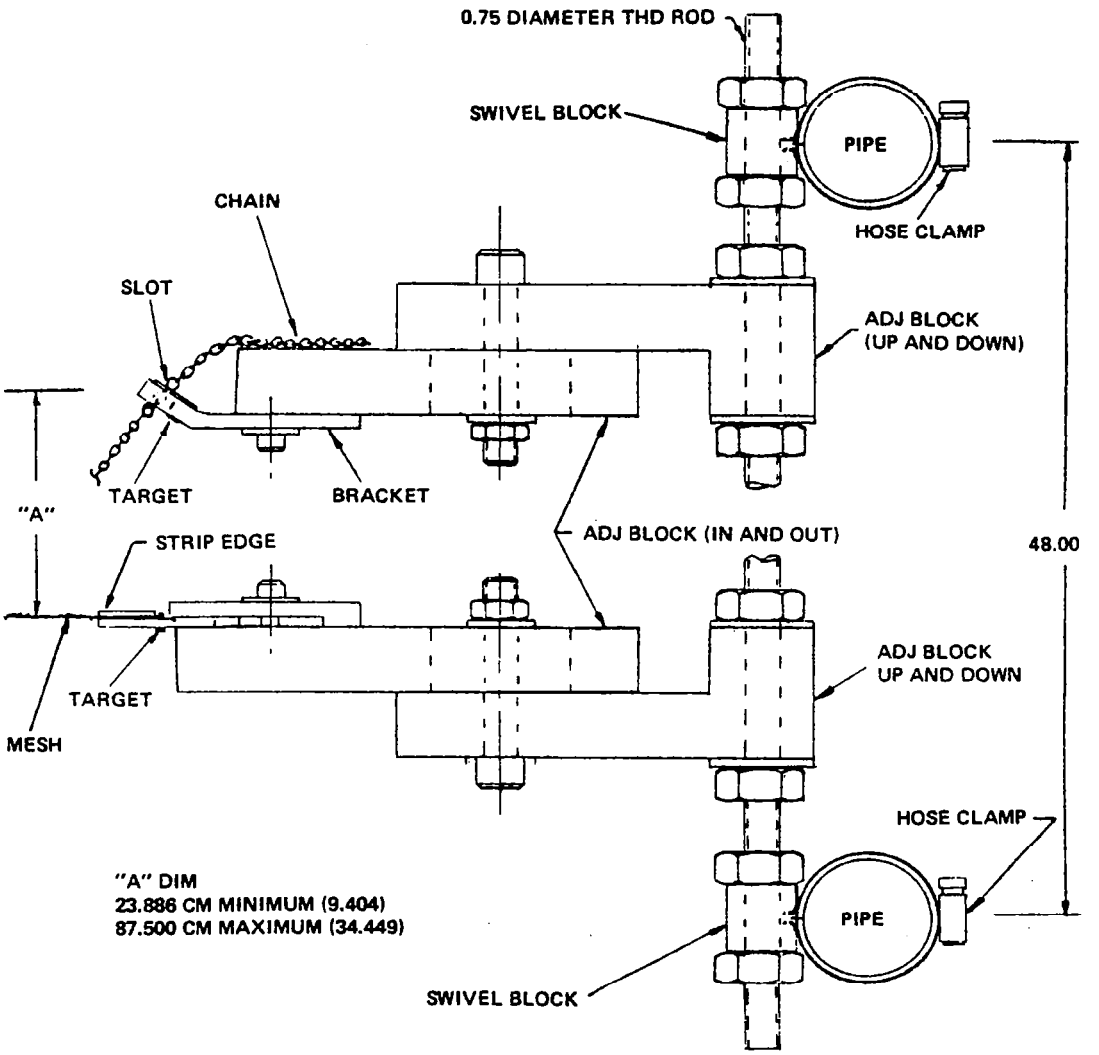


Figure 9.1.3-1. Surface Attachment

The central features of the simulated mast is a vertical pipe section rigidly held by a rectangular pipe frame. This central vertical pipe section supports a bracket to which three radial spring housings are attached. Each housing (shown in Figure 9.1.3-2) encloses a pair of 4-inch turnbuckles and a pair of springs. Hooks on the ends of the springs are placed through the holes in the end fittings of mast interface cords. The lower mast interface cord has a crimped-on end fitting with a hole which will accommodate number 4 hardware. The end fitting of the mast interface cord is attached to the front cord system inboard termination fitting which is likewise attached to the rear cord system inboard fitting.

The turnbuckles within the spring housing allow adjustment of the radial position of the surface inboard fittings and hard points. The springs are sized to accommodate adjustment of the turnbuckles while maintaining correct tension levels in the mast interface cords.

The upper and lower mast interface cords attach to the spring hooks in an identical manner, but the upper mast interface cord must attach to a fiberglass tab. This is accomplished by use of a wedge tab accommodating an aluminum fitting riveted to the upper end of the mast interface cord. The tab and fitting mate such that the $60^{0}$ inclined surfaces are bearing surfaces, held in contact by number 2 hardware.

Each of the five hoop posts (vertical pipe section) has an interface bracket attached such that the analytical nodal point is positioned at an elevation of 1.829 meters above the floor and 25.000 meters from the mast section centerline. Three axis adjustment of the hoop interface points is possible. Interface cords as shown in Figure 9.1.3-3 provide the connection between the surface and the hoop interface bracket. A turnbuckle in-line with the lower interface cable permits gore edge cord tensioning and height adjustment.

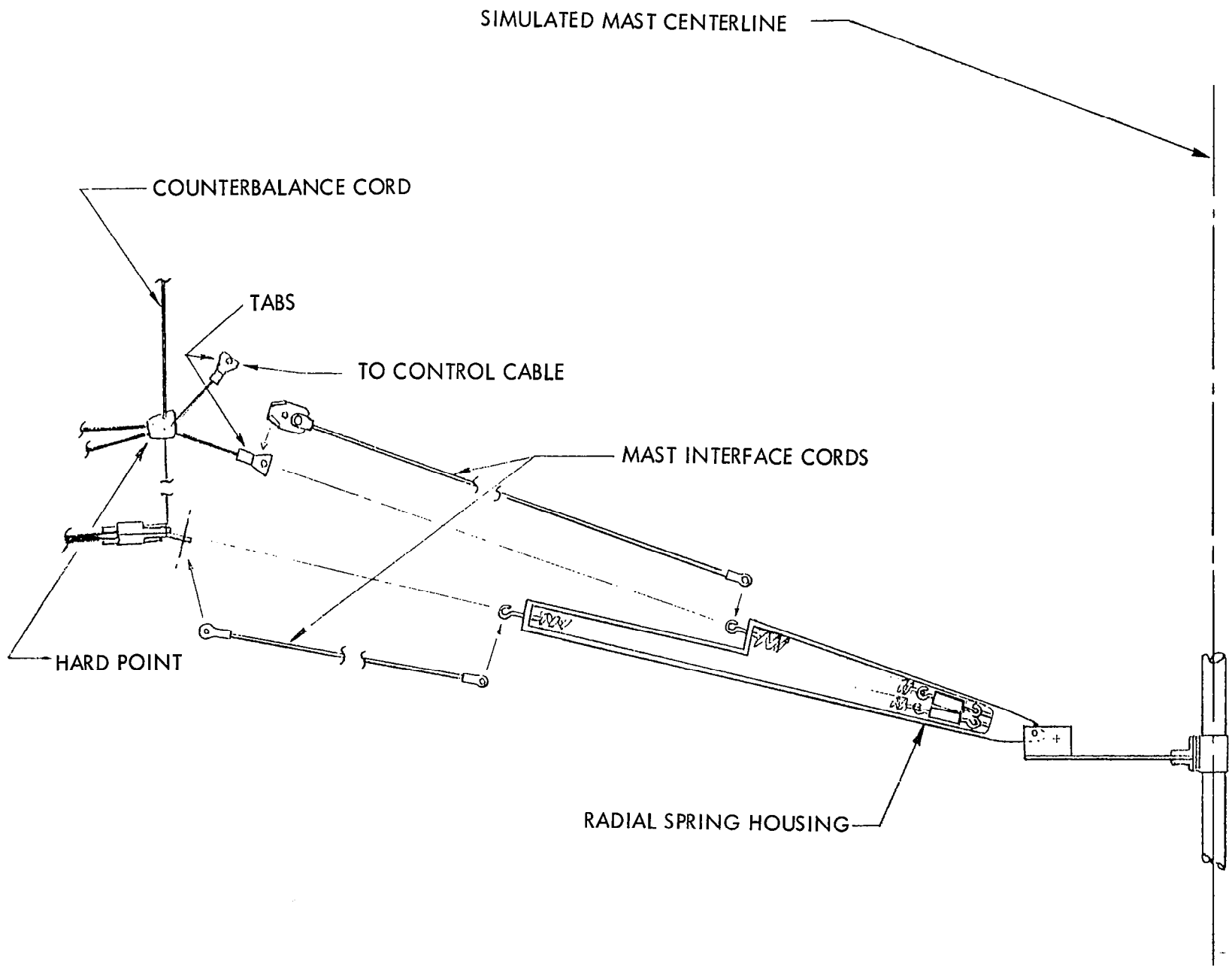


Figure 9.1.3-2. Mast Interface

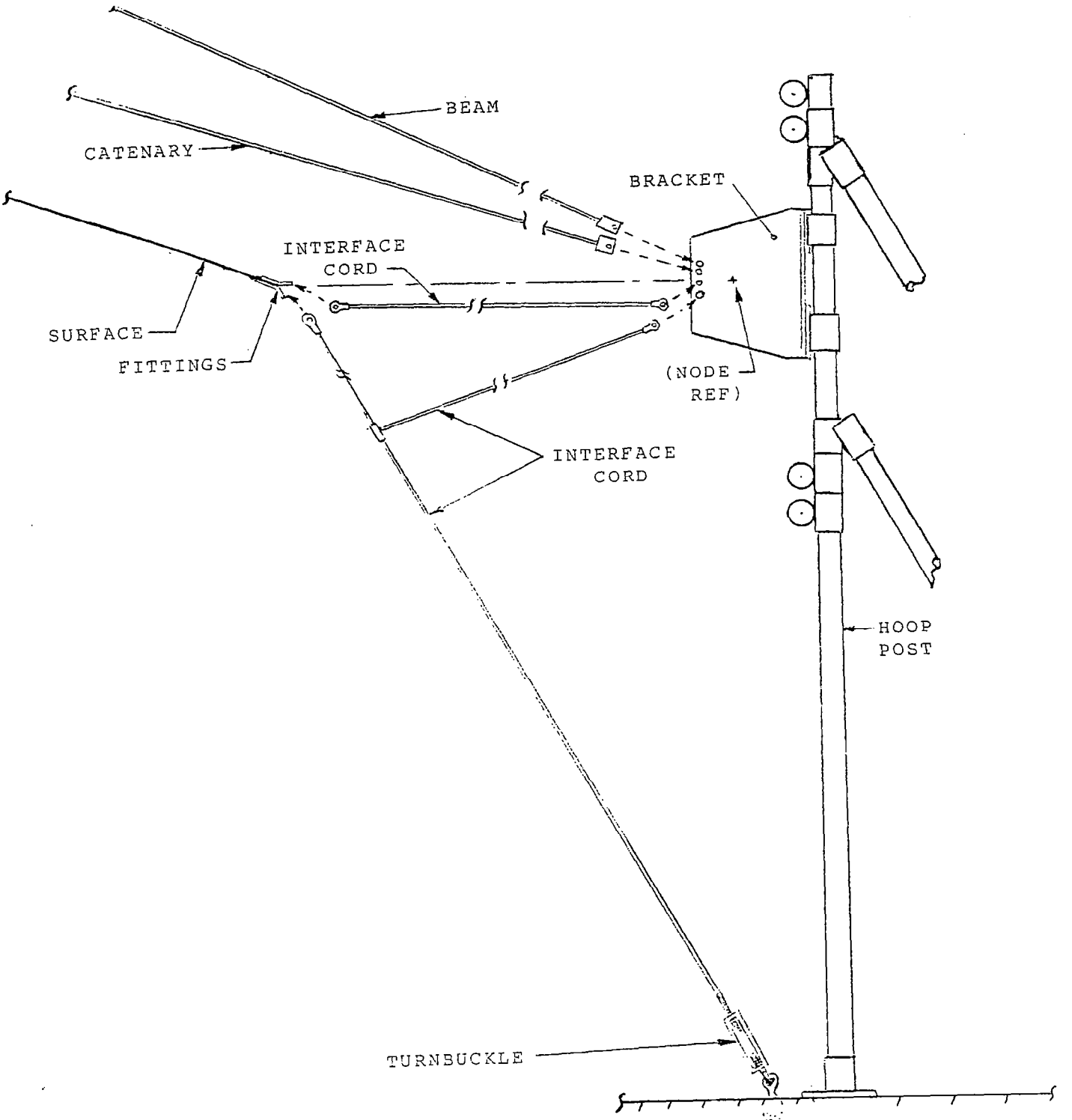


Figure 9.1.3-3. Hoop Interface

The model design assumes very stiff radial boundary structures, i.e., no deflection of the radial interfaces from a control cable adjustment. The inclined supports, interconnecting trusses, and connection to the hoop assembly make the boundary sidewalls stiff with respect to applied circumferential loads. The surface attachment assemblies shown in Figure 9.1.3-1 are also very stiff relative to the applied circumferential loads. The chain and strip assemblies can be adjusted in a direction normal to the surface or circumferentially. Targets permit optical verification of the proper boundary geometry by the theodolite measurement system (TMS).

## 9.2 50-Meter Surface Analysis

### 9.2.1 Introduction

The 50-Meter Surface Verification Model demonstrates the ability to manufacture and adjust an LSST antenna surface. The surface analysis considers the effects of gravity, manufacturing and flat panel mapping to predict both position and stiffness of the surface structure. Also, surface adjustment to improve the roughness and focus is a function of surface analysis.

The 100-Meter Point Design has been established for the zero-G environment. To provide maximum information about the point design, the design of 50-Meter Surface Verification Model was selected to be a geometric duplicate. Some deviation from the exact 1/2 scale design exists. These deviations enhance the ability of the model to meet the objective of providing information about the point design. They are:

1. The 100-meter cord size and element loads are maintained. This provides information for manufacturing on the cord termination points and show load performance for the point design.
2. Mesh membrane elements are the same stiffness and pretension as the point design. This verifies manufacturing ability of mesh panels in the same cord load to mesh load ratio range. This will simulate the point design cord dominated structure more accurately.

3. The surface is counterbalanced at the control cord attachments. This allows cord loads and deflections to be more similar to the 100-meter zero-G situation.

The following pages describe the analytical models and show the results and conclusions of surface analysis.

### 9.2.2 Model Details

To analyze the 50-meter surface in areas of manufacturing, assembly and surface adjustment, two basic finite element models are used. The models are:

- One-for-one half-gore model
- One-for-one four-gore model

Both models are analyzed using the Harris proprietary nonlinear structural analysis (NLSA) computer program. This program is used to account for pretension stiffness in the cords (stringer elements) and mesh surface (membrane elements).

#### 9.2.2.1 One-for-One Half-Gore Model

The one-for-one half-gore model is a finite element model represented with one finite element for each continuous length of cord on the surface design. Node to node stringer elements represent cord junction to cord junction cord structure and triangular membrane elements represent cord junction to cord junction areas of the RF reflective mesh surface. Figure 9.2.2.1-1 reveals the above mentioned modeling technique.

The half-gore model represents an axi-symmetric structure which is similar to the four-gore surface verification model. The only deviation from the test fixture is that the half-gore model represents a full $360^{0}$ surface that is symmetric about the bore axis, while the four-gore test article is terminated and fixed at the boundary points. Comparisons for verification purposes are provided in the analysis section.

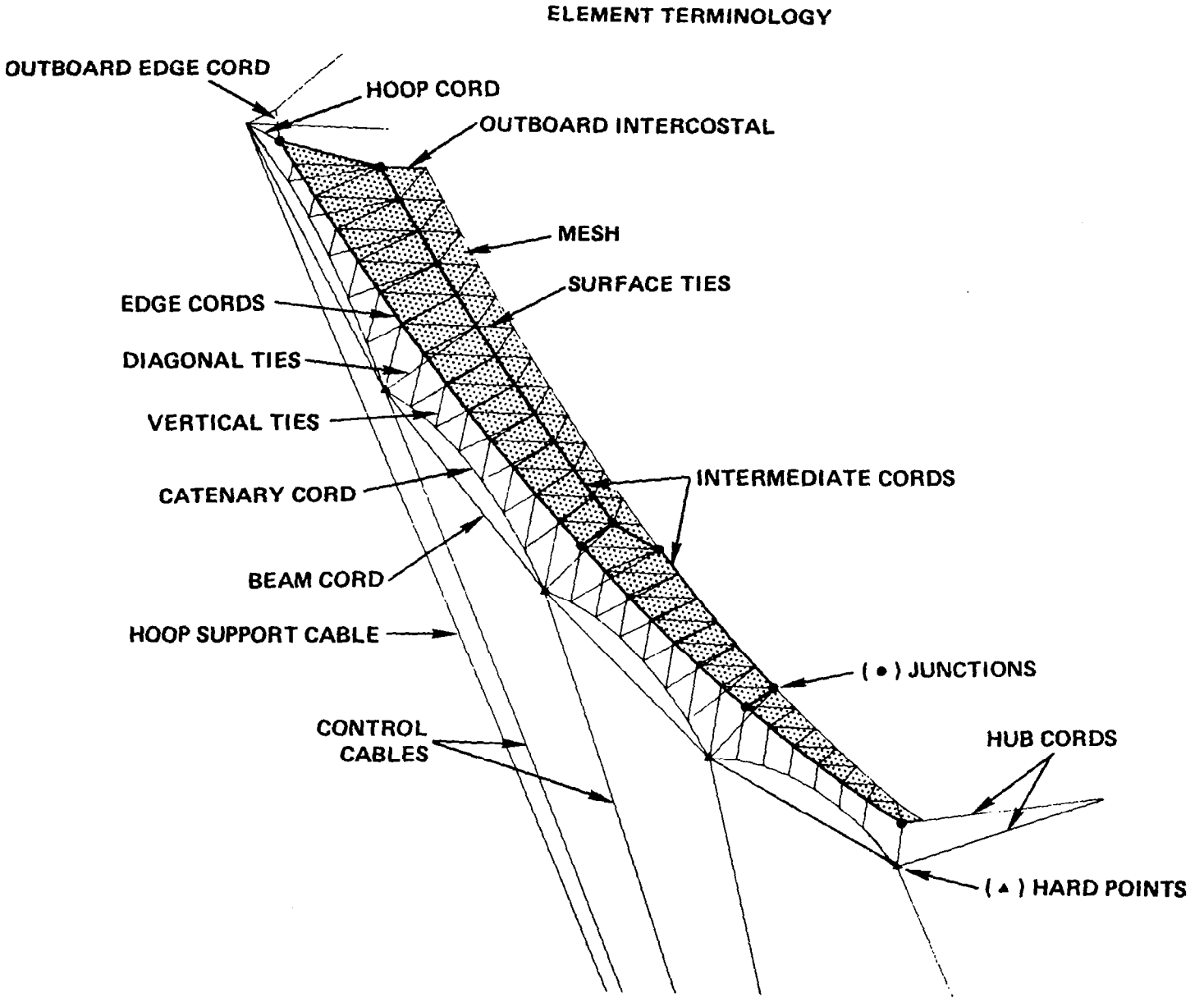


Figure 9.2.2.1-1. Element Terminology

The half-gore model geometry is depicted in Figures 9.2.2.1-2 through 9.2.2.1-4. Cord and mesh properties are given in Figures 9.2.2.1-5 and 9.2.2.1-6, respectively.

### 9.2.2.2 One-for-One Four-Gore Model

The four-gore model is a one-for-one representation of the four-gore surface verification model. The zero-G point design cord and mesh pretension and stiffness are used as the basis of this model. The four-gore model is comprised of four full gores of the antenna surface. The inner two gores of the four-gore surface are the active gores used in the analysis. The outer two gores act as the transition region between the fixed boundary and the inner two gores. Each gore is an image and mirror image of the half-gore model already described, with identical surface elements. However, finer detail is given to the mesh-outboard intercostal with an increased membrane element array. Also, an additional intermediate node is placed on the beam cords.

Model element descriptions are the same as the half-gore model and need not be repeated.

Three figures show the four-gore finite element model in detail: Figure 9.2.2.2-1 shows a view from the back of the surface of cord stringer elements as mounted in the surface verification model boundary fixture. Figure 9.2.2.2-2 shows the mesh membrane elements in the same orientation. Figure 9.2.2.2-3 shows the full four-gore surface with membrane and stringer elements as viewed in the Z axis.

## 9.2.3 Analysis

The one-for-one half-gore model is used for much of the analysis. This includes sensitivity analysis, tolerance studies and mapping effects. The four-gore model is used for 1-G effects and surface adjustment considerations.

There is good correlation between the half-gore model and the four-gore model. Figure 9.2.3-1 shows nodal displacements of the two models when subjected to the same load case. The load case is that of applying gravity to a zero-G configuration while facing down (1-G face-down).

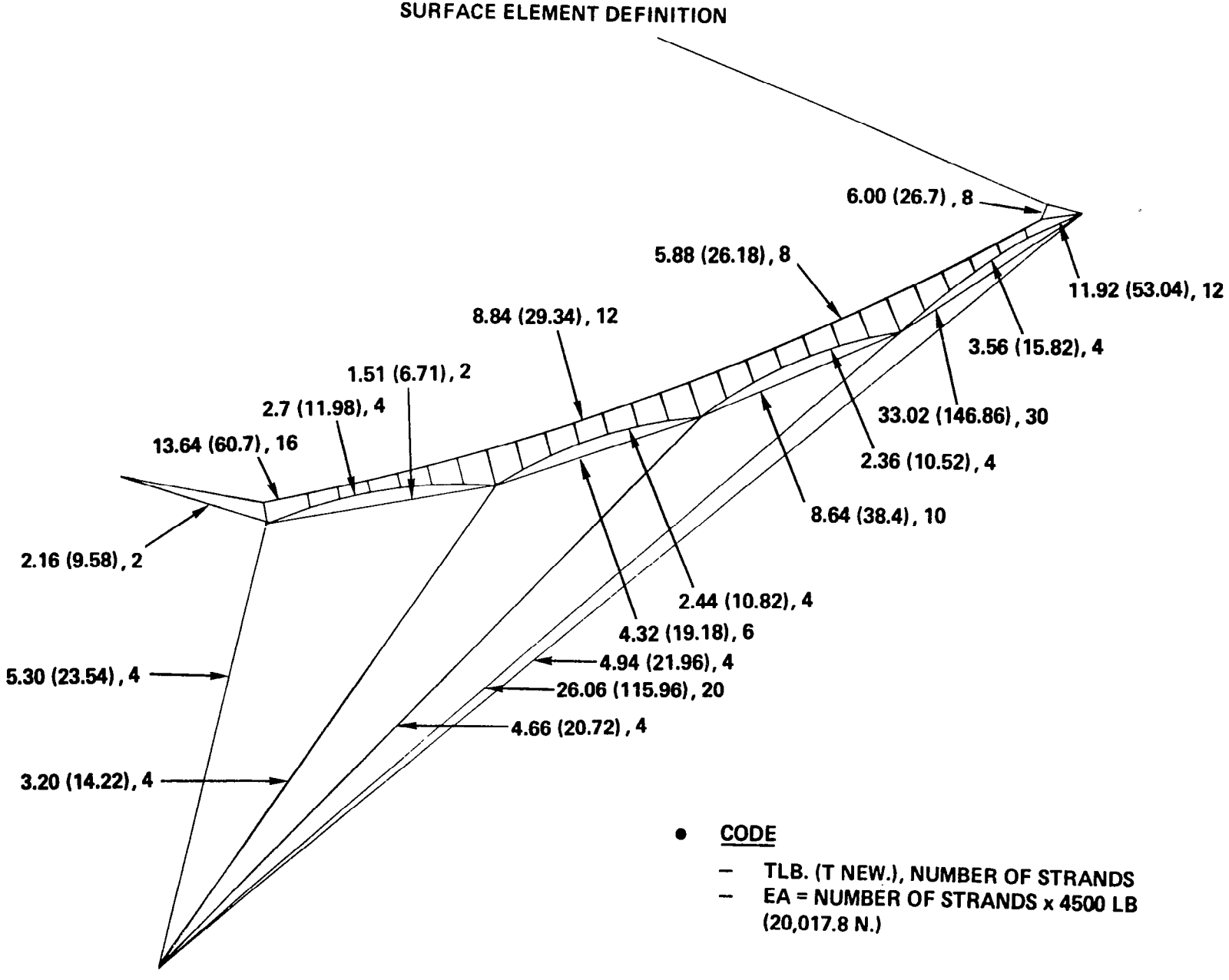


Figure 9.2.2.1-2. Surface Element Definition

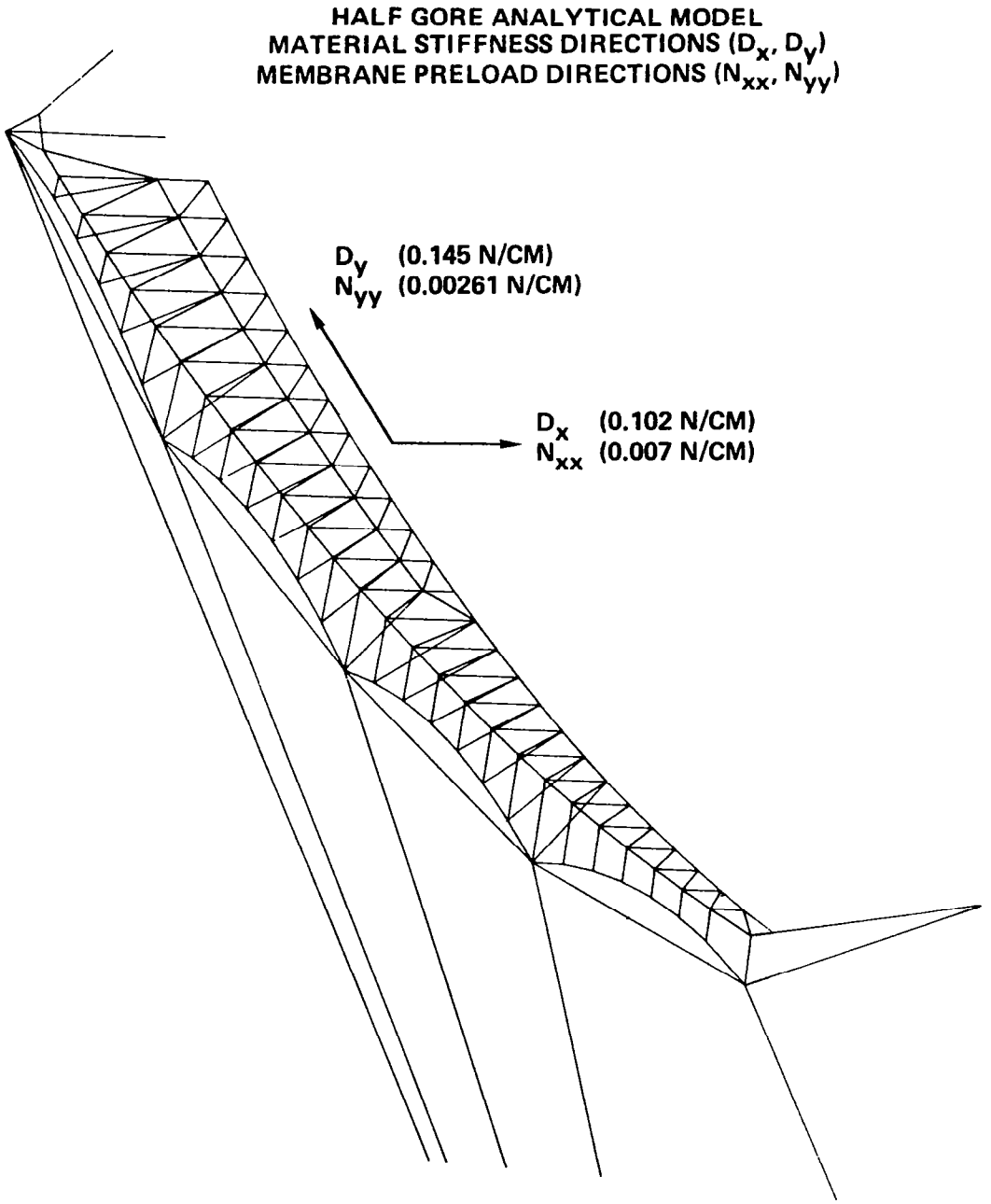


Figure 9.2.2.1-3. Half-Gore Analytical Model

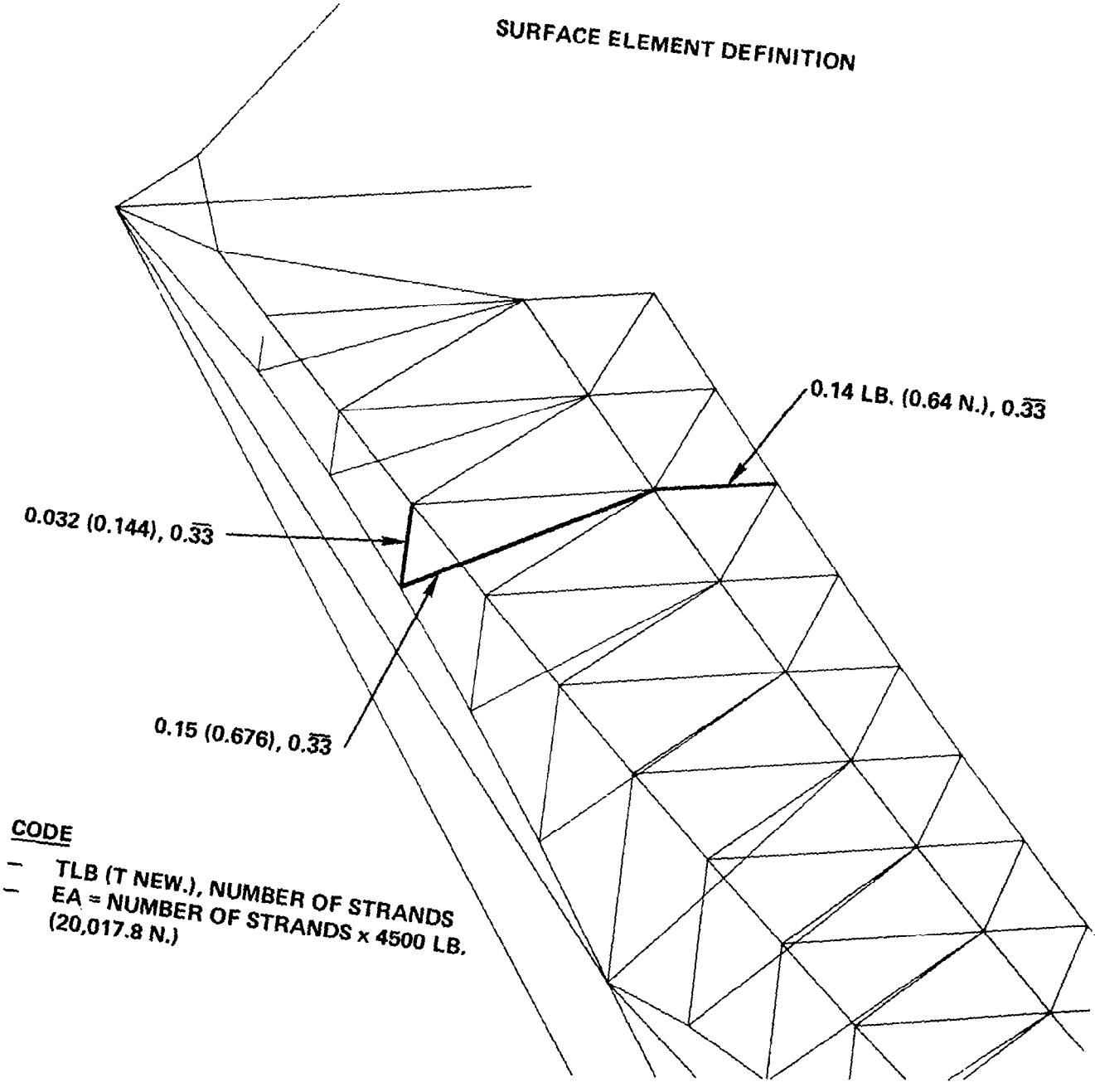


Figure 9.2.2.1-4. Surface Element Definition

CORD PROPERTIES (PER STRAND)

- 3000 GRAPHITE (CELION 3000) FIBERS
- EA = 4000 LB (17793.6 NEWTONS)
- CTE = $-0.25 \times 10^{-6}/^{o}F$
- BREAK STRENGTH = 23 LB (102.3132 NEWTONS)
- WEIGHT = $13.024 \times 10^{-6}$ LB/IN, ($2.28 \times 10^{-5}$ NT/CM)
- OPERATING TENSION 0.5 LB to 1.2 LB (2.2242 TO 5.338 NT)

Figure 9.2.2.1-5. Cord Properties (Per Strand)

## MESH PROPERTIES

- MATERIAL: TRICOT KNIT, 0.0012 IN. DIAMETER, GOLD PLATED MOLYBDENUM WIRE
- TENSION: $N_x$ = 0.004 LB./IN. = 0.0070 N./CM.
  $N_y$ = 0.0015 LB.IN. = 0.0026 N./CM.
- STIFFNESS: LB./IN. (N./CM.)

| SAMPLE | $D_x$ | $D_y$ | $D_1$ | $D_{xy}$ EST. |
|---|---|---|---|---|
| 1 | 0.054 (0.095) | 0.083 (0.145) | 0.056 (0.098) | |
| 2 | 0.062 (0.109) | 0.083 (0.145) | 0.058 (0.102) | |
| AVG. | 0.058 (0.102) | 0.083 (0.145) | 0.057 (0.100) | 0.035 (0.061) |

- WEIGHT

  $\gamma = 9.97 \times 10^{-6}$ LB./IN$^2$ = $6.87 \times 10^{-6}$ N./CM.$^2$

- COEFFICIENT OF THERMAL EXPANSION

  $\alpha = 3. \times 10^{-6}$ CM./CM./$^{o}$F

- OPENING

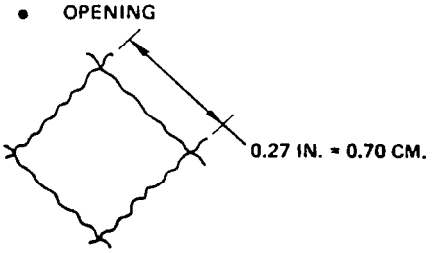


Figure 9.2.2.1-6. Mesh Properties

CORD STRINGER ELEMENTS

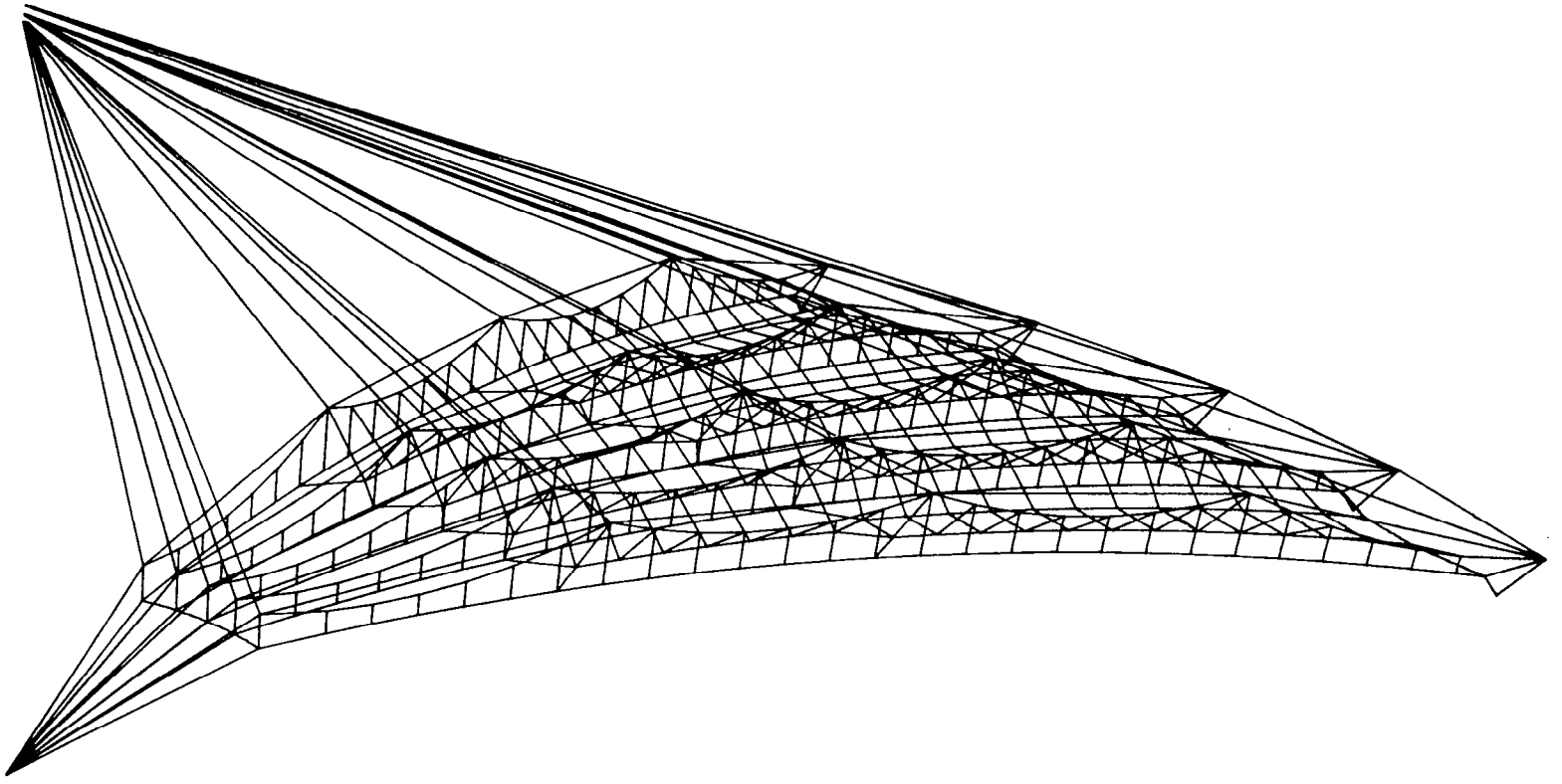

Figure 9.2.2.2-1. Cord Stringer Elements

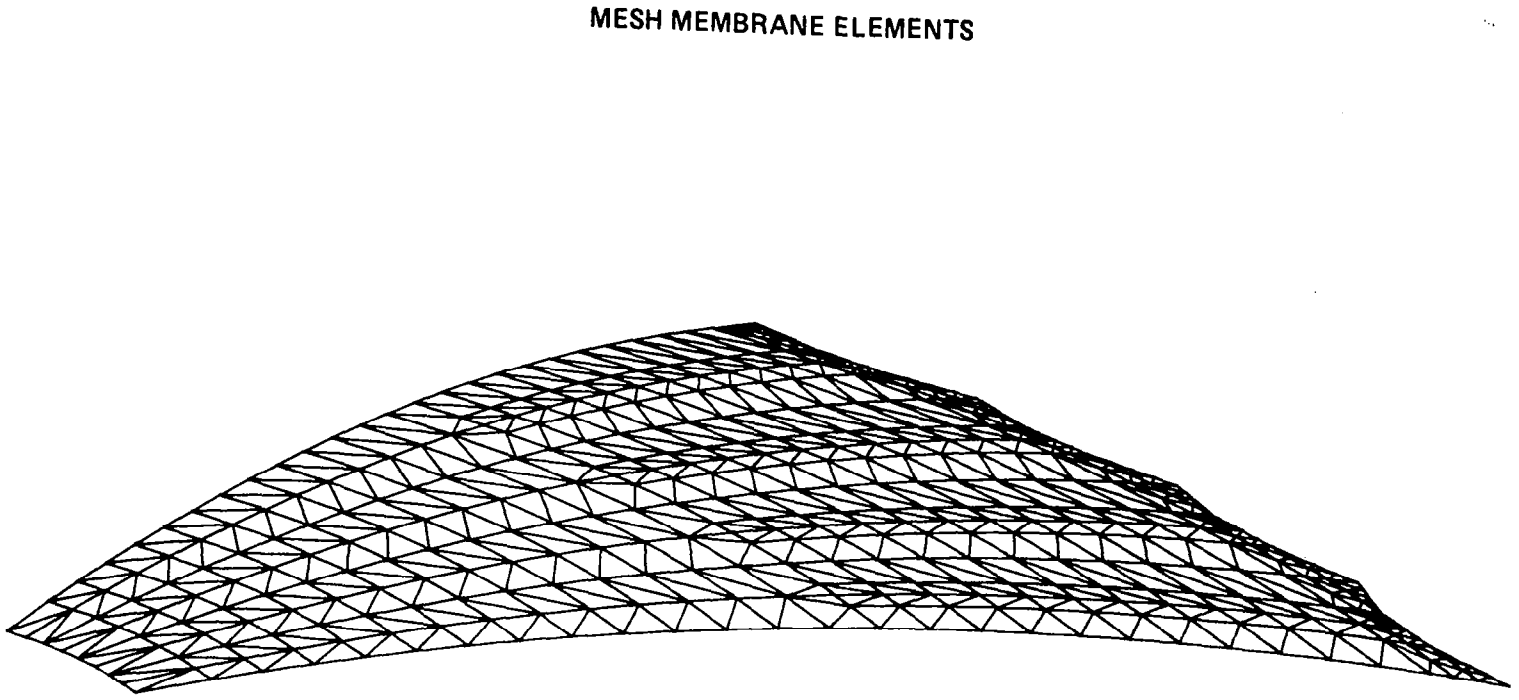


Figure 9.2.2.2-2. Mesh Membrane Elements

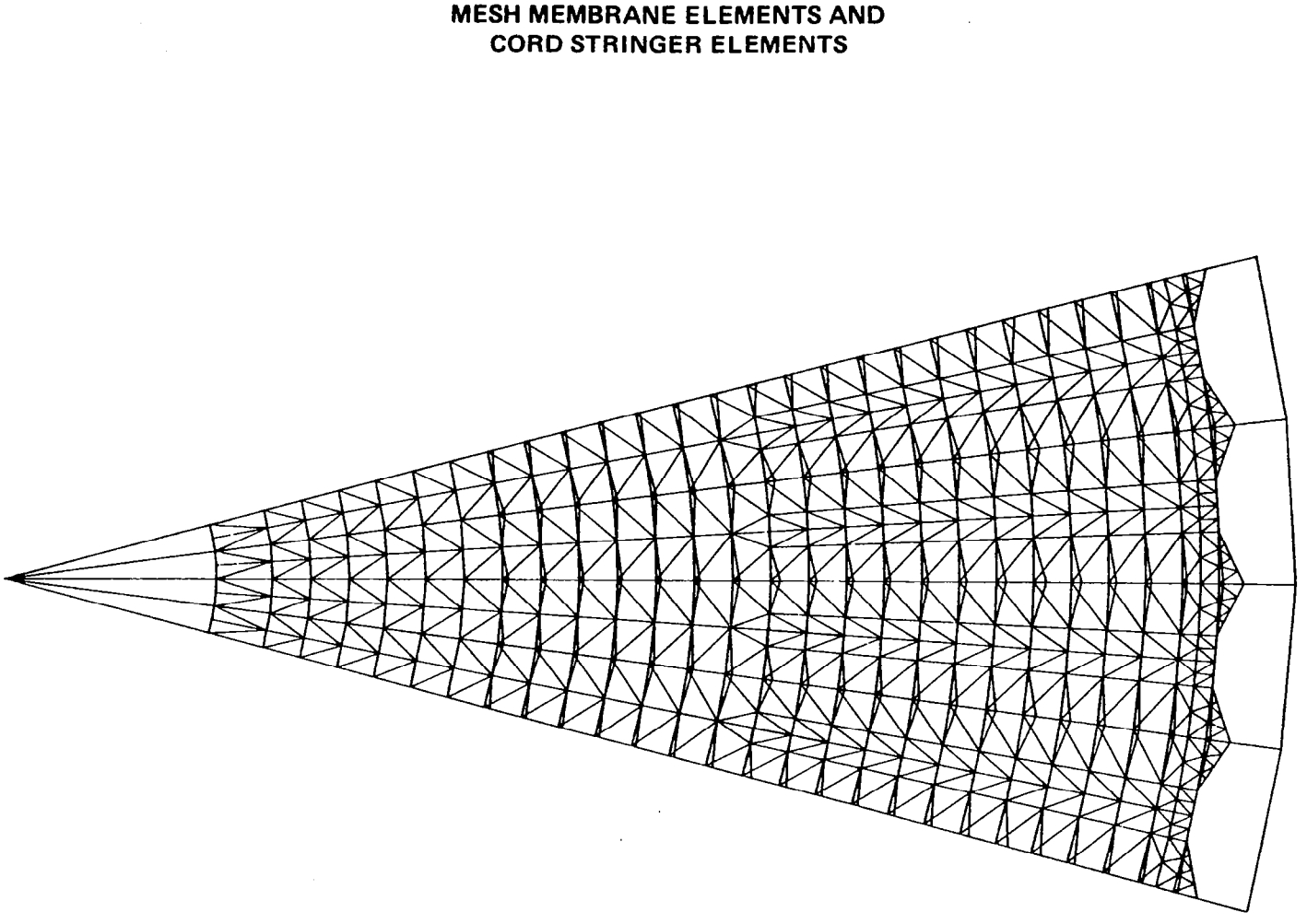


Figure 9.2.2.2-3. Mesh Membrane Elements and Cord Stringer Elements

- LOAD CASE RESULTS (APPLICATION OF GRAVITY)

NODAL DISPLACEMENTS
+Z DIRECTION (DIRECTION OF GRAVITY)

| NODE | HALF-GORE MODEL | FOUR-GORE MODEL |
|---|---|---|
| 15 | -0.0003 IN. | -0.0003 IN. |
| 18 | -0.022 IN. | -0.024 IN. |
| 50 | 0.027 IN. | 0.034 IN. |
| 58 | 0.216 IN. | 0.219 IN. |
| 83 | 0.072 IN. | 0.072 IN. |
| 85 | 0.019 IN. | 0.018 IN. |
| 115 | 0.642 IN. | 0.657 IN. |
| 131 | 0.022 IN. | 0.022 IN. |
| 133 | 0.063 IN. | 0.063 IN. |

1-G CORD TENSIONS (HALF LOADS)

| JA – JB | HALF-GORE MODEL | FOUR-GORE MODEL |
|---|---|---|
| 15 – 20 | 2.222 LB | 2.208 LB |
| 80 – 85 | 2.332 LB | 2.304 LB |
| 128 – 131 | 6.015 LB | 6.054 LB |
| 81 – 84 | 2.296 LB | 2.316 LB |
| 17 – 27 | 3.829 LB | 3.895 LB |
| 87 – 91 | 2.367 LB | 2.408 LB |

Figure 9.2.3-1

### 9.2.3.1 Sensitivity Studies

Many sensitivity studies were done using the half-gore model to understand the effects on the structure due to variations in material properties, cord and mesh pretensions, and manufacturing tolerances. The effects are evaluated in terms of surface contour system effects, i.e., surface roughness (RMS value) and antenna defocus. The individual cases considered and results are presented in what follows.

#### Mesh Sensitivity Studies

The mesh stretched across the cord truss structure forms the RF reflective surface of the antenna. The antenna structure is designed to be highly cord dominated. This means that mesh stiffness and pretension should be second order when compared to the cord stiffness and pretension. Therefore, a large variation in mesh properties would have to be present to effect system characteristics. For the sensitivity studies the effects of extreme mesh property changes were used.

To undestand the effect of mesh stiffness (Dx, Dy, Dl properties) variations, the 3σ mesh stiffness value was used. Mesh stiffness values are arrived at by repeatedly testing samples of mesh material and statistically fitting the results. A normal distribution is applied to the data values obtained to determine the standard deviation (σ) of the data points. Three standard deviations (3σ) represents a large percentage of all possible data values, and therefore designates a worst-case effect. The increased (+3σ) stiffness case was used because the mesh stiffness approaches the cord stiffness, and mesh stiffness become more dominant in the overall structural stiffness. Figure 9.2.3.1-1 shows the results of the sample testing values.

The results shown in Figure 9.2.3.1-2 show that the structure remains cord dominated and that the predicted surface (compared to baseline) will vary only slightly with increased mesh stiffness.

- STIFFNESS CHARACTERIZED BY NUMEROUS TESTING OF SAMPLES
  - STATISTICAL RESULTS

| | DX( $\mu$/CM) | DY( $\mu$/CM) | D1 ( $\mu$/CM) |
|---|---|---|---|
| $\mu$ (MEAN) | 0.058 | 0.083 | 0.057 |
| $\sigma$ (STA. DEV) | 0.010 | 0.030 | 0.011 |

Figure 9.2.3.1-1. Mesh Sensitivities

MESH SENSITIVITY

| SENSITIVITY | RMS | ( $\triangle$F + $\triangle$ Z) |
|---|---|---|
| MESH + 3 $\sigma$ | (0.00054 IN.) | (-0.009 IN.) |
| MESH TENSION x 3 | (0.051 IN.) | +1.465 IN. |

Figure 9.2.3.1-2. Mesh Sensitivity

Another mesh sensitivity considered is the mesh pretension. The nominal values of mesh pretension are 0.0026 NT/CM radially and 0.007 NT/CM circumferentially (Figure 9.2.2.1-6). For the sensitivity case the nominal value of pretension was tripled, or the pretension value changed to 0.0078 NT/CM radially by 0.021 NT/CM circumferentially. This is equivalent to a strain rate of +0.315016 CM/CM circumferentially (soft direction) and +0.180192 CM/CM radially (hard direction). This large strain rate will not be encountered in manufacturing. However, the analysis was performed as an extreme upper bound condition.

As indicated in Figure 9.2.3.1-3 a tripling of mesh pretensions affected the surface system characteristics to a notable degree. However, the mapping results (Paragraph 9.2.3.3) indicate very small dimensional changes in the mesh surface due to mapping and manufacturing has proven to have good workmanship in mesh panel production. Therefore large effects due to variations in mesh pretensions are not expected.

Cord Sensitivity Studies

Manufacturing of many of the truss structure cords will be done using loading and geometry techniques. The effects of loading variations will be analyzed in this section and geometry variation effects will be analyzed in the tolerance study section.

To analyze the sensitivity of the cords to loading variations, key cords were selected and initial loads varied by approximately 10% change in load. The key cords selected are the beam cords on the back surface and the radial cords on the front surface. Also the control cord tensions were changed to study surface cord loads when making surface adjustments. Figure 9.2.3.1-3 shows the results of the sensitivity studies. The results indicate that of the cords analyzed, the beam cords are the most critical. However, the adjustment process will greatly reduce system errors in focal length and help reduce surface roughness (Paragraph 9.2.3.4). The control cords have the greatest effect on the system. This is, of course, the design purpose of the control cords.

## CORD SENSITIVITY RESULTS

| SENSITIVITY ELEMENT (JA – JB) | LOAD VARIATION | RMS (CM) | (△F + △Z) (CM) |
|---|---|---|---|
| BEAM CORD (132 – 110) | -10.0% | 0.0063 (0.0025 IN.) | -0.1913 (-0.0632 IN.) |
| BEAM CORD (110 – 81) | -10.0% | 0.0419 (0.0166 IN.) | 0.0851 (0.0335 IN.) |
| BEAM CORD (81 – 46) | -10.0% | 0.0846 (0.0333 IN.) | 1.9728 (0.7767 IN.) |
| BEAM CORD (46 – 12) | -9.8 % | 0.0533 (0.0210 IN.) | 1.8363 (2.7229 IN.) |
| RADIAL CORDS (17 – 82, 87 – 111) | -10.0% | 0.0203 (0.0080 IN.) | 0.2889 (0.1138 IN.) |
| | TOTAL (RSS) | 0.111 CM | 2.718 CM |

Figure 9.2.3.1-3. Cord Sensitivity Results

### 9.2.3.2 Tolerance Effects

Dimensional variation due to manufacturing has been shown to be within 80 parts/million on cord lengths. This number has been arrived at by past performance of manufacturing showing good workmanship capabilities. Therefore, this tolerance has been applied to the most significant cords of the surface structure (but not less than 0.050 CM minimum). These cords are:

Beam Cords
Radial Surface Cords
Outboard Intercostal
Surface Ties
Hoop Cord

The locations of the cords are shown on a typical half-gore of the surface in Figure 9.2.2.1-1.

The results of the tolerance studies are shown in Figure 9.2.3.2-1.

The worst-case total of roughness is 0.151 CM and defocus is 4-361 CM.

By adjusting the surface and by using a tensioning device on the radial cords at the mast, most of the effects can be removed. The radial tensioning device is discussed in the surface adjustment section.

### 9.2.3.3 Flat Gore Mapping

The process for manufacturing and assembling a flat two-dimensional surface so that it may be transformed to a three-dimensional doubly-curved predetermined position, is called mapping the surface. The simplest method is to start with the three-dimensional surface and maintaining element lengths, construct the surface in two dimensions. This simple method works well with the LSST antenna concept, because of the relative flatness of each panel. Very small dimensional changes occur in the mesh elements and the stringer elements as the results in Figure 9.2.3.3-1 indicate.

The flat panel manufacturing occurs under controlled conditions with specified cord intersection points and specified cord loads.

**TOLERANCE EFFECTS**

| ELEMENT | TOLERANCE | RMS (CM) | (△F + △Z) (CM) |
|---|---|---|---|
| BEAM CORD | +0.050 CM | 0.119 | 2.311 |
| RADIAL SURFACE CORD | +0.100 CM | 0.058 | -1.387 |
| OUTBOARD INTERCOSTAL | +0.050 CM | 0.058 | -0.150 |
| SURFACE TIES | +0.050 CM | 0.020 | -0.373 |
| HOOP CORD | +0.050 CM | 0.041 | -0.140 |
| | TOTAL (RSS) | 0.151 CM | 2.729 CM |

Figure 9.2.3.2-1. Tolerance Effects

MEMBRANE MAPPING EFFECTS (LARGEST VARIATION)

CHANGE IN MESH PRE-TENSION (1)

RADIAL 0.00011 NT/CM

CIRCUMFERENTIAL. 0.00012 NT/CM

STRINGER MAPPING EFFECTS (LARGEST STRAIN)

CHANGE IN CORD LENGTH = $69.4 \times 10^{-6}$ CM/CM

$\Delta L = 0.0076$ CM

Figure 9.2.3.3-1. Mapping Effects

### 9.2.3.4 Surface Error Budget Manufacturing Contribution

The total contributing defocus and surface roughness due to manufacturing processes is listed in Figure 9.2.3.4-1. This table includes effects on the cord lengths and flat panel coordinates as a result of measurement in accuracy.

#### Uncertainties Budget

Inherent in any analysis is the area of uncertainty. The uncertainty is not within the mathematical model but with inputs into the mathematical model. For the 50-Meter Breadboard Model the uncertainties list consists of only the element material properties and the mesh pretension. The total contribution to the system is small and can be seen in Figure 9.2.3.4-2.

#### 50-Meter Contour Budget

The 50-Meter Model contour budget is presented in Figure 9.2.3.4-3; all contributions to the distortion are listed as well as the contribution of surface roughness (pillowing) due to doubly curved surface. The total predicted defocus is therefore:

$$\Delta F + \Delta Z = 4.879 \text{ CM}$$

and the total predicted surface roughness is:

$$\text{RMS} = 0.241 \text{ CM}$$

these values represent a change in defocus and surface roughness from the nominal 1-G surface.

### 9.2.3.5 1-G Effects

The surface verification model is oriented in the face-down configuration with the 1-G environment. The analytic surface position simulates the 50-meter model surface. The analytic position is arrived at by applying the force of gravity on the one-for-one four-gore model originally in the zero-G environment. The deflected model with the new cord tensions, membrane tensions, and nodal coordinates become the analytic 1-G surface verification finite element model.

## MANUFACTURING CONTRIBUTION TO BUDGET

| BUDGET ARTICLE | BUDGET CONTRIBUTION | |
|---|---|---|
| | ($\triangle F + \triangle Z$) (CM) | RMS (CM) |
| ASSEMBLING EFFECTS (DUE TO $\Delta$ CORD LOAD MESH SENSITIVITY) | 2.718 | 0.111 |
| TOLERANCE EFFECTS | 2.729 | 0.151 |
| FLAT PANEL MAPPING | 0.015 | 0.000 |
| MEASUREMENT ACCURACY | 0.100 | 0.022 |
| TOTAL (RSS) | 3.853 CM | 0.189 CM |

Figure 9.2.3.4-1. Manufacturing Contribution to Budget

## UNCERTAINTIES CONTRIBUTION

- AREA OF CONCERN
  - UNEXPECTED VARIATIONS IN AS DESIGNED AND AS ANALYZED MATERIAL PROPERTIES AND ELEMENT PRETENSIONS

| BUDGET ARTICLE | BUDGET CONTRIBUTION ($\triangle F + \triangle Z$) (CM) | RMS (CM) |
|---|---|---|
| • MESH SURFACE | | |
| – MESH STIFFNESS ( $\pm 3\sigma$ ) | 0.018 | 0.001 |
| – MESH PRE-TENSION ( ±50%) | 0.620 | 0.008 |
| • GRAPHITE CORDS | | |
| – STIFFNESS ( ± 5%) | 0.388 | 0.017 |
| TOTAL | 1.026 CM (SUM) | 0.019 CM (RSS) |

Figure 9.2.3.4-2. Uncertainties Contribution

1-G CONTOUR BUDGET

| | (△F + △Z) (CM) | RMS (CM) |
|---|---|---|
| MANUFACTURING EFFECTS | 3.853 | 0.189 |
| UNCERTAINTIES | 1.026 | 0.019 |
| PILLOWING | 0.000 | 0.148 |
| TOTAL | 4.879 CM (SUM) | 0.241 CM (RSS) |
| | (1.921 IN) | (0.095 IN) |

Figure 9.2.3.4-3. 1-G Contour Budget

By applying the force of gravity to a structure defined for the zero-G environment, a new 1-G structure is defined. Based upon elementary laws of statics, a new equilibrium position is reached and is reflected in the 1-G model. The equilibrium position is created when the action generated by gravity super-position is reacted by changing element tensions within the structure. To maintain the changing element tensions to a minimum an external force should be used to counteract the new gravity force. The external force is applied in the form of a counterbalance.

The counterbalance allows the 1-G environment analytics to better simulate the zero-G point design analytics. This increases the accuracy of the implications gained from the 1-G surface verification model.

The analytically chosen counterbalance points are indicated in Figure 9.2.3.5-1. Only three counterbalance points are needed per gore of surface which simplifies manufacturing considerations.

Using the counterbalanced structure greatly reduced tension changes and therefore reduced nodal displacement. The largest displacement occurred at mesh nodal points and is 1.67 CM. Most nodal displacements are less than 0.127 CM.

The change in system characteristics are:

$\Delta F$ = 3.593 CM
$\Delta Z$ = 0.470 CM
$\Delta RMS$ = 0.348 CM

A view of the finite-element four-gore model membrane elements is plotted in Figure 9.2.3.5-2. The 1-G displacements are amplified by a factor of 10 for visual enhancement. The displacement view should be compared with the zero-G view in Figure 9.2.2.2-2 to notice displacements.

### 9.2.3.6 Surface Adjustment

The one-for-one four-gore finite-element model is used in the analysis or surface adjustment considerations.

CONTROL CABLE ADJUSTMENT

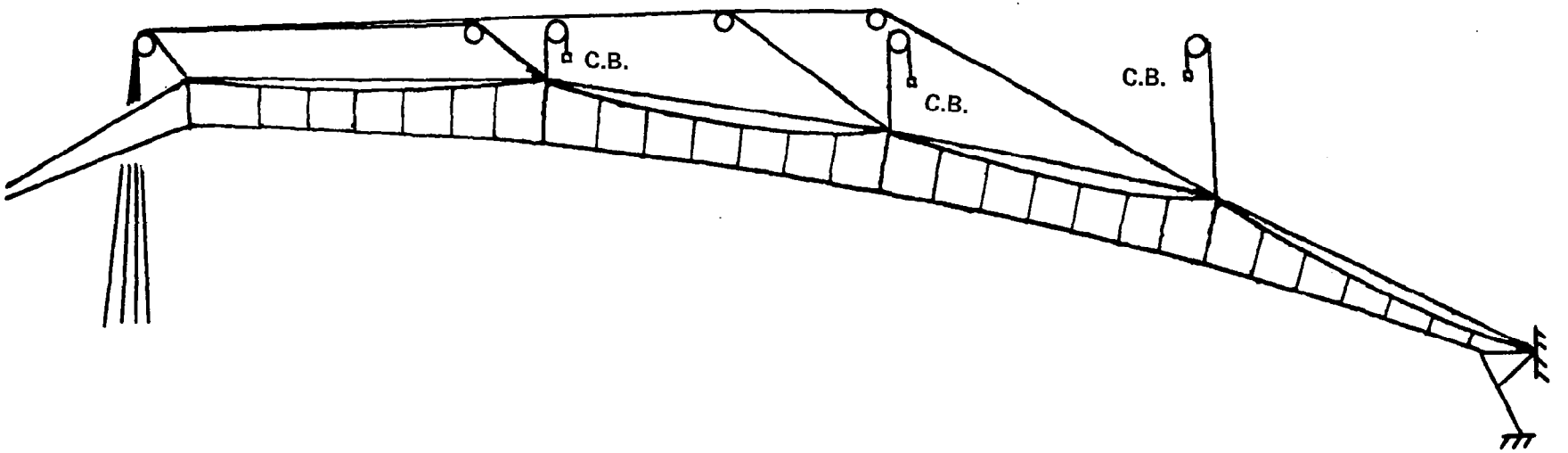


C.B. = COUNTERBALANCE POINTS

Figure 9.2.3.5-1. Counter Balance System

1-G FACE-DOWN CONFIGURATION

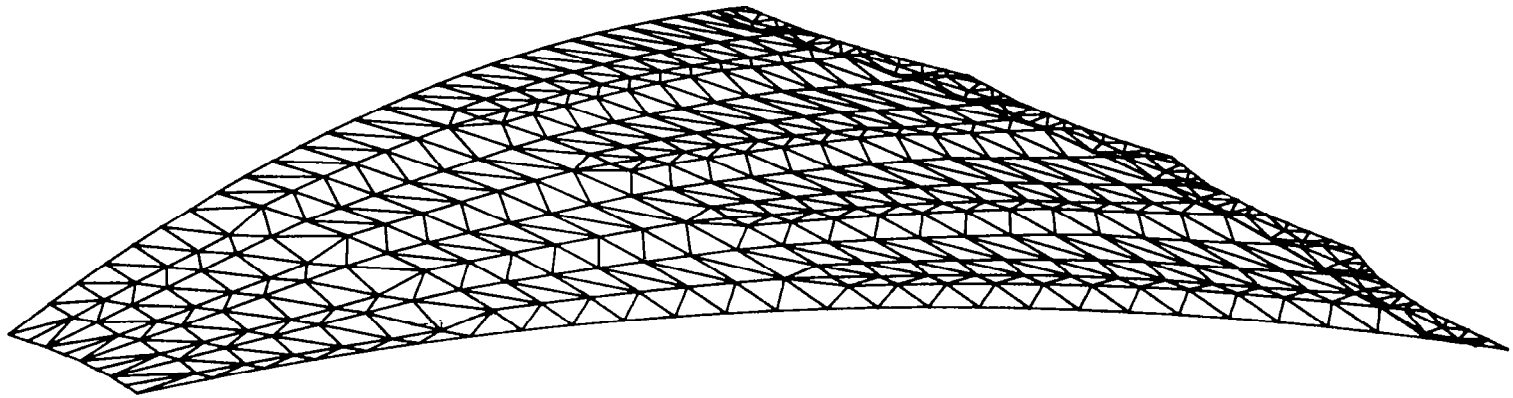

Figure 9.2.3.5-2. 1-G Face-down Configuration

There are 12 surface control cords on the four-gore surface verification model. The control cords are primarily designed to make desired surface adjustments which are normal to the surface (Figure 9.2.3.6-1).

Surface adjustment affects surface position and cord loads. The surface adjustment process is based upon the analytical cord tensions. Therefore, to simulate accurately a large variation of surface adjustments a mechanism is used to maintain a near constant cord load on the surface radial cords. The mechanism is a simple low stiffness, extension spring. The spring is attached in line with the two radial cords of each panel as shown in Figure 9.2.3.6-2.

The radial spring is desired for adjustment purposes, however, it is not desired for on-orbit thermal-elastic (TE) purposes. Therefore it will be locked out during on-orbit operation. As an example, the following comparison is made on the point design antenna (100 meter).

T.E. CASE ECLIPSE

POINT DESIGN

| | RMS | $\Delta F + \Delta Z$ |
|---|---|---|
| Radial Spring Free | 1.029 CM | 9.068 CM |
| Radial Spring Locked Out | 0.030 CM | 1.323 CM |

The surface adjustment scheme is based upon the following principles.

An interaction matrix (I) is determined analytically from the four-gore finite-element model. This is determined by normalizing displacements of the surface (in the normal direction) caused by a unit adjustment of a single control cord. Thus the interaction of other surface points is related to the adjustments of the control cords.

## SURFACE ADJUSTMENT

- FOUR-GORE MODEL USED FOR ANALYSIS
- DESIRED ADJUSTMENT MOTION IN DIRECTION NORMAL TO SURFACE

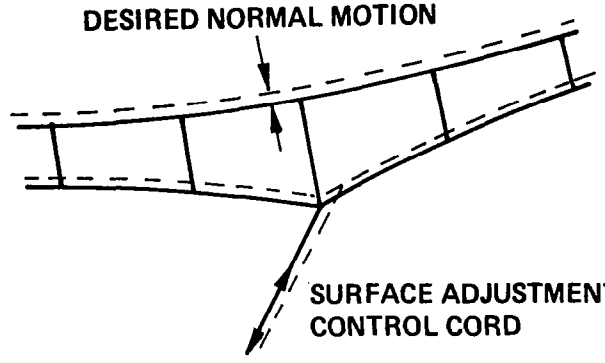


- SURFACE ADJUSTMENT AFFECTS CORD LOADS AND SURFACE POSITION
- INTERACTION ADJUSTMENT IS BASED UPON KNOWN ANALYTIC CORD LOADS
- ACCURACY AND CONVERGENCE OF ADJUSTMENT PROCESS INCREASED BY MAINTAINING CORD LOADS
- RADIAL SPRING MAINTAINS RADIAL CORD LOAD ACCURACY



Figure 9.2.3.6-1. Surface Adjustment

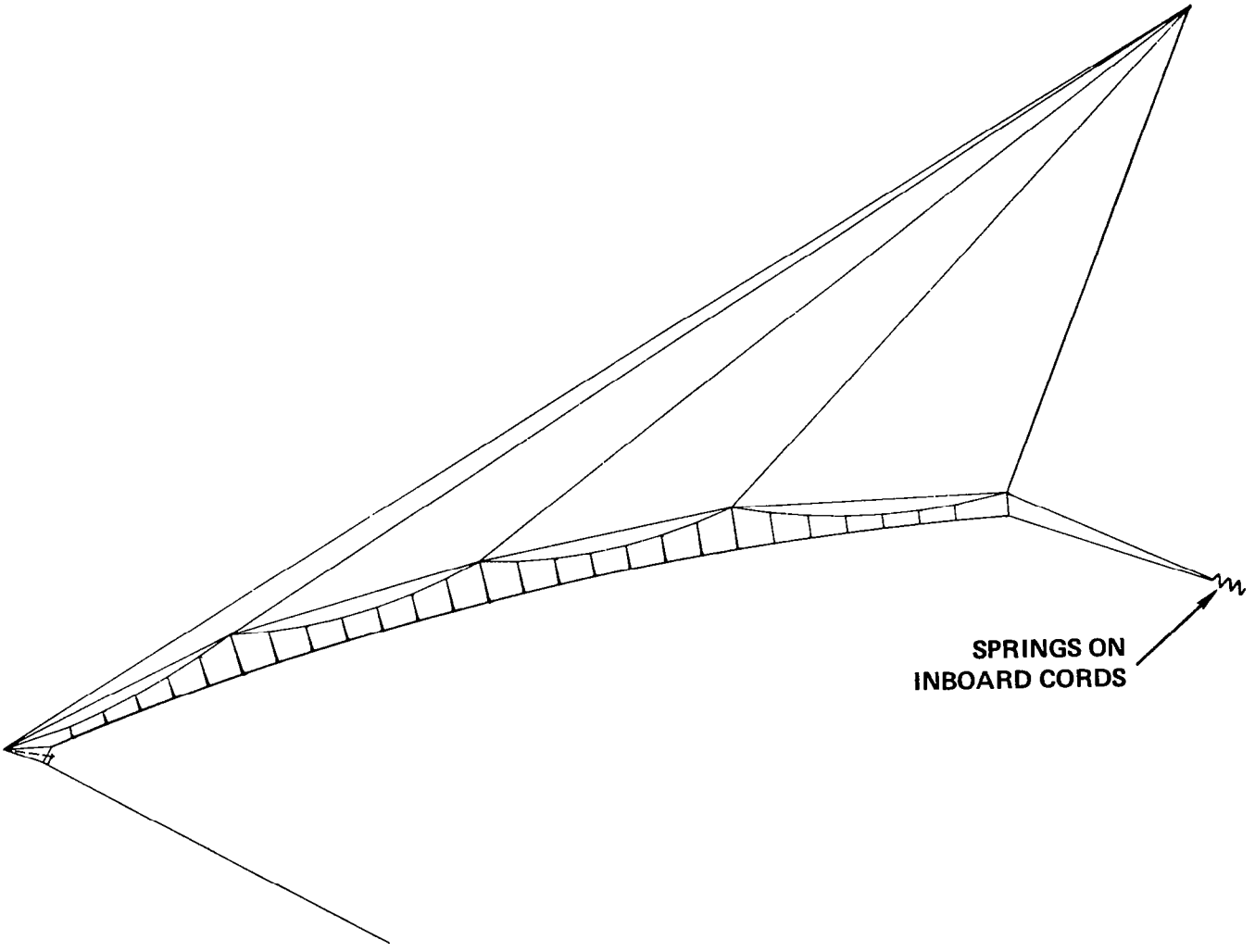


Figure 9.2.3.6-2. Radial Spring Location

In matrix notation this is written as follows:

$$\left\{\begin{array}{c}\text{Control}\\ \text{Cord}\\ \text{Adjustment}\end{array}\right\} \quad X \quad \left[\begin{array}{c}\text{Structural}\\ \text{Stiffness}\\ \text{Matrix}\end{array}\right] = \left\{\begin{array}{c}\text{Normal}\\ \text{Surface}\\ \text{Displacement}\end{array}\right\}$$

or

$$\{ai\} \times \left[\kappa\right] = ' \{\phi\}$$

Where; ai $\triangleq$ possible adjustments

$i = 1, 12$

$\kappa$ $\triangleq$ stiffness matrix

$\phi i$ $\triangleq$ corresponding set of displacements for each unique adjustment.

$i = 1, 12$

Next, the surface is measured and a set of deviations of the nodal points from the desired nodal points is established. Knowing the normal deviations, the error vector' {e} is assembled with the deviations becoming the super-position of some portion of each of the twelve adjustment mode shapes $\phi i$.

or $$' \{e\} = \sum_{i=1}^{12} ai \ \phi i = \left[\phi\right] \{a\}$$

Where $\left[\phi\right]$ is a matrix consisting of columns of' $\{\phi i\}$ vectors.

Finally the least squares best-fit adjustment amplitudes are given by:

$$' \{a\} = \underbrace{\left[\left[\phi\right] + \left[\phi\right]\right]^{-1}}_{I} \left[\phi\right]^{+} \ ' \{e\}$$

I is the interaction matrix and is formed previous to the measurement process and stored on the computer disc.

The adjustment amplitudes are calculated real time after each measurement set until surface set is achieved. The iterative process is shown in Figure 9.2.3.6-3. For this process to work efficiently the individual adjustment should produce, at best, a local effect. This would allow the $\phi$ matrix to be definite as desired. Figures 9.2.3.6 A, B, C, and D show the normal displacements of the surface when subjected to a control cord adjustment. For each case shown, the back control cord was shortened by 0.10 inches. The corresponding displacements are normal to the surface. The plots shown are of the four-gore analytic surface verification model in the 1-G environment. The numbers indicate mostly local effects in the region of the adjustment, as is desired. (The adjustment point is circled.) This indicates that convergence will be achieved by the adjustment procedure.

### 9.2.3.7 Analysis Conclusions

Through the use of the analytical models, the following conclusions are reached.

Sensitivity results show that current manufacturing abilities can produce a structure in the 1-G environment which will correlate well with the analytical model.

Tolerances in the main surface cords, (i.e., radial surface cords and beam cords) should be small, however, more importantly tensions in the cords can be controlled accurately with the radial spring device.

Surface mapping effects are small due to the surface flatness, which provides good manufacturing accuracy.

1-G effects can be reacted and controlled with a counterbalance system. This will allow good simulation of the zero-G surface adjustment process.

The surface-adjustment interaction is shown to be a desired local effect, indicating the adjustment procedure will converge.

SURFACE ADJUSTMENT FLOW

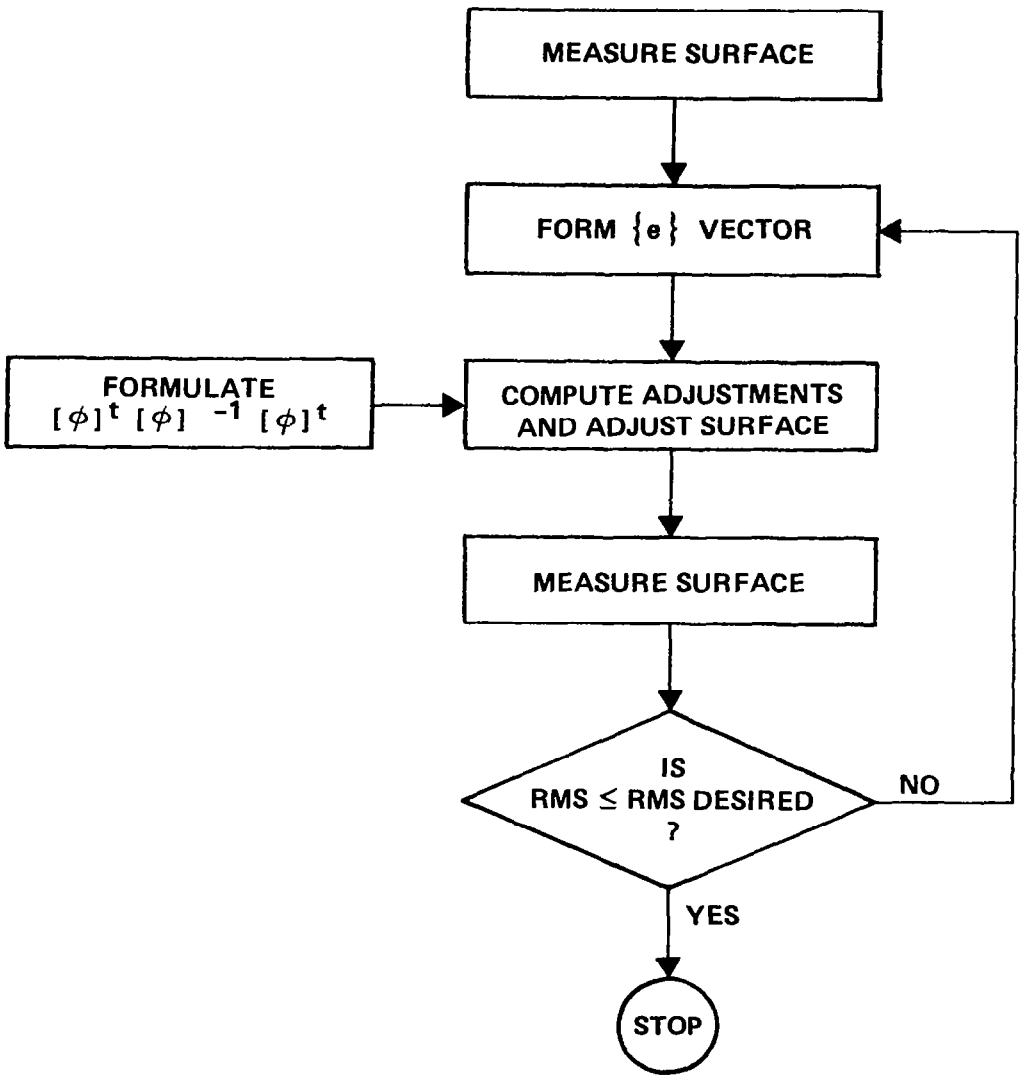


Figure 9.2.3.6-3. Surface Adjustment Flow

## FIRST CONTROL CORD

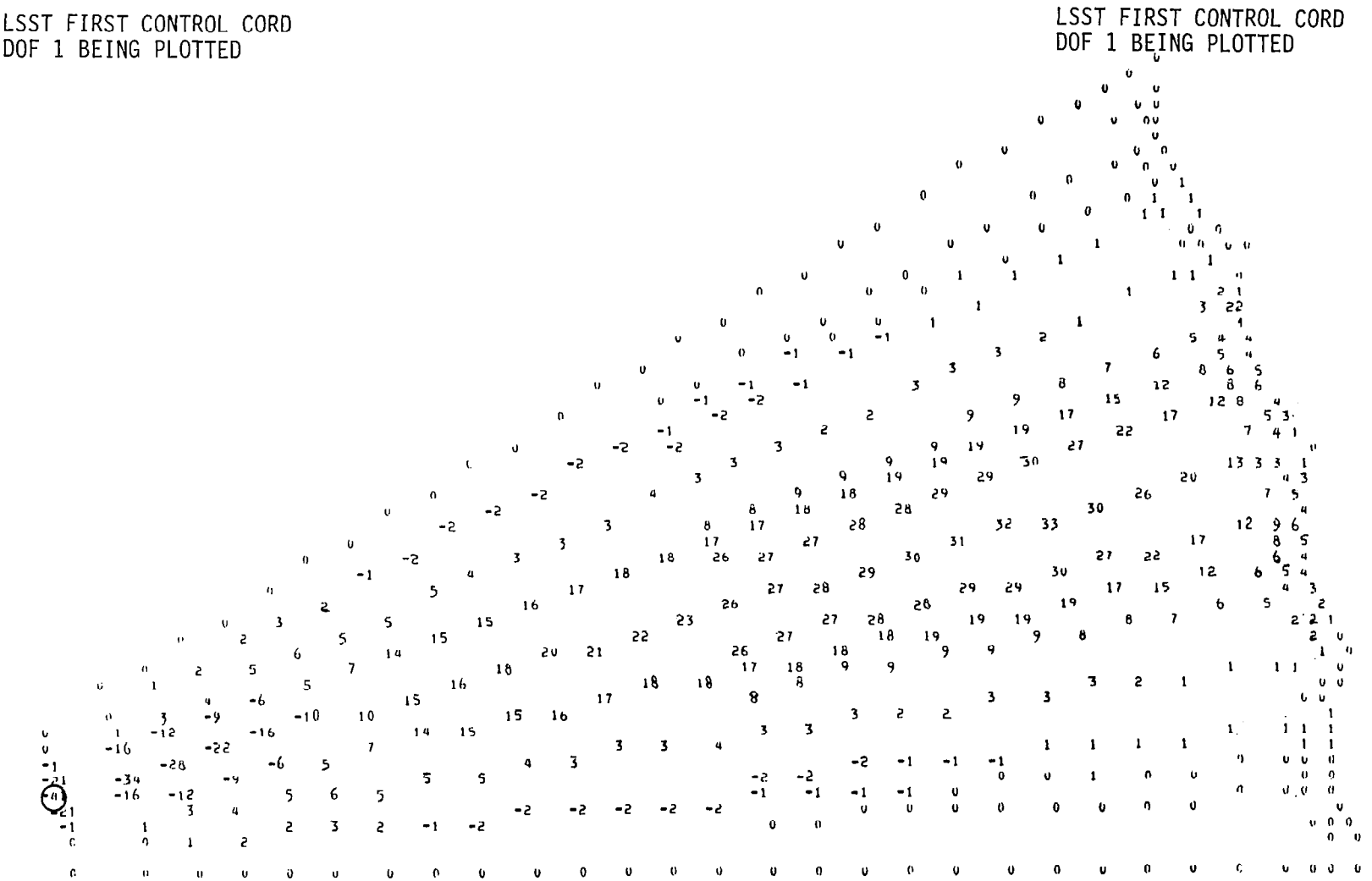


Figure 9.2.3.7-4A. First Control Cord

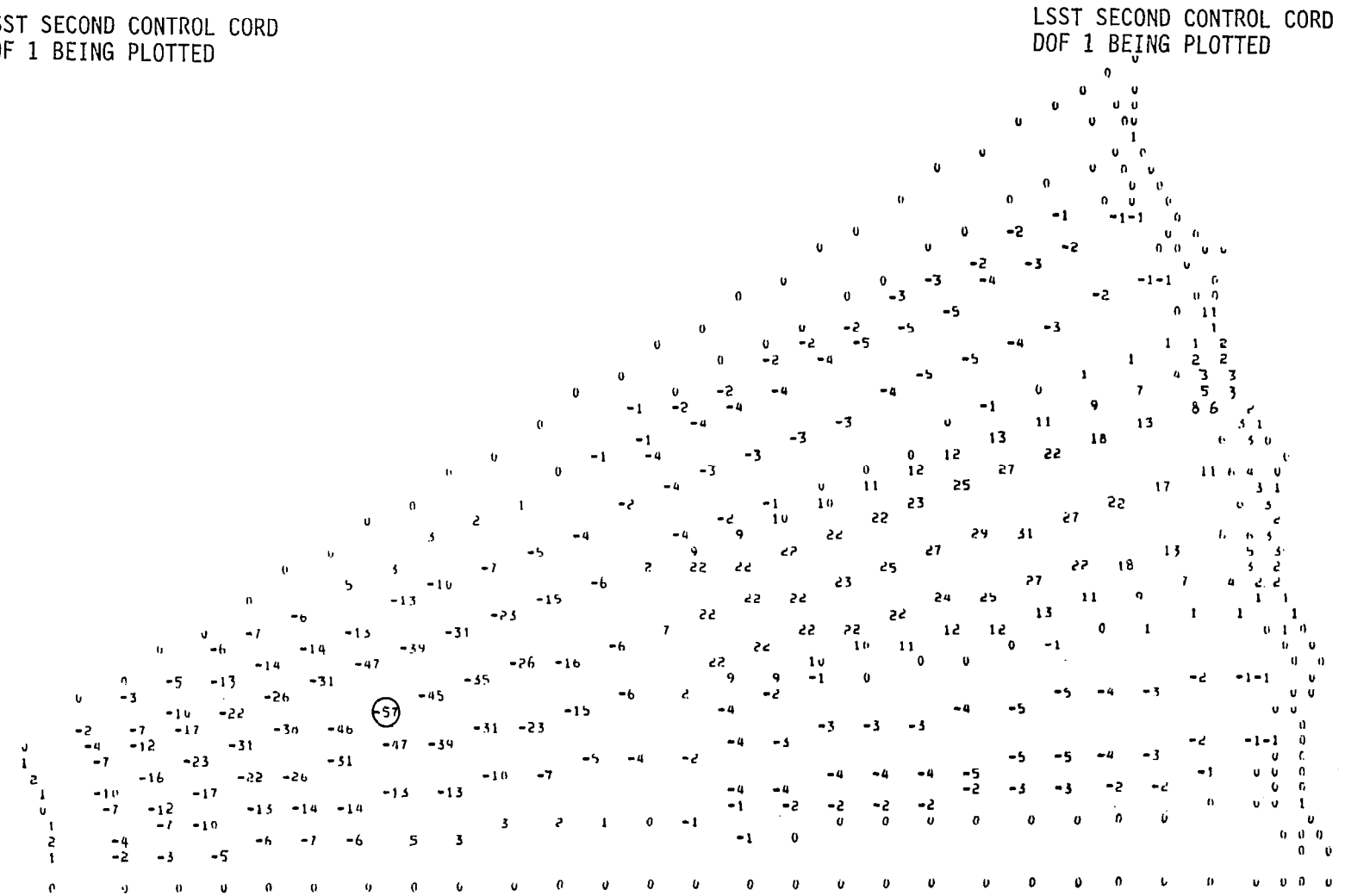


Figure 9.2.3.7-4B. Second Control Cord

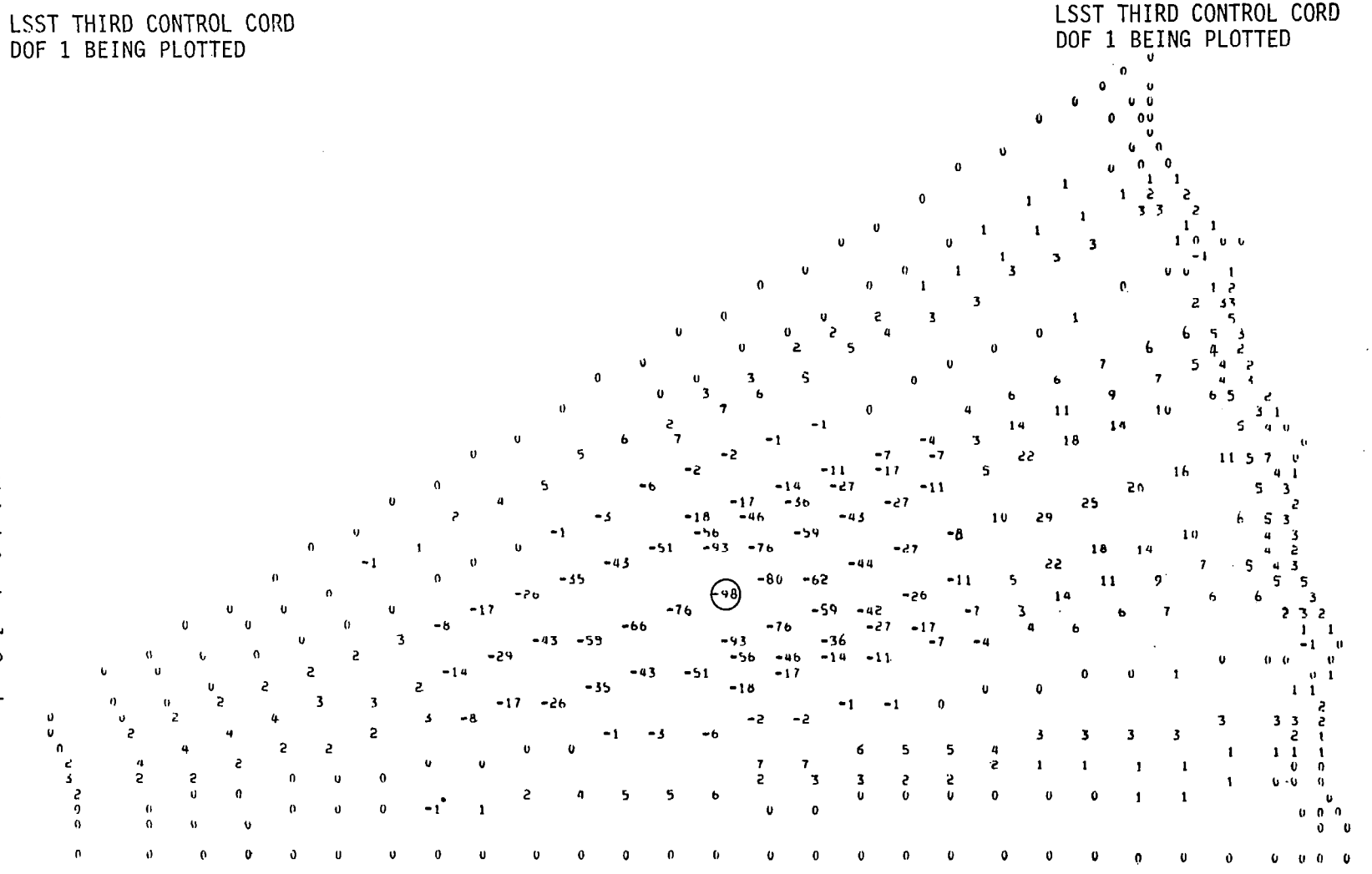


Figure 9.2.3.7-4C. Third Control Cord

15.,15.
DOF 1 BEING PLOTTED

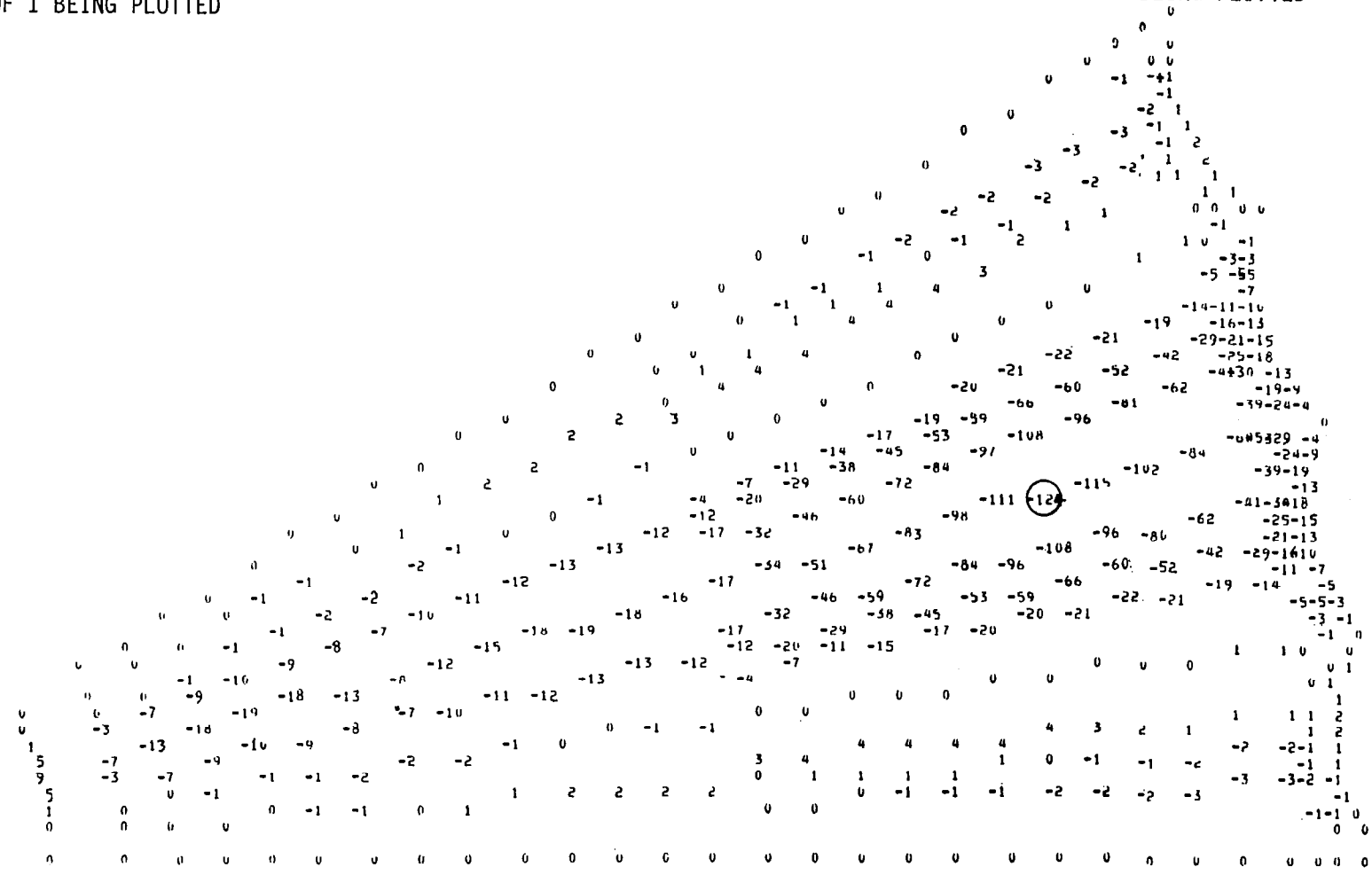

Figure 9.2.3.7-4D. Fourth Control Cord

## 9.3 Boundary Design

The boundary for the 50-Meter Model consists of simulated mast, simulated hoop, and side boundary. A quick assembly structure shown in Figure 9.3-1 is used to construct the boundary. More detailed boundary description is given in the following paragraphs.

### 9.3.1 Simulated Mast Assembly

The simulated mast assembly shown in Figure 9.3.1-1 supports the bracketry to which inboard interface cords are attached. The structure is comprised of standard 1.5-inch diameter IPS pipe sections assembled into a stiff rectangular frame structure by means of cast fittings. The entire frame supports a vertical pipe section at the center of the frame. The spring housings/bracket of the inboard cords attach to this vertical pipe section at a height of 5.27 meters above the floor. Four preloaded guy wires $30^{o}$ from the surface radial load component vector serve to stabilize the structure. The resultant frame structure has a minimal deflection under the 70-pound (32-kilogram) horizontal load applied by the model surface.

Adjustments to each interface cable tension, the height of the bracket, guy wire tensions, and interface points can be made due to the design of the simulated mast. A plumb line dropped through the center of the vertical pipe section serves to position a theodolite used during boundary structure and surface assembly setup. This location is the convergence point for radials of the model.

### 9.3.2 Simulated Hoop Assembly

The simulated hoop shown in Figure 9.3.2-1 is comprised of five vertical pipe sections equally spaced to form four $7.5^{o}$ angles with the simulated mast at 25.2 meter radii. Each pipe section is supported by two pipe supports inclined at $60^{o}$ to the floor in the plane of the radials. Each pipe section is also connected to adjacent pipe sections by two horizontally attached pipe sections (forming a simulated hoop section). The outer pipe sections are also tied into the boundary assembly for stiffness.

## CONSTRUCTION OF BOUNDARY ASSEMBLY, MAST, AND HOOP TOOLING

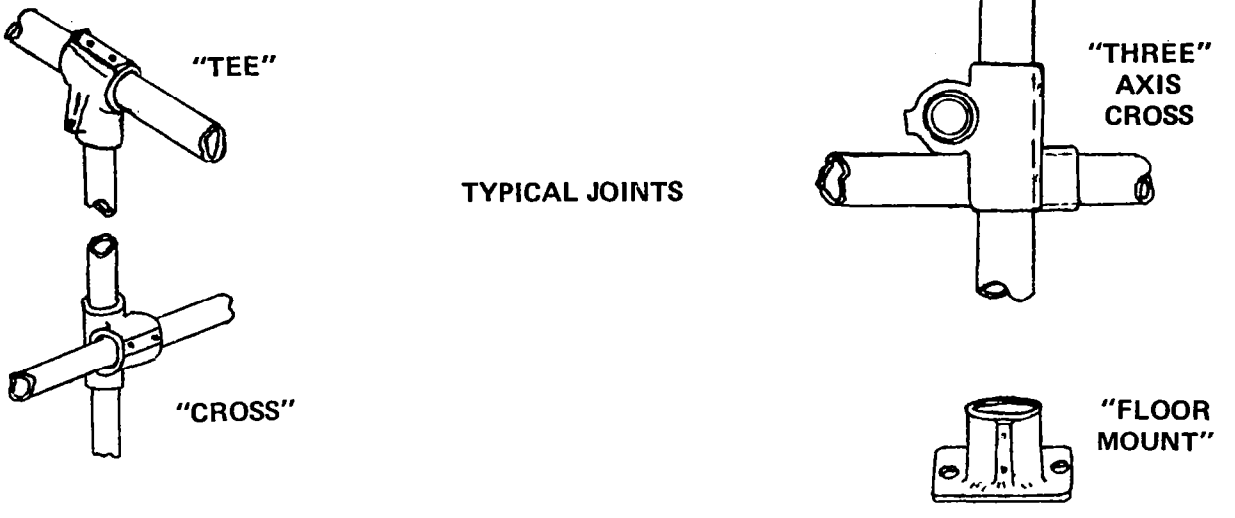


### CHARACTERISTICS

- EASILY ASSEMBLED AND ADJUSTED
- BASIC ELEMENTS ARE 11/2 INCH STD IPS PIPE AND SELECTED "INSTANT STRUCTURE" FITTINGS
- PIPE IS 6063-T6 AL ALY (25 KSI YIELD) ANODIZED WITH .145 IN. THICK WALLS, 1.900 IN. O.D.
- FITTINGS CAPTURE PIPE BY MEANS OF STAINLESS SETSCREWS
- PIPES LOADED AXIALLY IN ALL BOUNDARY STRUCTURES
- STRUCTURE IS READILY DISASSEMBLED
- STRUCTURE WAS NOT DESIGNED TO BE MAN-RATED BUT WOULD SUPPORT A MAN ANYWHERE IF NECESSARY (ANALYTICALLY DETERMINED)

Figure 9.3-1. Construction of Boundary Assembly, Mast, and Hoop Tooling

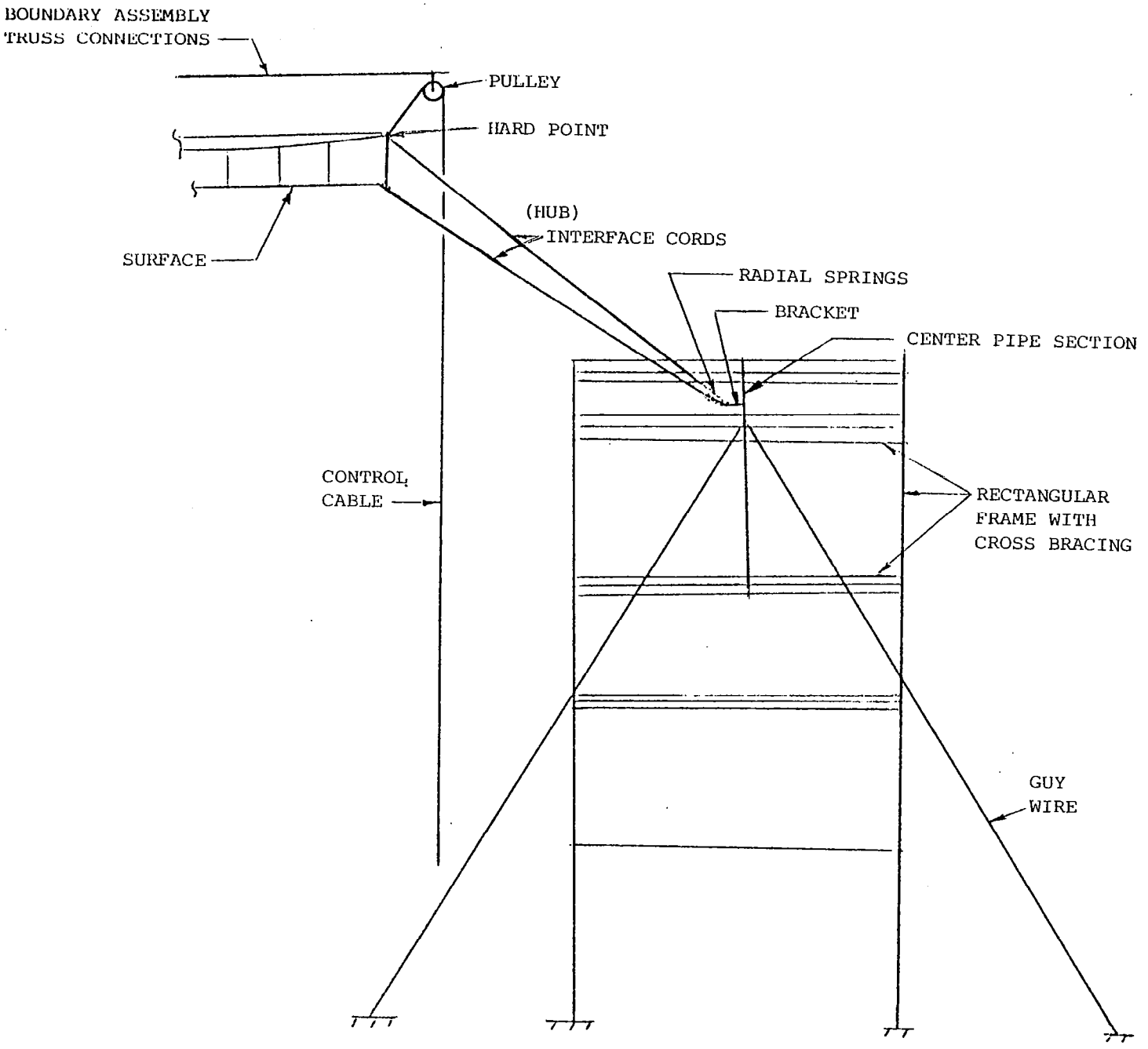


Figure 9.3.1-1. Simulated Mast Assembly

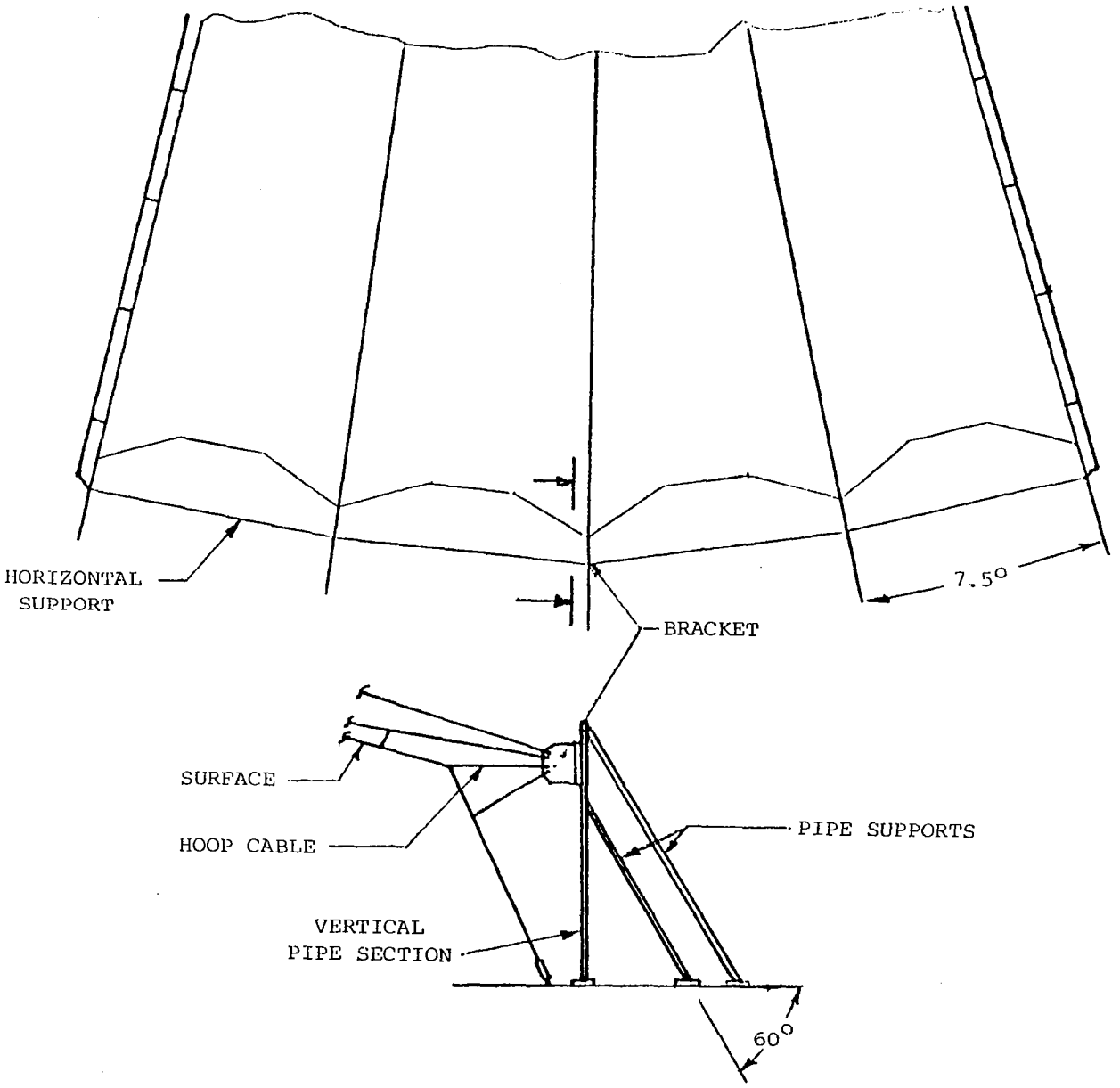


Figure 9.3.2-1. Simulated Hoop

No hoop joints are involved in this design since only surface adjustment and not hoop kinematics is being addressed in the model. The simulated hoop does provide a rigid boundary (i.e., deflection under load is less than 0.05 inch) and duplicates the geometry of the point design except that no hoop control cables are present in the model.

Each bracket on a vertical pipe section has four 0.125 diameter holes for attachment of cord terminations. The upper two connections attach the rear cord system beam cord and catenary. The center hole is used to connect the (hoop) interface cord from the surface. The bottom connection is for attachment of the simulated upper hoop support cable.

### 9.3.3 Boundary Assembly

The boundary assemby is the most involved of the boundary structures and serves several purposes. It provides a stiff radial boundary for the outer transition panels of the model surface. It provides a stiff overhead truss network which supports pulleys for control cables and counterbalance cables. The boundary assembly also provides control cable adjustment devices near the simulated mast structure.

The two sidewalls of the boundary assembly are constructed of Instant Structure pipe and fitting as shown in Figures 9.3-1 and 9.3.3-1. The sidewalls are skewed relative to another by an angle of $30^{o}$. Overhead trusses span the distance between the sidewalls, creating a structure approximately 20 meters along each sidewall, 7.32 meters in height, and 12.8 meters at its widest point (not including inclined supports).

Each sidewall supports parallel pipe sections separated by 48.0 inches and connected by 27 surface attachment assemblies. The inner seven surface attachments connect to the surface only (no diagonal ties are present) while the outer twenty clamp surface edge strips and connect to chain links on the transitional panel diagnonal ties (see Figure 9.1.3-1). Each surface attachment point along the boundary sidewall provides a rigid interface as prescribed by the analytical model.

BOUNDARY ASSEMBLY SIDEWALL

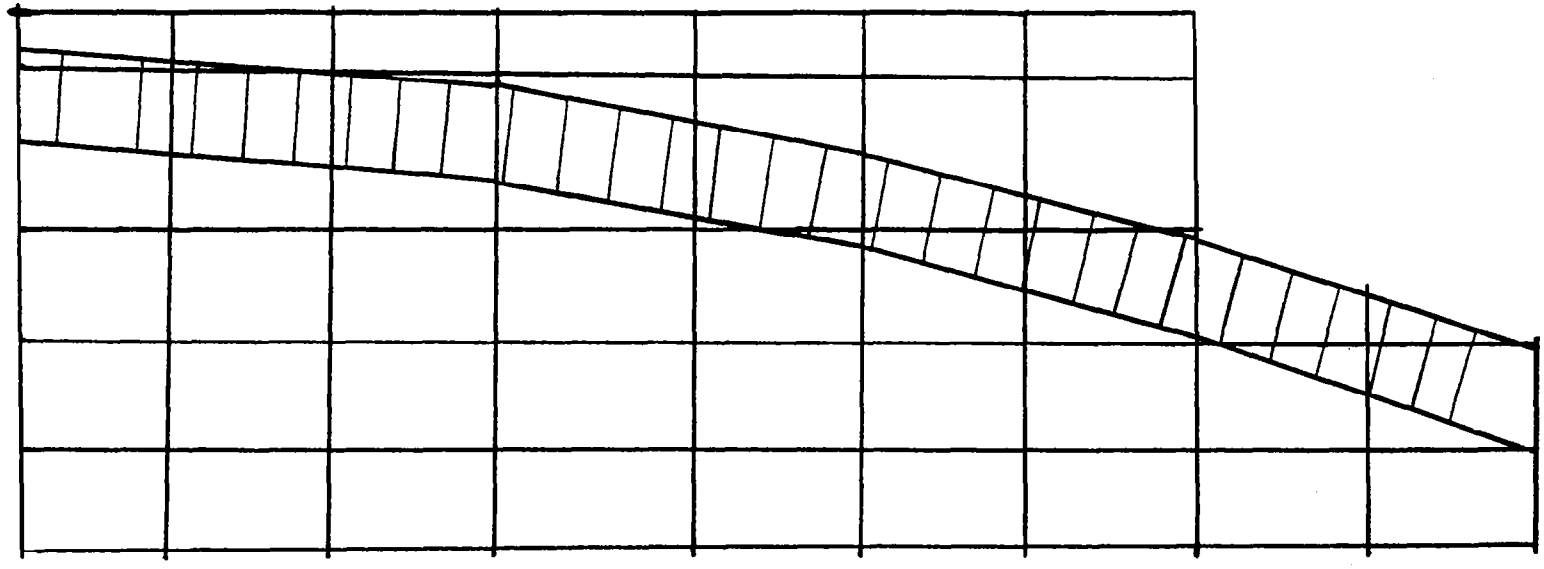

CONSTRUCTED FROM "INSTANT STRUCTURE" PIPE AND FITTINGS
PIPE IS 6063-T6 AL ALLOY, 1.925" O.D., 0.145" WALLS
FITTINGS ARE 6063-T6 AL ALLOY, SECURE PIPE WITH SET SCREWS.

Figure 9.3.3-1. Boundary Assembly Sidewall

An ideal boundary structure would allow control cables to duplicate the point design geometry between the mast and hard points. However, because of the height constraint in the facility being used, the required 50-foot high mast could not be accommodated; therefore the simulated mast represents primarily the hub region, and additional structure is required to re-direct and truncate the control cables. A network of interconnected trusses spanning from sidewall to sidewall over the model surface serves this purpose as shown in Figure 9.3.3-2.

Eight trusses 8 feet to 37 feet (2.44 to 11.28 meters) in width and up to 54 inches (1.37 meters) in depth are interconnected by radial and oblique pipe sections lying in horizontal planes above and below the trusses. Twenty-one pulleys are attached to the radial pipe sections to accommodate nine counterbalance cords and 12 control cables.

As with all boundary structures, stiffness is an important criteria of the design. As discussed in the section on tooling analysis, a duplicate of the largest truss was proofloaded with 147 pounds, at the center. The measured center deflection was 0.022 inch for this case. The highest vertical load from a single control cable should be about 15 pound, so minimal deflections can be expected.

Troughs or bearings can be attached to the trusses or radial pipe sections to minimize control cable sag along the horizontal run of the cables. The sag does not effect control cables adjustment because targets near hard points are used to determine surface contour changes.

Adjustment of the 12 control cables will be critical during the model testing phase. Analytical predictions of effects on the surface contour associated with a hard point adjustment cannot be correlated unless accurately measured adjustments are made.

The adjustment required to initially set up the surface to a nominal contour may need to be large, and small adjustments are needed during test. Both coarse and fine adjustments can be made with the designed adjustment devices. Coarse changes are made by pulling the cable through a

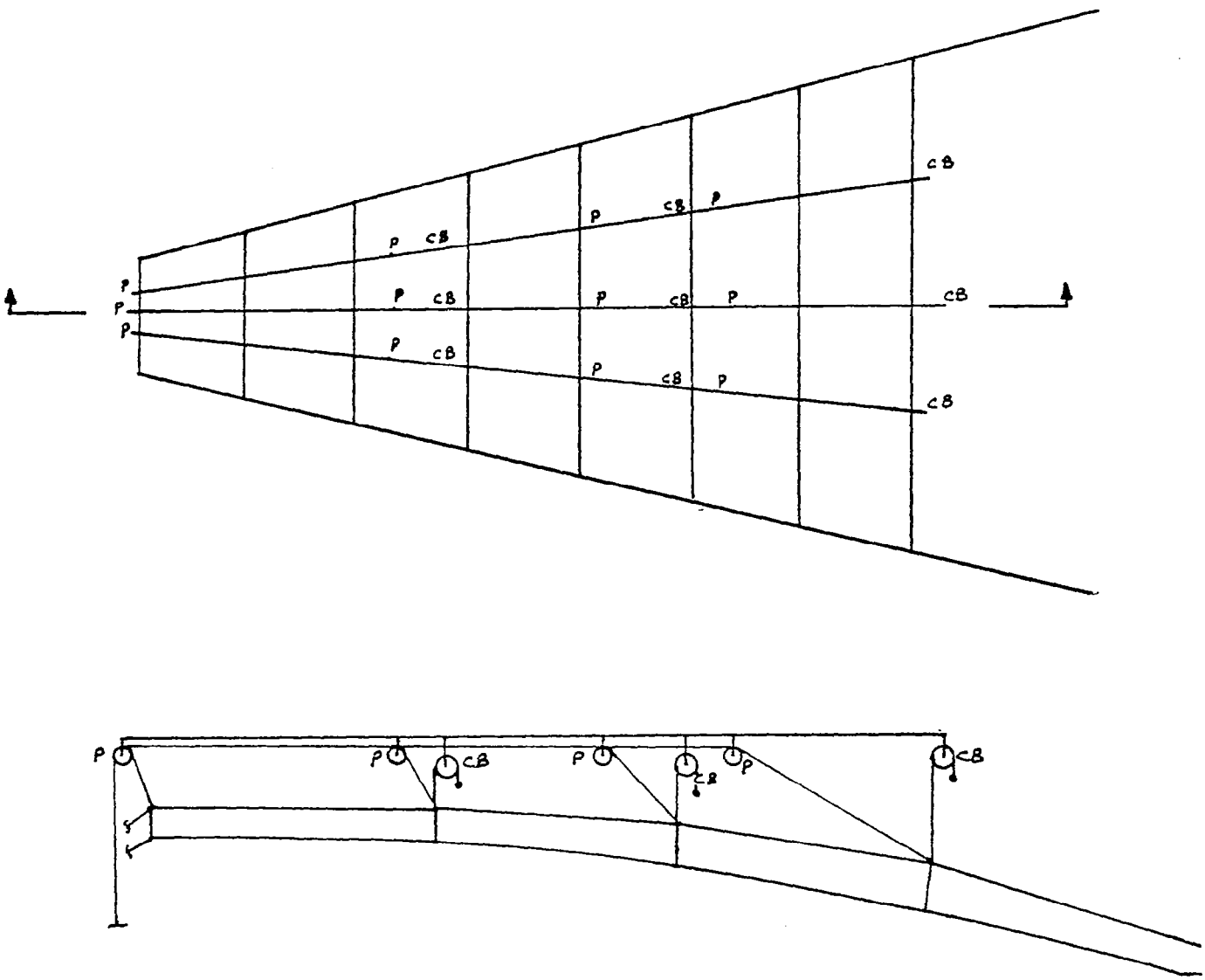


Figure 9.3.3-2. Overhead Trusses, Pulleys and Counterbalances

tube which is externally threaded and then clamping the cable by wedging against the inner walls of the tube. Fine adjustments are made by rotating the threaded tube in a thick plate. For the 1/2-14 ASA pipe thread, one full revolution provides 0.071" (0.181 CM) of adjustment.

The plates that support the threaded tubes are attached to the boundary sidewalls below the mast inboard truss at a convenient working height. Nuts above and below the plate enable the tubes to be fixed. However, targets positioned near the hard points will be optically measured to determine the effective magnitude of the adjustment, eliminating any errors associated with the boundary structure.

### 9.3.4 Boundary Analysis

A structural analysis was prepared for the LSST support tooling, which includes the mast, hoop, and side boundary, to evaluate the integrity and stiffness under handling loads. The mast, hoop and boundary represent the principle tools used to support the 50-Meter Model. A LSST structural analysis criteria was written to define the structural loading requirements and safety factors to be used in determining margins of safety.

The mast, hoop and boundary tools will be fabricated utilizing Hollaender "Instant Structure." "Instant Structure" is a truss type assembly made up of 6063-T6 aluminum pipes and aluminum/magnesium slip on joint fittings. "Instant Structure" was selected since it meets the strength and stiffness requirements and allows for the incorporation of additional structure should loads or stiffness requirements change.

#### MAST

The mast is a vertical truss type tower used to react forward lateral loads caused by cord loading of the 50-Meter Mesh Model. A finite element model of the mast was constructed for use on a CDC Stardyne Computer Program. The computer model was made to determine internal member loads under two loading conditions. Condition 1 is a nominal case involving normally expected tooling loads in a 2g environment. It consists of:

Condition 1

- 70 lb live load representing the antenna cord loads applied along the lateral axis.
- 50 lb lateral load representing a ladder resting along the mast top. 50 lb load was applied in the same direction as the 70 lb load.
- Each of four guy wires, used to support the tower, were preloaded to 100 lb.

Condition 2

Is a survivability case incorporating the 3 above loads with the addition of a 250 lb man standing on the mast top edge in a 2g environment (500 lb). A factor of safety of 3 on ultimate loads and 2 on yield loads was utilized in determining margins of safety for Condition 1 (nominal) loads. Factors of safety were used to evaluate the survivability or "accident" type loading environment.

The strength and stability of the beam elements of the mast structure were analyzed for both loading conditions. The mast fitting and joints were analyzed for the nominal (Condition 1) loading case.

The results of these analyses indicate the mast meets the margin of safety requirements outlined in the structural analysis criteria for the nominal case. The mast structure also had ample margin for the worst case survivability loading. Also, the mast stiffness for lateral loading was determined to be 4141 lb/in.

HOOP

The hoop is a circular segment of beam supported by floor mounted stanchions. The hoop reacts AFT lateral loads resulting from the 50-Meter Mesh cord loads. Like the mast, it is constructed entirely of "Instant Structure" aligned in circular segments with ground supports.

A finite element model was created to evaluate the internal member loads and overall hoop stiffness using a CDC Stardyne Program. The hoop is loaded by 45 lb radial mesh cord loads. A structural analysis of this beam elements was performed. The results of this analysis yielded very high margins of safety since the beam internal loads were insignificant. The hoop radial stiffness was found to be 10,000 lb/in.

BOUNDARY

The boundary is the principal truss structure used to support and control to 50-Meter Mesh Model. The boundary tool is a series of vertical frames interconnected by numerous interlacing beams. Lateral support is achieved by floor mounted support beams. As in the mast and hoop, the boundary is primarily made of "Instant Structure." A finite element model of the complete boundary structure was made. Loads were applied to the model as follows:

- Mesh loads and rear cord loads were applied along the edge to the attachment pipes.
- Counterbalance and mesh control cord loads were applied to the overhead "Instant Structure."

A geometry run was made to evaluate the dimensional accuracy of the full model. A second finite element model was made of a critical frame section. The reduced model was selected for evaluating strength, stability and stiffness of a representative frame due to the complexity of making the full model run. A 500 lb lateral (ladder load) were applied to the model. These handling loads were judged more severe than the mesh and control cord loads acting on the full model. The results of the analysis indicate the frame has ample safety margin. The margins of safety were determined using the safety factors outlined in the structural analysis criteria. The frame laternal stiffness was determined to be 1664 lb/in.

The minimum margins of safety calculated on the frame were:

Bending (ultimate) M.S. = +2.54
Bending (yielding) M.S. = +3.70

MODEL VERIFICATION

A test versus analysis correlation was made to verify computer model accuracy. A simple truss was constructed utilizing "Instant Structure" pipes and fittings. A finite element model of the test truss was made. A test load was applied to the actual truss centerspan and deflections recorded. The model was run using CDC Stardyne and a like centerspan load. A comparison of measured versus predicted centerspan deflection indicated excellent correlation between the model and actual hardware.

## 9.4 Cord Tooling

Cord tooling for the 50-Meter Surface Model refers to the tooling required to construct (1) Vertical, diagonal, and surface ties, (2) the front cord panel assemblies, and (3) the rear cord trusses. The general approach taken for fabrication of these cord assemblies is to duplicate the desired geometry of the analytic model on templates, position cords under correct loads and then capture this geometry and tension state by bonding junctions. Tooling tolerances must be kept extremely low. An error of less than the required 80 parts per million can be obtained using a theodolite measurement system to locate adjustable junction positioners, pins, and pegs. Wherever size allows, large vernier calipers can be used to position, measure, and verify dimensions (as on the tie assemblies) with greater accuracy.

### 9.4.1 Front Cord Panel Template

The panel template consists of approximately thirty 4 x 8 foot plywood sheets laid out in a pattern encompassing the panel flat pattern as shown in Figure 9.4.1-1. These plywood sheets are laid out on the floor of the facility (Building 21) and three patterns are marked: (1) Front cord system, i.e., flat pattern, (2) Tensioned mesh pattern, (3) Measurement target pattern. Using multiple patterns enables the fabrication of front cord systems and mesh panel assemblies at the same location which is between the boundary sidewalls.

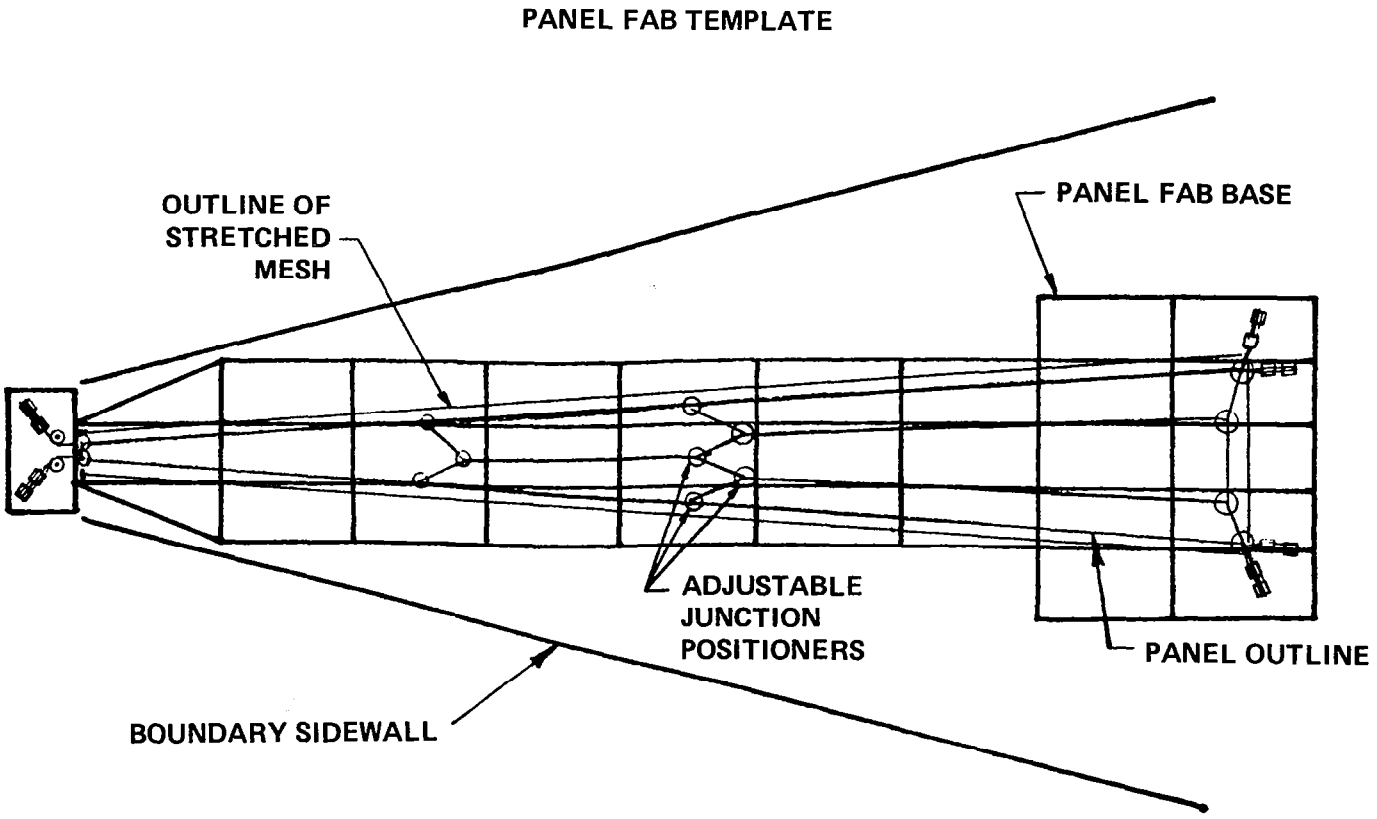


Figure 9.4.1-1. Panel Fab Template

The critical element in cord system fabrication is to achieve a geometry duplicating the analytical model. The theodolite measurement system is used during setup of the template to locate the adjustable positioners shown in Figure 9.4.1-2. Once the front cord system is bonded and cured in place, the mesh can be unrolled over the cords. Mesh holes are counted and stretched to the appropriate dimensions radially and circumferentially. The mesh edges are attached to rows of pegs outside the perimeter of the cord system. Then targets are installed, mesh and cords are joined, excess mesh is trimmed away, and the completed panel assembly is moved to storage.

### 9.4.2 Rear Cord Truss Template

In a manner similar to that of the front cord system, the rear cord truss system is fabricated on a pattern established on 4 x 8 foot plywood panels. The theodolite measurement system is again used to adjust the positioners and pegs to minimize the geometrical error.

### 9.4.3 Tie Fabrication Tooling

The three types of ties present in the surface design require that a large number of lengths of ties be constructed. For this reason, a tool which can be adjusted to provide ties over a wide range of dimensions is necessary to minimize tooling costs.

Since most ties are constructed using very fine diameter graphite cord, handling, loading, and measurement accuracy were critical factors in the design of this tool. The tool performs the functions shown in Figure 9.4.3-1. It is readily measured to 0.001 inch accuracy (end-to-end) up to 50 inches in overall length using a large vernier caliper. Loading is done by hooking weights to clips attached to ends of the cord material. Handling involves threading cords around or between closely spaced pins or pegs to achieve desired loop sizes, bend radii, and hook shapes. Local stripping of Teflon from the cords is facilitated by aluminum plates behind the area to be stripped and eventually bonded.

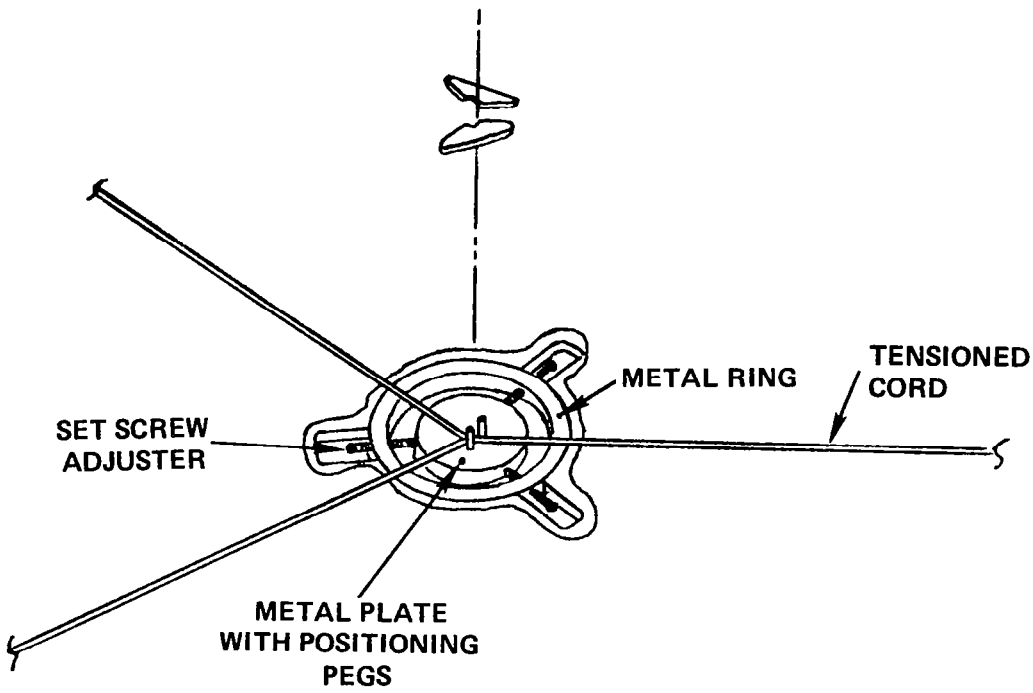


Figure 9.4.1.2. Cord System Fabrication
- Junction Positioner -

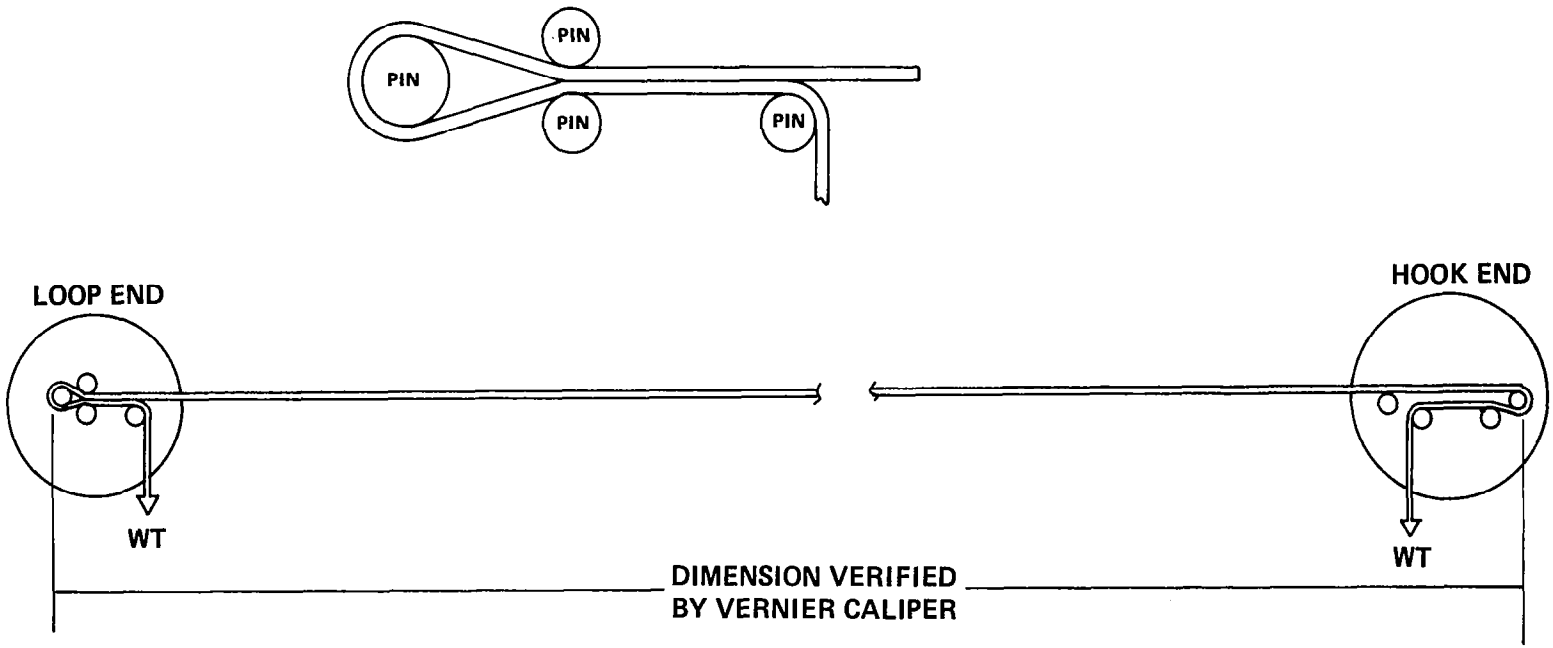


- PINS INSTALLED ON ALUMINUM PLATES WHICH CAN BE ADJUSTED IN SLOTS TO PROVIDE VARIOUS PIN TO PIN DIMENSIONS REQUIRED OF TIES
- HOOKS OR LOOPS CAN BE FORMED BY APPROPRIATE PATTERN OF PINS ON PLATES
- MAXIMUM LOAD IN ANY TIE IS 0.61 LB. (0.28 KG)
- MAXIMUM TIE LENGTH REQUIRED IS 48.81 INCHES

Figure 9.4.3-1. Tie Fabrication Tooling

## 9.5 Manufacturing and Assembly Flow

The 50-Meter Surface Model manufacturing and assembly flow plan is shown in Figure 9.5-1. It consists of procurement, template layouts, boundary fabrication, and surface piece part fabrication and assembly activities.

## 9.6 Facilities and Equipment

### 9.6.1 Facilities

The 50-Meter Surface Model will be assembled in the west half of Building 21 on the grounds of the Harris Corporation plant. The west half of the building provides approximately a 75' x 105' floor space, with a sloping roof that is at a minimum height of 35' at the west wall. A partition through the center of the building separates the west half of the building in which various equipment is stored. Another portion of this building is caged off for a parts storage area and workshop area. The building frame is constructed of steel beams and girders assembled on a concrete foundation. The walls and roof are galvanized steel sheet with white paint on the exterior side and vinyl-backed insulation on the interior. The building has several air conditioning ducts along the north wall but a constant $74^{o}F$ cannot be maintained throughout the building during the summer. Temperature gradients of $10\text{-}12^{o}F$ from floor to ceiling can be anticipated in the noonday heat (and must be accounted for in the analytical correlation to measured target data). The building entrance has a simplex combination lock, and the entire building is surrounded by an 8-foot chain link for added security.

### 9.6.2 Equipment

Special equipment reqired to perform this task include:

1. Manually-operated Zeiss optical theodolites
2. Temperature and humidity monitoring devices
3. Load cells and strain gages (for cord tension determination)
4. Computer/printer (for test analytics)
5. Up-pup or similar elevated platform (for tooling assembly)
6. Eight-foot Mitsutogo vernier caliper
7. Band saw (for cutting tooling pipe)

## 50 METER SURFACE CONTOUR MODEL MANUFACTURING/ASSEMBLY FLOW CHART

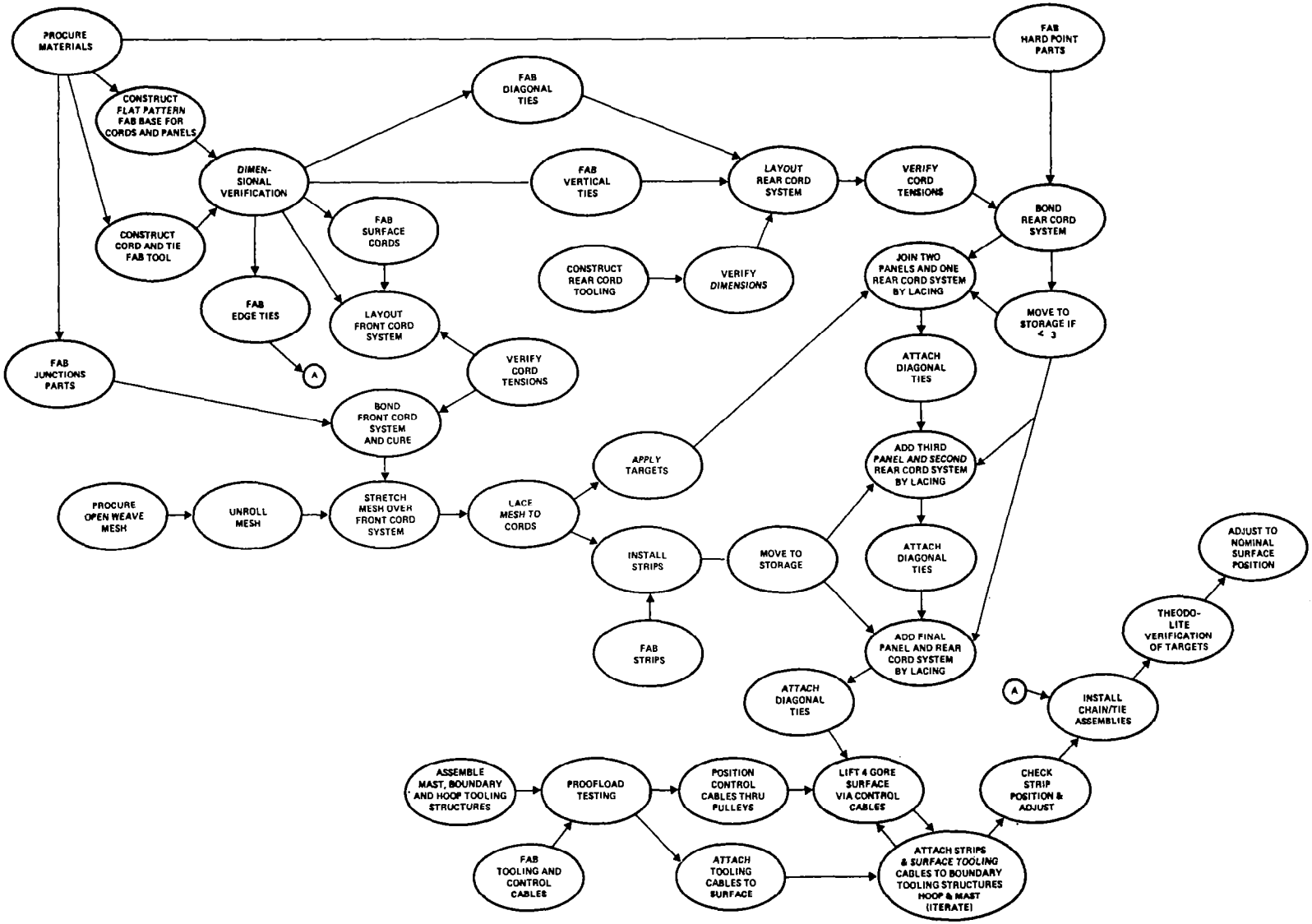


Figure 9.5-1. 50-Meter Surface Contour Model Manufacturing/Assembly Flow Chart

### 9.6.3 Theodolite Measurement System (TMS)

The preliminary locations for the theodolites are shown in Figure 9.6.3-1. These locations allow the measurement of all targets on the test surface by at a least three theodolites, establishment of true radials in the model, and minimized error in cord system fabrication. The various theodolite positions between the sidewalls have a unique trigonometric relationship between one another.

This type of optical measurement system has been used at Harris on other programs, including TDRSS Airborne. The achievable measurement accuracy for this system is approximately ±0.005" (0.0127 CM).

## 9.7 Test Plan

Following assembly of the 50-Meter Surface Model, the test phase commences. The testing is performed to demonstrate the capability of a Hoop/Column reflector surface to be manufactured and adjusted in a manner which provide surface enhancements and to verify the analytical prediction capability.

The test flow summary is presented in Figure 9.7-1, and a generalized outline of the test is:

- Verify boundary conditions
- Calibrate the TMS
- Measure as-built, unadjusted surface
- Evaluate discrepancies and modify surface of TMS software
- Re-measure/re-evaluate as required
- Run single control cable adjustment predictive analysis
- Adjust cord per predictive analysis
- Measure surface
- Compare measured versus predicted results
- Update predictive model
- Repeat single cord adjustments/surface measurements on all cords comparing results

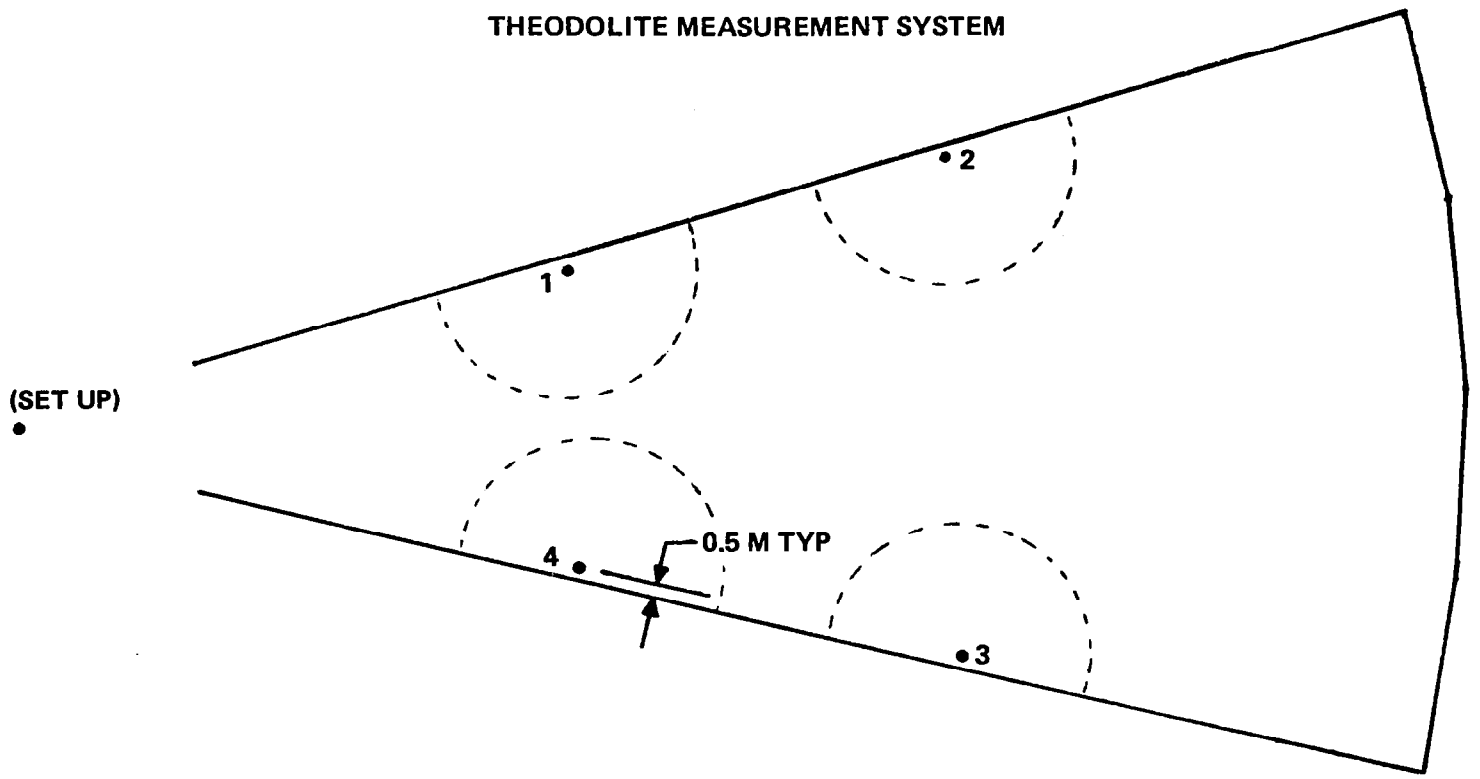


- EACH THEODOLITE CAN MEASURE ANY TARGET OUTSIDE OF ITS SEMICIRCULAR BLOCKAGE AREA
- ANY TARGET CAN BE SEEN BY AT LEAST THREE THEODOLITES
- THEODOLITE LOCATIONS SELECTED TO PREVENT OVERLAPPING BLOCKAGE AREAS

Figure 9.6.3-1. Theodolite Measurement System

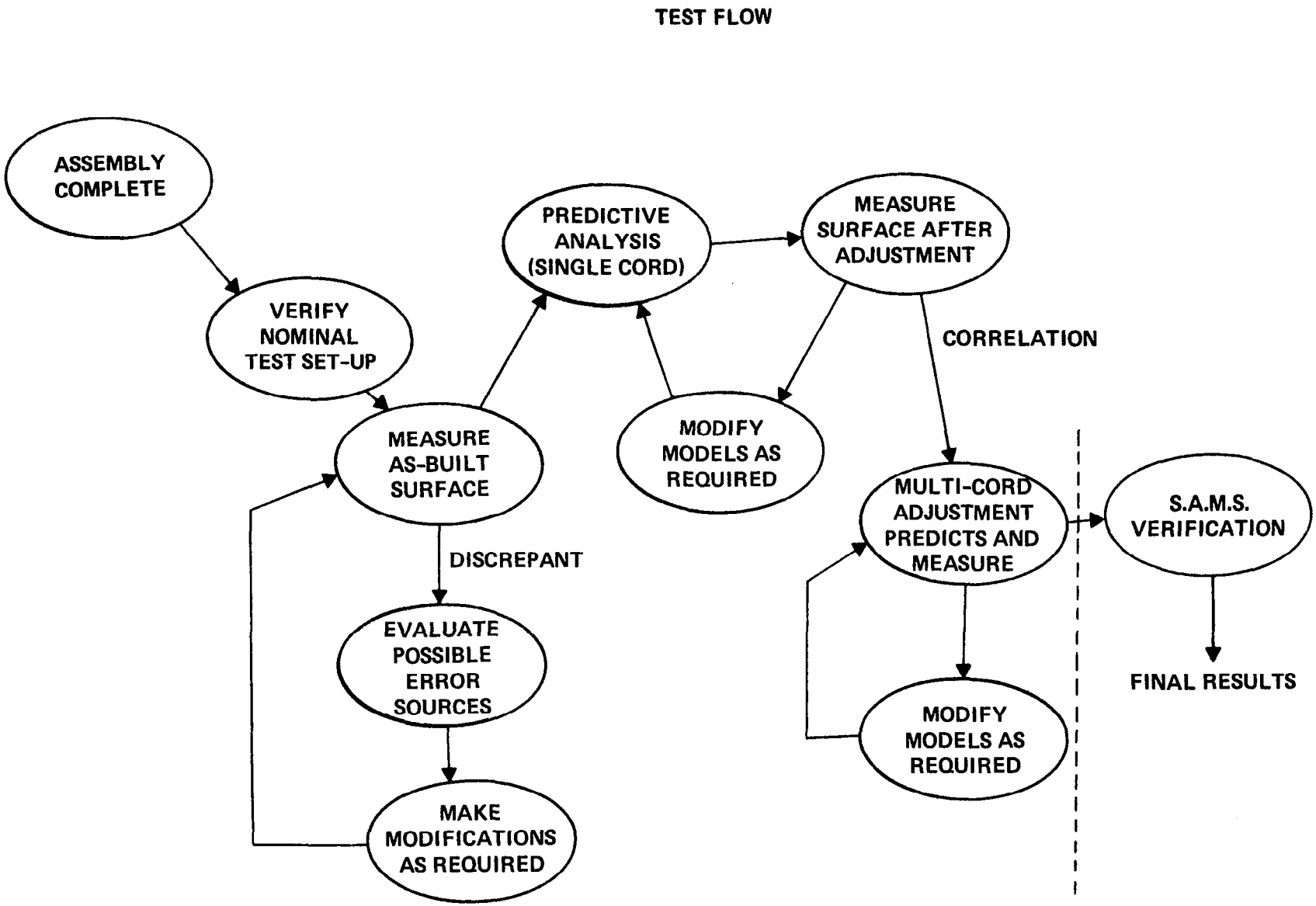


Figure 9.7-1. Test Flow

- Update predictive model
- Run multiple control cable adjustment predictive analysis
- Adjust cords per predictive analysis
- Measure surface
- Compare measured versus predicted results
- Repeat for all multiple control cable adjustments
- Update predictive model

After completion of this phase of the testing, the model is available as a "test bed" for an operations demonstration of a Surface Accuracy Measurement System (SAMS) as shown in the right side of Figure 9.7-1, Test Flow.

## 9.8 Summary (50-Meter Surface Model)

The objectives of the 50-Meter Surface Model address the gathering of preliminary information on performance, manufacturing techniques, and cost applicable to the Hoop/Column Point Design. Phase I (FY'80) objectives were to design and analyze a half scale representative segement of the point design surface. Phase II (FY'81) objectives are to proceed into procurement, assembly, test, and evaluation stages.

FY'80 objectives were generally met, though design of several tooling items was not completed. Major items achieved included design and analysis of all surface elements and boundary structures, and the generation of test plans, manufacturing documents, drawings, and reports. Performance and manufacturing techniques are consistent with the point design.

The timing of the 50-Meter Model relative to other tasks in the program enables its output to serve as input to the point design and to the 15-Meter Hoop/Column Model.

## 10.0 15-METER MODEL

This section describes the conceptual design activities performed on the 15-Meter Model during Phase I of the program. Final design, fabrication, and testing of the model occurs in the Phase II follow-on effort described in Section 12.0.

### 10.1 Objective

The basic objective of the 15-Meter Model is to verify the 100-Meter Hoop/Column antenna point design. More specifically, it verifies deployment kinematics, deployment reliability, failure modes investigation, surface interaction, manufacturing techniques, and scaling theory.

### 10.2 Description

The model is a Hoop/Column design shown in Figure 10.2-1. This design utilizes a central column or mast as one primary compression member and a 48-segment hoop, symmetrically located with respect to the mast, as the other compression member. This hoop is connected to the mast with 48 upper cables and 48 lower cables that extend from the hoop segments to the top and bottom of the mast. When these cables are loaded in tension, a rigid structure is formed on which a parabolic surface can be formed. The mast consists of a central hub with eighteen telescoping sections. The 48-hoop sections fold in towards the hub. The deployment begins by the mast sections telescoping out and latching into place. Then the hoop is released from the mast and unfolds outward. Deployment is completed when the cables are tensioned. This stabilizes the structure and shapes the surface.

The model will be constructed in a radome at Harris Corporation's Palm Bay, Florida, facilities as shown in Figure 10.2-2. In Figure 10.2-3 the stowed configuration is shown. This figure also shows the proposed support system, a single support tube that will extend into the lower half of the mast when deployed. This allows the entire antenna model to remain at a central elevation (22.5 feet) whether stowed or deployed and, therefore, more closely simulate deployment kinematics and loads. By removing the stowed antenna from the support tube and inverting it, the ability to deploy cup-up or cup-down is realized. This ability will be useful when evaluating the effects of gravity on the surface.

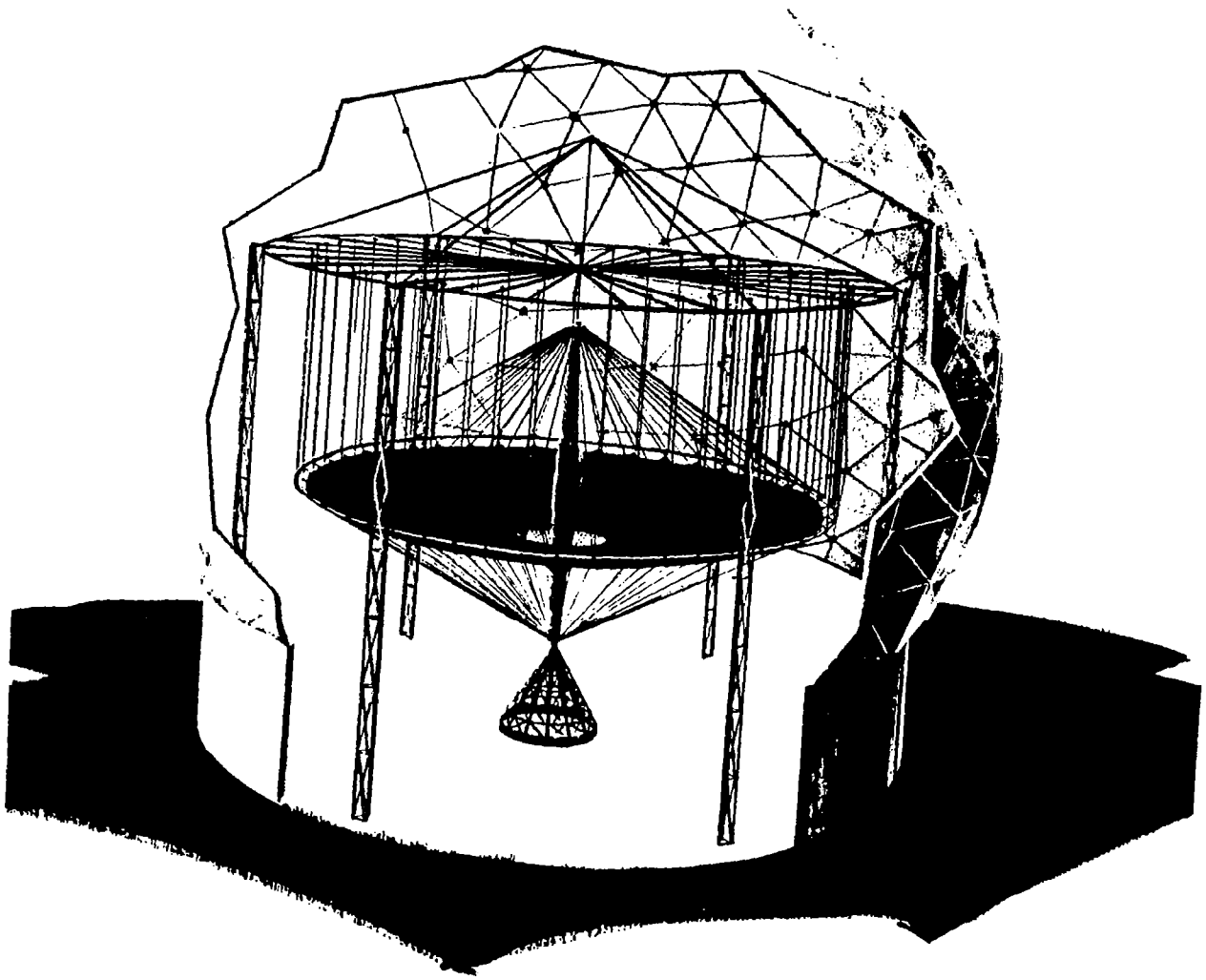

Figure 10.2-1. 15-Meter Model

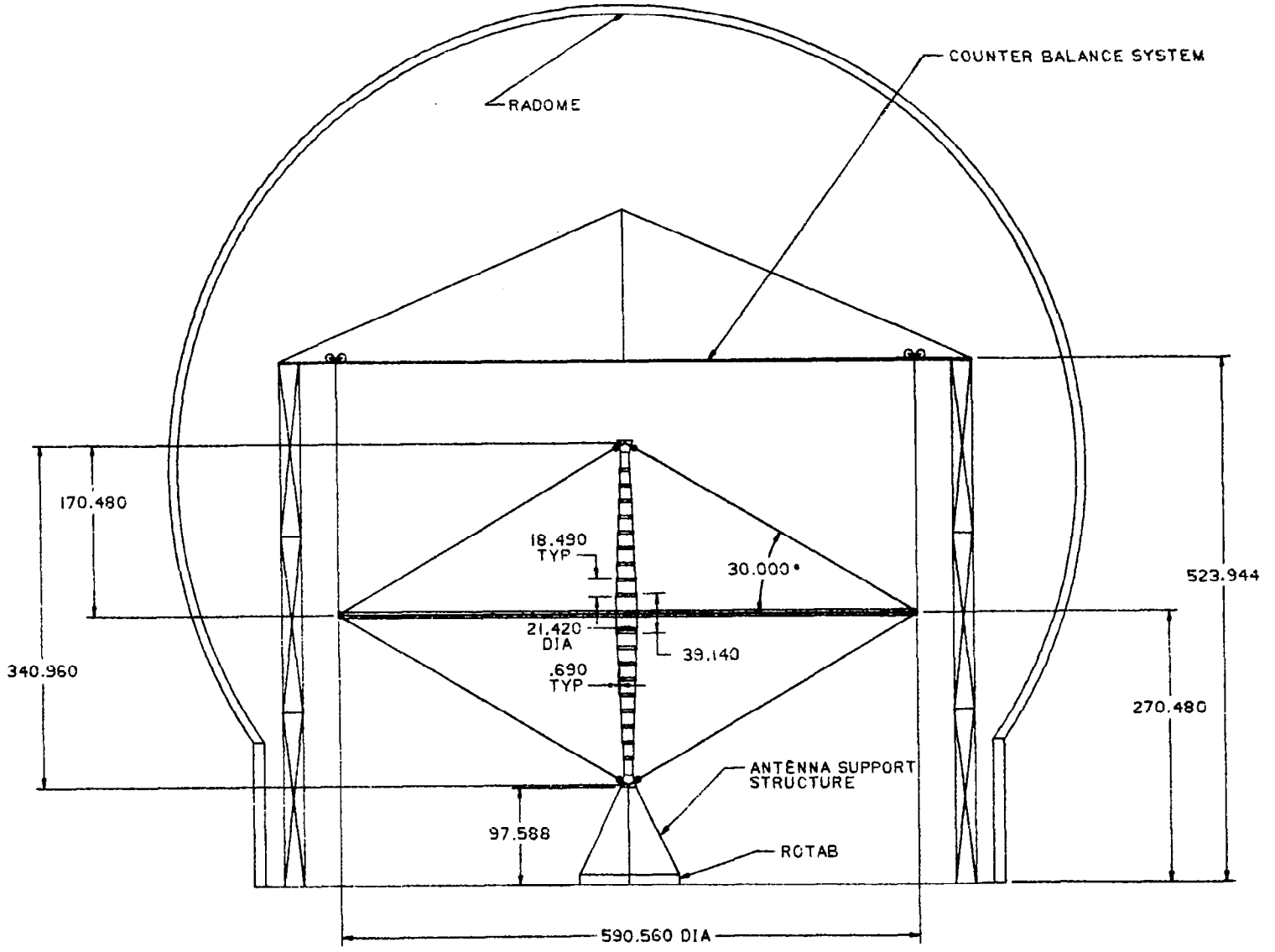


Figure 10.2-2. 15-Meter Geometry, Deployed

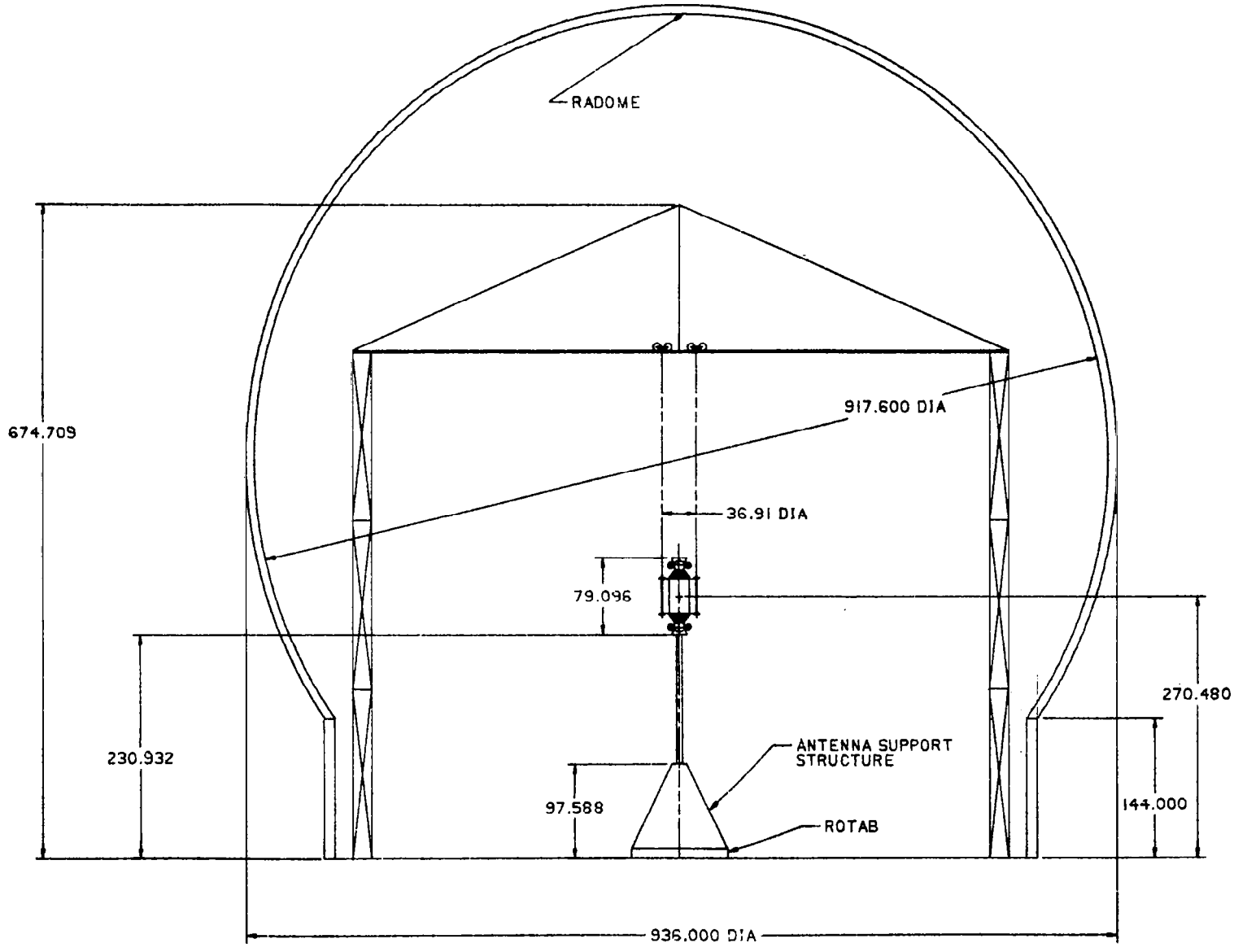


Figure 10.2-3. 15-Meter Geometry, Stowed

## 10.3 Requirements

The requirements for the 15-Meter Model are listed in Figure 10.3-1. These requirements apply to the antenna as a whole and to the hoop, mast, and surface specifically. The requirements have been generated from the initial task letter, discussions with the customer, and discussions among Harris engineering and management personnel. The design of the model will be guided by these requirements.

The 15-Meter Model is a breadboard of the 100-Meter Point Design. The diameter of 15 meters (49.2 feet) is measured across the corner of the hoop segments at their respective centerlines. The model, as originally planned, was to be 20 meters in diameter. The decision to reduce this dimension to 15 meters was made in early July 1980, after it was determined that the model could be subjected to thermal vacuum testing at a later date. A survey of existing thermal vacuum chambers indicated that the NASA Johnson Space Center in Houston, Texas, contained the largest operational facility. Drawings of this facility pointed out the need to reduce the overall diameter of the model to 15 meters. As shown in Figure 10.3-2, the reduced size fits the Houston chamber while allowing adequate side clearance to accept instrumentation and/or counterbalance supports.

While the reduced size of 15 meters ensures the physical ability to fit into a thermal vacuum chamber for possible future testing, the model is not designed for a thermal vacuum environment, i.e., there will be no thermal controls (blankets, heaters, etc.) and materials for the model will be selected on a design efficiency/cost basis. Any future vacuum testing will require a refurbishment of the model.

The 15-Meter Model, like the 100-Meter Point Design, is a quad aperture configuration. This scheme effectively separates the antenna into four distinct offset reflectors. The breadboard model does not have a feed or support tower.

Direct scaling from the 100-meter design will be performed where cost constraints, hardware availability, and design considerations allow.

General

- Hoop/Column concept
- Model of 100-Meter Point Design
- Quad aperture design
- Hoop diameter is 15 meters (49.2 feet)
- Direct scaling where possible
  - Cost constraints
  - Hardware availability
- No feed or feed tower
- No thermal control
- Cup-up - Cup-down capability

Hoop

- Single stage deployment
- 48 sections - graphite construction
- Restowable
- Four motors spaced at $90^{o}$

Mast

- 18 sections plus hub
- Aluminum construction
- Cable deployment
- Sections will be hexagonal truss
- Restowable

Surface

- Surface will be built-to-dimension
- Focal length is 366.85
- Surface will be gold-plated molybdenum wire mesh
- Mesh opening size is 0.25 inch
- Secondary drawing surface to shape mesh
- RMS is TBD
- No active surface control
- Mesh management technique will be implemented
- No requirement to restow surface to original configuration automatically

Control Cables

- Deployed from negator spring controlled spools

Materials

- Selection will be based on design considerations and cost

Figure 10.3-1. 15-Meter LSST Reflector Model - Summary of Requirements

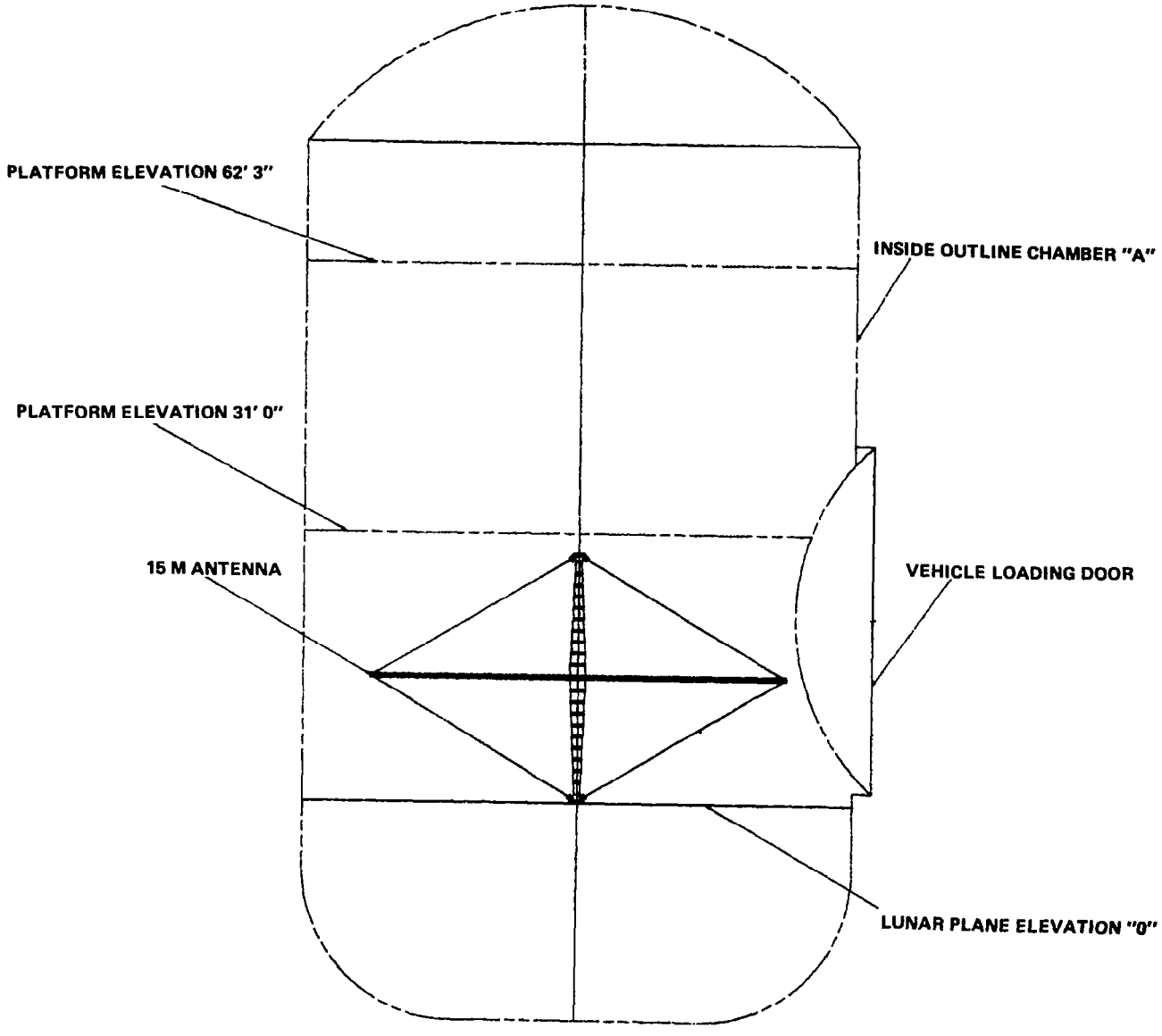


Figure 10.3-2. NASA Johnson Space Center Thermal-Vacuum Test Facilities Chamber "A"

Cup-up, cup-down capability will be incorporated into the handling fixtures to allow surface measurements averaging with the gravity force in two directions.

The surface for the 15-Meter Model will demonstrate the build-to-dimension approach of the 100-meter design. The sections of the surface are built to preset dimensions and the surface accuracy compared to predictions after assembly. The RF reflective surface is gold-plated molybdenum wire mesh with an opening size of 0.25 inch. The mesh will be shaped by the cord and tie system to a TBD inch RMS accuracy. A technique for managing the mesh during deployment to prevent snagging is implemented on the model. The scheme for mesh control contains provisions for hand packing before deployment. There is no requirement to automatically restow the mesh to its stowed configuration, however, there is a requirement that the mesh not interfere with the restowing of the hoop and mast.

The hoop is a single stage deployment type, i.e., one motion carries the hoop segments from a vertical stow position to the horizontal deployed configuration. There are 48 segments constructed of graphite/epoxy composite with aluminum fittings. The hoop is driven via four motors spaced at $90^{o}$ intervals. There is a requirement for the hoop to be restowable (reversible). The position of the hoop relative to the mast is controlled with 96 control cables which are tensioned with negator spring spools. These spools are instrumental in determining the need for a hoop counterbalance. The counterbalance is discussed in Section 10.5.

The mast consists of a central hub section with 18 telescoping sections emanating from it. The mast is required to be restowable and contain the preload section to preload the hoop cables after deployment is complete.

All of the above requirements for the 15-Meter Model and its subassemblies will be added to and updated as the design progresses.

## 10.4 Design

To begin the design of the 15-Meter Model, it is necessary to determine the loads and the load cases that components of the structure are to experience to successfully function. Two load cases are identified. During deployment, the model is subjected to one case while the fully deployed model experiences a different load case (operating loads). In general, the operating loads are compressive while the deployment loads involve bending and torsion.

### 10.4.1 Deployment Loads

The deployment load case for the mast begins with the extension of the mast segments and ends with the mast latching into place. The deployment load case for the hoop begins when the hoop is released from the stowed position and ends when the hoop reaches its completely deployed position, forming a 15-meter diameter circle. The deployment loads for both the mast and the hoop are approximated by studying the kinematics and geometry of both systems and by assuming certain cord loads. The cord loads come from the 100-Meter Point Design and specifically refer to the tension in the hoop control cables. This tension is maintained in the cables during deployment by the negator springs in the take-up spools. The purpose of the tension is to provide a method of controlling the hoop orientation with respect to the mast. If the hoop becomes skew to the mast, the component of the tension acting on the hoop changes in a manner that tends to realign the hoop. This cord tension is a driver in determining deployment loads.

Each mast half must deploy against a 48-pound force (48 cables x 1 pound/cable). Added to this force is the weight of the mast segments, the preload section, and the spool carriers. In the cup-up position the top half of the mast must deploy against this gravity force whereas in the bottom half this force aids or adds to the deployment force. The opposite is true for the cup-down deployment. Therefore, the worst-case deployment load for either mast half is 48 pounds plus the mast segment weights of approximately 50 pounds.

The deployment loads for the hoop can also be determined by using the cord tension as a starting point. For the hoop, however, only the horizontal component of this tension acts on the hoop (assuming that the hoop is not misaligned with the mast). The vertical component is reacted by the vertical tension from the opposite top or bottom cable. When the hoop begins deployment, the horizontal component is small and increases to a maximum of 0.866 pound at full deployment. The kinematics of the deploying hoop indicate the torque needed to deploy the hoop against a resisting force is greatest at the stowed position (worst mechanical advantage) and decreases to the deployed position (greatest mechanical advantage). When the changing mechanical advantage is combined with the inversely changing resisting force, a maximum torque requirement is realized at about one-half of the deployment cycle ($40^{o}$).

The point design (and a requirement for the 15-Meter Model) has four motors with 48 hoop segments. This results in each motor driving 12 segments, six on either side of the motor. The torque requirements for each hoop joint are additive, meaning that the motors must be sized to handle 12 times the single joint torque. As six segments are driven on either side of the motor, the hoop tubes beside the motors must carry six times the bending load that is required in one joint.

Using this information it is possible to size the hoop tubes for bending load based on control cable tension, i.e., maximum required torque (at $40^{o}$) times six. Additional load is added to override possible mesh snag loads.

### 10.4.2 Operating Loads

The operating loads for both the mast and the hoop are applied after complete deployment. The preload section of the mast is started as the final deployment step. This section expands to lengthen the mast to tension the control cables, surface cables, and surface in the final configuration. This loads the mast and the hoop in compression which is the operating load case. The desire for a stiff structure and therefore high loads is bounded by

the stability of the hoop and mast. This stability is a function of cord tension and cord stiffness and can be optimized using a stability analysis (see analysis section). Preliminary analysis was performed using the same loads and stiffnesses as are on the 100-Meter Point Design.

An important point should now be made concerning a relationship between deployment loads and operating loads that is unique to the 15-Meter Model. Because the model will be operated in a 1-G environment, the operating loads which size the control cables also influence the deployment loads. As stated previously, the deployment loads are dependent on cable tension induced by negator spring spools. The minimum cable tension is the weight of the cable plus the load required for the spool to retrieve the cable during restow. As the operating load and cable size is increased, the minimum deployment tension (weight of cable) is also increased. Of course, the ability to control the hoop position relative to the mast increases with deployment cable tension as does the member loading. Therefore, a trade-off among operating loads, deployment loads, and member sizing is needed in the Phase II final design.

### 10.4.3 Kinematic Anomaly

The kinematic anomaly was discovered through observation of the hinge joint model. The problem is that deployment kinematic loads are induced in the hoop of a magnitude undetermined at this time. Qualitative analysis indicates that the anomaly and the accompanying loads can be minimized through proper design. The loads encountered is a function of number of hoop members with the problem growing worse as the number of segments decreases. As stated previously, the problem appears to be relatively minor with 48 segments. The basic problem, which initiated the study, is that the hoop segments do not move at identical rates over certain positions in the deployment sequence.

A kinematic study was performed beginning with a simple 4-bar linkage in 2-dimensional space and proceeding through a Computervision 3-dimensional model. The 4-bar linkage represents the push rod/pivot arm hinge concept that is used in the 100-Meter Point Design. The initial 2-D

linkage, as shown in Figure 10.4.3-1, was studied to determine the displacement angle of one pivot arm relative to the other. The ideal situation would be a linear or one-to-one change in angle. This linear relationship was found not to exist as one pivot arm lags the other at angles between $0^{\circ}$ and $90^{\circ}$. To minimize this error, an analysis was performed to determine the correct relationship between pivot arm length and hinge line separation in order to yield identical displacement at $0^{\circ}$, $45^{\circ}$, and $90^{\circ}$. The correct relationship is shown in Figure 10.4.3-2 as is the graph of pivot arm displacement versus pivot arm displacement for this particular geometry. As can be seen from the graph, identical displacements have been achieved at $0^{\circ}$, $45^{\circ}$, and $90^{\circ}$.

Once the error in displacement is identified and minimized, it is necessary to study how this error effects the hoop. Figure 10.4.3-3 demonstrates how the error in displacement is accumulated from joint-to-joint if all hinge mechanisms are constructed the same, i.e., all drive pivot arms being male or female and all driven pivot arms being female or male.

The problem associated with this displacement arises when the 2-dimensional hoop is projected into 3D. To make a hoop from the 2D drawings in Figure 10.4.3-3, the hinge lines on each platform (normal to the paper in 2D) must be moved with respect to each other so that the angle between them is $7.5^{\circ}$ (48 segments) and the plane that they lie in is normal to axis A of Figure 10.4.3-3. When this is performed in a hoop exhibiting the above mentioned displacement error, a helix is formed, i.e., the ends of the hoop do not join. Forcing the hoop ends to meet introduces strain energy into the hoop segments which manifests itself as bending stress and torsional shear stress. An in-depth quantitative analysis of this phenomenon has not been performed because of the complexity of the hoop model. A qualitative feel for how this stress arises and how the geometry relates to it can be determined by noting the apparent shift in the hoop axis from A to B, Figure 10.4.3-3. This shift, equal to the original displacement angle, causes the projected angle of the hinge lines on the plane normal to the new axis to be less than the original $7.5^{\circ}$. This angular reduction, resulting in a misalignment of tube ends (hinge line to hinge line), induces bending and torsion into the hoop tubes. Magnitude approximations indicate error of less than $1.0^{\circ}$.

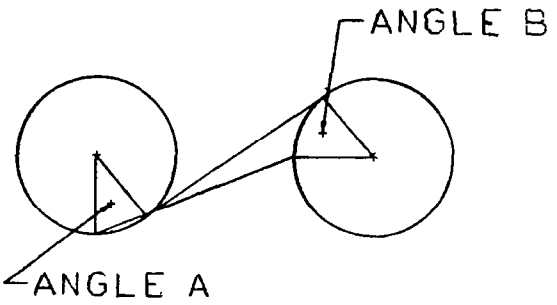


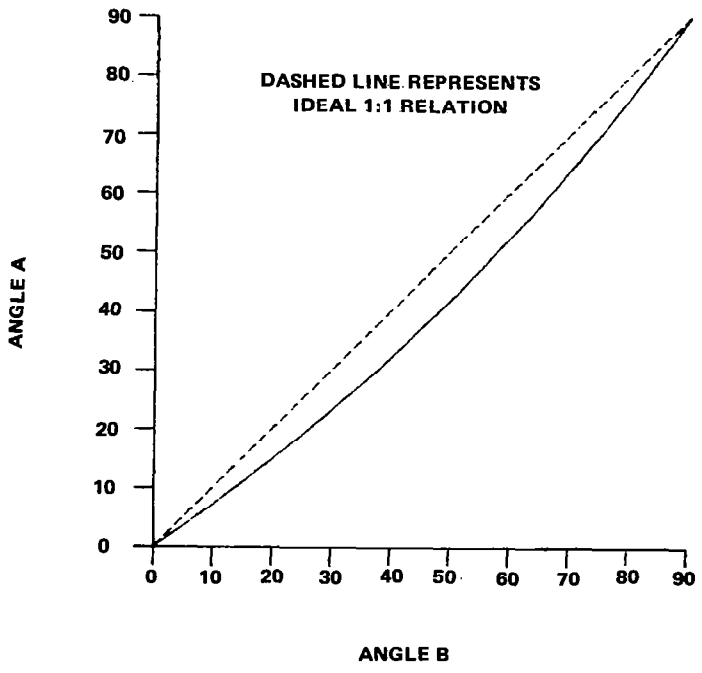


Figure 10.4.3-1. Kinematic Study

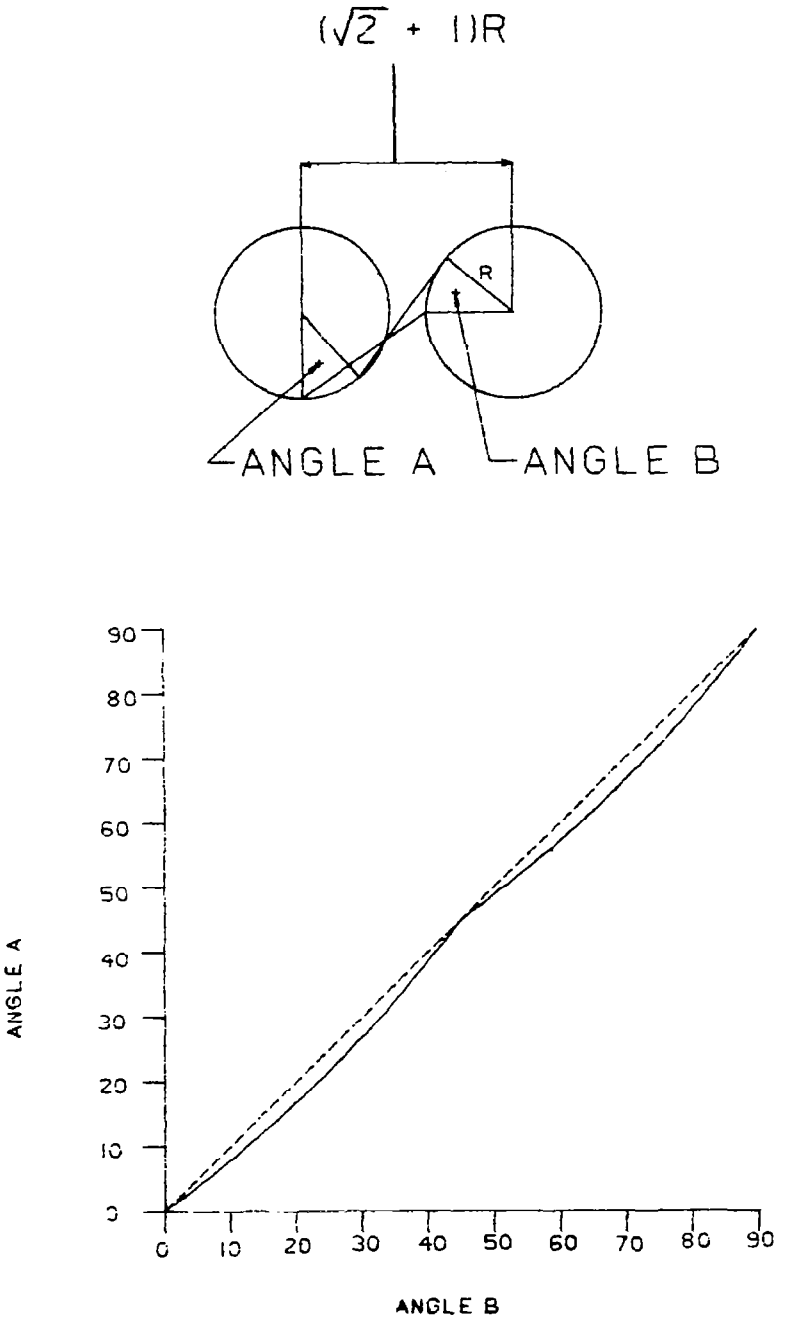


Figure 10.4.3-2. Kinematic Study - Optimized Geometry

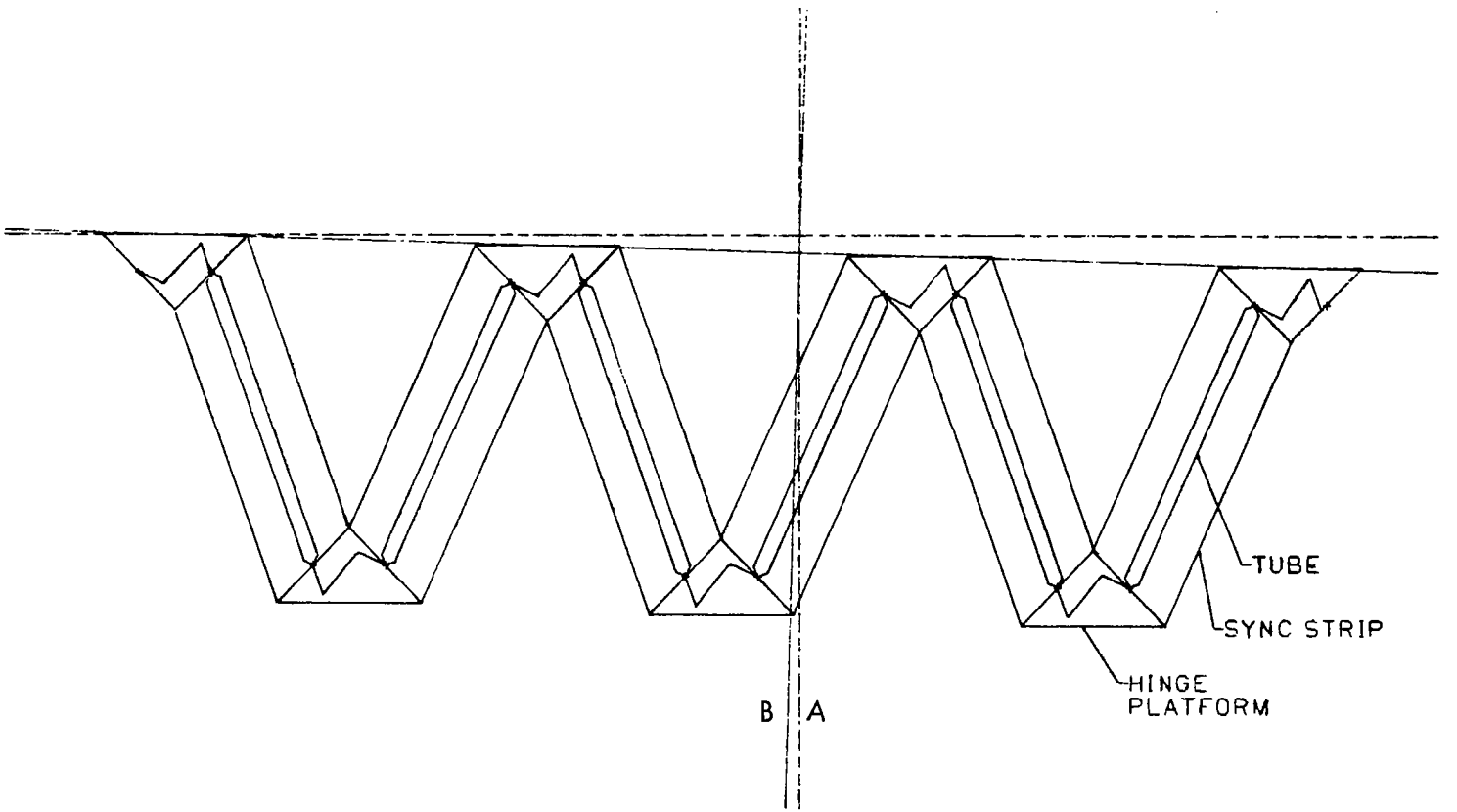


PHANTOM LINES=DESIRED CENTERLINE OF HOOP, NORMAL TO HINGE PLATFORMS

SOLID LINES=ACTUAL HOOP CENTERLINE NECESSARY FOR ENDS OF HOOP TO MEET

Figure 10.4.3-3

The solution to this problem is to reduce or eliminate the displacement error caused by nonuniform pivot arm rotation during deployment. Reduction of the error can be accomplished by proper assembly of component parts of the hoop as depicted in Figure 10.4.3-4. If the hoop member end fittings (male and female) are selectively assembled, the displacement error can be reduced significantly with a resulting reduction in bending and torsional stresses. Total elimination of the error would mean changing to a gear or cable/pulley system.

The Phase II 15-Meter Model design will study the feasibility of using a gear, cable/pulley, or other zero error mechanism for the hoop hinge. The possibility of making the push rod design acceptable for the 15-Meter Model through certain design changes will also be studied. The 100-Meter Point Design will still use the push rod mechanism because the error introduced for a 48-member hoop with 20+ foot long sections is acceptable. An alternate gear approach for the 15-Meter Model is shown conceptually in Figure 10.4.3-5 and a pulley/cable concept in Figure 10.4.3-6.

### 10.4.4 Hoop System

The two main structural pieces of the hoop system are the tube segments and the hinge joints. Associated with these are the surface connections and the hoop cable connections. The function of these components and the level of detail reached in their design is described below.

The hoop tube segments are required to perform deployment by carrying bending loads from the motors to adjacent hoop segments, and in the fully deployed geometry the tubes serve as main compression members. The initial sizing of the tubes was based on an operating load from the 100-Meter Point Design of 600-pound compression. Using this load, a 1.25-inch diameter graphite tube with a 0.025-inch wall thickness gives a design margin of 1.0 (capable of accepting twice the design load). This margin is based on a graphite modulus of $10 \times 10^6$ psi. Assuming a strength allowable for the graphite of 20,000 psi, the maximum bending moment is approximately 600 in/lb, a value that leaves little margin during deployment to accept snag loads or

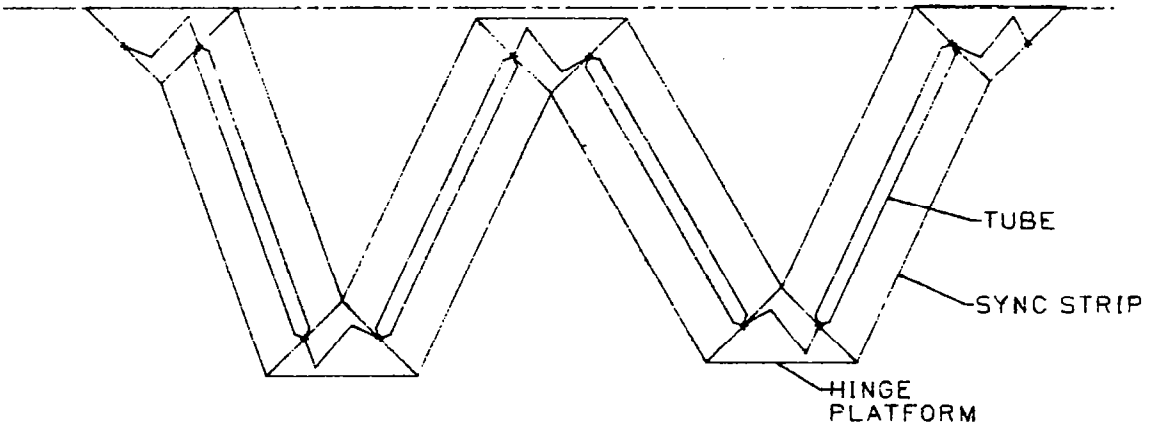


USING SELECTIVE ASSEMBLY OF END FITTINGS, THE ERROR CAN BE PARTIALLY CORRECTED

Figure 10.4.3-4. Cancelling Error Assemble Method

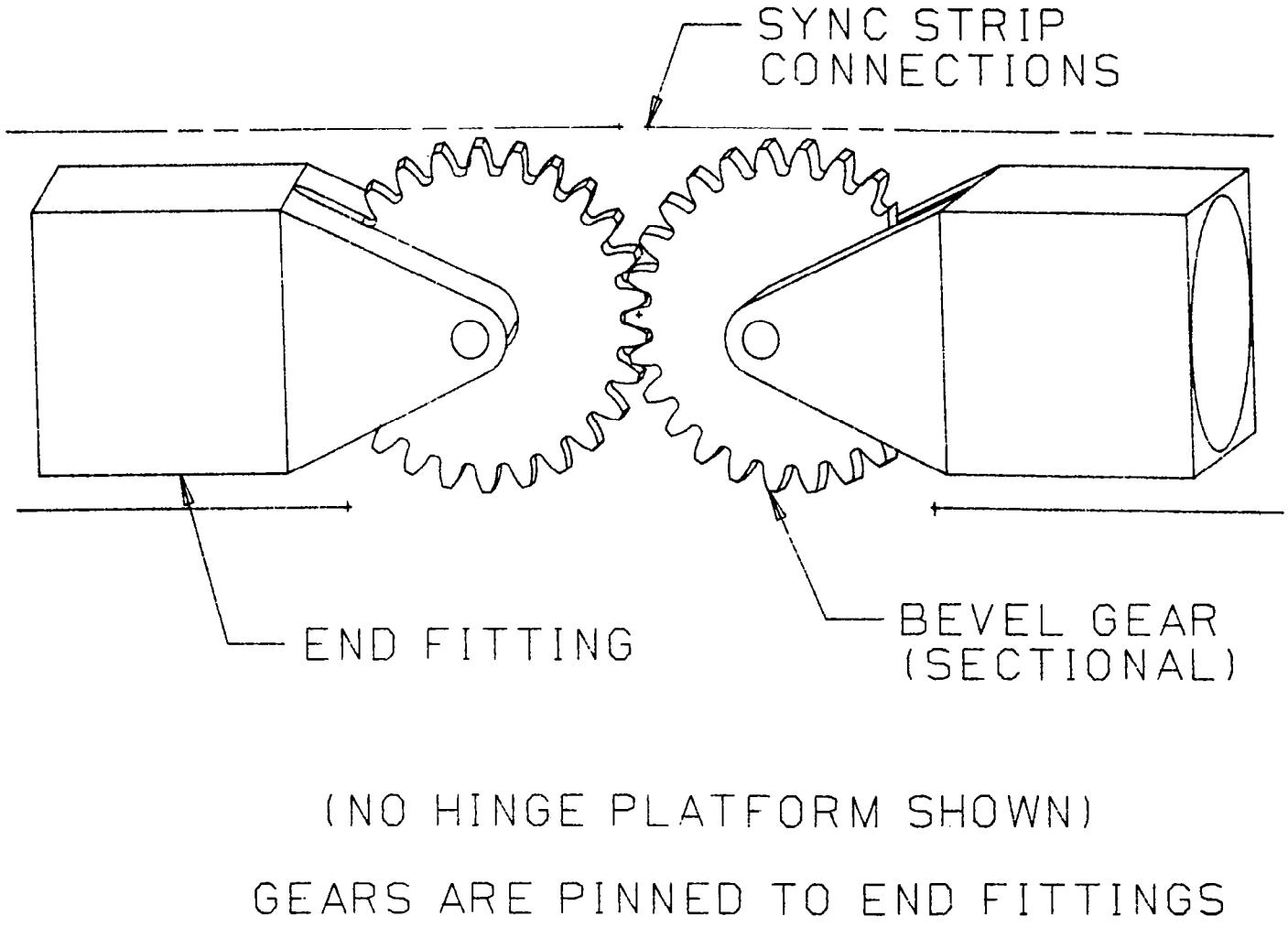


Figure 10.4.3-5. 15-Meter Hinge Joint Gear Concept

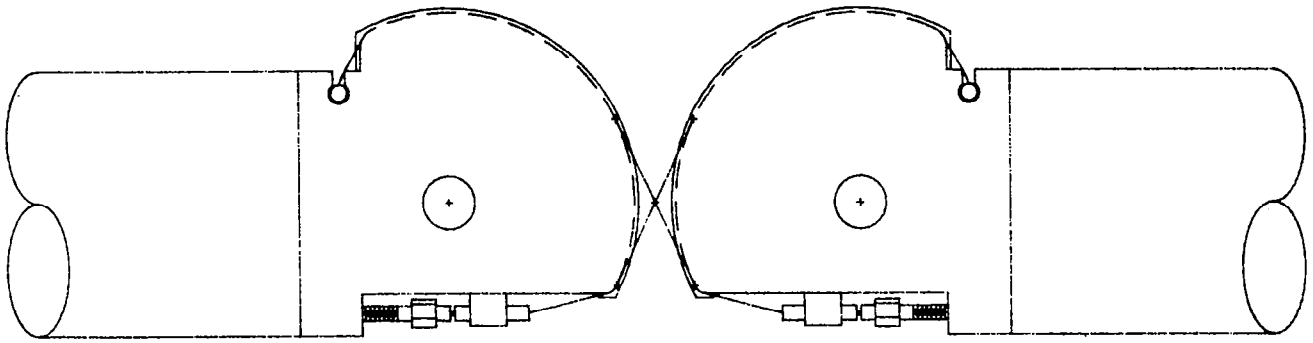

(NO HINGE PLATFORM SHOWN)

Figure 10.4.3-6. 15-Meter Hinge Concept - Pulley Cable

deployment anomalies. Therefore, this tube design is marginal with respect to performance and yet it should be noted that a direct scale from the 100-meter tube design yields a 0.9-inch diameter tube, significantly smaller and unacceptable for the loads anticipated. This emphasizes the fact that direct scaling is not adequate for hoop segments and joints. To provide more margin on the 1.25-inch diameter tubes may require that the philosophy of using 100-meter loads on the 15-Meter Model be revised. As stated in the loads determination section, the entire idea of not scaling loads and cord sizes will be reviewed with respect to hoop stability and design considerations in the next phase of the design task.

The hoop segment graphite layup is $0^{o}$, $90^{o}$, $\pm 45^{o}$ which has good torsional rigidity and yields a weight of approximately 0.25 pound.

The design of the hinge joint was directed exclusively toward the push rod concept until late July when the kinematic anomaly was discovered. At that point a decision was made to shift the effort toward developing the gear and pulley/cable concepts in the remaining time of the first design phase. Because this decision came near the end of the design work for this fiscal year, the level of detail for the two alternate hinges is not equal to the design detail for the push rod hinge.

The push rod hinge design for the 15-Meter Model is shown in Figure 10.4.4-1. The kinematics of the 100-Meter Point Design are reproduced with this design although the appearance is quite different. The side plates serve to support the hinges and sync strips without the costly and difficult to assemble truss structure of the point design. The plates are designed to be stamped from 1/8-inch thick steel in a fairly inexpensive operation. The two side plates, stabilizing the hinge pins and the synchronizer strips, are held apart by machined X struts. They also serve as the sync strip pin connection and allow access for assembly and adjustment.

The push rod has a length adjustment and swivel couplings at both ends that resemble a U-joint. A commercially available ball joint end fitting was initially considered but the size would have increased the push rod length by approximately 1 inch with corresponding changes in all hinge joint components.

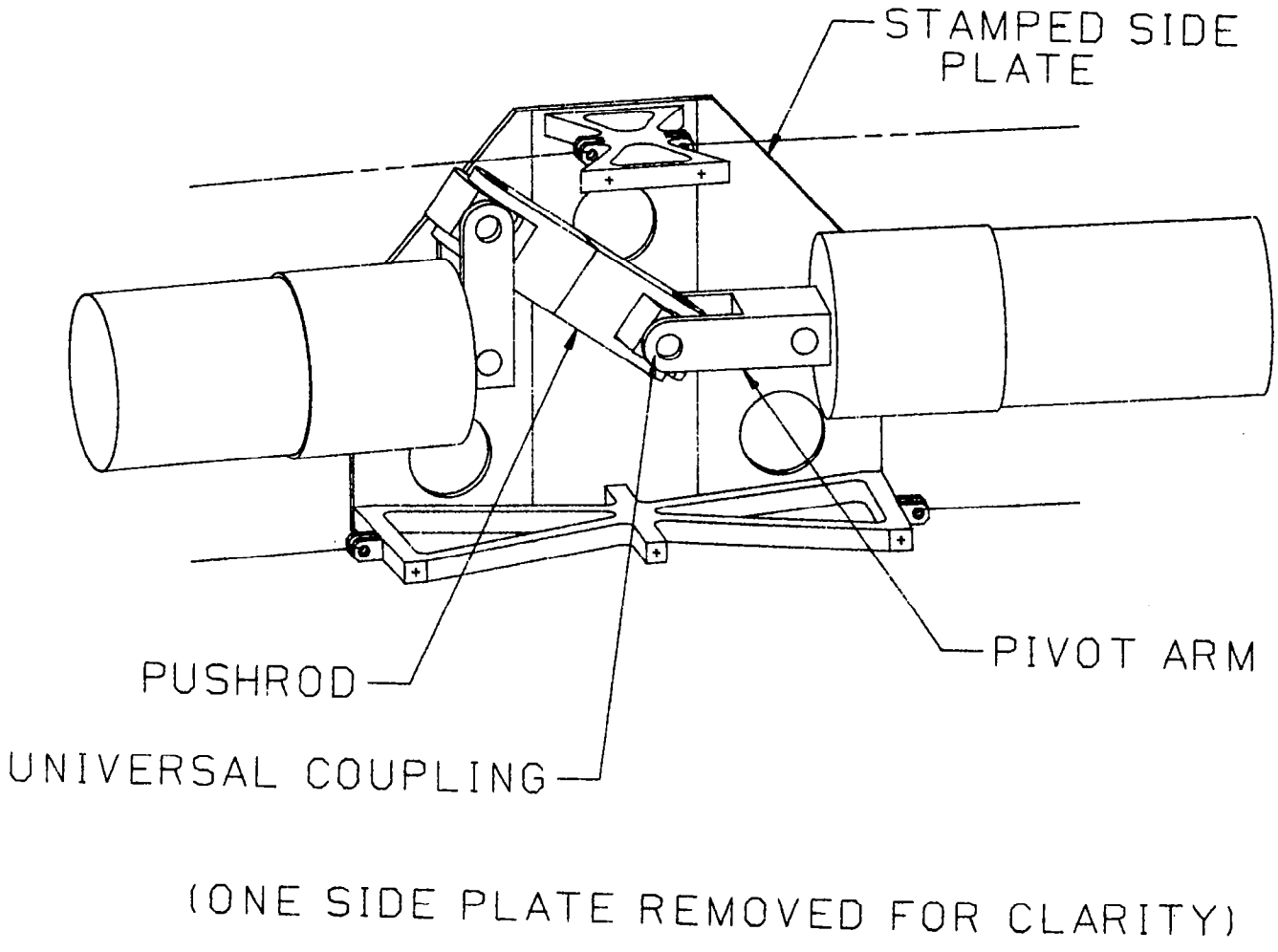


Figure 10.4.4-1. 15-Meter Hinge Joint Push Rod Design

The pivot arms, both male and female, are 1-inch long, and integral with the aluminum end fitting. These fittings are bonded directly to the graphite tubes.

The hinge joint shown represents one of the nondriven joints. The four motor driven joints are of a similar design that allows the mounting of a ball screw drive unit. This unit drives the deployment in exactly the same way as the point design. An enlarged clevis fits over one end of the push rod and through the ball screw to be driven by the motor.

As noted earlier, this design is not a direct scale of the 100-Meter Point Design. Direct scaling would yield a pivot arm length of 0.48 inch, which would be very difficult to implement considering the size and loads expected.

The two hinge concepts that were worked after the kinematic problem was discovered are the gears and the pulley/cable. The pulley/cable concept was studied and drawn by the customer. Little work was performed at Harris except to note that the lack of backlash in this type of joint is very desirable.

The gear concept is shown in Figure 10.4.3-5. Due to the $7.5^{0}$ angle between hinge lines (48-segment hoop) the gears would need to be beveled. Also, to provide proper clearance for the synchronous strips when stowed, the gears are sectional. This last requirement exists only if a two-gear set is used. If a gear train of smaller gears is used, the clearance problem is avoided.

Some problems or difficulties encountered in the gear design are weight, backlash, and the need to rigidly align shafts. the weight problem might be avoided with proper design although excessive machining could increase costs. The backlash problem appears unavoidable as a conventional antibacklash design adapted to a bevel sectional gear could be heavy and expensive. the need to rigidly align and hold the shafts appears to be consistent with the push rod concept and has already been addressed in this design.

The remaining components of the hoop system have not been studied. The next design phase will address these parts and finalize the design of the tubes and the hinge joints.

### 10.4.5 Mast System

The mast for the Hoop/Column antenna is the central compression member which telescopes to the proper length upon deployment. The mast supports the carriers for the cable spools and the preload section in addition to the motors and controls for its own deployment. This section will describe the geometry and current design for the 15-meter mast.

The basic mast geometry and kinematics are identical to the 100-Meter Point Design and the 20-Meter Mast Model that is being built. To gain the greatest stiffness and strength for the lowest weight, a truss design is used. The nine top sections, nine bottom sections, and the hub are all similar built-up trusses with only basic dimensions different. The truss is composed of six vertical tubes forming a hexagonal cross section, connected at top, center, and bottom by circumferential tube members (see Figure 10.4.5-1). In addition, the truss is stiffened by diagonal cables in every face of the hexagonal. Since the hub is longer than the telescoping sections, it has several levels of circumferentials between top and bottom.

The mast is deployed using a four-cable pulley system. Two cables operate the top nine mast segments and two operate the bottom nine segments. The cables run over a series of pulleys on two opposite vertical tubes in the hexagonal truss. As the cables are reeled in by two motors (one motor for top, one for bottom), the segments telescope to their fullest extent. At this point a limit switch stops the motors. A retention cable assembly consisting of a cable attached to the last segment and a motor and drum then retracts the mast segments into their fully latched position. These cable systems are shown schematically in Figure 10.4.5-2.

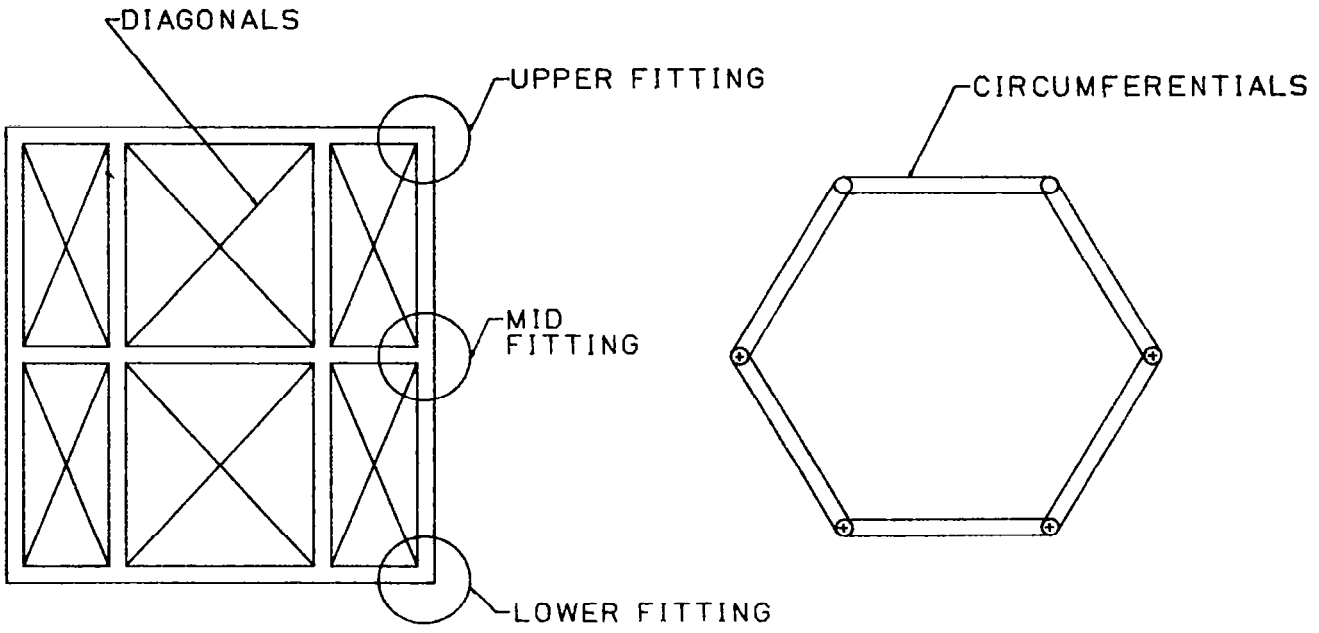


Figure 10.4.5-1. 15-Meter Mast Segment

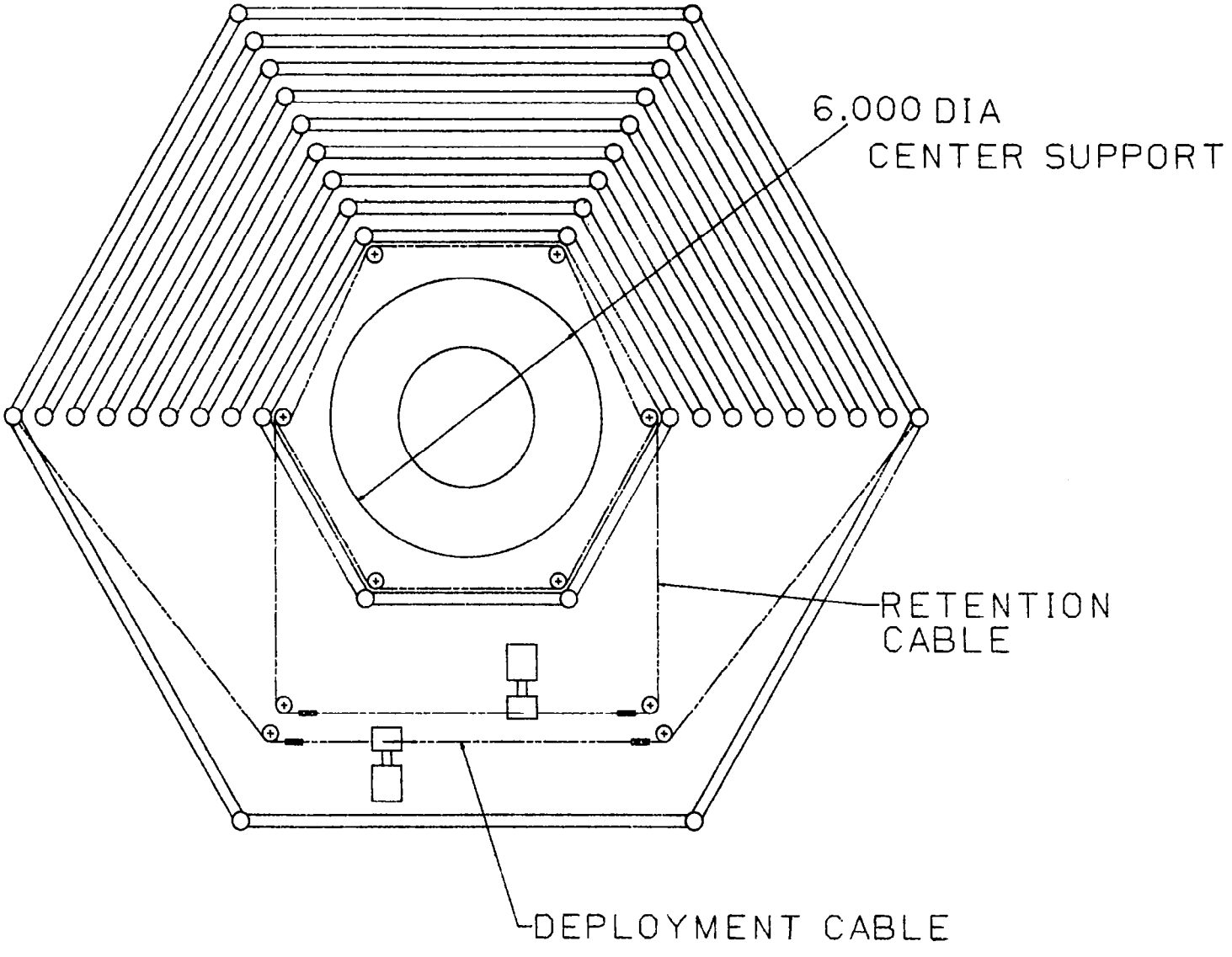


Figure 10.4.5-2. 15-Meter Hoop Top View

The latch mechanism, shown in Figure 10.4.5-3, is located on each mast segment and at six points on the truss. This mechanism requires each segment to overshoot its latched position to activate the latch. After the latch is activated, the segments must be retracted as described above to fully engage the latch. This latch can be released in the same manner, i.e., deploy past latched position and then stow completely.

The length of the mast when deployed is 320.95 inches. The distance between the imaginary intersection of the top 30° hoop cables and the bottom 30° hoop cables is 340.95 inches. The extra 10 inches at top and bottom allow room for the spool carriers and the preload segments which will be designed during the next phase. The mast geometry is shown in Figure 10.4.5-4.

The diameters of the mast sections are defined as the distance across corners on the hexagon from centerline of one vertical tube to the centerline of the opposite tube. As these sections nest into each other, there will be ten different diameters (nine sections, one hub). A direct scale from the 100-meter design yields diameter ranging from 3.0 inches for the smallest section to 7.8 inches for the hub. As can be seen from Figure 10.4.5-4, the 15-Meter Model will have diameter ranging from 9.0 inches to 21.42 inches at the hub. It was necessary to increase their diameter over the scale dimensions to allow for the support tube that will protrude into the center of the mast and serve as a holding fixture for the hub. Analysis has shown that a natural frequency of 5 hertz for the antenna/support tube system is necessary to enable accurate surface measurements to be taken after deployment. This requires a support tube diameter of 6.0 inches and a 1.5-inch wall thickness. Using a 6.0-inch diameter for an inscribed circle of the hexagonal cross section, and allowing for clearance due to tube thickness, a 9.0-inch diameter for the smallest mast segment is arrived at.

The vertical tubes in the hexagonal truss are 3/8-inch OD aluminum tubing. This size tubing, when assembled in the current truss geometry, provides a buckling strength approximately double the expected loads. All piece parts are aluminum to reduce cost. Piece parts from the 20-Meter Mast Model will be redesigned for this application in the next phase.

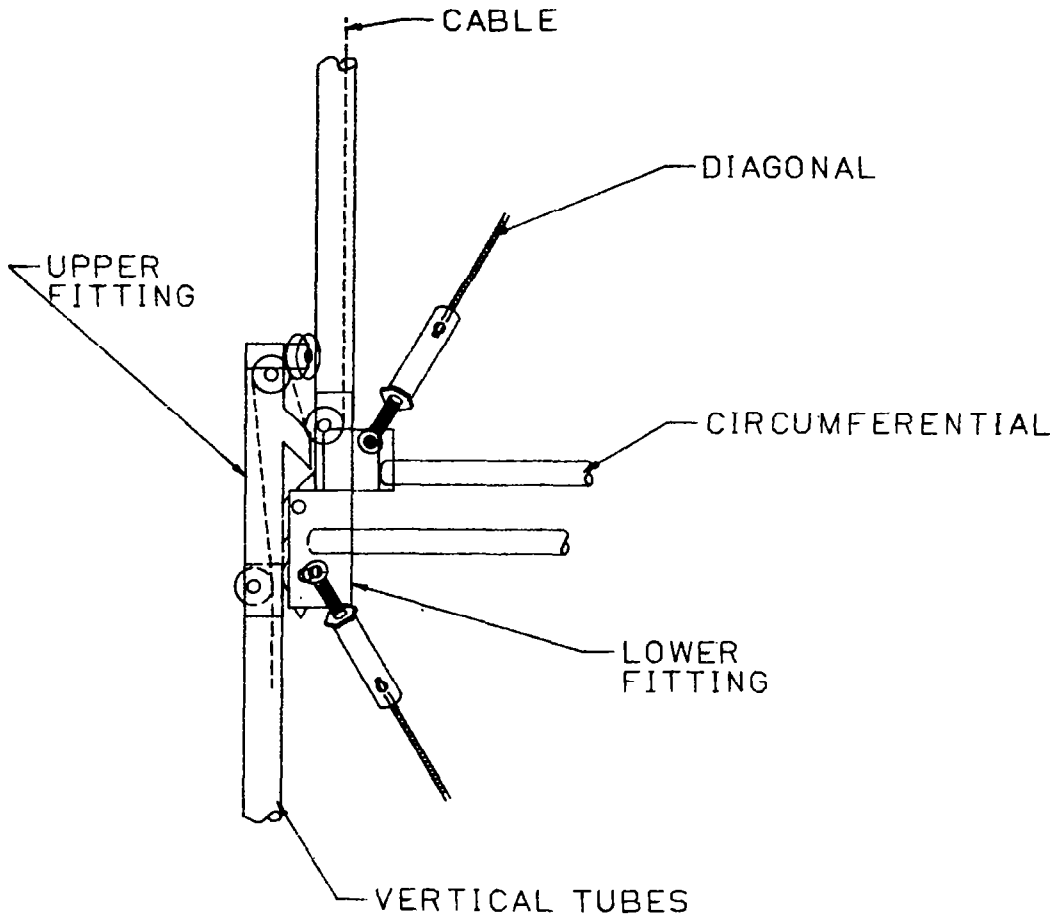


Figure 10.4.5-3. 15-Meter Model Deployed Upper and Lower Mast Fittings

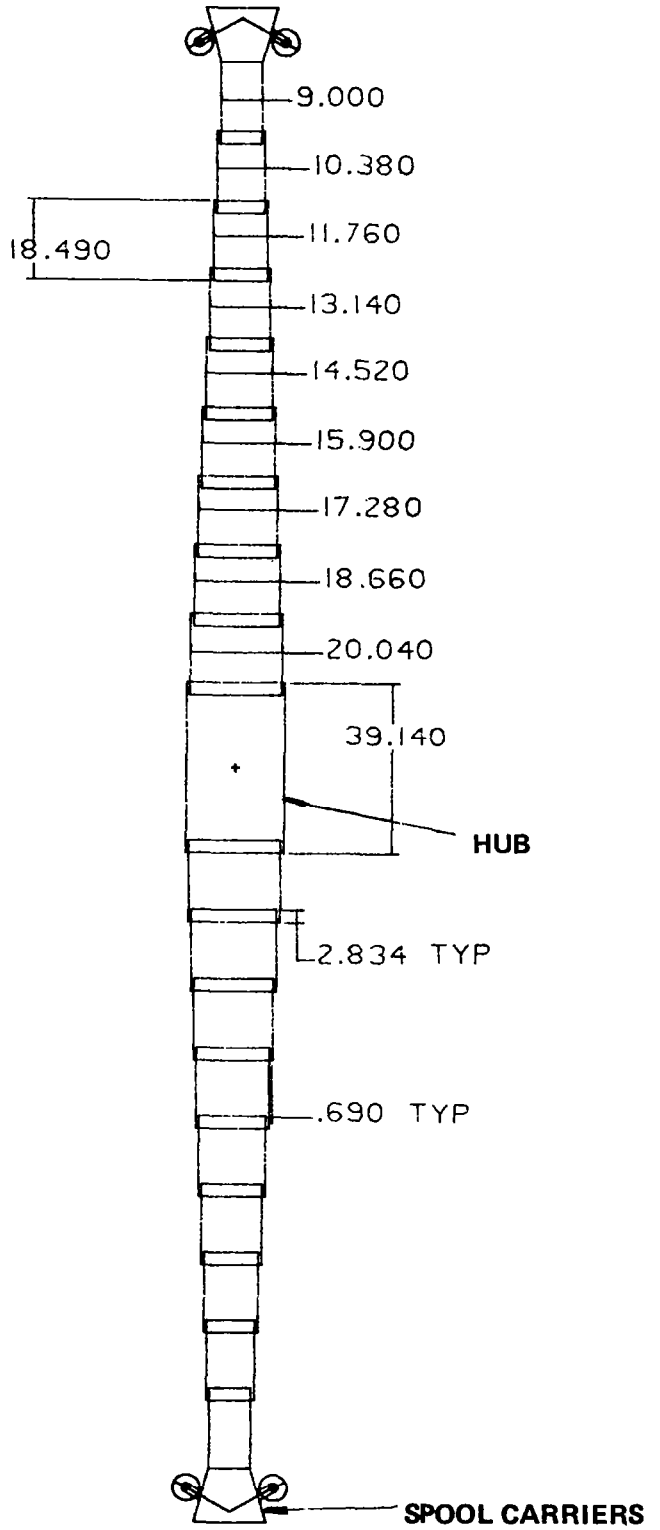


Figure 10.4.5-4. 15-Meter Mast Geometry

## 10.5 Counterbalance Study

A counterbalance study was performed with the following objectives:

1. Determine if the hoop system should be counterbalanced
2. Determine if the mast/column system should be counterbalanced

### Background

The purpose of the 15-Meter Hoop/Column Model is to demonstrate the hoop kinematics and mast kinematics of the 100-Meter Point Design. To accomplish these kinematic studies, the mechanical concepts of the 100-meter design should be incorporated in the 15-Meter Model. As these concepts and mechanisms were not designed to operate in a gravity field, it may be necessary to negate the 1-G force via a counterbalance system. These systems and how gravity effects them will be discussed in the following paragraphs.

### Hoop Counterbalance

The hoop system consists of hoop segments, hinge joints, and a series of cables and spools designed to control the position of the hoop relative to the mast during deployment (see Figure 10.5-1). The spools exert a force on each control cable by means of a constant force (negator) spring. Although the tension in each cable is uniform, the component of this tension that acts on the hoop is dependent on the angle the cable makes with the hoop as shown in Figure 10.5-2. As the hoop deploys away from the mast, the angle between the hoop and each cable changes. Although the force component is changing, all cables are exerting equal forces at a given time. If the hoop becomes asymmetric relative to the mast, for whatever reason, the cable tension components increase or decrease to correct the position as shown in Figure 10.5-3.

The self-correcting hoop system relies on a complete set (48) of upper cables and a complete set of lower cables to control the hoop. The system is designed to operate in a 0-G environment. The top cable tension is equal to the bottom cable tension. If the hoop system is deployed in a gravity field, the weight of the hoop adds a significant downward component of force that causes unbalance between upper and lower control cables (see Figure 10.5-4). Not only does this unbalance in tension affect the self-

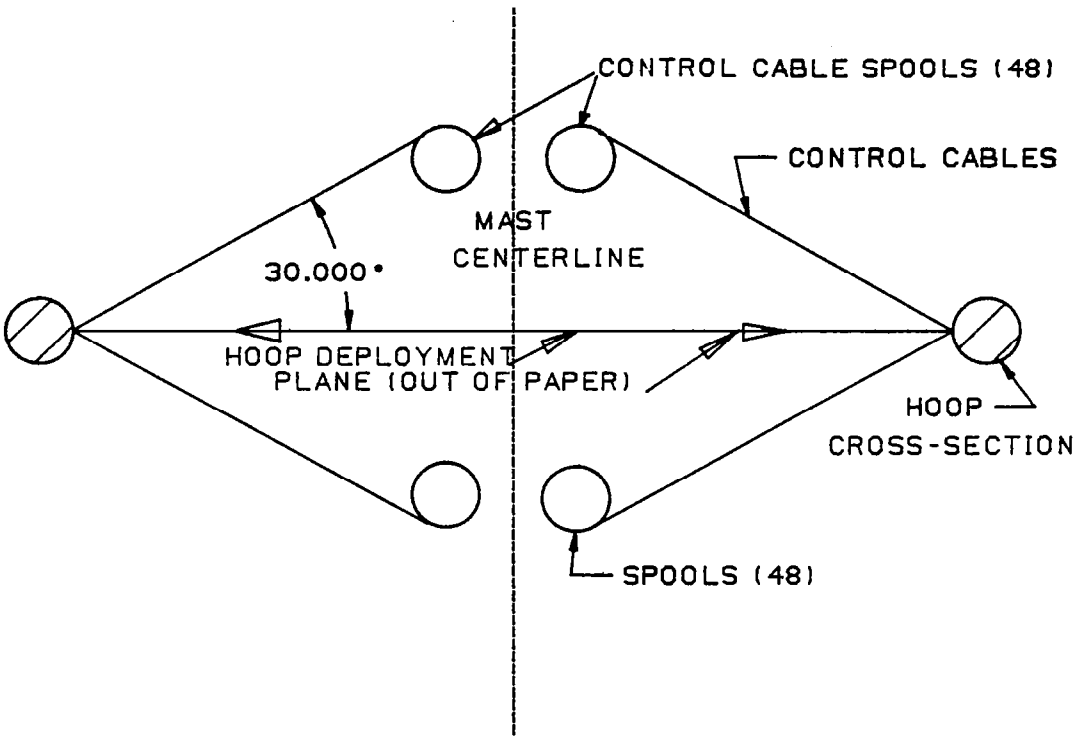


Figure 10.5-1. Hoop System Geometry - Deployed

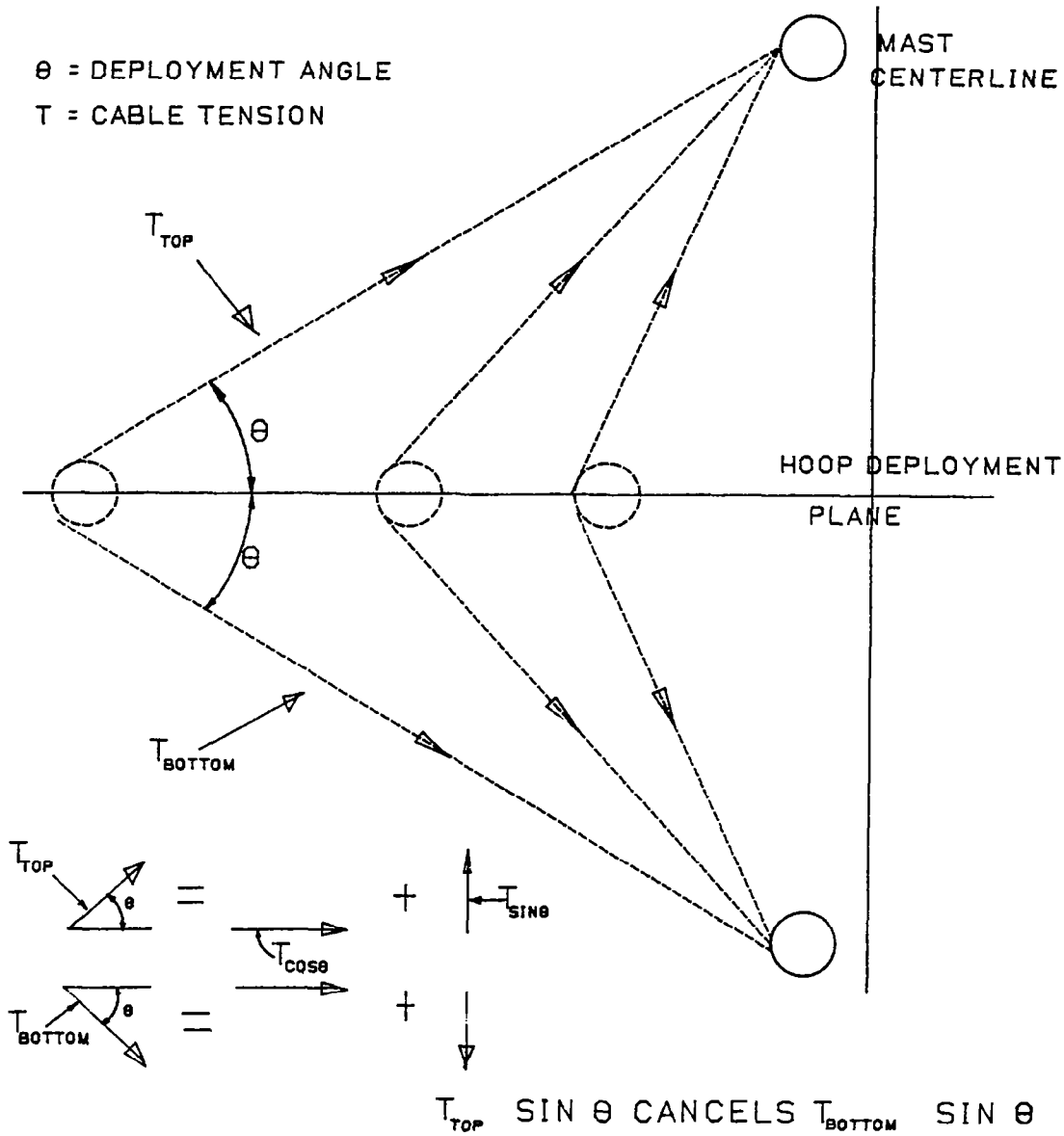


Figure 10.5-2. Hoop Deployment Sequence

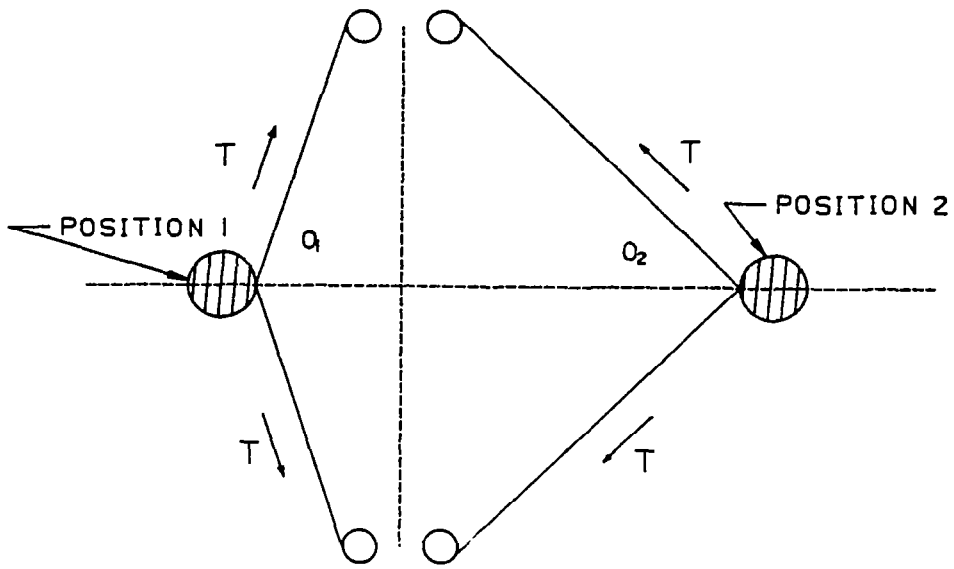


MISALIGNED HOOP

FORCES ACTING ON HOOP

POSITION 1

⟶ = 2T COS $O_1$

POSITION 2

⟵ = 2T COS $O_2$

THE LARGE FORCE AT POSITION 2 WILL TEND TO PULL THE HOOP INTO ALIGNMENT WITH THE MAST

Figure 10.5-3. Hoop Self-Centering Mechanics

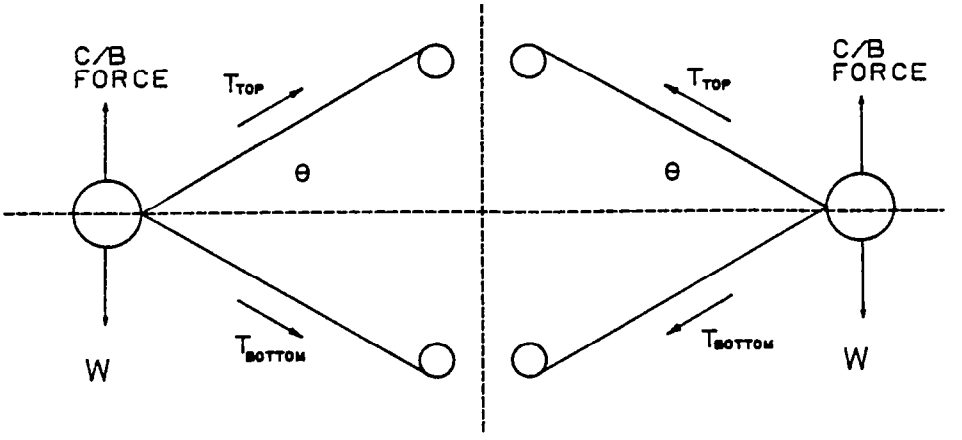


WITH COUNTERBALANCE

$$T_{TOP} = T_{BOTTOM} = T$$

WITHOUT COUNTERBALANCE

$$T_{TOP} = T + W/\sin\theta$$

$$T_{BOTTOM} = T - W/\sin\theta$$

T MUST BE > $W/\sin\theta$ TO PREVENT:

1. HOOP FROM DROPPING
2. BOTTOM CORDS FROM GOING SLACK

Figure 10.5-4. Counterbalance Effect on Cable Tension

correcting design, but the weight of the hoop dominates the spool tension causing the hoop to fall as it is disconnected from the mast. If the top cable/spool tensions are increased to support the hoop weight, the problem arises of varying this force as a function of the deployment angle to maintain the hoop at its proper elevation during deployment. The addition of hoop weight to cable tension also increases the required motor torque. This can be seen in Figure 10.5-4 where the motor torque must drive against the horizontal component of cable tension.

$T \cos 30°$ with counterbalance

$(T + \frac{W}{\sin \theta}) \cos 30^{o}$ without counterbalance

To maintain the deployment kinematics, loads relationships, and motor sizing of the 100-Meter Point Design, a counterbalance should be employed on the 15-Meter Model hoop.

Mast Counterbalance

The 100-meter mast system consists of a center hub section, 18 deployable sections that telescope into position during deployment, and a spool carrier on both ends that holds the hoop control cable spools. Deployment of the mast is accomplished by a cable/pulley system that drives the movable sections to their farthest position from the hub. At that point, latching mechanisms are activated and a retention cord assembly draws the sections back slightly to firmly engage the latch.

The mast for the 15-Meter Model contains the same mechanisms as the 100-Meter Point Design and will demonstrate the same kinematics. The current 15-meter design has the hub supported on a vertical support with the top nine sections deploying upward and the bottom nine sections deploying downward. In a 0-G field, the deployment scenario is the same as the 100-meter design. In a 1-G environment, the deployment and retention cables on the upper segments perform the same tasks because the weight vector is toward the hub. However, on the lower half of the mast, the retention cables are required to perform both deploy and stow tasks. During deployment the retention cables serve to

restrain the lower mast half as gravity attempts to lower the segments. When the nine segments are at the bottom of their travel and the latches are activated, the retention cables reverse to pull the segment into their latched position.

The presence of a gravity vector away from the hub, as in the lower segments, eliminates the need for the deployment cable/pulley assembly as the mast segments tend to deploy themselves. Also, when the gravity vector is toward the hub as in the upper segments, the retention cable assembly is not needed as the mast segments tend to stow themselves. Of course, if a hangup due to racking or misalignment occurs in either top or bottom mast halves, the appropriate cable systems are needed to overcome the hangup.

Since the deployment cable assembly and the retention cable assembly can be adequately demonstrated on upper and lower masts respectively, there is not a need for a mast counterbalance. The small space inside the mast and the cost of designing and building a mast counterbalance also influences this decision. An additional complexity in the design and implementation of a mast counterbalance is the independent motion of the mast segments before they are latched in place.

Summary

A counterbalance is required on the hoop system. The mast is designed to operate in a 1-G environment without a counterbalance.

## 10.6 15-Meter Contour Analysis

The main tasks for contour analysis on the 15-Meter Kinematic Model are:

- Establish and describe the 15-meter surface
- Predict system characteristics in the 1-G face-up/face-down configuration
- Provide design analysis support

The contour analysis for the 15-Meter Kinematic Model was performed using a geometrically scaled finite element model. The scaling of the point design consisted of maintaining the same number of elements and element properties, but changing the element length to 0.15 times their original length. Figure 10.6-1 shows the half-gore model used in the analysis. A detailed description of the finite element model is presented in Paragraph 5.3 under the 100-Meter Point Design description. The hoop and mast design in 15-Meter Model consists of the reduced properties as described in tube design and mast design description.

The primary function of the surface analysis on the 15-Meter is to describe the system characteristics in a gravity environment, and describe cord loads as a result of gravity.

Figure 10.6-2 lists the system characteristics for the 15-Meter Kinematic Model. There is good face-up/face-down linearity, as evidenced by the magnitudes and opposite sign of the defocus values. This is necessary if a 0-G surface contour is to be established. The 0-G surface can be closely approximated by measuring the displaced surface face-up and then face-down and averaging the coordinates.

Also of concern is cord tension changes due to the gravity vector. Analysis indicates that cords will remain in tension in both the face-up and face-down configuration. This is not the case on 100-Meter Point Design, due to its larger relative size.

A counterbalance will be used to aid in the deployment/stowage of the kinematic model, however, once full deployment has been accomplished the counterbalances should be removed. A counterbalance on the deployed model increases the distortion of the surface. Another conclusion of the analysis is that the hoop is under high stress loads under full deployment conditions and should be redesigned for the 15-Meter Kinematic Model.

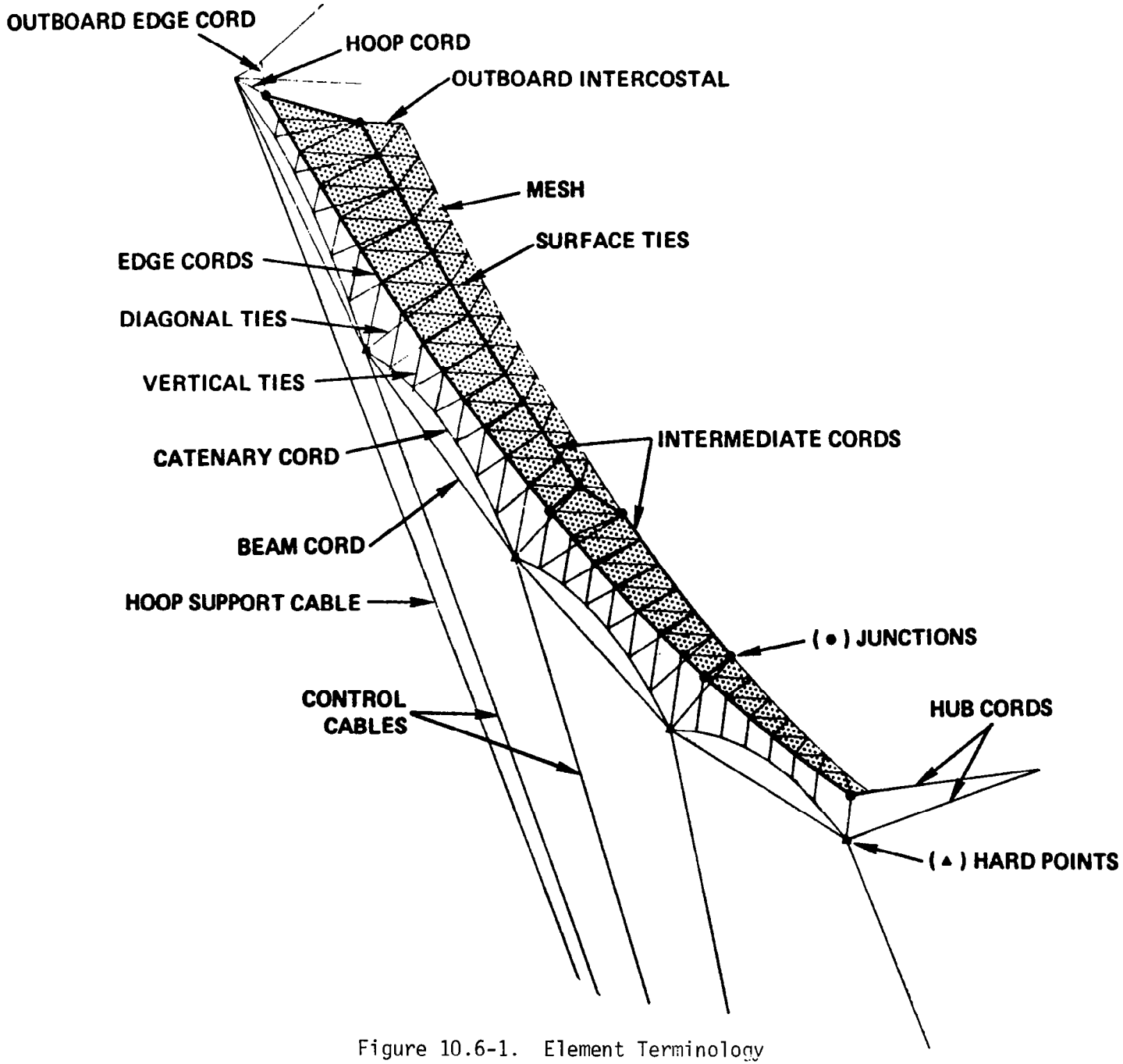


Figure 10.6-1. Element Terminology

– SYSTEM CHARACTERISTICS

| CONFIGURATION | △F (CM) | △RMS (CM) |
|---|---|---|
| 1-G FACE-UP | -0.485 | 0.039 |
| 1-G FACE-DOWN | 0.470 | 0.043 |

Figure 10.6-2. 15-Meter Kinematic Model

## 11.0 ECONOMIC ASSESSMENT

### 11.1 Task Objective

The objective of the Economic Assessment task of the LSST Program is to determine using a parametric model: (1) the estimated hardware cost of a Hoop Column 100-meter diameter Space Deployable Antenna, (2) perform the hardware cost of alternate diameter antennas of the same or similar configuration.

### 11.2 Model Description

The mechanism selected to accomplish this task is the RCA Price hardware model version 83B. There are several reasons for selecting the Price model to do this job.

a. Historical Usage - NASA and Harris have been Price users for several years. Harris has been a subscriber of the RCA Price since early 1976. During the past 4 years many of the items in the Harris technology product line have been characterized using the Price model. A particular area of model usage and method customization is space structures. Harris has a corporate history of at least 10 year's experience in the design development and construction of space structure hardware assemblies. These space structure programs directly involved the incorporation of graphite, aluminum, titanium and beryllium materials. In addition to exotic materials, space structures employ many mechanisms and complex interfaces that have evolved during the design process.

b. Compatibility - The RCA Price model is a universally used cost estimating tool with terminology and input data requirements. Assumptions and input characterizations of the LSST hardware are in a common language format for NASA review and evaluation. Since the Price model is compatible to both customer and contractor, NASA has the real-time option to adjust the input model parameters and perform internal trade-off analysis.

c. Credibility - How believable are the estimated costs generated by the Price model? As previously discussed, the model has undergone extensive usage and customization especially in the area of space structures. One must remember that the model is hardware oriented and the cost reflects the current design status. Hardware costs of a creditable nature can be generated at a detail level even though a detail design is not completed. This process will be further discussed in Paragraph 11.5 of this report.

d. Deliverables - In addition to this final report, Harris is to provide the Price input data files to NASA. The data files will represent all diameters and configurations characterized as a requirement of this study.

## 11.3 Hardware Description

a. Design Description - The subject of this study is a Hoop/Column or Maypole design Space Deployable Antenna. The baseline diameter of the Hoop Column design is 100 meters. A structure of this size has never before been designed or built. The antenna has many unique features, one of which is that hardware must be stored aboard the Space Shuttle and deployed in space. Packaging volume and weight are critical design parameters. The current design employs many components and material types that have been incorporated in previous Harris antennas. The fact that many of the antenna components are not new is one of elements that lends credence to the use of Price as the estimating vehicle for the Hoop/Column Antenna.

b. Weight Analysis - One of the required inputs to the Price model is weight. Weight had to be calculated for each component that was characterized. There is a certain amount of risk associated with the calculation of weight at the hardware tree level since a detail design at the same has not been completed.

Weights were estimated based upon a conceptional description of the component, material type and function. As with any parametric model an error in the weight or other physical characteristic will cause a corresponding incorrect cost. Because of the methodology employed in the Price characterization of the subject hardware the risk has been reduced or as a minimum not compounded.

The total weight for the 100-meter antenna is approximately 3,600 pounds. Alternate diameter antennas of the same configuration have scaled weights based upon tube diameter reduction, cord length, tube length reduction and mesh square area reduction. The following is a table of total estimated antenna weights:

| Diameter in Meter | Quad Aperature Weight in lb | Symmetrical Surface Weight in lb |
|---|---|---|
| 100 | 3600 | 3600 |
| 70 | 2900 | 2900 |
| 50 | 2300 | 2300 |
| 30 | 1900 | 1900 |

Estimated total weights for the Quad aperature and symmetrical surface are identical. The difference between the two is only in the surface adjustment and mesh selection area.

c. Assumptions - In order to estimate the hardware costs at this stage of development, one has to make certain assumptions in order to bound the task scope. The assumptions are divided into three main areas: economics, schedule and hardware.

Economic - All dollar values, i.e., costs, are calculated in constant 1983 dollars. The Price model version 83B escalates from 1979 actuals using predicted annual rates to the year 1983. After 1983, the rate remains constant way out escalation during the length of the schedule. The reader must be aware that the predicted rates in the 83B version are lower than the current Price 84 version.

In addition to being calculated in constant 1983 dollars the costs are at cost and do not include any CAS or FEE. The estimated costs do include the contractor's forward pricing rate for G&A.

Schedule - The Price model requires schedule dates as an input parameter. A program start data of 1 January 1983 was used to begin the Price characterization. For the initial characterization the schedule end dates were floated.

The Price model floating technique was used to determine the optimum schedule duration for each characterized component and assembly. The Price model was further used to determine the total length of time required to design, build and test the hardware.

The detail process and results will be discussed in the methodology and results section of this report.

d. Hardware - The hardware assumptions for the economic assessment activity include several limiting factors. At this stage of the study many areas remained undefined and those areas have been omitted from the characterization. Some of the significant items are as follows:

- Antenna/Spacecraft interface.
- Feed assembly and feed support structure.
- Antenna deployment and re-stow electronics package.

All diameters of the Hoop/Column Antenna design are built using the protoflight philosophy, that is to say, that the qualification or testing model is refurbished as flight hardware. The total calculated hardware costs for each antenna diameter do include many development hardware and test specimen assemblies. Components, subassemblies, and assemblies that have high ECMPLX values or that represent new technology are

modeled. The following specific items are included in the Price characterization along with the typical design, analysis, documentation and testing associated with a flight hardware program:

- Refurbishment activity.
- Part shrinkage during assembly.
- Partial wiring and cabling mockup.
- Thermal control blanket mockups at initial assembly areas.
- Partial hum deployment model.
- 2 gore surface breadboard.
- Hoop Joint Test Model.
- Model of upper and lower type 9 and 8 most assemblies.
- Restraint system mockup.
- Restow mechanism model.
- Deployment cable model.

All assembly and test tooling is included in the cost estimate. Tooling global values are consistent with other space structure programs.

## 11.4 Hardware Characterization

a. Methodology - The key to accurately using Price to estimate costs is to construct a very granular model. The distribution of predicted weight is critical to generic characterization. The Price model is weight-driven and generally speaking the heavier the characterized part the higher the cost.

During the past four years several unsuccessful attempts have been made to develop a top level or even second level set of MCPLXS values that are representative and repeatable of deployable structures. Diameter changes with a non-solid surface are the major factors contributing to the modeling difficulty. Harris' experience with mechanical items has shown that the granular approach is the only way to go. There are several advantages and few disadvantages to this approach.

The advantages:

- Deployable antennas incorporate many exotic material types that have wide ranges of MCPLXS values. A very granular method of characterization allows characterization as a minimum, by homogeneous material type.
- A granular approach allows the user to access the complexities of design integration and assembly integration. Often time, the costs of assembly and testing at the subassembly or assembly level far outweighs the sum of the components.
- Scheduling of components, subassemblies, and assemblies is more accurate than a lump item characterization.
- Price empirical data values for generic types of hardware have prior history. An example of the empirical data is the MCPLXS values for graphite tubes, titanium and aluminum fittings and joints, motors, gear boxes, mesh, ties, pins and other structural components.
- The current method of characterization allows the Price analyst to discuss in detail with the design/analyst folks about mechanisms and interfaces that are not designed but are conceptual in nature.
- The prime advantage to the granular approach is that the estimated costs are much more accurate than they would be if lumped hardware items were characterized.
- Review of the Price input assumptions and results with engineering especially ECMPLEX values is a more thorough method of evaluation.
- This granular approach allows for the modification of design to be accessed in terms of dollars and schedule.
- Detail design changes at a sub hardware level can be evaluated at the system or assembly level by simply reprocessing the LF file.

The disadvantages:

- The only disadvantage to the granular method of characterization is the size of the LF data file.

b. Hardware Tree and Price Characterization - The Price model was constructed using a series of LU files that are consistent with the organization of the hardware tree.

To demonstrate how the process works and why the estimated costs have a high degree of credibility, we will characterize a segment of the hoop assembly and show how these segments are integrated to form the hoop assembly.

The hoop assembly is composed of four major subassemblies plus hardware designed and installed at the final stage. The major subassemblies are: (1) Pivot Frame assembly, (2) Drive Unit assembly, (3) Tube assemblies, (4) Push Rod assemblies. In addition to hardware definition, the hardware tree defines how many of each component are required per assembly.

Let us now look at how the Pivot Frame assembly is characterized. The following is a listing of the components required to construct the Pivot Frame assembly.

| Item | Description |
|---|---|
| 1 | Pivot Fitting |
| 2 | Motor Fittings |
| 3 | Fitting W/O Motor |
| 4 | Lower Fitting with Stabilizer |
| 5 | Clevis Housing |
| 6 | End Fitting |
| 7 | Tube Assembly T-1 |
| 8 | Tube Assembly T-2 |
| 9 | Tube Assembly T-3 |
| 10 | Tube Assembly T-4 |
| 11 | Tube Assembly T-5 |
| 12 | Sync Bracket Inboard |
| 13 | Pivot Frame Assembly and Integration |

Item Number 1, Pivot Fitting - At the time of Price characterization this part was not detailed, however, enough data is known about the part to characterize. The function of the part is known as is the material type and the type of integration. History has shown the aluminum fitting with a graphite bond has an MCPLXS value in the mid 6's range to 7.0 at the high end. The value selected to describe this pivot fitting is 6.8 and the percent design is 100. The engineering complexity is new but of routine complexity.

Item Number 2, Motor Fittings - The motor fittings are much larger than the pivot fittings and have to perform a more difficult function. The function of the motor fitting is similar to the MDS mechanism designed and built on a previous program. The MDS assembly has a value of 7.92. This fitting does not have quite the same degree of complexity and thus the MCPLXS value is a slightly lower. The percent new design is 100 and the ECMPLX value is slightly higher than the pivot fitting.

Item Number 3, Fitting W/O Motor - The geometry of this fitting is almost identical to Item Number 2, however, the motor interface is omitted. The descriptors for this item are slightly less than Item Number 2. Reference the Price input file for specific values.

Item Number 4, Lower Fitting with Stabilizer - This is a smaller aluminum fitting with intricate machining required. History has shown that items that perform the same function are characterized in the low 7.0's for manufacturing.

Item Number 5, Clevis Fitting - This small fitting interfaces with Item Number 4 above. Machine tolerance are critical for precise deployment movement. The material type is aluminum. Clevis type hardware items have been used on Harris antenna designs for several years. The part is not that difficult but the integration drives the complexity.

Item Number 6, End Fitting - This is a critical part for mechanism success and the difficulty is reflected in the selection of ECMPLX value.

Items Number 7-11 - Straight tube segments. Values for these are lower than other members of the Pivot Frame assembly because the tubes are very easy to manufacture. The only area of complexity is tube sizing.

Item Number 12, In-board Sync Brackets - These brackets are for mounting of the synchronizer (in-board strips). We have designed and manufactured many aluminum brackets. The MCPLXS values are based upon previous type brackets.

Item Number 13, Frame and Design Assembly and Integration - This segment of the file is a mode 5 box or point of design integration and not a piece of hardware. The input values for degree of design difficulty and manufacturability describe the total subassembly. This assembly has never been built before and this fact is reflected in the values.

The process used to characterize the above hoop segments was utilized to estimate the LSST hardware. The range of manufacturing complexity (MCPLXS) values is from a low of 5.3 to high of 7.9. Each of the values are based upon experience of a generic family of components. The generic hardware value is the prime reason why Price is a credible tool to be used on a hardware program that ha not yet been designed.

Summarizing parts to characterize on assembly would also be very difficult because of the wide range of complexity values. The granular approach takes a little more time to characterize, however, the repeatable results by part type make it a worthwhile task.

c. Schedule - Each characterized item has a Price requirement, a schedule start and stop data. The intermediated dates are calculated by the model based upon the PRNF values. The first run utilized floating dates for the intermediate and completion times. The Price model calculated optimum time intervals based upon ECMPLEX and PRNF values. The defined length of time was then input on the schedule input line. In order to construct a structure of this magnitude each item cannot start on the first day of the program. Experience with flight hardware has shown that because of hardware/subassembly relationships a certain order is required. Each part has been ordered and the dates are contained in the Price input file. Calculated dates would appear on a LSKIP CR output.

d. Stacking Technique - The stacking is a process where the antenna model is built up. LFS boxes at stacking generally have much higher values than individual items. This is due in part to the amount of unknowns and the physical size of the LSST hardware. The dates in stacking boxes usually account for a greater period of time than the greatest interval of any sub-box. This is due to the fact that the integration box also includes the overall design/analysis effort for that assembly.

## 11.5 Results

a. Total Cost - The results of the Price characterization for both the quad aperture and symmetrical surface configurations are presented in both dollars and relative values in Figures 11.5-1 through 11.5-4. Each configuration was evaluated for four different diameters. Data points and Price runs are included for diameters of 30, 50, 70 and 100-meters.

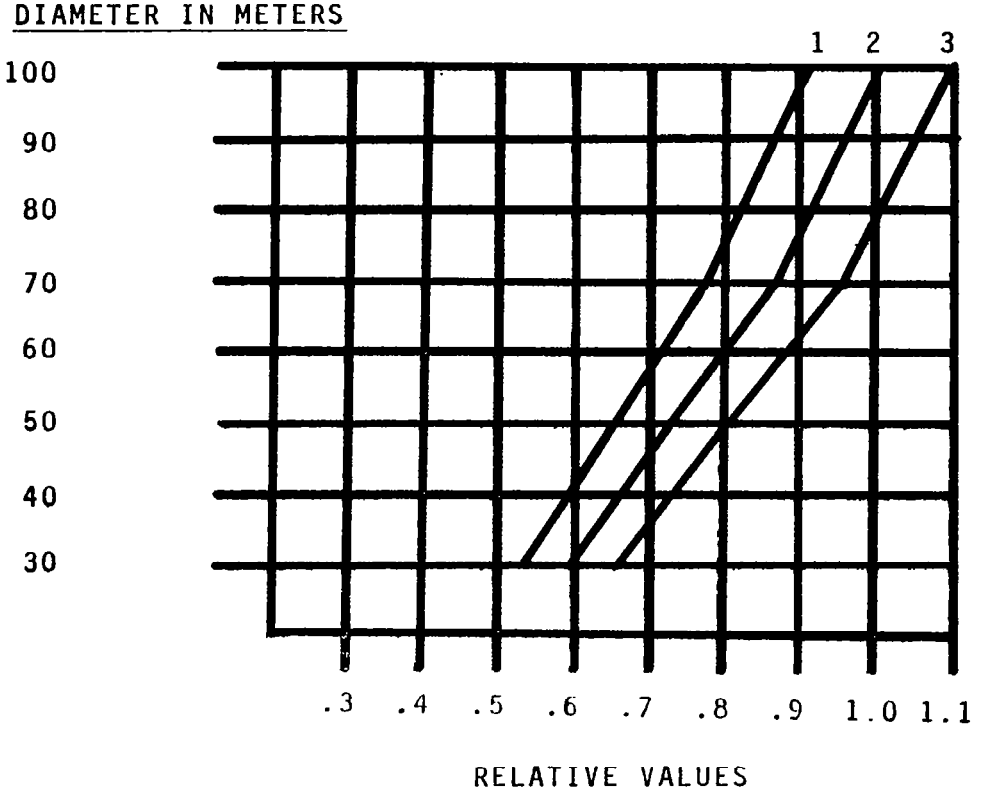


Figure 11.5-1. LSST Quad Aperture Cost Uncertainty as Calculated by Price Cost Versus Diameter (Point Design)

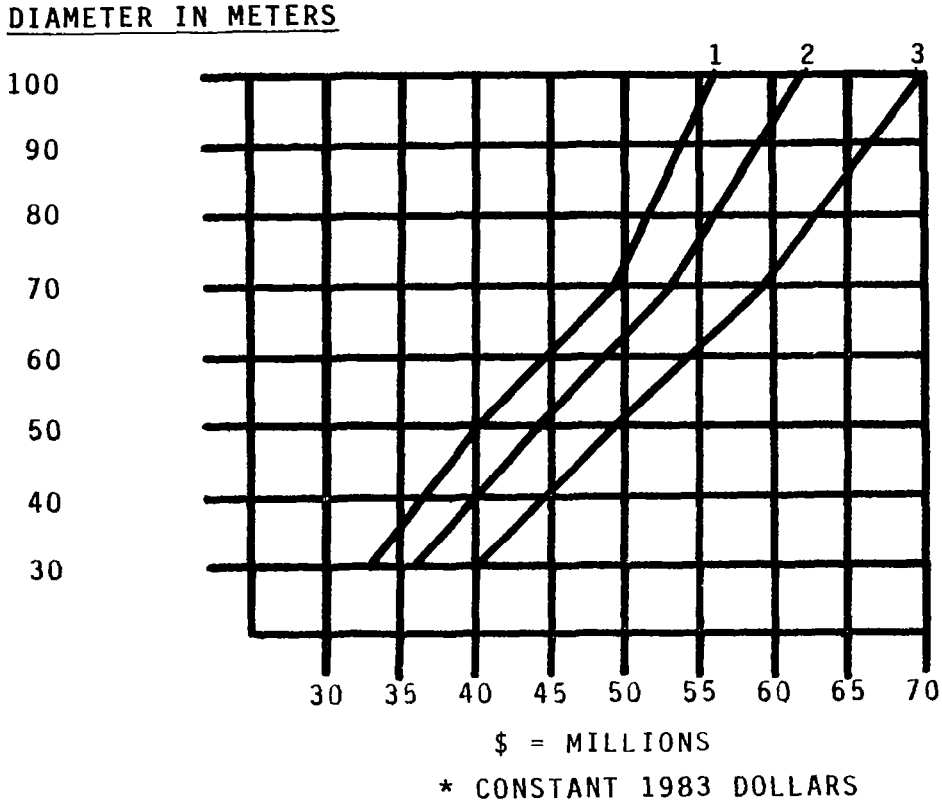


Figure 11.5-2. LSST Quad Aperture Cost Uncertainty as Calculated by Price Cost* Versus Diameter (Point Design)

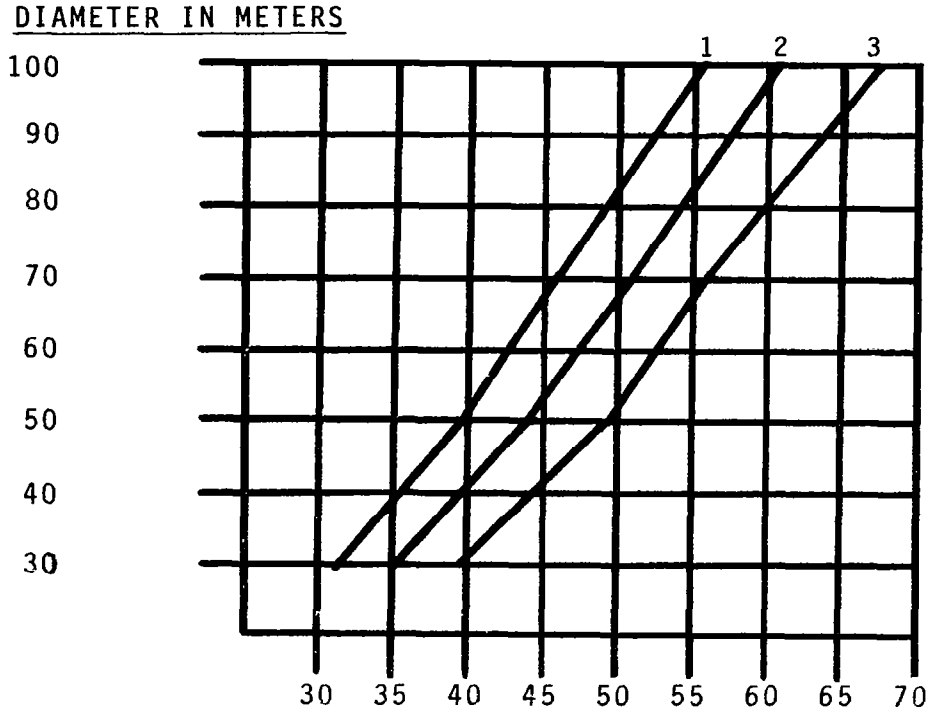


$ = MILLIONS

* CONSTANT 1983 DOLLARS

1 = LOWER BOUNDARY

2 = MEAN COST

3 = UPPER BOUNDARY

Figure 11.5-3. LSST Symmetrical Surface
Cost Uncertainty as Calculated by Price Cost* Versus Diameter

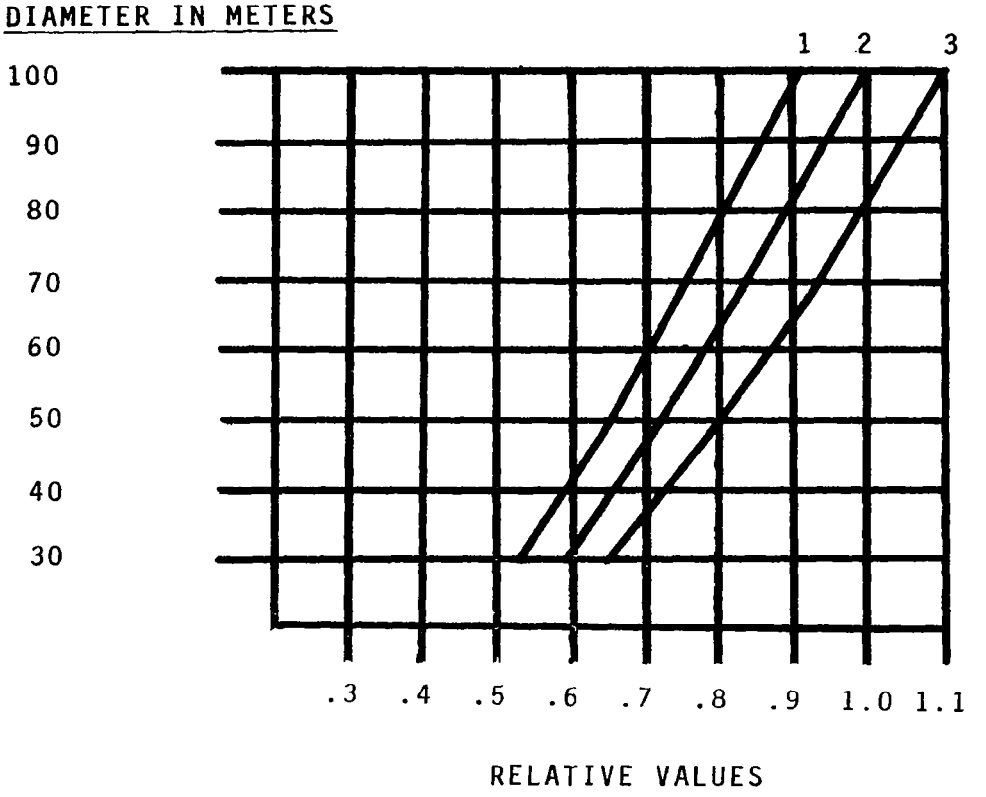


1 = LOWER BOUNDARY
2 = MEAN VALUE
3 = UPPER BOUNDARY

Figure 11.5-4. LSST Symmetrical Surface
Cost Uncertainty as Calculated by Price Cost Versus Diameter

b. Costs - For alternate diameters, the 100-meter diameter is considered the baseline for all characterizations. The Price files for the other diameters are stand-alone cost configurations and do not assume the completion of a 50-meter design. Cost data points appear linear because of the direct scaling. If, for example, a 50-meter diameter were the target of the design, actual hardware would be deleted from the 100-meter configuration. The cost curves probably represent a worst-case cost for each diameter less than 100 meters.

c. Schedule - The total time required in months to deliver a 100-meter antenna is 54, using optimized durations as calculated by the Price mode.

## 11.6 Technology Risk Areas

a. Risk Area - Specific components and assemblies that are considered risky in nature based upon Harris' experience are any ECMPLX values that are greater than 1.3. The following is a summary of these areas:

- Restowable Restrain Mechanism
- Thermal Control system particularly in areas of deployment mechanisms
- Hoop Control Mechanism
- Hoop Joint Area
- Restraint Mechanism
- Cord Assembly
- Most Deployment
- Final antenna assembly and checkout

b. Risk Reduction Tasks - The preceding identified risk areas are as of this stage in the study. Harris will evaluate the cost impact of these areas and reduce the degree of uncertainty through the construction of the 15-meter and 50-meter mockups. The Price model values and detail characterization are to be updated and the mockup task progresses.

## 12.0 PHASE II FOLLOW-ON PLAN

The Maypole Hoop/Column antenna development program objectives (see Section 1.0) are accomplished in two phases. Phase I activities are completed and the results are reported in this document. The Phase II follow-on effort is described in this section.

The Phase II program schedule is shown in Figure 12.0-1. There are five tasks which are briefly defined below. Task 1, Antenna Design and Performance, consists of evaluating the performance impact of dielectric hoop control cables in the first 3 months of FY'81, and then updating the antenna design and performance predictions in the last half of FY'83. The update will incorporate the experience and results from all of the program tasks. In Task 2, Materials Development, dielectric and graphite cable development and testing will be completed in FY'81. The Task 4, Economic Assessment, will periodically update the "PRICE" model and cost projections as additional experience and knowledge is obtained. In Task 5, the 50-Meter Surface Model and the RF Verification Model are designed, fabricated and tested in FY'81 and FY'82. At the beginning of FY'82, the Task 6, 15-Meter Kinematic Model Final Design, is initiated. Procurement, fabrication and testing of the Hoop/Column structure of the model assembly is completed by the end of FY'83. In FY'84 the surface is fabricated and installed on the structure. The model is then tested to evaluate surface repeatability, mesh stowage design, and deployment reliability. Final reports will be written at the completion of each of the tasks. More detailed descriptions of the tasks are specified in the following paragraphs.

### 12.1 Task 1: Antenna Design and Performance

#### 12.1.1 Scope of Work

This task will provide a final update of the 100-Meter Point Design. The final update will occur during the last half of FY'83 (see schedule, Figure 12.1.1-1) and will incorporate all information and experience gained during the preceding years on all tasks. The activity is divided into four subtasks: (1) Antenna Requirements Document, (2) Baseline Antenna Point Design, (3) Manufacturing Flow Plan and Philosophy, and (4) Final Report.

## PHASE II SCHEDULE

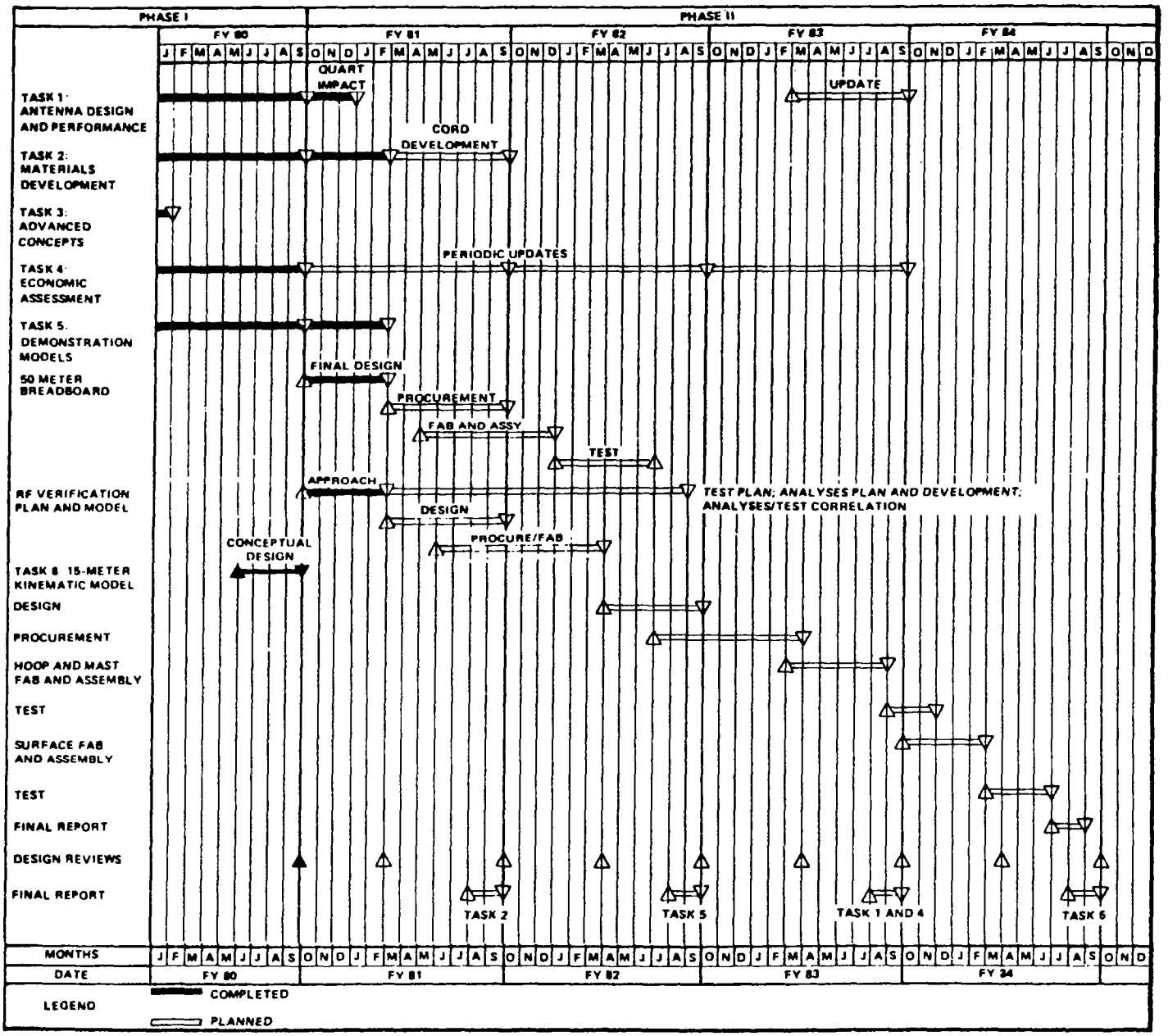


Figure 12.0-1. Phase II Schedule

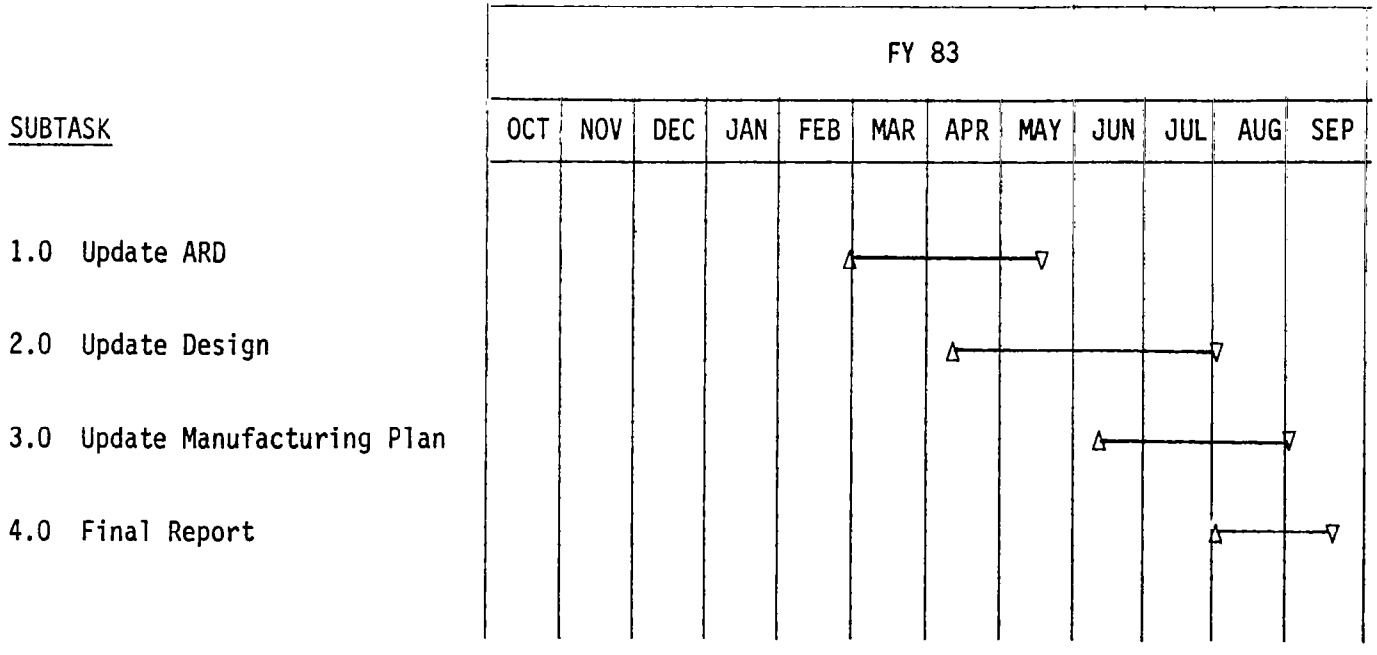


Figure 12.1.1-1. Task 1: Antenna Design and Performance

12.1.2 Task Description

Subtask 1.0: Antenna Requirements Document

This subtask will provide a final update to the ARD. This document shall contain all the most current geometrical constraints, environmental profiles, system integration requirements, mass properties, surface control and measurement requirements and ground handling requirements. The quality of the document should be sufficient for use as a procurement document for a flight experiment.

Subtask 2.0: Baseline Point Design

In this task the 100-meter point design will be evaluated against the experience gained in the design, procurement, fabrication, assembly and test of the Task 5 and Task 6 breadboard models. Where appropriate, the design will be modified to incorporate features to improve performance. An updated mass properties analysis will be provided utilizing the information obtained from the 50-Meter Surface Breadboard Model and the 15-Meter Kinematic Model. All performance projections will be updated. Parametric scaling data which define the validity of extrapolation to various size antennas will be finalized.

Subtask 3.0: Manufacturing Flow Plan and Philosophy

This subtask will provide a final update to the Manufacturing Flow Plan. The Manufacturing Flow Plan will incorporate all experience gained on the program and be of sufficient quality and detail to provide a baseline for a flight program.

Subtask 4.0: Final Report

The Phase II Final Report will consist of five volumes:

Volume 1: Antenna Design and Performance

Volume 2: Material Development

Volume 3: Economic Assessment

Volume 4: 50-Meter Surface Breadboard

Volume 5: RF Verification

Volume 6: 15-Meter Kinematic Model

This subtask will prepare and deliver Volume 1 which will contain an overview summary and schedule of the entire Phase II Program, and detailed discussion of Task 1: Antenna Design and Performance work and results. Volumes 2 through 6 will be prepared by the appropriate following task.

## 12.2 Task 2: Material Development

### 12.2.1 Scope of Work

Cable technology has been identified as a critical element and design driver for the LSST Hoop/Column Antenna 100-meter point design. An area recently identified as requiring additional information is the radio frequency scattering effects produced by the graphite (conductive) hoop control cables in front of the quad apertures. The use of dielectric (nonconductive) cables has been determined to minimize the scattering effect. Therefore, a suitable dielectric cable must be developed that can be used as a front hoop control cable. The effort will occur in FY'81 as shown in the Figure 12.2.1-1 schedule. In addition to developing dielectric cables, the task will include the determination of a statistical base of properties for graphite and dielectric cables. The statistical base properties testing will occur in the late summer of FY'81 to take advantage of an advanced cable testing facility presently being developed on Harris funds and scheduled to be completed in September 1981.

### 12.2.2 Task Description

The specific subtasks are:

Subtask 1.0: Dielectric Cable Material Identification

This subtask will identify candidate nonelectrical-conducting materials for use as a hoop control cable. Basic material properties will be determined and trade-offs performed.

Subtask 2.0: Dielectric Cable Construction Identification

This subtask will identify and select construction methods for the selected dielectric cable materials. The selected cable construction will meet the design requirements of the hoop control cable.

SUBTASK

1.0 Dielectric Cable Material Identification

2.0 Dielectric Cable Construction Development

3.0 Test and Evaluation

4.0 Final Report

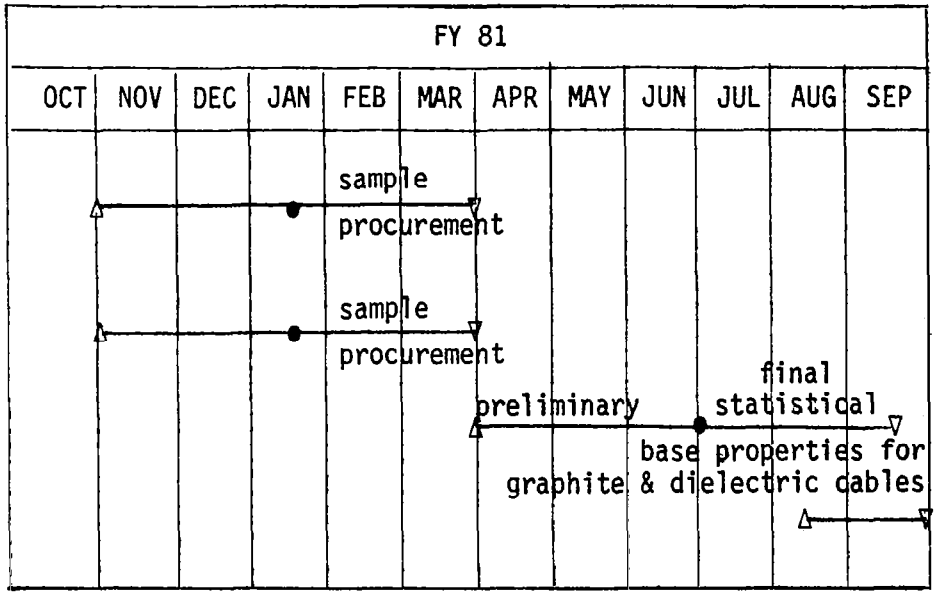


Figure 12.2.1-1. Task 2: Material Development

Subtask 3.0: Test and Evaluation

This subtask will test and evaluate graphite and dielectric cable designs. Testing will include residual strain, coefficient of thermal expansion, stiffness (EA), strength, and folding/spooling endurance. This task provides the data required to substantiate the cord properties and determine the standard deviation of those properties under the normal expected manufacturing tolerance variations.

Subtask 4.0: Final Report

This subtask will document in the form of a final report all activities and results from the Phase II Material Development Task.

## 12.3 Task 3: Advanced Concepts

There are no Phase II activities presently planned for the Task 3: Advanced Concepts.

## 12.4 Task 4: Economic Assessment

### 12.4.1 Scope of Work

The purpose of this task is to provide updated cost projections for a family of Hoop/Column Antennas as defined in the technical/mission requirements of the LSST Program. The "PRICE" model will be updated to account for new data generated by all program tasks. The model will be used to project the cost of the 50-Meter Surface Breadboard and then compared with actual costs after completion of the breadboard. The updated "PRICE" model will be used to update the Work Breakdown Structure (WBS) projected costs. The projected schedule is shown in Figure 12.4.1-1.

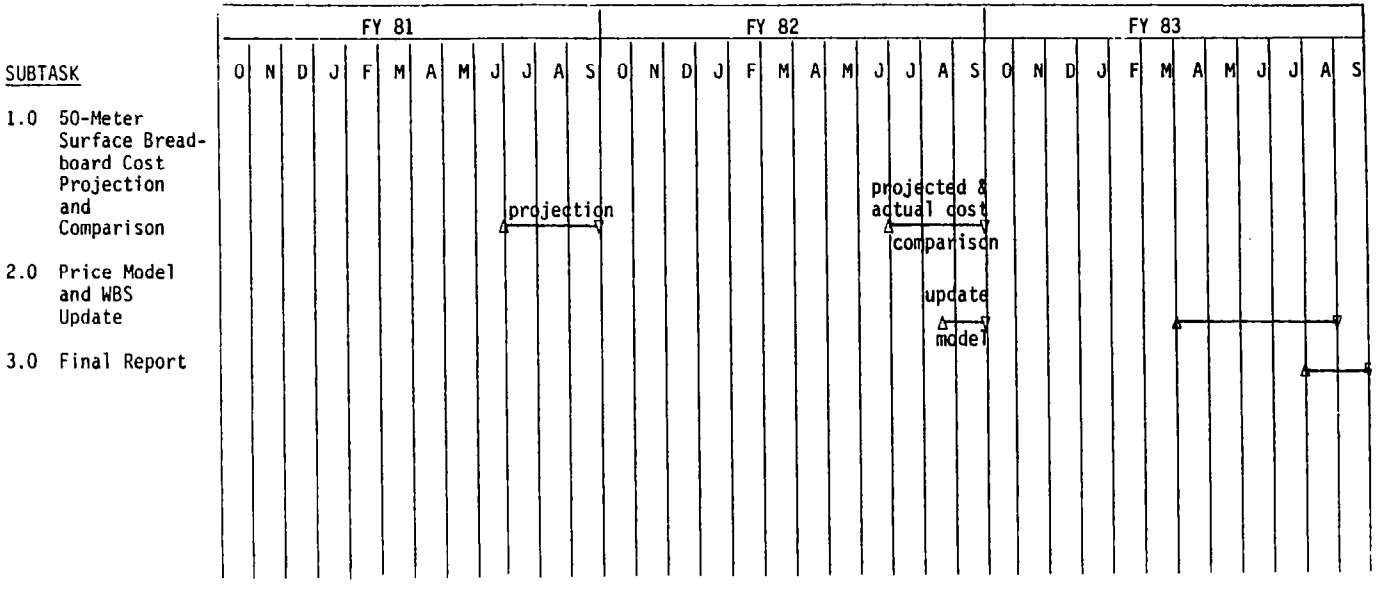


Figure 12.4.1-1. Task 4: Economic Assessment

12.4.2 Task Description

Subtasks activities are:

Subtask 1.0: 50-Meter Surface Breadboard Cost Projection and Comparison

This subtask will project the manufacturing costs of the 50-Meter Surface Breadboard prior to the commencement of work. These costs will then be compared to the actual breadboard costs. Deviations between the projected and actual costs will be used to update the "PRICE" model as appropriate.

Subtask 2.0: PRICE Model and WBS Update

This subtask updates the "PRICE" model by using the experience and outputs of all the other tasks. The model is then used to update the WBS cost projections.

Subtask 3.0: Final Report

This subtask documents the activities and results of the Phase II Task 4: Economic Assessment in a final report.

12.5 Task 5: Demonstration Models and Full Scale Elements

12.5.1 Scope of Work

The purpose of this task is to show the feasibility of the 100-meter Hoop/Column design by fabricating and testing models and full scale element. The Phase II Task 5 is comprised of two major subtasks: (1) the 50-Meter Surface Breadboard, and (2) RF Verification Model. These subtasks are described below.

12.5.2 Task Description

Subtask 1.0: 50-Meter Surface Breadboard

The design of the 50-Meter Surface Breadboard (see Figure 12.5.2-1) was completed in Phase I (FY'80) of the program. The purpose of the breadboard is to:

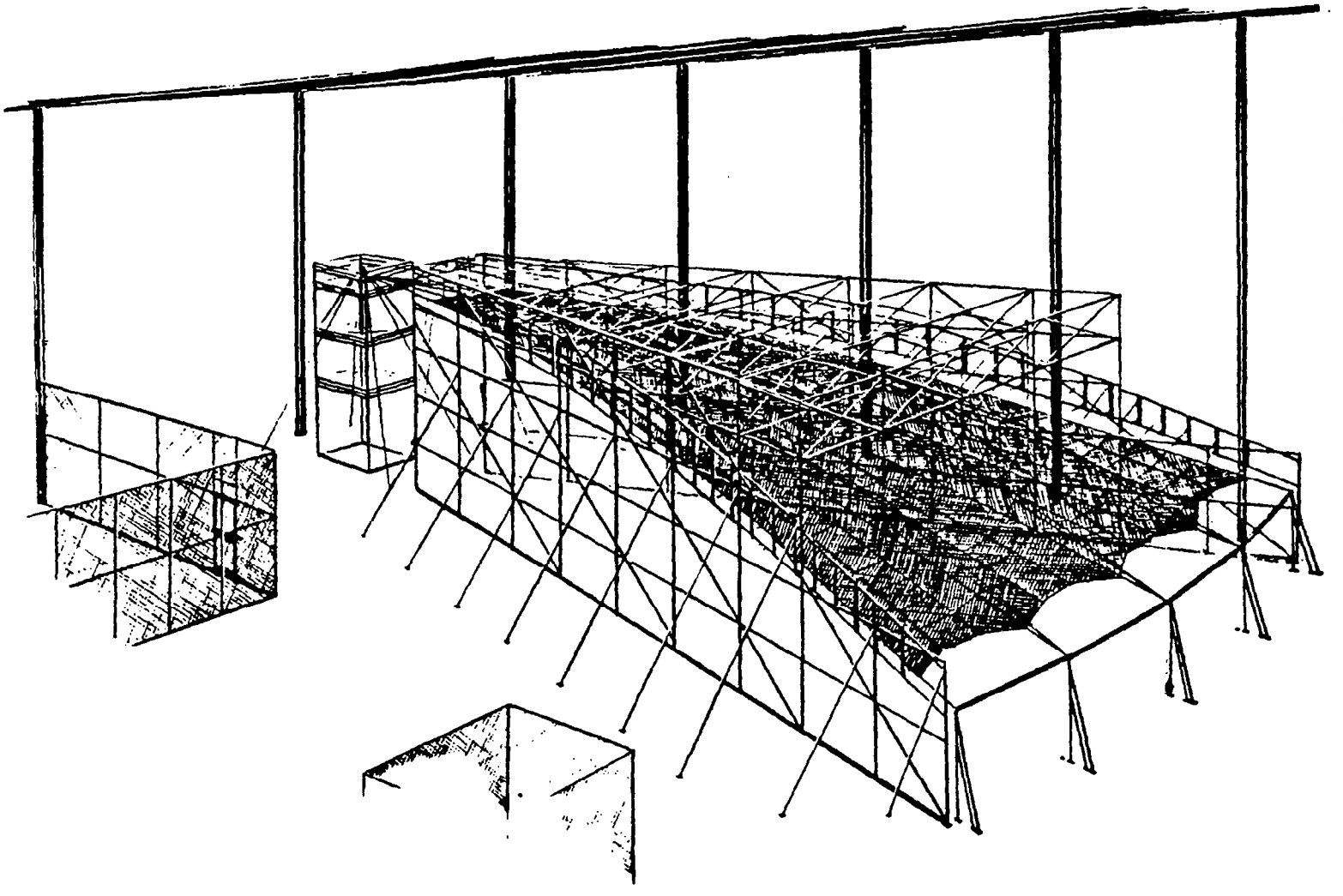

Figure 12.5.2-1. 50-Meter Surface Breadboard

a. Establish fabrication and assembly procedures for large size mesh reflectors that are cable supported
b. Demonstrate that a large scale mesh reflector can be set to a prescribed curvature within acceptable tolerances using the Hoop/Column concept
c. Determine the compatibility of a Surface Accuracy Measurement System (SAMS), supplied by NASA, with the Hoop/Column design
d. Establish the surface adjustment characteristics of a cable supported mesh reflector from some distorted shape to the desired curvature
e. Compare the experimental results of surface adjustment on the model to analytical predictions of adjustment interaction and the net effect on the overall surface shape of any particular adjustment

The subtask schedule is shown in Figure 12.5.2-2.

Subtask 1.1: Breadboard Procurement, Fabrication, Assembly, and Test Plan

The subtask includes the procurement of all model and tooling hardware as defined during the design phase of this task. Control shall be exercised to ensure the most economical costs possible are achieved for this hardware.

Upon receipt of the hardware, fabrication and assembly operations will commence in order to complete the model assembly by February 1, 1982. The manufacturing flow as defined from the output of Phase I will be utilized as appropriate in order to validate the process. Experience gained during this operation will be applicable to the 15-Meter Model described under Task 6 and any changes required will be reflected in an updated manufacturing plan developed under Task 1.

A test plan will be formulated which describes in detail the specific tests which will be performed on the completed model. Provisions for the integration and testing of a TBD surface measurement system will be made. The test plan will be submitted to NASA LaRC for review and approval at least 2 months prior to the proof-of-concept demonstration test.

SUBTASK

1.0 50-Meter Surface Breadboard

- Cable and Mesh template layout drawings
- Procurement
  - Piece Parts
  - Boundary
  - Mesh
- Tooling Fab (Gore and Cable)
- Boundary Assembly
- Surface Fab and Assembly
  - Cables
  - Gores
  - Assembly/Setting
- Testing
  - Surface Characterization
  - SAMS Integration and Test
- Final Report

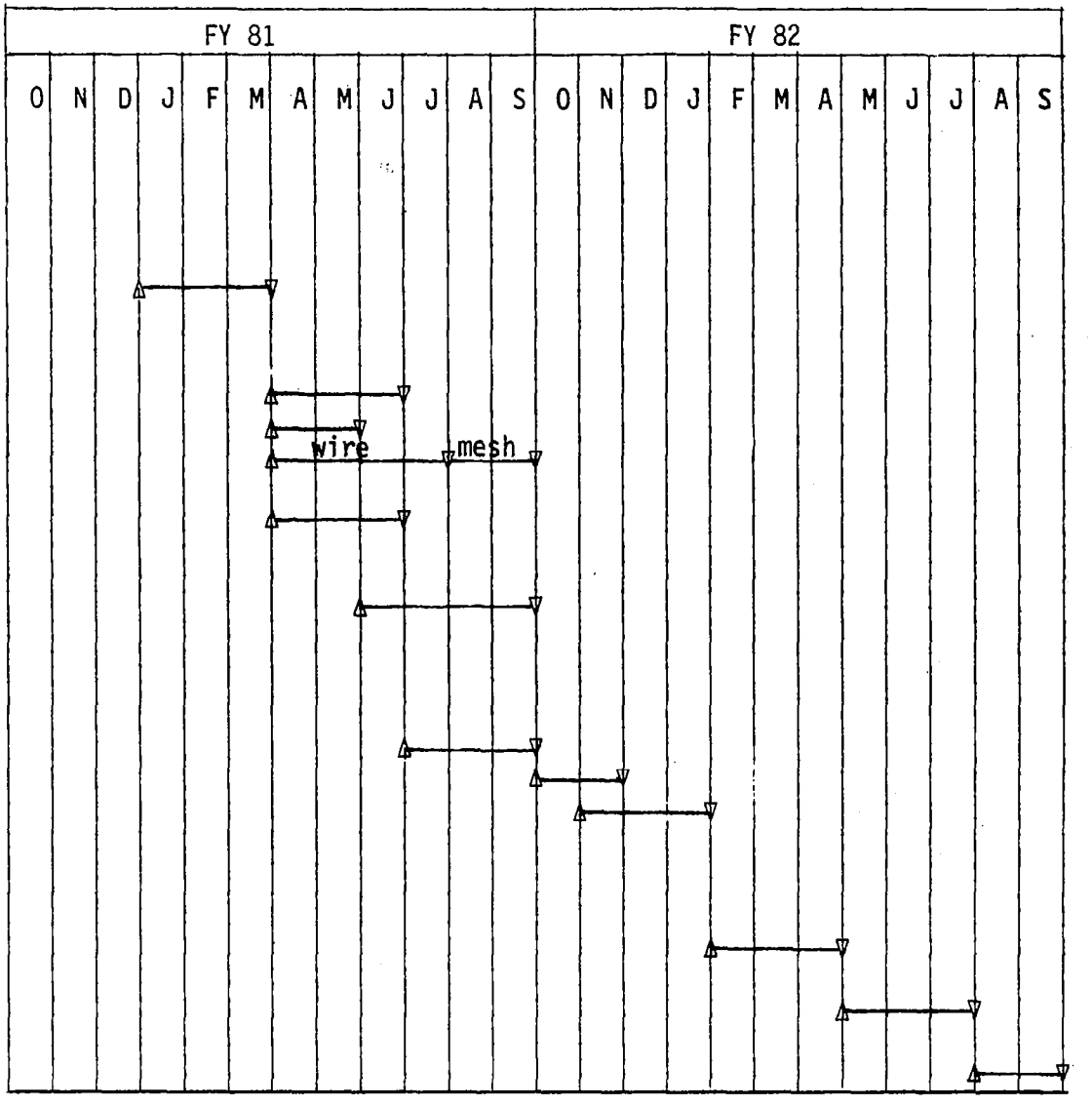


Figure 12.5.2-2. 50-Meter Surface Breadboard Schedule

Subtask 1.2: Breadboard Testing

This subtask requires the tests defined and approved from the previous subtask be accomplished. The tests will demonstrate the capability of the Maypole Hoop/Column concept to be adjusted to enhance the surface shape. Analytical support will be provided as required in the areas of setting and measuring the surface. Computer models are generated to predict the effects of various adjustments on the overall reflector surface. Measurements of the breadboard model will provide data necessary to permit analytical correlation.

Subtask 1.3: Final Report

This subtask will document all activities and results of the 50-Meter Surface Breadboard task in a final report.

Subtask 2.0: RF Verification

The RF Verification Plan objectives are three-fold:

1. Address all RF performance parameters of the quad-aperture antenna that are critical to a multibeam implementation
2. Provide verification of these critical parameters through test, analysis, or test and analysis
3. Implement each task in the most cost- and schedule-effective manner

The quad-aperture performance parameters, as outlined in the antenna requirements document (ARD), are summarized in Figure 12.5.2-3. These parameters are the most influential parameters in determining the configuration for the RF Verification Plan. The Plan is designed to answer the questions concerning the performance of the 100-Meter model as outlined in the ARD. Figure 12.5.2-4 shows that all of the critical performance parameters of the quad-aperture concept will be addressed by test or analysis. The surface effects, such as mesh construction, surface roughness and polarization effects caused by mesh hard and soft directions, will be predicted analytically using techniques and software developed on the TDRSS Program. The software is capable of predicting hard and soft direction

| PERFORMANCE PARAMETER | SPECIFIED VALUE | DESIGN PARAMETER AFFECTING PERFORMANCE |
|---|---|---|
| • GAIN | • 55.4 dB | • CABLE BLOCKAGE<br>• SURFACE ROUGHNESS<br>• MESH TRANSMISSIVITY<br>• COMATIC ABBERATION (EDGE OF SCAN |
| • BEAM INTERLEAVING | • 219 BEAMS (55 INTERLEAVED FROM EACH APERTURE) | • FEED ARRAY POSITION<br>• SPECIFIC FEED ARRAY DESIGN |
| • BEAM-TO-BEAM ISOLATION | • 30 dB | • FEED ILLUMINATION FUNCTIONS<br>• SIDELOBE LEVEL (-35 dB)<br>• REFLECTOR POLARIZATION PURITY<br>• CABLE DIFFRACTION EFFECTS<br>• FEED ARRAY RELATIVE STABILITY<br>• LOW COMA LOBES<br>• IMPLEMENTATION OF A GOOD FREQ/ POL BEAM PLAN<br>• SECONDARY BEAM SHAPE (SECONDARY REFLECTOR SHAPE) |
| • SIDELOBE LEVEL | • 30 - 35 dB | • WIRE BLOCKAGE<br>• FEED EDGE TAPER |

Figure 12.5.2-3. Quad-Aperture Performance Parameters at Issue

| KEY PARAMETERS | VERIFICATION TECHNIQUE | |
|---|---|---|
| | TEST | ANALYSIS |
| MULTIBEAM INTERLEAVING | X | X |
| BEAM-TO-BEAM ISOLATION | X | X |
| BEAM PARAMETERS | | |
| GAIN | X | X |
| BEAMWIDTH* | X | X |
| SIDELOBES* | X | X |
| POLARIZATION EFFECTS | X | X |
| EDGE-OF-SCAN EFFECTS | X | X |
| DUAL-BAND EFFECTS | X | X |
| SURFACE EFFECTS | | X |
| MESH CONSTRUCTION | | X |
| • HARD AND SOFT | | X |
| • REFLECTIVITY | | X |
| ROUGHNESS | | X |
| • PILLOWS | | X |
| • CONTOURING | | X |
| RIM | | X |
| CABLE EFFECTS | X | X |

* SOLID ANGLE COVERAGE

Figure 12.5.2-4. Key Parameters Verification Matrix

effects, mesh/reflectivity, surface roughness effects such as mesh pillow and tie points, and mesh resistance effects. The analysis has been correlated with measurements. The quad-aperture test bed is shown in Figure 12.5.2-5. In this test bed there are two 3.6-meter offset solid reflectors with an f/D of 1.5. The size of the reflectors, when operating at the chosen X-band frequency, are approximately 96 wavelengths in diameter and provide beam widths of approximately 0.6 to 0.7 degree.

For the X-band frequency there are two three-horn feeds, each independently mobile in the focal plane. The three-horn feed configuration consists of two horns permanently fixed together and a third mobile horn that can be moved in relation to the two fixed horns. The configuration will allow for complete characterization of the edge of scan effects by moving the horns independently. Each horn provides a dual linear output to provide for measurement of polarization isolation.

The breadboard will have (TBD) sets of removable support cables. These support cables are scaled representations of the 100-meter model and are made of appropriate materials such as graphite and quartz.

The effective diameter of one of the offset reflectors may be reduced by placing microwave absorber material around the outside to allow for dual-band operation with a third feed. This third feed will operate at Ku-band providing an evaluation of dual-band performance.

The techniques for quad-aperture analysis are shown in Figure 12.5.2-6. The figure shows generally tools used to verify multibeam performance, individual beam performance, surface effects, and cable effects. It is the intention to examine the commonality between NASA-Langley and Harris analytical tools at a meeting early in the program. This meeting will determine what techniques need to be utilized or augmented, and what NASA (or Harris) may have uniquely to offer to solve a particular problem associated with predicting the multibeam performance.

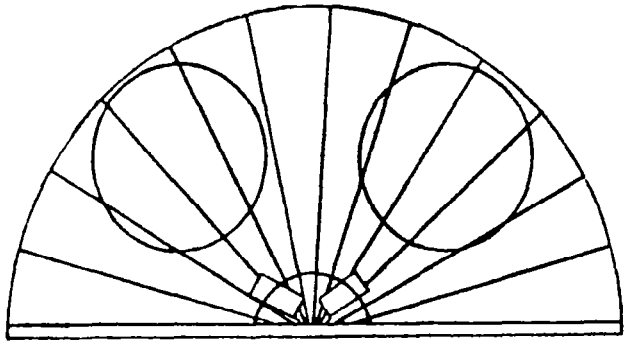

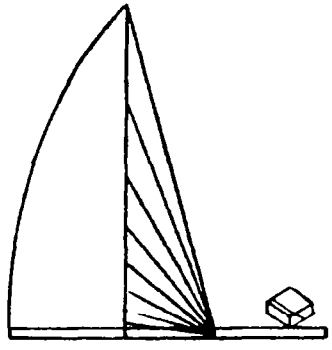

- BREADBOARD
  - TWO CUSPED 3.6M OFFSET SOLID REFLECTORS WITH F/D' 1.5.
  - THREE 3-HORN FEEDS, EACH WITH AN INTERDEPENDENTLY MOVABLE FEED, WHICH CAN BE POSITIONED ANYWHERE.
  - OPERATION AT X-BAND (EACH REFLECTOR ~ 96 , BEAMWIDTH ~ .7$^{0}$).
  - 5 SETS OF REMOVABLE CABLES.
  - REMOVABLE CUTOUTS BETWEEN REFLECTORS.
  - OUTER RING OF ONE REFLECTOR REMOVABLE, ALLOWING DUAL-BAND OPERATION WITH 3RD FEED.
- RANGE
  - DEDICATED OUTDOOR RANGE UTILIZING SAZOZIC AUTOMATED RANGE EQUIPMENT.
  - AUTOMATED SOLID ANGLE MEASUREMENTS.



Figure 12.5.2-5. Quad-Aperture Test

| PERFORMANCE PARAMETER TO BE PREDICTED | HARRIS OR NASA TECHNIQUE/TOOL TO BE USED |
|---|---|
| MULTIBEAM PERFORMANCE<br>• INTERLEAVING<br>• ISOLATION<br>• EDGE OF SCAN | SURFACE CURRENT INTEGRATION (SCI)<br>• GAIN, BEAMWIDTH, CO AND CROSS-POL<br>• MEASURED OR ANALYTIC FEEDS<br>• PILLOW, ROUGHNESS AND ARBITRARY SHAPE |
| BEAM PERFORMANCE<br>• GAIN<br>• BEAMWIDTH<br>• SIDELOBES<br>• POLARIZATION EFFECTS | SCI-GTD (OSU GTD)<br>• NEAR FIELD CALCULATION<br>• $360^{o}$ PATTERNS |
| SURFACE EFFECTS<br>• MESH<br>• ROUGHNESS<br>• CONTOUR<br>• RIM | MESH SCI<br>• CALCULATES VECTOR REFLECTION COEFFICIENT<br>• CONDUCTIVITY AND CONTACT RESISTANCE<br>• USED ON TDRSS |
| CABLE EFFECTS<br>• DIELECTRIC<br>• SIZE<br>• SPACING | SUPERPOSITION USING MOMENT METHOD SOLUTION; NASA HAS SUCH A TOOL ALREADY DEVELOPED |

Figure 12.5.2-6. Quad-Aperture Analysis

Figure 12.5.2-7 contains a summary description of the major software tools which Harris anticipates will be used in the RF Verification Task. Among these tools are the Surface Current Integration Program (SCI) and the Mesh Surface Current Integral Program (MSCI). The MSCI incorporates surface effects into prediction of secondary performance, i.e., gain, beam width, side lobes, null depths, etc.

The test facility for the quad-aperture model is shown in Figure 12.5.2-8. The geometry associated with this range is shown in Figure 12.5.2-9. The equipment to be used is the SA 2021C or equivalent. The SA 2021C is capable of providing swept-frequency and solid-angle measurements and automatically reducing the data. A typical example of the SA2021C output is shown in Figure 12.5.2-10. Both contour and 3D plots of the antenna radiation patterns are shown. These will be available on either the SA2021C or alternate equipment described in Figure 12.5.2-11. The alternate automated range consists of a software modification to an existing SA 2030 System with a microprocessor-driven acquisition and plot capability. The automatic data acquisition and plot capability was installed in Radome R2 for the TDRSS Program. The requirements of that program dictated an automatic data acquisition system. We are presently programming the software modification so that the microprocessor will be able to drive the SA 2030 System in both solid angle and frequency.

Figure 12.5.2-12 shows a connectivity diagram for the tasks required in the RF Verification Plan and Figure 12.5.2-13 shows the schedule. The tasks will be discussed in more detail in the following paragraphs.

Subtask 2.1: Breadboard Design

This task incorporates the RF and mechanical designs into the quad-aperture test bed. Included in the RF Design are considerations of RF geometry, three horn feed complexes, materials and diameters of the cables and pointing budgets for the breadboard model. These tasks will be accomplished coincidently with the mechanical design to achieve a coordinated effort. This is particularly true for the specification of the cables and the analysis of the pointing budgets.

I. SCI: SURFACE CURRENT INTEGRATION (SCI) UTILIZES VECTOR KIRCHHOFF INTEGRATION TO OBTAIN FAR-FIELD PATTERN PREDICTIONS.

1. PREDICTS SECONDARY PATTERN OF PARABOLIC OR SHAPED ANTENNA.
   - ACCEPTS POLYONOMIAL DESCRIPTION OF SURFACE
   - CAN INCLUDE RMS ROUGHNESS
2. USES HORN PATTERN OF ACTUAL SCATTER PATTERN (MEASURED DATA) AT PRIME FOCUS.
   - WILL ACCEPT MEASURED PATTERN DATA
   - FEED CAN BE OFFSET OR TILTED
   - ANALYTICAL HORN PATTERN OF COS TYPE
3. ONLY GOOD FOR 1ST TWO OR THREE SIDELOBES.

II. MSCI: MESH SCI INCORPORATES THE INFLUENCE OF MESH ON THE PREDICTED SECONDARY PATTERN.

1. SAME AS SCI BUT INCLUDES SOFTWARE TO CALCULATE MEAN REFLECTION COEFFICIENT AND INCLUDES MESH LOSS.
2. MESH PARAMETERS INPUT AS 1) WIRE SPACING, 2) WIRE SIZE, 3) WIRE CONDUCTIVITY, AND 4) WIRE CONTACT IMPEDANCE.

III. SCI GTD: SCI AUGMENTED BY GEOMETRIC THEORY OF DIFFRACTION (GTD) TO PROVIDE ACCURATE SIDELOBE PREDICTIONS.

1. CALCULATE FULL SECONDARY PATTERN ($360^{o}$) OF APEX OR CASSAGRIAN PARABOLIC SYSTEM.

IV. OFFSET SCI GTD: SCI WITH GTD APPLIED TO OFFSET REFLECTORS.

1. CALCULATES FULL SECONDARY PATTERN ($360^{o}$) WITH OFFSET REFLECTORY AND TILTED FEED; (CAN CALCULATE NEAR FIELD).

Figure 12.5.2-7. RF Software Available for Use in the RFVP (Sheet 1 of 2)

V. GTD PAR: GTD ONLY PROGRAM FOR SIDELOBE PREDICTION.

1. CALCULATES FAR OUT SIDELOBES OF PARABOLIC SYSTEM

VI. GTD HVP: GTD ONLY PROGRAM FOR HYPERBOLIC SUBREFLECTOR RADIATION PATTERNS.

1. CALCULATES FULL SCATTER PATTERN OF HYPERBOLIC SUBREFLECTOR.

VII. RAYTRACE: GEOMETRIC OPTICS/FAST FOURIER TRANSFORM COMBINATION UTILIZES APERTURE THEORY TO PREDICT FAR-FIELD PERFORMANCE.

1. CALCULATES SECONDARY PATTERN OF SHAPED OR PARABOLIC SYSTEM USING GEOMETRICAL OPTICS.

IX. RAYTRACE FFT: (2-DIMENSIONAL) LIKE RAYTRACE, EXCEPT MORE VERSATILE; CAPABLE OF PROVIDING DATA FOR CONTOUR PLOTS.

1. USES RAYTRACE TO CALCULATE THE APERTURE DISTRIBUTION AND USED THE FFT TO CALCULATE THE FAR-FIELD.

X. CONTOUR PLOT:

1. USES THE OUTPUT OF THE FFT PROGRAM TO CALCULATE THE FAR-FIELD CONTOURS.

XI. HORN PATTERN:

1. CALCULATES HORN PATTERN FOR CIRCULAR OR RETANGULAR HORN. CALCULATES NEAR OR FAR FIELD.

XII. EFFICIENCIES:

1. ASSUMES CIRCULARY SYMMETRIC DISH; CALCULATES AMPLITUDE, PHASE, SPILLOVER, AND BLOCKAGE EFFICIENCIES.

Figure 12.5.2-7. RF Software Available for Use in the RFVP (Sheet 2 of 2)

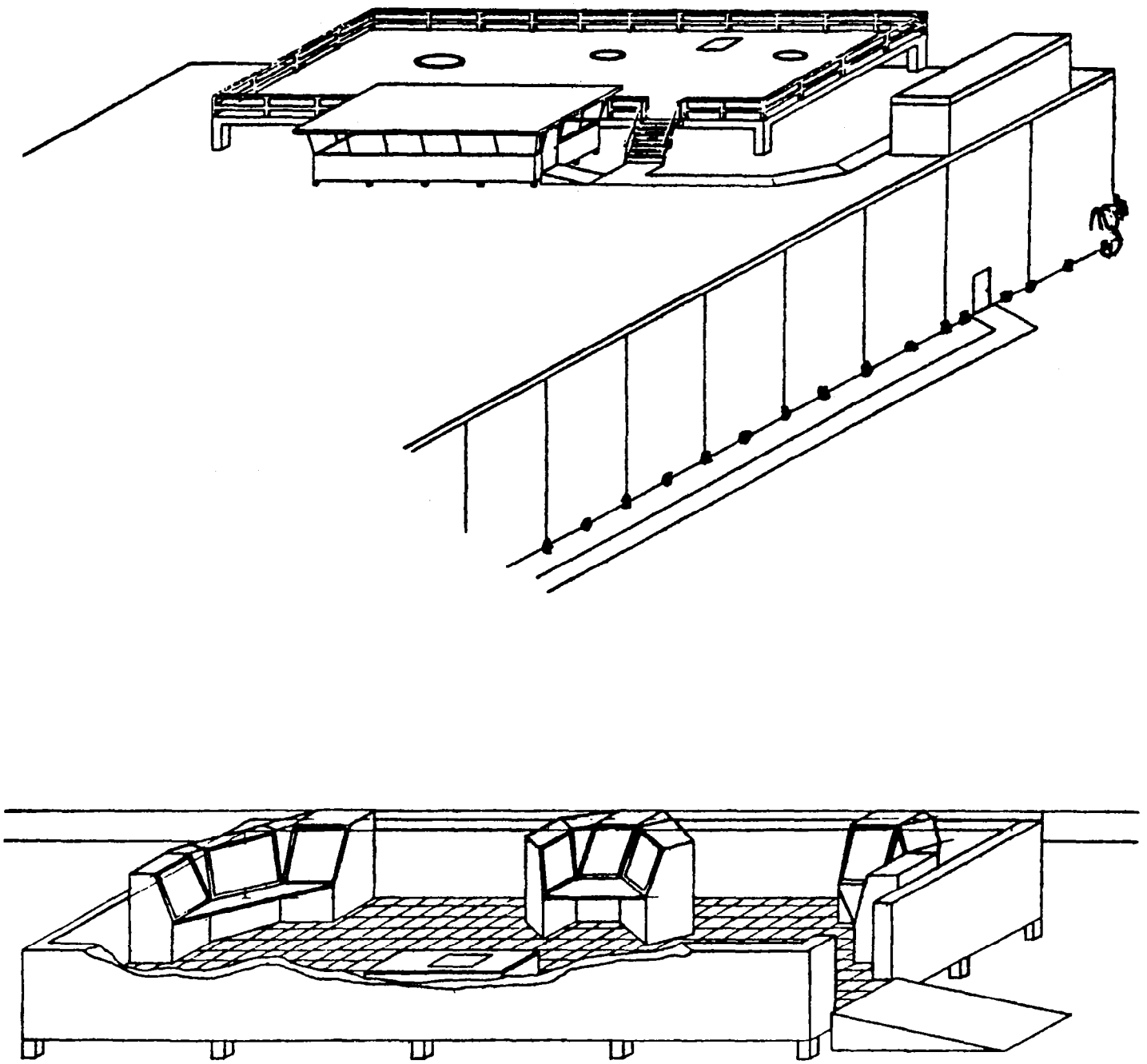

Figure 12.5.2-8. Building 5 Elevated Range

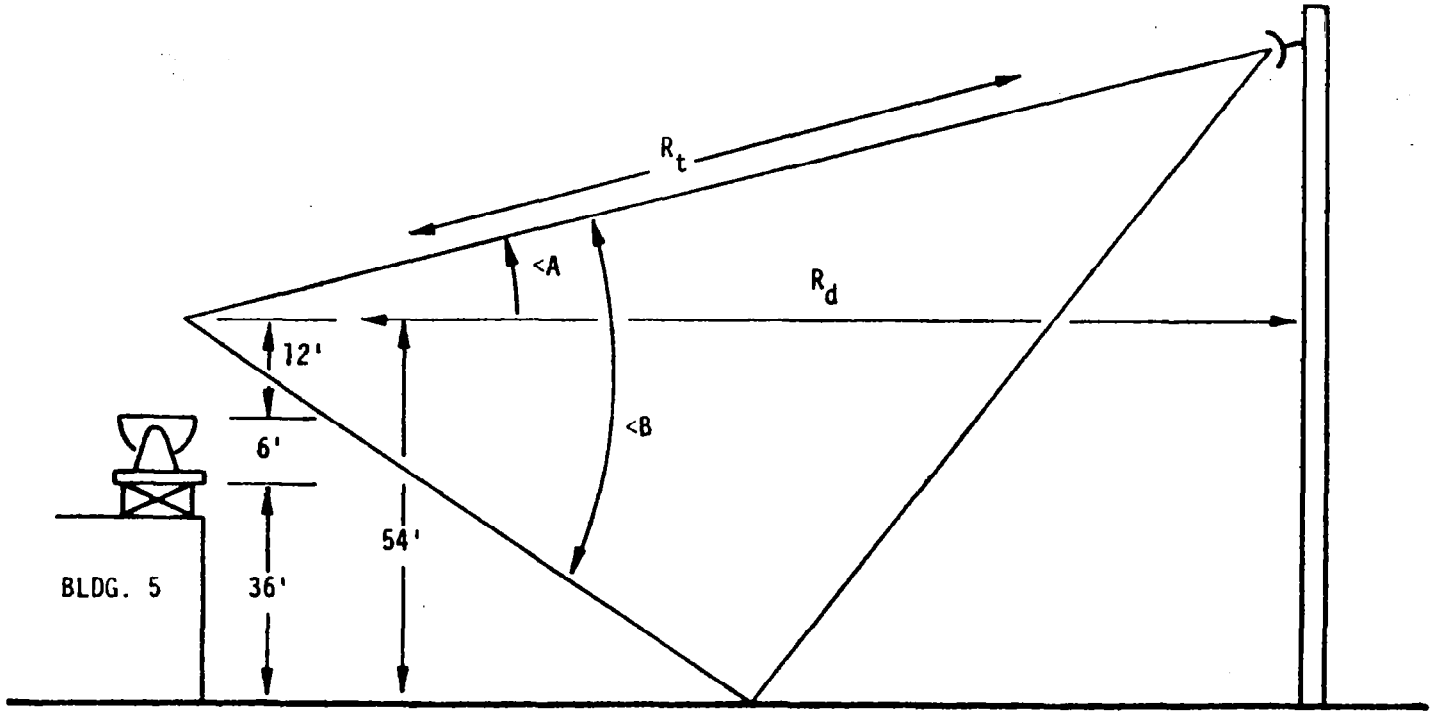


| | 400' TOWER | OLD 150' TOWER | NEW 150' TOWER |
|---|---|---|---|
| <A = | 2.8° | 2.9° | 5.0° |
| <B = | 6.6° | 9.2° | 15.7° |
| $R_t$ = | 6548' | 1846' | 1088' |
| $R_d$ = | 6540' | 1844' | 1084' |

Figure 12.5.2-9. Building 5 Range Layout

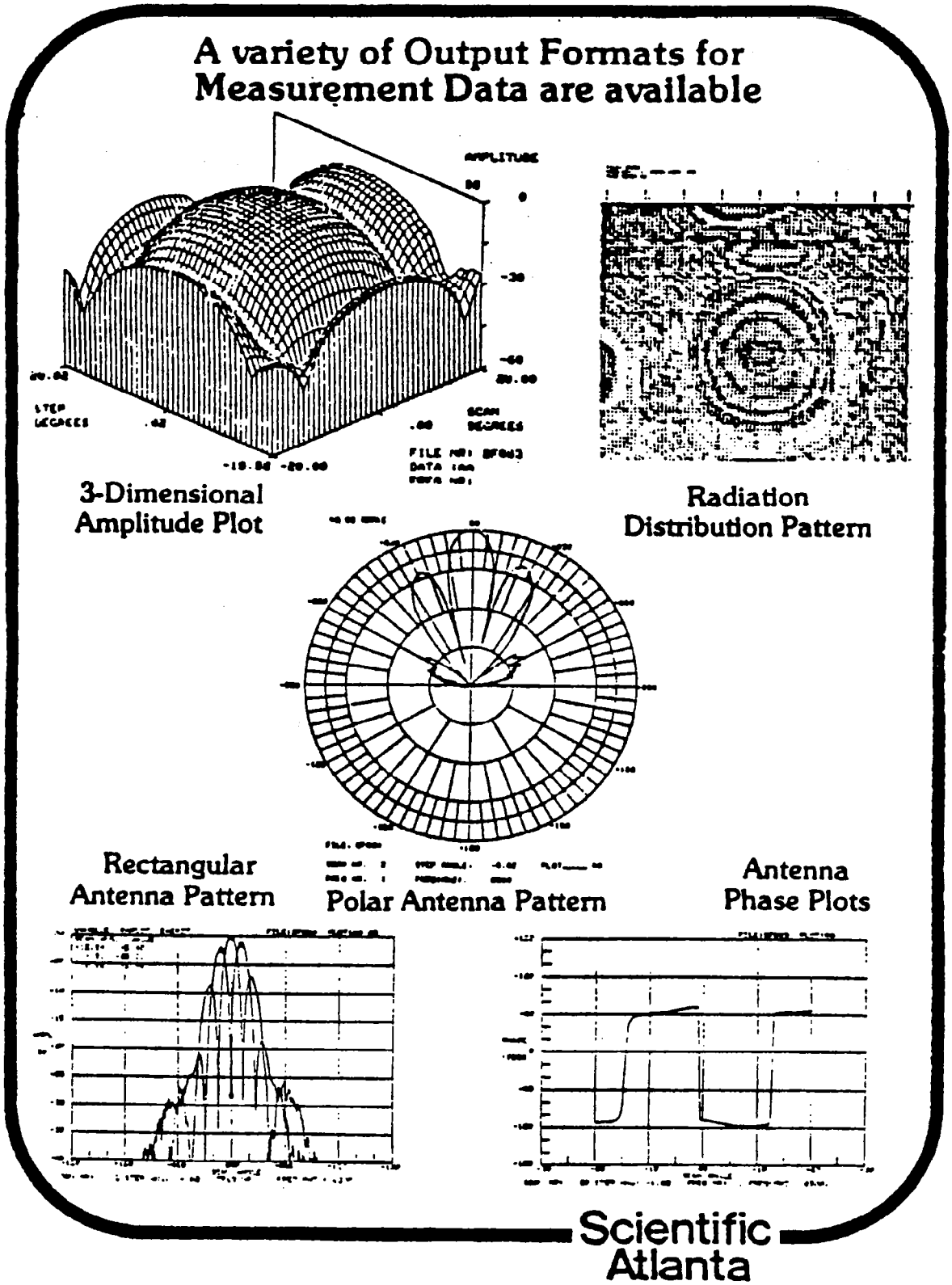


Figure 12.5.2-10. Automated Range Typical Data Output

- SOFTWARE MODIFICATION TO EXISTING RANGE EQUIPMENT
- SA 2030 SYSTEM WITH MICROPROCESSOR DRIVEN ACQUISITION AND PLOT
  - VECTOR-GRAPHIC MICROPROCESSOR WITH 10.8 MB DISC DRIVE
  - INTERFACE TO HP2648A SMART TERMINAL WITH HARD COPY CAPABILITY
  - BETTER (MORE READABLE) OUTPUT
- SOFTWARE MODIFICATION COMPLETE BY MARCH 1981

Figure 12.5.2-11. Alternate Automated Range

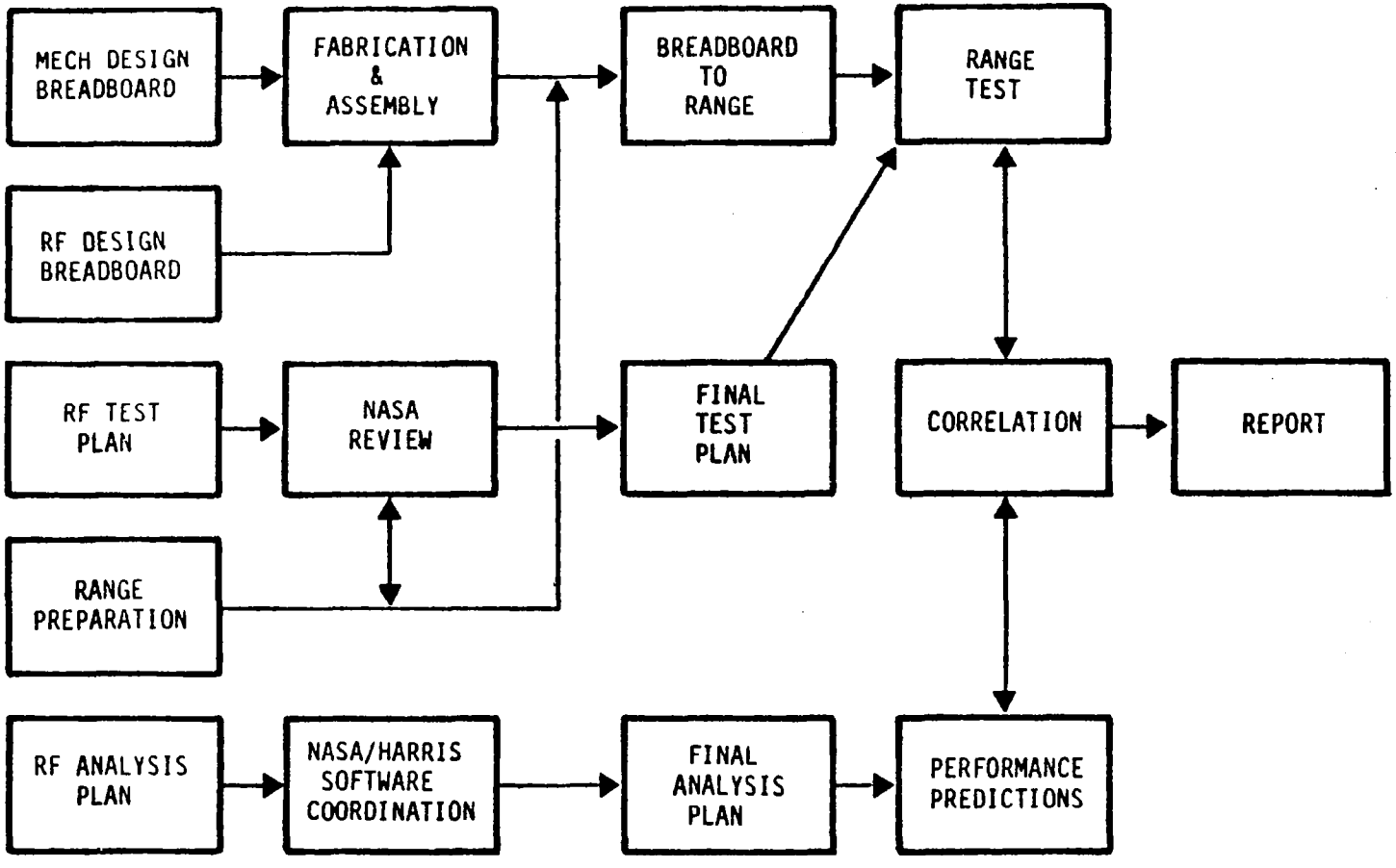


Figure 12.5.2-12. RF Verification Plan Task Flow

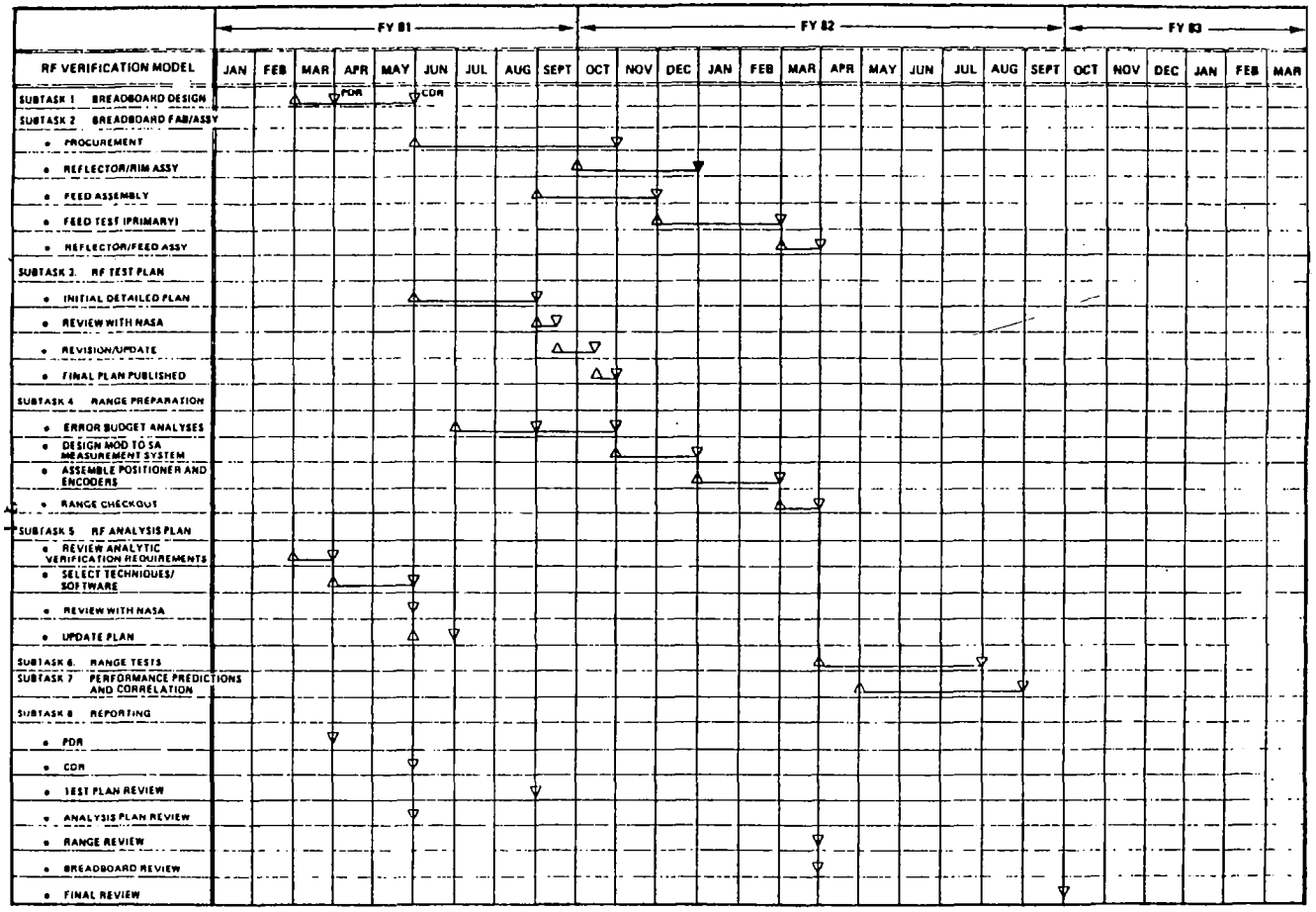


Figure 12.5.2-13. RF Verification Plan Schedule

The mechanical design and analysis of the test bed will include: the two horn feeds, and a movable third horn, the movable fixture in the focal plane of the offset reflectors and supporting structure. The mechanical design will accommodate an outside environment in terms of protection of the structure from the weather. The structure will be analyzed to determine the appropriate safety factors for handling and design pointing budgets in terms of reflector droop and mispointing due to mechanical deflection. Included in this design task is support of reviews with NASA-Langley.

Subtask 2.2: Fabrication and Assembly

This task procures appropriate parts for the breadboard, such as, off-the-shelf horns, OMT's and coaxial switches. In addition, the fabrication of the structure, reflectors and feeds will occur. The cables will be fabricated and set aside for use in the range measurements.

Primary tests of the horn designs will be carried out and secondary results extrapolated from the data.

Subtask 2.3: Test Plan

This task defines detailed tests to be performed on the RF Verification Model. After a detailed set of procedures are written they will be reviewed with NASA for comment and question. The final test plan will result from this review.

Subtask 2.4: Range Preparation

The range will be prepared for the test bed measurements through analysis of the range errors and design modifications as necessary to the SA measurement system to ensure that the azimuth and elevation accuracy requirements are achieved. The range is checked for accuracy by probing with the test antenna "window" as necessary.

Subtask 2.5: RF Analysis Plan

The purpose of the RF Analysis Plan will be to review the analytic verification requirements as determined from the verification matrix and select the appropriate techniques and software currently available at Harris. These analytic techniques and software will be reviewed with NASA for

commonality. Where there are common programs resident at both NASA and Harris, duplication of effort may be eliminated. Harris will use the expertise of NASA-Langley in certain areas of antenna modeling for cable effects. We also plan to utilize NASA expertise to reduce the programming effort required for new software by using existing NASA software where applicable. In addition, consultation between NASA and Harris engineers should result in the best approach for verifying the quad-aperture performance in terms of surface effects that will be present when a mesh is used as a surface for the offset reflectors.

Subtask 2.6: Range Tests

The range test on the quad-aperture test bed will occur as scheduled in Figure 12.5.2-13. The range tests will be performed according to the detailed procedure written up in the range test document as an output of Task 3. It is anticipated that the tests to be performed will be solid angle, frequency, swept gain, side lobe, beam width tests, as well as edge of scan tests and principal plane cuts.

Subtask 2.7: Performance Predictions and Correlation

According to the RF Analysis Plan, the performance predictions of the quad-aperture test bed will be computed and the mission critical items, as identified in the key parameters matrix, will then be verified by both test and analysis. These include the multibeam performance, the individual beam performance and the cable effects. The analysis isolated in the RF Analysis Plan as being applicable to surface effects will be used to generate performance predictions for the quad-aperture test bed as if the surfaces were mesh.

Subtask 2.8: Reporting

The reporting of the RF Verification plan will include: (1) Preliminary and Critical Design Reviews for the Quad-Aperture Test Bed, (2) Thorough and Detailed Reviews of the RF Analysis and Test Plan, and (3) Interim and Final Reports on the progress on the RF Verification Plan.

## 12.6 Task 6: 15-Meter Kinematic Model

### 12.6.1 Scope of Work

The proposed task will focus on the design fabrication and test of a 15-Meter diameter Deployable Kinematic Reflector model shown in Figure 12.6.1-1. The purpose of the model will be to provide verification of the design in terms of deployment kinematics, deployment reliability, failure modes investigation, surface interaction, manufacturing techniques and scaling. The task schedule is shown in Figure 12.6.1-2.

### 12.6.2 Task Description

#### Subtask 1.0: Model Design

All design work required to support procurement, fabrication, and operation of the 15-meter breadboard model will be accomplished under this subtask. The design will be representative of the 100-meter Maypole Hoop/ Column "point" design. Scaling to the extent possible will be accomplished. The model will consist of a deployable mast, a deployable hoop consisting of 48 segments powered by motors, a mesh reflector surface and cords for hoop stabilization and surface shaping. The model will be fabricated and assembled to a prescribed surface accuracy which is consistent with the objective of verifying scaling laws and accuracy predictions.

Investigation into the requirements of a counterbalance system will be accomplished and a system incorporated into the design if necessary. The design description will include drawings of sufficient detail to permit fabrication and assembly of the hardware. Material selection will be of flight type materials where possible and other materials when they functionally represent the requirements of the flight design without significantly degrading the model's overall performance. Analytical support of this subtask will include piece part analysis, Kinematic Analytical models, and Reflector Surface models.

## OBJECTIVES

- DESIGN, FABRICATE AND TEST A 15M DIAMETER FULL HOOP/ COLUMN ANTENNA BREAD-BOARD MODEL

| TASK | COMMENTS |
| --- | --- |
| 15M VERIFICATION BREADBOARD MODEL | • PRELIMINARY DESIGN IN PROGRESS. SCHEDULED COMPLETION DATE MAY 81 |

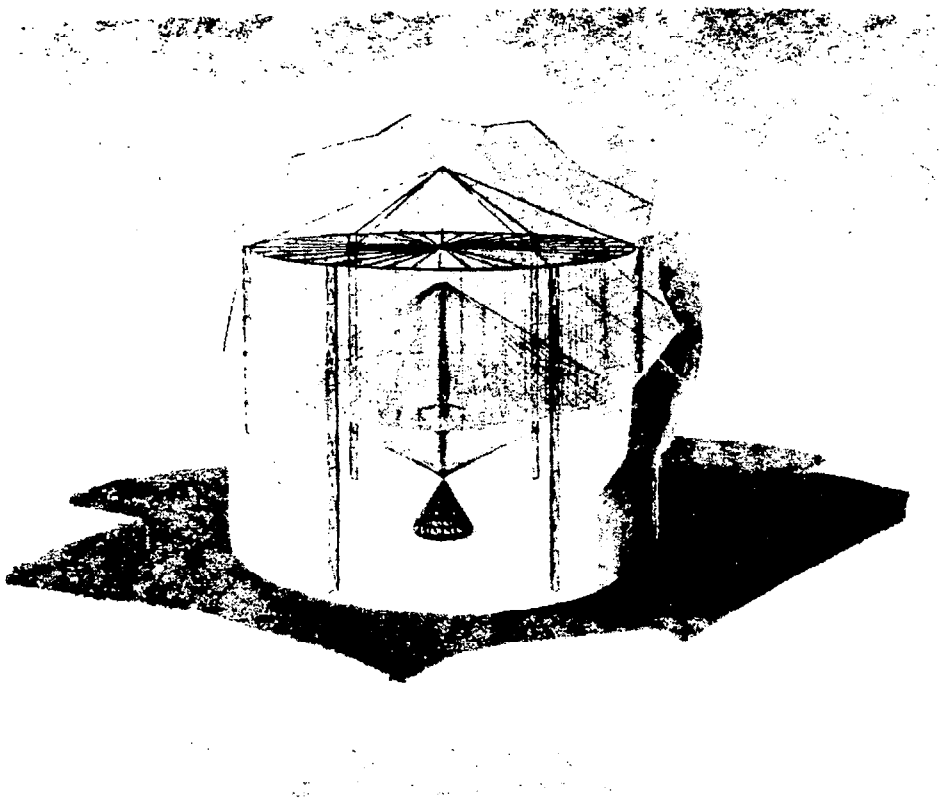

Figure 12.6.1-1. 15-Meter Kinematic Model

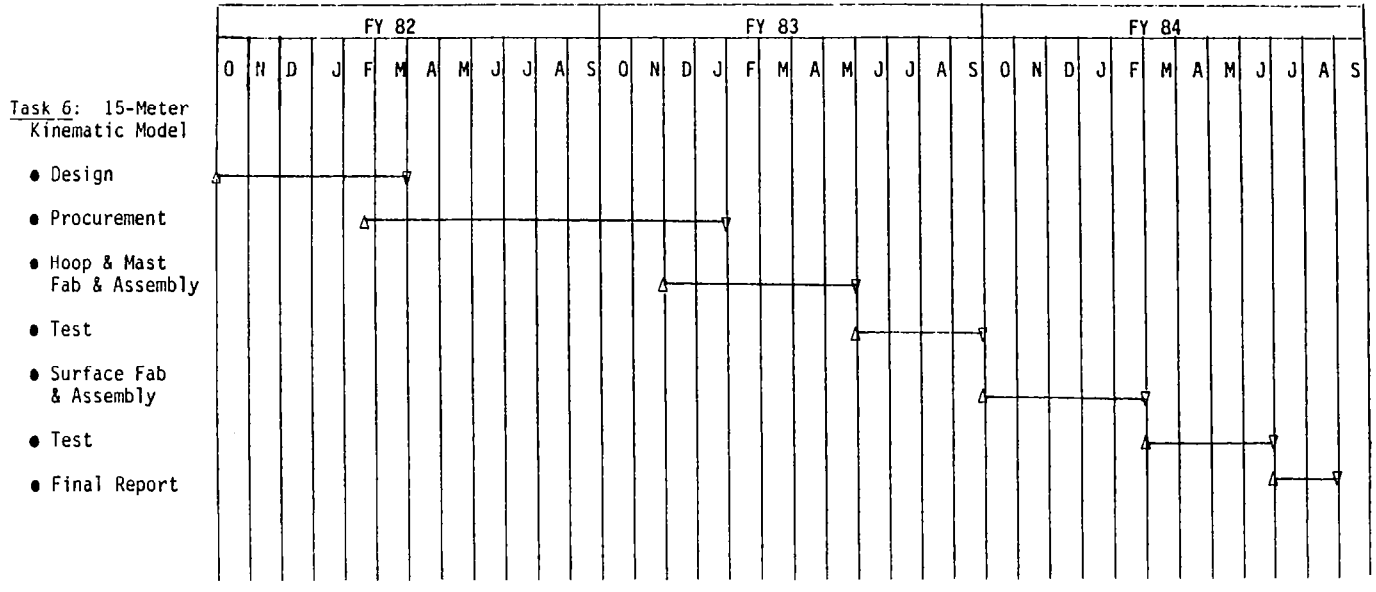


Figure 12.6.1-2. Task 6: 15-Meter Kinematic Model Schedule

Subtask 2.0: Tooling Design

All tooling required for the construction and operation of the 15-meter model will be designed under this subtask. The manufacturing sequence developed under Task 1 of the program will be considered to design tooling consistent with the proposed manufacturing flow. Tolerances will be kept to a minimum within reasonable costs in order to assess the impact of these tolerances on the reflector surface budget.

Subtask 3.0: Fabrication, Assembly and Testing

This subtask is divided into the following task areas.

Subtask 3.1: Procurement

All hardware necessary to permit fabrication and assembly of the full 15-meter model will be procured. This includes all tooling. Control will be exercised to ensure the most economical costs possible are achieved for this hardware.

Subtask 3.2: Fabrication and Assembly

The Kinematic model will be assembled in two phases. The first phase consists of the primary structural elements of the design; namely: the hoop, deployable mast, and hoop control cables. Appropriate tests will be performed upon the completion of this level of assembly.

The second phase of assembly will incorporate the surface elements. These include mesh, mesh shaping ties and cords, and the basic string truss cord system.

Subtask 3.3: Test Plan and Model Testing

A test plan will be developed describing in detail the specific tests to be performed on the model. The plan will be submitted to NASA LaRC for review and approval at least 2 months prior to the start of any testing.

The testing of the model consists of two phases. The first phase will utilize the hoop and mast to evaluate deployment kinematics failure modes, synchronization, etc. The second phase will evaluate the full reflector system. Tests will validate the design in terms of overall performance plus the effects of the surface elements on deployment reliability. The reflector repeatability will also be determined.

Subtask 4.0: Final Report

All activities and results of Task 6 will be documented in a Final Report.

| 1. Report No. | 2. Government Accession No. | 3. Recipient's Catalog No. |
|---|---|---|
| NASA CR-3558, Part 2 | | |

| 4. Title and Subtitle | 5. Report Date |
|---|---|
| LSST (HOOP/COLUMN) MAYPOLE ANTENNA DEVELOPMENT PROGRAM | June 1982 |
| | 6. Performing Organization Code |
| 7. Author(s) | 8. Performing Organization Report No. |
| Marvin R. Sullivan | |
| | 10. Work Unit No. |
| 9. Performing Organization Name and Address | |
| Harris Corporation, Government Systems Group<br>Electronic Systems<br>P.O. Box 37<br>Melbourne, FL 32901 | 11. Contract or Grant No.<br>NAS 1-15763 |
| | 13. Type of Report and Period Covered |
| 12. Sponsoring Agency Name and Address | Contractor Report |
| National Aeronautics and Space Administration<br>Washington, DC 20546 | 14. Sponsoring Agency Code |

15. Supplementary Notes

Langley Technical monitor: Thomas G. Campbell
Phase I final report, Part 2

16. Abstract

The first of a two-phase program was performed to develop the technology necessary to evaluate, design, manufacture, package, transport and deploy the Hoop/Column deployable antenna reflector by means of a ground based program. The Hoop/Column concept was originated in a previous contract and consists of a cable stiffened large diameter hoop and central column structure that supports and contours a RF reflective mesh surface. NASA supplied mission scenarios for communications, radiometer and radio astronomy provided the data to establish technology drivers that resulted in a specification of a point design. The point design is a multiple beam quadaperture offset antenna system which provides four separate offset areas of illumination on a 100 meter diameter symmetrical parent reflector. The periphery of the reflector is a hoop having 48 segments that articulate into a small stowed volume around a center extendable column. The hoop and column are structurally connected by graphite and quartz cables. The prominence of cables in the design resulted in the development of advanced cable technology. Design verification models were built of the hoop, column, and surface stowage sub-assemblies. Model designs were generated for a half scale sector of the surface and a 1/6 scale of the complete deployable reflector. These models will be fabricated in Phase II of the program and will verify the 100 meter point design in terms of surface accuracy and adjustment, deployment kinematics, manufacturing techniques and analytical models correlation. An RF verification model and test was also planned for the Phase II effort.

| 17. Key Words (Suggested by Author(s)) | 18. Distribution Statement |
|---|---|
| LSST Technology<br>Large space deployable antenna<br>Quadaperture<br>Cable stiffened hoop/column | Unclassified - Unlimited<br>Subject Category 03 |

| 19. Security Classif. (of this report) | 20. Security Classif. (of this page) | 21. No. of Pages | 22. Price |
|---|---|---|---|
| UNCLASSIFIED | UNCLASSIFIED | 300 | A13 |

For sale by the National Technical Information Service, Springfield, Virginia 22161

NASA-Langley, 1982